CRANFIELD UNIVERSITY
LIBRARY

Cranfield University

HEEYOON KANG

HEAT TRANSFER CHARACTERISTICS OF HEAT PIPE HEAT EXCHANGERS FOR LOW AND MEDIUM TEMPERATURE HEAT RECOVERY

School of Mechanical Engineering

MPhil Thesis

ProQuest Number: 10832144

All rights reserved

INFORMATION TO ALL USERS
The quality of this reproduction is dependent upon the quality of the copy submitted.

In the unlikely event that the author did not send a complete manuscript
and there are missing pages, these will be noted. Also, if material had to be removed,
a note will indicate the deletion.

ProQuest 10832144

Published by ProQuest LLC (2018). Copyright of the Dissertation is held by Cranfield University.

All rights reserved.
This work is protected against unauthorized copying under Title 17, United States Code
Microform Edition © ProQuest LLC.

ProQuest LLC.
789 East Eisenhower Parkway
P.O. Box 1346
Ann Arbor, MI 48106 – 1346

CRANFIELD UNIVERSITY
LIBRARY

Cranfield University
School of Mechanical Engineering

MPhil Thesis
1996/1997

HEEYOON KANG

HEAT TRANSFER CHARACTERISTICS OF HEAT PIPE HEAT EXCHANGERS FOR LOW AND MEDIUM TEMPERATURE HEAT RECOVERY

Supervisor : Dr. O. BADR

July 1997

This thesis is submitted for the degree of MPhil

ABSTRACT

Heat pipe heat exchangers (HPHEs) offer many advantages over other types of heat exchangers for the recovery of heat from industrial gaseous waste streams in the low and medium temperature ranges. Heat pipes employed in industrial heat exchangers can be made with or without wicks. Although the thermal performances of single heat pipes and HPHEs have been extensively investigated, comparative studies concerning behaviours of HPHE with different types of heat pipes, at the same operating conditions, appear to be very limited. Such studies are useful in evaluating the significance of the parameters pertinent to thermal performance and in selecting the most appropriate HPHE for a particular application.

Taking into account previous studies, the present work was focused on comparative studies between heat pipe and thermosyphon, at the same operating conditions, with following the objectives :

- Further studying the heat transfer characteristics of heat pipe and thermosyphon to obtain additional information regarding thermal performance, at the same operating conditions.
- Providing some guide-lines for HPHEs design which relate to the thermal performance of heat pipe and thermosyphon.

To achieve these objectives, two computer models, a 'Heat Pipe and Thermosyphon Thermal Performance Model' and a 'Heat Pipe Heat Exchangers Design Model', were developed. The former model facilitates the prediction of the axial temperature distributions of the working fluid and the tube wall ; heat-transport limitations; and the thermal performances of thermosyphons and heat pipes with different type of wicks. An experimental investigation of the steady-state behaviour of the thermosyphon was carried out to validate this computer model and the results were compared with the corresponding predictions of the computer model developed. According to the experimental results, Nusselt's film theory for continuous liquid film could not be employed for predicting thermal performances in the condenser and evaporator film region of inclined thermosyphons. Liquid film could only be maintained circumferentially in vertical thermosyphon tubes,

even though might not the smooth continuous film. In the evaporator pool region, the change in saturation temperature due to the hydrostatic height of the pool should be considered for predicting the axial temperature distributions. The results of the behaviours of heat pipes and thermosyphons were utilised to develop a 'Heat Pipe Heat Exchangers Design Model' to facilitate both the design and the prediction of performances of HPHEs. These models enable the designers of waste-heat recovery systems to choose the most appropriate type of heat-transfer elements and optimise the design parameters of a HPHE for a given application.

ACKNOWLEDGEMENT

I would like to express my sincere gratitude to my supervisor Dr. Ossama Badr for his expert supervision, advice, encouragement and caring attitude throughout this study. It is really a pleasure to work with him.

Thanks must also go to the technicians in the Design Office and Department of Applied Energy, in particular Mr. Charlie Knight, for their help in the experimental work of this study.

Many thanks are due to my company, POSCO, for providing all their support.

Last but not least, I would like to thank all of my family particularly my parents and my wife for all their support and the sacrifices they have made.

Heeyoon Kang
July 1997
Cranfield University

CONTENTS

	Page
ABSTRACT	A
ACKNOWLEDGEMENTS	C
CONTENTS	D
LIST OF FIGURES	G
LIST OF TABLES	I
NOMENCLATURE	J
CHAPTER 1 INTRODUCTION	1
1.1 HEAT PIPES AND THERMOSYPHONS	1
1.2 THE PRESENT STUDY	3
1.3 STRUCTURE OF THESIS	4
CHAPTER 2 LITERATURE SURVEY	5
2.1 HISTORIC DEVELOPMENT OF HEAT PIPES AND HPHES	5
2.2 HEAT-TRANSFER CHARACTERISTICS OF HEAT PIPES	7
2.3 REVIEW OF PREVIOUS WORK ON HEAT PIPE AND HPHES	10
2.3.1 Previous Studies on Characteristics of Heat Pipes	10
(a) Heat-transfer characteristics and thermal behaviour	12
(b) Heat-transport limitations	21
2.3.2 Comparative Studies of Heat Pipes and Thermosyphons	30
2.3.3 Previous Studies on Heat Pipe Heat Exchangers	32
2.4 SUMMARY OF THE REVIEW ON PREVIOUS WORK	35

CHAPTER 3 ANALYTICAL STUDY AND COMPUTER MODELLING OF THE BEHAVIOUR OF HEAT PIPES 40

3.1 ANALYSIS OF THE BEHAVIOUR OF HEAT PIPES 40

3.1.1 Analysis of Thermal Performances 40

(a) Steady-state performance 40

(b) Comparison between the heat pipe and thermosyphon 46

3.1.2 Analysis of Heat-Transport Limitations 47

3.1.3 The Simple Mathematical Model for Thermosyphons 53

3.2 HEAT PIPE AND THERMOSYPHON THERMAL PERFORMANCE COMPUTER MODEL 54

3.2.1 Computer Program Design 55

3.2.2 Computer Program Notes 61

CHAPTER 4 EXPERIMENTAL SET-UP AND PROCEDURE 64

4.1 DESIGN OF TEST APPARATUS 64

4.2 INSTRUMENTATION 69

4.3 EXPERIMENTAL PROCEDURE 71

CHAPTER 5 EXPERIMENTAL RESULTS AND DISCUSSION 74

5.1 EXPERIMENTAL RESULTS 74

5.2 COMPARISON BETWEEN EXPERIMENTAL RESULTS AND ANALYTICAL PREDICTIONS 91

5.3 DISCUSSION 104

5.3.1 Condenser and Evaporator Film 104

5.3.2 Evaporator Pool 104

5.4 VALIDATION OF THE COMPUTER MODEL 105

CHAPTER 6 HEAT PIPE HEAT EXCHANGERS 107

6.1 THERMAL PERFORMANCES OF HPHES 107

6.2 HPHE DESIGN MODEL 114

6.2.1 Computer Program Design 114
6.2.2 Computer Program Notes 114
6.2.3 Case Study 119

CHAPTER 7 CONCLUSIONS AND RECOMMENDATIONS FOR FURTHER WORK 121

7.1 CONCLUSIONS 121
7.2 EXPERIMENTAL INVESTIGATION 124
7.3 SUGGESTIONS FOR FUTURE WORK 124

REFERENCES 126

LIST OF FIGURES

		Page
Figure 2.1	A heat pipe with capillary structure	8
Figure 2.2	The thermosyphon and heat pipe	9
Figure 2.3	Experimental results of heat-transfer coefficient of heat pipe	14
Figure 2.4	Sketch of evaporative heat-transfer mechanism for groove wicks	15
Figure 2.5	Experimental results of fully-developed boiling in thermosyphon	19
Figure 2.6	Frictional coefficients for laminar flow	24
Figure 2.7	The functions f_1 and f_3 in the correlation for the CCFL	28
Figure 2.8	Experimental results of thermal performance of heat pipe with and without wicks	31
Figure 2.9	Experimental results of HPHE thermal performance test	34
Figure 3.1	Thermal resistance model	41
Figure 3.2	Heat-transport limitations of a heat pipe	48
Figure 3.3	Flow chart for Heat Pipe and Thermosyphon Thermal Performance Model	56
Figure 3.4	Example of Heat Pipe and Thermosyphon Thermal Performance Model	59
Figure 3.5	Example of comparison results using the computer model	60
Figure 4.1	Schematic drawing of the experimental apparatus	65
Figure 4.2	Photograph of the experimental apparatus	66
Figure 4.3	Thermosyphon test apparatus	68
Figure 4.4	Cross section of evaporator	70
Figure 4.5	Longitudinal cross section of the vapour temperature probe	70
Figure 4.6	Schematic drawing for test tube evacuation and filling	71
Figure 5.1	Working-fluid temperature variations	76

Figure 5.2 Wall-temperature variations 82

Figure 5.3 Heat-transfer coefficient in the condenser, evaporator film section, and evaporator pool 88

Figure 5.4 Comparison between experimental results and analytical predictions for the heat-transfer coefficient 92

Figure 5.5 Comparison between experimental results and analytical predictions for the thermal resistance 98

Figure 5.6 The effects of hydrostatic pressure in the evaporator pool 105

Figure 5.7 Comparison between reference and the computer model 106

Figure 6.1 Schematic diagram of HPHEs 108

Figure 6.2 Geometry of cross-flow tube arrays 110

Figure 6.3 Variation of average Nusselt number with Reynolds number for in-line and staggered tube banks 113

Figure 6.4 Correction factor F_2 113

Figure 6.5 Flow chart for the HPHEs Design Model 116

Figure 6.6 Example for the HPHEs Design Model 118

Figure 6.7 The case study of HPHEs Design Model 120

Figure 7.1 Comparison between thermal performances of thermosyphon and heat pipes in HPHEs 122

Figure 7.2 The effect of thermal performances of a single thermosyphon and grooved-wick heat pipe on the overall performances of HPHEs 123

LIST OF TABLES

		Page
Table 2.1	Typical operating characteristics of heat pipes	11
Table 3.1	Heat pipe thermal resistances	43
Table 3.2	Order of magnitude of thermal resistances for a water heat pipe	44
Table 3.3	Thermosyphon thermal resistance	46
Table 3.4	Comparison of thermal resistances	47
Table 3.5	Related equations for capillary limitation	50
Table 3.6	Thermophysical properties of saturated water	133
Table 4.1	Specification for test apparatus	67
Table 4.2	Experimental procedure	72
Table 5.1	Experimental results of steady-state temperature distribution	140
Table 6.1	Values of a and m	111
Table 6.2	Tube arrays commonly used in heat exchangers	112
Table 6.3	Thermophysical properties of air	148

NOMENCLATURE

a	correlation constant in equation (6.14)
A	Area
B_o	Bond number
C	effective thermal conductance constant in equation (3.28)
c_p	specific heat
d	pipe diameter
F	frictional coefficient fluid fill charge ratio in equation (3.28)
f	drag coefficient
g	gravitational acceleration
h	heat transfer coefficient
J	mechanical equivalent of heat
k	thermal conductivity
K	permeability
k_e	effective thermal conductivity of liquid-saturated wick
k_p	thermal conductivity of pipe material
K_p	dimensionless pressure parameter
L	heat pipe length
m	correlation constant in equation (6.14)
$\dot{m}$	mass flow rate
M	molar mass
M_v	Mach number
n	number of grooves number of heat pipes
N	screen mesh number number of rows in the heat pipe heat exchangers

Nu	Nusselt number
p	pressure
P	pipe pitch of heat exchanger
p_a	atmospheric pressure
p_{ah}	axial hydraulic pressure
p_{cm}	maximum capillary pressure
Pr	Prandtl number
p_v	vapour pressure
$p_\perp$	hydrostatic pressure in direction perpendicular to pipe axis
q	heat flux
Q	heat flow rate
Q_c	capillary limit on heat transfer rate
$(QL)_c$	capillary heat transport factor
r	radius of cylinder
R	thermal resistance
R	universal gas constant
r_c	effective capillary radius
Re	Reynolds number
r_h	hydraulic radius
r_m	mean radius of liquid flow passage
R_v	gas constant for vapour
s	wire screen crimping factor
S	cross sectional area in the heat pipe heat exchangers
T	temperature
T_o	stagnation temperature
T_v	vapour temperature
U	overall heat transfer coefficient
UA	specific heat conductance
V	velocity

w	groove width
w_f	groove fin width
We	Weber's number
x	distance from bottom

Superscripts

n	new value during iteration
o	old value during iteration

Subscripts

a	adiabatic section
b	bulk physical properties
c	condenser cold air
d	diameter
e	evaporator
f	film
h	hot air
i	inner input
j	section notation of heat exchanger
max	maximum
min	minimum
l	liquid
o	outer output
p	pool pipe

s	surface condition
sat	saturated condition
si	sink
so	source
t	total
v	vapour
w	wick outside wall surface of heat pipe

Greek letters

α	groove aspect ratio
δ	groove fin depth
ε	wick porosity
γ	specific heat ratio
λ	latent heat of vaporisation
μ	dynamic viscosity
ν	kinetic viscosity
θ	inclination angle
ρ	density
ρ_o	vapour density at stagnation condition
σ	surface tension coefficient

CHAPTER 1 INTRODUCTION

1.1 HEAT PIPES AND THERMOSYPHONS

Heat pipes and closed two-phase thermosyphons are highly efficient heat-transfer devices utilising the continuous evaporation and condensation of a suitable working fluid for two-phase heat transport in a closed system. As one of widely considered applications of heat pipes and thermosyphons, heat pipe heat exchangers (HPHEs) offer many advantages over other types of heat exchangers for the recovery of heat from industrial gaseous waste streams in the low and medium temperature ranges. Features of HPHEs which are attractive for industrial heat recovery applications are:

- No moving parts and no small external power requirements implying high reliability.
- Cross-contamination is totally eliminated because of a solid wall between the hot and cold gas streams.
- A wide variety of sizes are available, and the unit is in general compact and suitable for all, except the highest temperature, applications.
- The HPHEs are fully reversible (i.e. heat can be transferred in either direction).
- Collection of condensate in the exhaust gases can be arranged.
- The flexibility of using different fin spacings permits easy cleaning if required.

The application of these devices fall into three main categories:

- Heat recovery in air-conditioning systems, normally involving comparatively low temperatures and duties.
- Recovery of heat from a process-exhaust stream to preheat air for space heating.
- Recovery of waste heat from process for reuse in the process (e.g. preheating of combustion air) .

Although the heat pipe is similar in some respects to thermosyphon, there is an important difference in the mechanism of condensate return. A thermosyphon relies only on gravity, whereas a heat pipe may employ several forces (such as capillary force, centrifugal force, electrostatic volume forces) for the condensate return. Therefore, the thermosyphon is ineffective in zero gravity or in case where the condensate has to be returned against gravity. In most cases of terrestrial applications, the heat pipe operate with the condenser elevated so that gravity can assist the other forces. Thermosyphons have the advantages of simplicity in construction, cheap manufacturing cost and relatively high rates of heat transfer compared with conventional heat pipes. Because of those characteristics, comparative studies concerning the behaviours of heat pipe and thermosyphon, at the same operating condition, are important for their utilisation.

The available volume of literature on heat pipes and closed two-phase thermosyphons has become very huge. The first reports on heat-pipe theory and operation were written by Cotter (1965) and Marcus (1965), and a number of other reports followed. The first heat-pipe design handbook was authored by Skrabek and Binert (1972) and published by NASA. Various books and review reports have also been written by Dunn (1982), Chi (1976), Groll (1978), Chisholm (1971), and Ivanovskii (1982). International heat pipe conferences have been held since 1973, and the respective conference proceedings contain information in the whole field of heat-pipe theory, technology and application. Although the thermal performances of single heat pipes and thermosyphons have been extensively investigated, comparative studies, at the same operating conditions, appear to be very limited. Through the literature survey, only one such a study could be traced. Consequently, much studies still remains in the field of HPHEs to select the most appropriate heat pipes (or thermosyphons) for a heat exchanger for a particular application.

The aim of this research is to investigate the heat-transfer characteristics of HPHEs employing heat pipes with and without wicks for low and medium

temperature heat recovery. The results of the present study should enable designers of waste-heat recovery systems to select the most appropriate HPHEs for a particular application.

1.2. THE PRESENT STUDY

Taking into account previous studies, the present work is focused on comparative studies between heat pipe and thermosyphon, at the same operating conditions, with the following objectives :

- Further studying the heat transfer characteristics of heat pipe and thermosyphon to obtain additional information regarding thermal performance, at the same operating conditions.
- Providing some guide-lines for HPHEs design which relate to the thermal performance of heat pipe and thermosyphon.

To achieve these objectives, both experimental investigation and analytical techniques to evaluate the heat-transfer characteristics of heat pipe and thermosyphon are needed. Through the analytical studies adopted a computer model, namely 'The Heat Pipe and Thermosyphon Thermal Performance Model', is developed. The model facilitates the prediction of the axial temperature distributions of the working fluid and the tube wall ; heat-transport limitations; and the thermal performances of thermosyphons and heat pipes with different type of wicks. An experimental investigation of the steady-state behaviour of the thermosyphon is carried out to validate the computer model. The results are compared with the corresponding predictions of the computer model developed. The influences of the fluid fill charge ratio (FFCR), heat-supply rate to the evaporator, inclination angle, and the hydrostatic pressure in the pool are discussed. The results of the behaviours of heat pipes and thermosyphons are utilised to develop a 'Heat Pipe Heat Exchangers Design Model' to facilitate both the design and the prediction of performance of HPHEs. This model should enable the designers of waste-heat recovery systems to choose the most appropriate

type of heat-transfer elements and optimise the design parameters of a HPHE for a given application.

1.3 STRUCTURE OF THE THESIS

After this introduction, a literature review is given in Chapter two. Most of the important studies and observations in this field are briefly reviewed, including thermal behaviours of heat pipes and thermosyphons and previous studies on the HPHEs. Chapter three describes the analytical studies adopted for predicting thermal performances of heat pipes and thermosyphons. These analytical studies are utilised for developing the Heat Pipe and Thermosyphon Thermal Performance Computer Model. Chapter four provides detailed design information about the thermosyphon test rig, including specifications of the cooling assembly and the heat-supplying loop. The instrumentation for measuring temperatures and other control parameters, as well as the data acquisition system are detailed. The experimental procedure and measuring techniques for the present study are also presented. In chapter five, the results of the experimental investigation of the steady-state behaviour of the thermosyphon are presented. These results are compared with the corresponding predictions from the computer model developed. The influences of the FFCR, heat-supply rate to the evaporator, inclination angle, and the hydrostatic pressure in the pool are discussed. Chapter six provides the practical uses of the present study. The results of the former study on the behaviours of heat pipes and thermosyphons are utilised to develop a 'Heat Pipe Heat Exchangers Design Model', and case studies employing this model are presented. In Chapter seven, conclusions from the present work are drawn and proposals for possible future research are made.

CHAPTER 2 LITERATURE SURVEY

Heat pipes and closed two-phase thermosyphons are highly-efficient heat-transfer devices, utilising the continuous evaporation and condensation of a suitable working fluid for the transport of heat in a closed system. Due to a variety of advantageous features, these devices have found a number of applications both in space and terrestrial technology. The heat pipe was first proposed by Gaugler (1942) of the General Motors Cooperation. Since Cotter (1965) discussed the basic heat-pipe problems, research and development on the heat pipe has been encouraged by NASA and numerous other groups. Heat pipes have been applied to the thermal control of spacecraft, air conditioning, cooling of integrated circuits etc. One of the latest heat pipe applications, which is drawing world attention, is waste-heat recovery at low and medium temperature because of their superior characteristics.

This chapter outlines briefly the development and heat-transfer characteristics of single heat pipes and heat pipe heat exchangers (HPHEs), and then reviews some of the previous research related to the present study.

2.1 HISTORIC DEVELOPMENT OF HEAT PIPES AND HPHES

Historically, the first application of gravity heat pipes (i.e. Perkins tube) was in boilers and bakeries in the 19th century. External finning of the closed two-phase thermosyphon for better heat transfer from/to gases was proposed and patented by Gay (1929). His patent describes a finned gravity HPHE operating vertically with hot air stream below and the cold air stream above. In 1938, a patent was granted in the USA which describes a tube incorporating capillary grooves to aid liquid distribution and hence vaporisation in boilers. The first patent for a heat pipe employing a capillary wick for pumping liquid against gravity was applied for by Gaugler (1942) as a two-phase heat transport device for refrigerators. It was claimed that it allows

movement of the working fluid without pumps and without natural convection, by the utilisation of the capillary force generated by a capillary wick. In connection with the US space programme, Trefethen (1962) suggested the utilisation of the surface tension pumping of liquids, and the capillary-pumping principle was independently re-invented by Grover et al. (1963) at the Los Alamos Scientific Laboratory. Grover called the device a "Heat Pipe" and characterised it in the following way: "With certain limitations on the manner of use, a heat pipe may be regarded as a synergistic engineering structure which is equivalent to a material having a thermal conductivity greatly exceeding that of any known metal". The first heat pipe built by Grover et al. (1962) used water as the working fluid. Very soon a sodium heat pipe was investigated. Lithium and silver as working fluids followed. In the following years, investigations of ambient-(or low-) temperature and high-temperature heat pipes met with world-wide interest. The first cryogenic heat pipe was developed by Haskin (1966). The use of a heat pipe as a temperature-control element was first described in a patent application by Hall (1964) of the Radio Cooperation of America. The theoretical basis and technological development for temperature-controlled or variable- conductance heat pipes was advanced especially by Bienert (1971) and Brennan (1971). The first zero-gravity demonstration of a water heat pipe was conducted by Deverall et al. (1967) of the Los Alamos Scientific Laboratory. Today, heat pipes have become a standard thermal element in satellite technology. It took more time to find terrestrial applications for heat pipes. The first application was developed by the Radio Corporation of America for the cooling of transistors. Sooner, heat pipes have found wide applications in the cooling of electronic devices and especially as elements for devices (i.e. HPHEs) to recover thermal energy from hot waste gases. Although HPHEs have been in production for less than a decade, a review of manufacturers' literature and published studies on their development and use has indicated a very wide range of applications in industry. The general application areas for HPHEs are covered by most gas to gas systems.

The available volume of literature on heat pipes and closed two-phase thermosyphons has become very huge. The first reports on heat-pipe theory and operation were written by Cotter (1965) and Marcus (1965), and a number of other reports followed. The first heat-pipe design handbook was authored by Skrabek and Binert (1972) and published by NASA. Various textbooks and review reports have also been written by Dunn (1982), Chi (1976), Groll (1978), Chisholm (1971), and Ivanovskii (1982).

International heat pipe conferences have been held since 1973, and the respective conference proceedings contain information in the whole field of heat- pipe theory, technology and application.

2.2 HEAT-TRANSFER CHARACTERISTICS OF HEAT PIPES

Among the many outstanding advantages of using the heat pipe as a heat-transmission device are : constructional simplicity, exceptional flexibility, accessibility to control, ability to transport heat at high rates over considerable distances with extremely-small temperature drops, and non requirement of external pumping power. Moreover, they can operate in zero-gravity environment and against gravity. Figure 2.1 presents a schematic drawing showing the classical heat pipe with capillary structure. A circular pipe has a layer of wicking material covering the inside surface, with a hollow core in the centre. A condensible fluid is also contained in the pipe, and the liquid permeates the wicking material by the capillary action. When heat is added to one end of the pipe (i.e. the evaporator), the liquid in the wick is vaporised and the vapour moves to the central core. At the other end of the pipe (i.e. the condenser), the heat is removed and the vapour condenses back into the wick. The liquid is replenished in the evaporator section by the capillary action. Another thermal device, having a similar function to that of heat pipe, is the thermosyphon (or "wickless heat pipe").

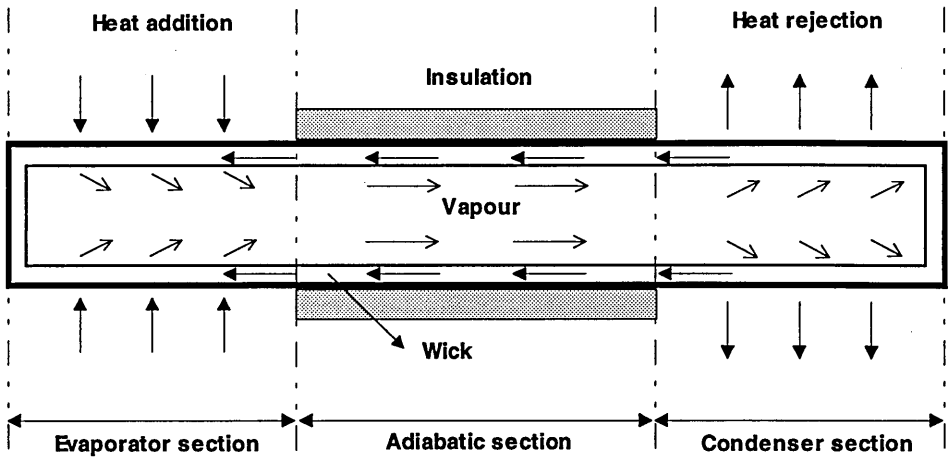

Figure 2.1 A heat pipe with capillary structure

The main difference is the mechanism of condensate return ; a thermosyphon relies on only gravity, whereas a heat pipe may employ several forces (such as capillary force, centrifugal force, electrostatic volume forces) for the condensate return.

In case of thermosyphon (see Figure 2.2), a small quantity of water is placed in a sealed tube from which the air is evacuated. When the lower end of the tube is heated the liquid vaporises and the vapour moves to the upper cold end of the tube where it condenses. The condensate is returned to the hot end by gravity. Since the latent heat of vaporisation is large, considerable quantities of heat can be transported with a very small temperature difference from end to end. Thus the structure will have a high effective thermal conductance. The thermosyphon has been used for many years and various working fluids have been employed. One of the serious limitations of the basic thermosyphon is that in order for the condensate to be returned to the evaporator region by gravitational force, the evaporator must be situated at the lowest point. In the heat pipe, however, the evaporator position is not restricted, and the pipe may be used in any orientation.

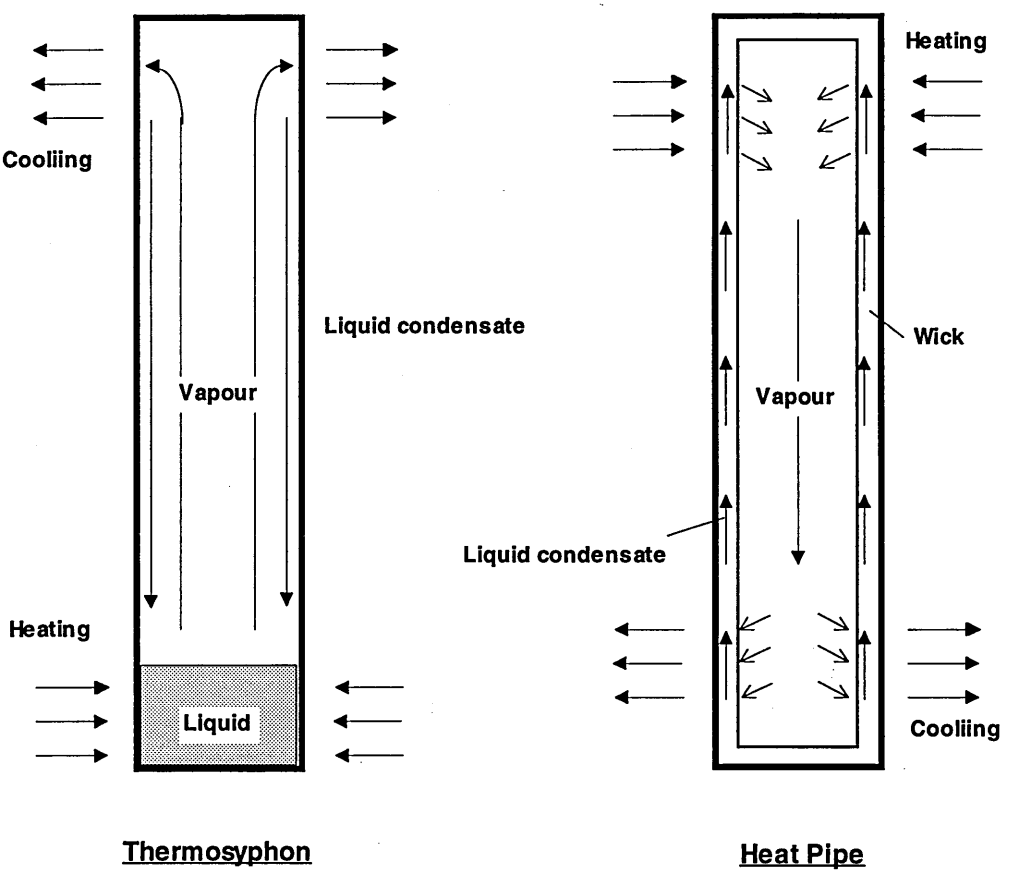

Figure 2.2 The thermosyphon and heat pipe

If the heat-pipe evaporator happens to be in the lowest position, gravitational forces will assist the capillary forces. Therefore, the thermosyphon is ineffective in zero gravity or where the condensate has to be returned against gravity. However, the thermosyphons have the advantages of simplicity in construction and cheap manufacturing cost compared with heat pipes, as well as relatively high rates of heat transfer compared with conventional types of heat pipes. The circulation of the working fluid is an important parameter in the operation of heat pipes and thermosyphons. The maximum possible circulation is required to obtain the maximum heat- transport capability. In the case of a heat pipe, the limitations on the heat transport capability include capillary pumping ability (i.e. capillary limitation), choking of vapour flow (i.e.

sonic limitation), tearing of liquid off the liquid-vapour interface by vapour flowing at high velocity (i.e. entrainment limitation), and disruption of the liquid flow by nucleate boiling in the wick (i.e. boiling limitation). In the case of a thermosyphon, three different performance-limitation phenomena can occur depending on operating conditions. A dry-out limitation can occur at comparably low filling of working fluid and the boiling (or burn-out) limitation appears under high radial heat fluxes in the evaporator section. If, under high axial heat fluxes, the high-velocity vapour flow from the evaporator to the condenser intensively interacts with the counter-current condensate flow, a counter-current flow limitation (CCFL) can occur. Additional factors that affect heat pipe thermal performance is the interface conditions between the heat pipe and its external heat source and sink. Practical designs of heat pipes employ a variety of working fluids, and pipe and wick materials according to the operating temperature. Some typical operating characteristics are summarised in Table 2.1.

2.3 REVIEW OF PREVIOUS WORK ON HEAT PIPE AND HPHES

2.3.1 Previous Studies on Characteristics of Heat Pipes

Laws of fluid mechanics and heat transfer have been used to establish the theory for predicting heat-transport limitations and other thermal performance phenomena of the heat pipe. The first heat pipe theory, dealing mainly with the capillary limitation and temperature characteristics, was put forward by Cotter (1965). The sonic limitation theory has been advanced by Levy (1968) and Kemme (1969). Kemme (1969) also discussed the theories of entrainment limitation and boiling limitation. Analysis of the controlled heat pipes has been treated in some detail by Binert (1969) and Marcus (1971). Theoretical models for the performances of heat pipes and thermosyphons were also proposed by Binert (1969), Skrabek (1972), Chi (1971), Marcus (1972), Winter (1971) and Barsch (1971).

Table 2.1 Typical Operating Characteristics of Heat Pipes, Dutcher (1970)

Temperature Range (°C)	Working Fluid	Vessel Material	Measured Axial Heat Flux [a] (kW/cm^2)	Measured Surface Heat Flux [a] (W/cm^2)
-200 to -80	Liquid Nitrogen	Stainless Steel	0.067 (at -163°C)	1.01 (at -163°C)
-70 to 60	Liquid Ammonia	Nickel, Aluminum and Stainless Steel	0.295	2.95
-45 to 120	Methanol	Copper, Nickel and Stainless Steel	0.45 [b] (at 100°C)	75.5 (at 100°C)
5 to 230	Water	Copper and Nickel	0.67 (at 200°C)	146 (at 170°C)
190 to 550	Mecury + 0.02%	Stainless Steel	25.1 [c] (at 360°C)	181 (at 360°C)
400 to 800	Potassium	Nickel and Stainless Steel	5.6 (at 750°C)	181 (at 750°C)
500 to 900	Sodium	Nickel and Stainless Steel	9.3 (at 850°C)	224 (at 760°C)
900 to 1500	Lithium	Niobium + 1% Zinconium	2.0 (at 1250°C)	207 (at 1250°C)
1500 to 2000	Silver	Tantalum + 5% Tungsten	4.1	413

a : Varies with temperature

b : Using threaded artery wick

c : Tested at Los Alamos Scientific Laboratory

Although the thermal performances of single heat pipes and thermosyphons have been extensively investigated, comparative studies concerning behaviours of HPHE with different types of heat pipes, at the same operating conditions, appear to be very limited. Such studies are useful in evaluating the significance of the parameters pertinent to thermal performance and in selecting the most appropriate HPHE for a particular application.

(a) Heat-transfer characteristics and thermal behaviour

The thermal behaviours of heat pipes and thermosyphons were developed initially during 1960's. Since then, further researches were carried out to evaluate the temperature variations and thermal performances in the evaporating part, the condensing part, and the overall heat-transfer performance of heat pipes. These characteristics have been investigated as function of the properties of the working fluid, wick specifications, container material and dimensions, fluid fill charge ratio, and inclination angle.

Heat pipe

The heat transfer characteristics of heat pipes were discussed by Chi (1976). According to him, the primary mechanisms of heat transfer in heat pipes are;

- heat conduction across the pipe wall and the liquid-saturated wick, at the evaporator section, with subsequent evaporation at the liquid-vapour interface of that section ;
- axial convective transport of latent heat by vapour from the evaporator to the condenser section ; and
- heat conduction across the liquid-saturated wick and the pipe wall at the condenser with subsequent condensation at that section.

The earliest study on the effective thermal conductivity of wicks was conducted by Gorring, et al. (1961). They formulated several heat transfer models for heterogeneous materials, most of which could be modified for application to liquid-saturated wicks. Their simple equation for effective thermal conductivity can be used for series or parallel arrangements of liquid

saturated wick structures. The exact solutions for in series or in parallel are, respectively,

$$k_e = k_l k_w / [\varepsilon k_w + k_l (1-\varepsilon)] \quad (2.1)$$

$$k_e = \varepsilon k_l + (1-\varepsilon) k_w \quad (2.2)$$

Larkin (1982) carried out an experimental study on a heat pipe to be used as a component in an air-to-air heat-recovery heat exchanger. Water and refrigerant 22 were employed as alternative working fluids in tubes with smooth inner surfaces and the surfaces with circumferential capillary grooves. The results showed that the modification of the surface can significantly change the heat-transfer performance (see Figure 2.3). In the case of water, bubble formation was proved difficult at comparatively low pressures. However, the grooves improved the evaporating heat-transfer coefficient. In the case of refrigerant 22, the smooth surface resulted in poor condensing heat transfer, and the results for a grooved surface were much higher. According to this study, when choosing a fluid, both the evaporating and condensing heat-transfer coefficients must be considered. Their relative importance depends to some extent on the relative lengths of the evaporating and condensing sections. Boiling heat transfer in a water-filled heat pipe was investigated by Ambrose et al. (1985) with the objective of relating the heat flux and temperature drop across the evaporator. Nucleate boiling was postulated as the heat-transfer mechanism at and near the wall. Rosenfeld (1987) presented a general model for heat-transfer to a heat pipe using a localised heat input. Conduction through the wall of the heat pipe and boiling in the interior structure were treated simultaneously. The model was derived from circumferential heat transfer in a cylindrical heat pipe evaporator and for radial heat transfer in a circular disc with boiling from the interior surface. This model can be used for design purposes if a boiling correlation is available and can be extended to provide improved predictions for the performances of heat pipes. Ikeda, et al. (1988) measured the effective thermal conductivity of screen wicks. For a screen wick containing a working fluid, this was found to be affected by the porosity of the wick.

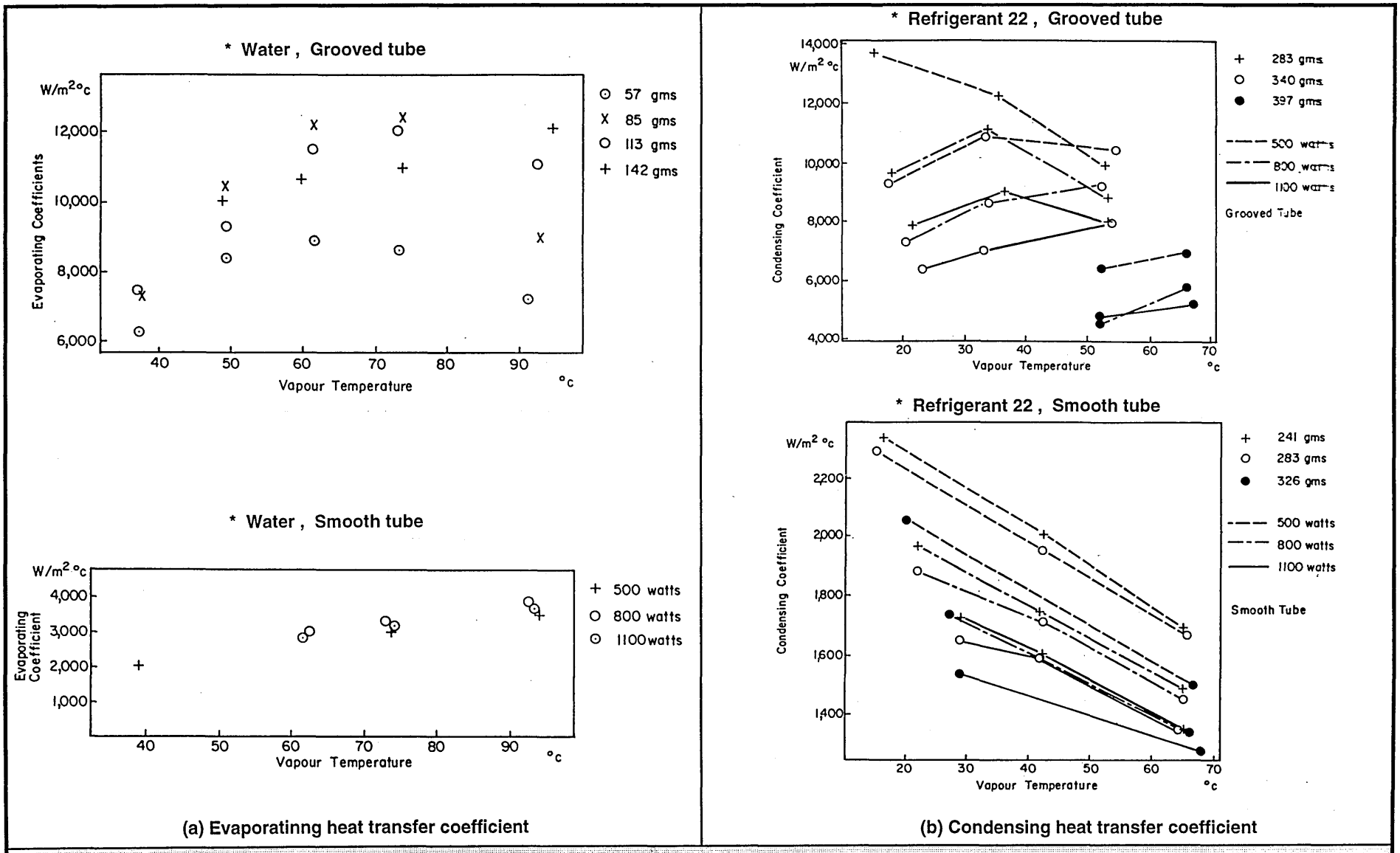

Figure 2.3 Experimental results of heat transfer coefficient of heat pipe (Larkin, 1982)

The effective thermal conductivity of a screen wick was the parameters of wire diameter, mesh number, coefficient of shrinkage, and inter-layer clearance. A similar study was performed by Imula et al. (1988). A horizontal planar heat pipe was employed, and the value of the effective thermal conductivity was calculated from the heat-transfer coefficient in the condenser of the heat pipe. They concluded that the thickness and porosity of multilayer screen wicks had to be estimated accurately by taking into account the intermeshing between screen layers.

One of the widely-used homogeneous wick is the grooved wick because of its good heat-transfer characteristics. Chi (1972) reported that for a grooved wick at the evaporator, and he concluded that the heat travels ;

- directly through the liquid film ; and
- through a series path consisting of the groove fin and a thin film of liquid adjacent to the tip of the liquid-fin interface (see Figure 2.4).

He presented a following correlation of the second path for estimating the film heat-transfer coefficient for the liquid-fin interface as a function of the fin width.

$$k_2 = k_l k_w \delta / (0.185 w_f k_w + \delta k_l) \qquad (2.3)$$

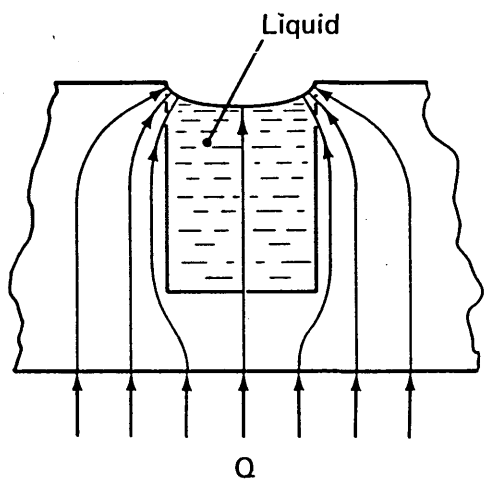

Figure 2.4 Sketch of evaporative heat-transfer mechanism for groove wicks (Chi, 1972)

Vasilev et al. (1981) performed an experimental study on a low-temperature, axially-grooved heat pipe to predict its characteristics, including its thermal

resistance, at zero gravity as well as for terrestrial applications. They proposed a criteria for maximising the rate of heat transfer based upon the amount of the working fluid and the heat-pipe inclination angle. Grakovich et al. (1988) also presented engineering formulae for calculating the overall coefficients of heat transfer in low-temperature, gravity-assisted heat pipes with rectangular axial grooves, which describes the heat transfer between the outer surface of the pipe and the saturated vapour in the vapour channel. Khrustalev et al. (1995) developed a mathematical model that describes heat transfer through thin liquid films in the evaporator of heat pipes with capillary grooves. The model accounts for the effects of interfacial thermal resistance, disjoining pressure, and surface roughness for a given meniscus contact angle. In their work, the importance of the surface roughness and interfacial thermal resistance in predicting the heat transfer coefficient in the grooved evaporator was demonstrated. Stephan et al (1992) also presented a model for the radial heat transfer of a grooved heat-pipe evaporator. They combined the solution of a two-dimensional heat conduction problem with the calculation of the shape of the liquid-vapour interface and its temperature, which takes into account the influence of meniscus curvature and adhesion forces on the volatility of the liquid. They demonstrated that the common assumption of an interface temperature equal to the saturation temperature of the vapour can lead to a large overestimation of the radial heat- transfer coefficient. Shishido et al. (1985) used two types of heat pipe to measure the axial saturation distribution of the working fluid in a heat pipe wick. For a horizontal heat pipe, it was found that the saturation distribution of the working fluid varies with heat input, the type of wick material, and the charge of working fluid. For an inclined heat pipe, the working-fluid saturation distribution depends also on the inclination angle. The effects of inclination angle on the transient operation of a gravity-assisted copper-water heat pipe was investigated experimentally by El-Genk et al. (1995). The heatup and cooldown time constants were used to assess the effect of the inclination angle at different power input and cooling rates. The experimental data of the transient vapour and wall temperatures and the effective power throughput

were used to benchmark a two-dimensional, heat-pipe transient analysis model.

Miyasaka (1995) assessed experimentally the heat-transport characteristics of capillary looped pipes. These heat pipes were tested to determine the flow direction of the vapour and the relationship between the quantity of fluid charge and the operating temperature. It was found that the flow regime changes when the heat density increase.

Thermosyphon

Shiraishi et al. (1981) conducted a series of test to evaluate the heat-transfer characteristics of a two-phase closed thermosyphon. In this study, the effects of the working fluid and its amount, the operating temperature and the heat flux were investigated. The heat-transfer coefficients at the condenser and the evaporator were estimated. By utilising the experimental results, a simple mathematical model was developed. Film condensation along the inside surface of the condenser, and evaporation from a liquid film above the pool and boiling of the liquid pool in the evaporator were considered as the heat-transfer mechanisms in the thermosyphon. Cheng et al. (1985) examined the steady- state operation and the heat-transfer characteristics of a closed two-phase thermosyphon for low-grade energy recovery. The working fluid was water and the tests were performed by varying the operating parameters (i.e. initial liquid-charge level, heat-source temperature, and cooling water flow rate). A maximum heat-transfer effectiveness of 40% was achieved. Gross et al. (1986) conducted an important study on the heat-transfer in a closed thermosyphon over a wide range of pressures and inclination angle. The mean evaporation heat -transfer coefficients were found to be strongly affected by pressure, but hardly at all by the angle of inclination. Condensation heat-transfer coefficients depend both on pressure and inclination, showing the characteristics of either a laminar or a turbulent condensate film. It was concluded that the overall performance of the thermosyphon results from the overlapping of the processes in the heating and cooling zones.

Imura et al (1973) proposed the following empirical correlation in the liquid pool which is based upon dimensional analysis.

$$h_p = 0.32\ [\ (\rho_l^{0.65} k_l^{0.3} c_{pl}^{0.7} g^{0.2})\ /\ \rho_v^{0.25} \lambda^{0.4} \mu_l^{0.1}\ ]\ (p_v / p_a)^{0.23}\ q_e^{0.4} \qquad (2.4)$$

Leidenfrost et al. (1987) performed a flow visualisation investigation of boiling heat transfer in a two-phase thermosyphon under various flow conditions and loop orientations. The results obtained agree very well with pool-boiling data. This indicates that the liquid motion induced in the boiling liquid under unstable and stable flow conditions does not influence measurably the heat-transfer process. Pioro et al. (1987) calculated the limiting heat flux for a liquid boiling in a two-phase thermosyphon. In this study, theoretical formulae from various sources were also examined. Boiling heat-transfer in the evaporator of thermosyhons studied experimentally by O-uchi et al.(1988). The occurrence of nucleate boiling in both the liquid film and the pool side was confirmed. As a result of the nucleate boiling in the liquid film, and because the heat-transfer performance is dependent upon the nucleate-boiling heat transfer coefficient, the capability of the thermosyphon has improved. However, the occurrence of a dry-out condition had a negative effect on the performance of the system. The heat-transfer coefficient for pool boiling within the heating zone of a two-phase closed thermosyphon was estimated by Bartsch et al. (1990). Typical empirical correlations describing the influence of the heat flux on the heat-transfer coefficient were verified analytically by applying the laws of thermodynamics. Niro et al. (1990) presented experimental results and an analytical model on the boiling mechanisms in a closed two-phase thermosyphon in order to define the frontiers between the main boiling regimes, particularly, between intermittent boiling and fully-developed boiling (see Figure 2.5). The boiling regimes were classified on the basis of the frequency of bubble nucleation and the ratio of bubble diameter to the pipe diameter. The criterion employed for defining the intermittent / developed-boiling frontier was based on the ratio of the bubble-nucleation waiting time and the bubble-growth time.

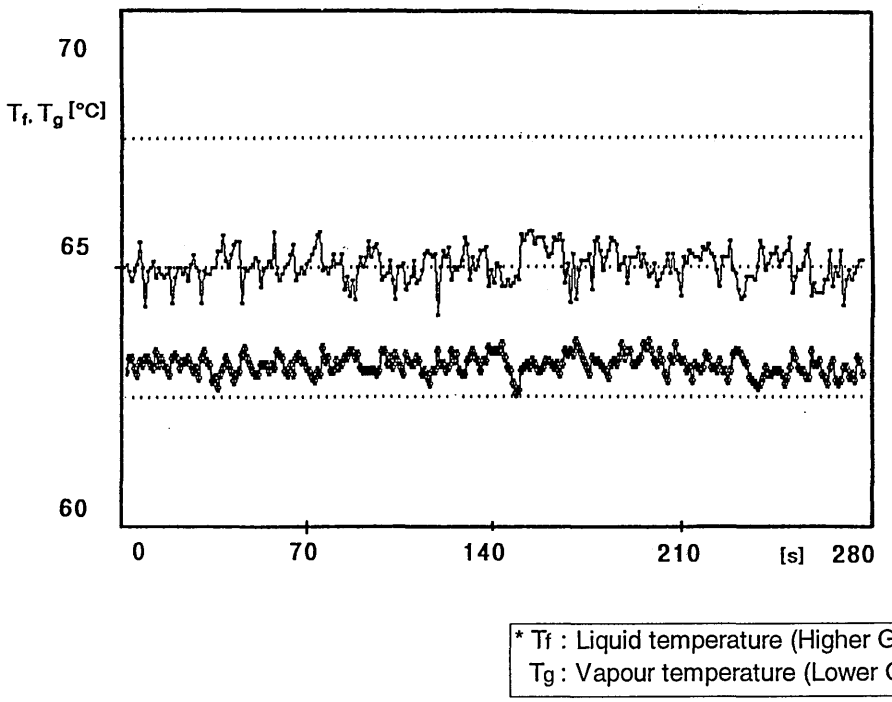

Figure 2.5 Experimental results of fully-developed boiling in thermosyphon (Niro, 1990)

Niro et al. developed a correlation between the power throughput, working-fluid pressure and nucleation critical superheat. Experimental data showed the same functional dependence as the proposed correlation.

Pande et al. (1990) also studied boiling in thermosyphon evaporators. This work was aimed at improving the design and operation efficiency of thermosyphon evaporators. Previous operating experience and research in two-phase systems revealed that boiling, accompanied by two-phase flow, was highly affected by the flow dynamics and stability of the system. The experimental results of Pande et al. revealed the effects of design parameters and operating variables on the thermo hydraulic performances of thermosyphon evaporators.

In addition to the study of boiling, the condensation process in thermosyphons was also investigated. Yiwei et al. (1989) studied condensation heat-transfer in vertical and inclined thermosyphons theoretically and experimentally. They took into account both vapour friction

and the inclination angle of a thermosyphon and presented a laminar film-condensation model. Li et al. (1996) also carried out condensing heat transfer in an two-phase closed thermosyphon. In their work, the heat-transfer performance of the closed thermosyphon was studied and a mathematical model for condensing heat transfer in a narrow annulus was developed based on Nusselt condensing heat-transfer model.

Al-Farah et al. (1991) examined the film condensation in tilted, two-phase thermosyphons by solving the governing equations. The azimuthal and axial distributions of the film thickness as functions of the tilt angle were determined. Unlike previously-reported results, their numerical solutions show that tilting the thermosyphon can result in either an increase or a decrease in the azimuthally-axially averaged film thickness. In addition to the study of boiling and condensation, numerical model for predicting the behaviours of thermosyphons have also been proposed. Reed et al. (1987) developed a comprehensive model to predict the steady-state and transient performance of the two-phase closed thermosyphon. The one-dimensional governing equations for the liquid and vapour phases were developed using available correlations for the shear stress and heat-transfer coefficients. Steady-state solutions agree well with data from several sources. Casarosa et al. (1988) investigated experimentally a closed two-phase thermosyphon, employing refrigerant-11 as the working fluid, and with imposed convection boundary conditions at the heated and cooled surfaces. They modelled the system analytically with a lumped-parameter model. The thermosyphon exhibited different operational modes depending on the heating and cooling fluids' temperature difference. An increase in this temperature difference produced at first a maximum heat transfer rate identifiable with the flooding heat-transfer limit. Beyond this limit, the thermosyphon operation reverted to a different steady-state through a transient non-equilibrium process. The new steady state, identified as the thermal blocking condition, produced a lower heat-transfer capacity. Zuo et al. (1994) modelled the steady-state performance of a two-phase closed thermosyphon. In their model, numerical techniques were incorporated to solve the non-linear governing equations

and respective boundary conditions. The parametric effects of operating temperatures, geometry, working-fluid inventory and condenser thermal-capacity were also studied. This model presented could be used for the optimisation of the design of a thermosyphon. Zuo et al. (1995) also presented a numerical model for an inclined-thermosyphon performance. They concluded that the behaviour of a thermosyphon relates to two important limiting mechanisms, the dry-out and flooding. The inclination - induced circumferential flow is unfavourable with respect to the dry-out because the thin top-side liquid film is easier to boil off, but, on the other hand, is favourable with respect to flooding because the thick underside film corresponds to a large gravity force. Minimum working-fluid inventory remains almost constant for a large range of inclination angles (i.e. between zero and 70°) and then significantly increases for any further increase in the inclination angle. At a certain inclination angle, the mean heat-transfer coefficient of the thermosyphon reaches a maximum value, which is related to the heat-transfer behaviour in both condenser and evaporator. The highest flooding limit is at an inclination angle in the range from 30 to 45°, which corresponds to the best balance of the two opposing effects: secondary circumferential flow and gravity reduction.

(b) Heat-transport limitations

The physical processes occurring during the operation of heat pipes (or thermosyphons) impose a number of constraints on their operating parameters. These constraints, which determine the maximum heat-transfer rate and fix the range of parameters for achieving normal working of the pipes, are going to be considered. Factors which limit the heat transfer in heat pipes are:

- Attainment of the speed of sound by the vapour flow in some part of the pipe, usually at the start of the condensation zone.
- The ability of a given capillary structure to provide circulation of the given medium only up to a certain limit.

- Friction in the vapour phase at low temperatures limiting the circulation of the medium and thus leading to the occurrence of a viscous limitation.
- Entrainment of liquid from the wick in the vapour stream.
- Boiling of the medium and other effects lead to critical phenomena and to a limitation of the heat flux.
- The possibility of carrying the heat away from the pipe.

Studies of these limitations in both heat pipes and thermosyphons are reviewed in the following two subsections.

Heat pipe

Since the effect of the capillary limitation on the performance of a heat pipe was suggested by Cotter (1965), further studies were carried out to evaluate the capillary limitations of heat pipes.

The capillary limitation of a heat pipe is dictated principally by the permeability of the wick and this permeability varies widely as a function of the wrap tightness in case of screen wicks. For a loosely-wrapped wick, permeability can be approximated by a series of parallel annular passage. Experimental data on the tightly-wrapped screen wicks were presented by Marcus (1972). He correlated the results via a modified Blake-Kozeny equation as follows;

$$K = d^2 \varepsilon^2 / [\, 122\, (1-\varepsilon)^2 \,] \qquad (2.5)$$

The permeability of screen wicks was also studied by Noda et al. (1991). They expressed the permeability as a function of the hydraulic diameter, and the product of the friction factor and the Reynolds number. The hydraulic diameter was defined in the terms of the wire diameter and porosity of the screen wick. The friction factor was evaluated experimentally since it is influenced by the specifications of the screen and wick thickness. The value of the friction factor decreased with the increase of the porosity and varied with the ratio of the wick thickness per layer. Kays (1966) presented solutions of laminar-fluid flow in rectangular passages showing the relationship between friction coefficient and the passage aspect ratio (see

Figure 2.6). These solutions give for calculating permeability in the rectangular grooved wick by using known aspect ratio and porosity. He also presented solutions for the friction coefficient in circular annular flow passage. Imura et al. (1987) predicted heat-transfer coefficients and maximum heat-transfer rates due to the capillary limitation in horizontal heat pipes using water as the working fluid. Another investigation on capillary limitations on screen-wick heat pipes was conducted by Noda et al. (1987). The effects of inclination angle, number of layers and the evaporator length on the heat-transfer limit were determined by using a planar heat pipe. An analysis was performed to predict the heat- transfer limit assuming a linear relationship between the receding of the liquid-vapour interface and the capillary pressure. The effective pore (or capillary) radius of a screen wick is an important factor for the prediction of maximum heat-transfer rates due to capillary limitation. Kozai et al (1990) derived an equation for the effective pore radius based on screen geometry.

Levy (1968) first derived an following equation (i.e. Levy's equation) for calculating the maximum heat-transport rate in a heat pipe, at its sonic limit, which occurs when the vapour velocity at the evaporator exit is sonic (i.e. when the Mach number at the evaporator exit is unity).

$$Q_{s,max} = A_v \rho_o \lambda \left[\rho_v R_v T_o / 2 (\gamma_v + 1)\right]^{1/2} \qquad (2.6)$$

Deverall et al. (1970) also presented equations for sonic limitation. Silverstein (1985) developed correlations for the sonic limit, entrainment limit, and boiling limit of heat pipes as simple power-law functions of the pressure of the heat-pipe vapour. The maximum heat-transfer rates, calculated using these correlations, agree very well with the values obtained using the actual heat-transport limit equations. Kemme (1967) detected the phenomenon of entrainment in heat-pipe tests, by monitoring the sounds made by liquid droplets striking the condenser end of the heat pipe and through the abrupt overheating of the evaporator, and discussed the theory of entrainment limitation.

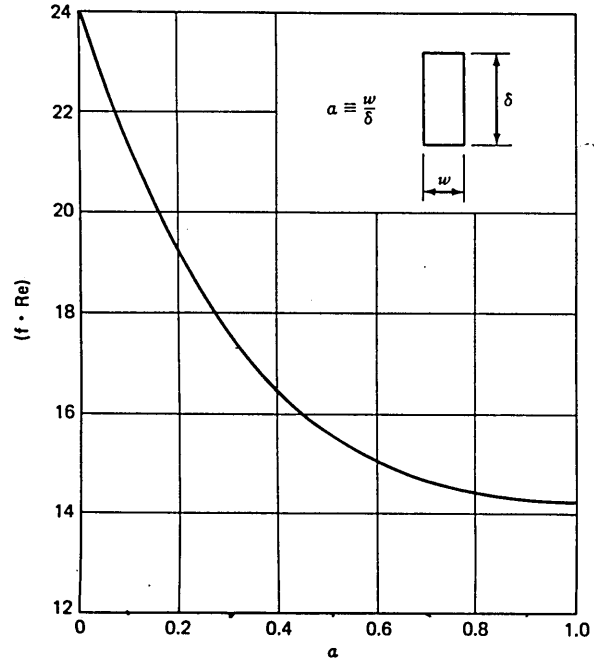

(a) Rectangular tubes

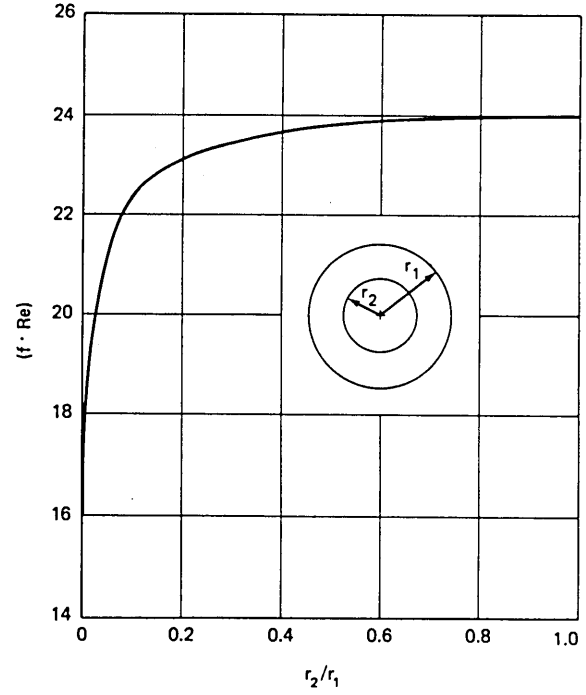

(b) Circular annuli

Figure 2.6 Frictional coefficients for laminar flow (Kays , 1966)

He and Coyne (1981) also carried out experiments with gravity assisted heat pipes employing simple wick structures in order to arrive at a correlation which could be used to predict the entrainment limits. This work led to the conclusions that the entrainment limits are vapour-dominated and are essentially independent of the fluid inventory. The entrainment limits were successfully correlated in terms of a critical Weber number and the correlation can be written as

$$Q_{e,max} = A_v \lambda [\sigma \rho_v / 2 r_{h,s}]^{1/2} \quad (2.7)$$

Tien et al. (1978) presented equations which enable the user to predict the maximum heat-transfer rate due to the entrainment limitation. Some experimental data, for gravity-assisted wicked heat pipes, horizontal heat pipes, grooved heat pipes, and rotating heat pipes, suggested that the equations give accurate results. Peterson et al. (1991) developed entrainment-modelling techniques. A review of the analytical methods, used to predict the liquid entrainment as a function of the pipe's physical parameters and working-fluid properties was included in their study. Analysis of the boiling limitation involves the theory of nucleate boiling. According to Griffith et al.(1958), nucleate boiling is very dependent on the heated surface, and factors such as the release of absorbed gas, surface roughness, surface oxidation and wettability greatly effect the surface to bulk liquid temperature difference. A useful correlation, applicable to water and organic liquids was developed by Rohsenhow (1955). In his model, he considered the convective heat transfer due to vapour bubbles.

$$q / (\lambda \rho_v) = 0.012 [(\rho_l - \rho_v) / \rho_v]^{0.6} \quad (2.8)$$

An important parameter, used when evaluating boiling limitations is the nucleation radius of the vapour bubbles. Griffith et al. (1959) carried out nucleation experiments involving immersing copper sheets in water. The results indicated that the nucleation radius varies from 2.54×10^{-3} to 2.54×10^{-2} mm. However, the results of such experiments, conducted at atmospheric pressure, are affected by the presence of dissolved noncondensible gases in the water. In the absence of noncondensible

gases, the nucleation radius can be orders of magnitude smaller. For a conventional heat pipe, which has been carefully processed to eliminate all noncondensible gases, nucleation radii of the order of 2.54×10^{-5} to 2.54×10^{-4} mm have been observed (Marcus, 1972). Dry-out characteristics of heat pipes were analysed by Kuramae et al. (1985). They developed a simple model for heat pipes having capillary wicks to study the effect of axial heat conduction.

Thermosyphon

The three most important performance-limitation phenomena are the dry-out, burn-out and count-current flow limitation (CCFL). The dry-out limitation usually can be avoided by selecting a sufficient fluid fill charge ratio for the thermosyphon. Takuma et al. (1986) studied the dry-out limitation in an annular thermosyphon . A simple analytical model, based on a mass-flow balance over a control surface in the evaporator, was developed taking into account evaporation and droplet generation due to nucleate boiling inside the condensate film. The following model resulted in an implicit correlation between the radial dry-out heat flux, fluid properties, the heated length of the evaporator and the working-fluid fill charge ratio.

$$F = 1 - \frac{1}{1 + C \{ [q_{max} / \lambda^2) (2\sigma \rho_v)] [3 q_{max} \mu_l L_e) / (\rho l (\rho_l - \rho_v) g \lambda)]^{1/3} \}^{3/4}} \qquad (2.9)$$

Lienhard et al. (1973) developed a simple correlation for the burn-out limitation. The following equation applies only for pool boiling, (i.e. in the lower regions of the evaporator).

$$Q_{max} = 0.12 \pi d_e L_e \lambda (\rho_v)^{1/2} [\sigma g (\rho_l - \rho_v)]^{1/4} \qquad (2.10)$$

A large number of analytical models, for the study of CCFL, are available. These were partly developed from work on the flooding phenomenon, and partly generated in the context of research on thermosyphon. A correlation for the CCFL was presented by Berenson (1962). According to his study, the CCFL heat flux can be expressed in terms of the three functions f_1, f_2, and f_3,

where f_1 is a function of the Bond number, f_2 is the function of a dimensionless pressure parameter. and f_3 is a function of the inclination angle of the thermosyphon and the Bond number (see Figure 2.7). Much of the experimental evidence, on the performance of thermosyphons, indicate that the maximum heat-transport capability occurs when the thermosyphon is at 60° to 80° to the horizontal (Groll,1989 and Terdtoon, 1990). The amount of liquid is governed by two considerations; too small a quantity can lead to dry-out, whereas an excess of liquid can lead to quantities being carried up to the condenser, where blockage of surface for condensation can result. Bezrodnyi et al. (1977) recommended that the liquid fill should be at least 50% of the volume of the evaporator. Dobran (1985) presented an analytical investigation for determining the steady-state characteristics and stability thresholds of a closed two-phase thermosyphon. The analytical model is based on a lumped-parameter description of the system that includes the thermohydraulics of vapour core, liquid film, and liquid pool of the evaporator. The steady-state solutions and the linear stability analysis of the governing equations revealed the existence of two operating limits: one associated with flooding and the other with drying of the liquid in the evaporator. A parametic study was also performed to determine the effects of heat pipe geometry, liquid filling, and fluid characteristics on the operating limits. Pioro (1985) carried out an experimental study on the boiling patterns in the thermosyphon evaporator over a wide range of heating fluxes. He derived an equation for determining the maximum heat-flux, which is applicable over a wide range of geometries, operating conditions, and working fluids. Tu et al. (1985) performed some experiments to predict the optimal fluid fill charge ratio of the working fluid within a two-phase, closed, carbon steel/water thermosyphon. Their results indicated that optimal ratio of fill charge to inner volume of the evaporator section is 0.25 to 0.33. Fukano et al. (1988) observed the flow patterns inside a closed two-phase vertical thermosyphon to determine the operating limits. The parameters varied were the inner diameter of the thermosyphon, the properties and the fill charge of the working fluid and the system pressure.

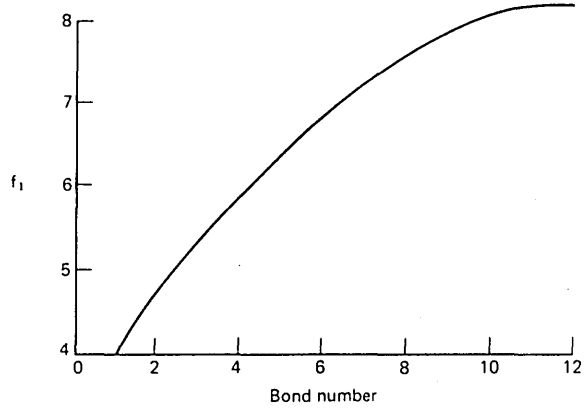

(a) Variation of function f1 with Bond number

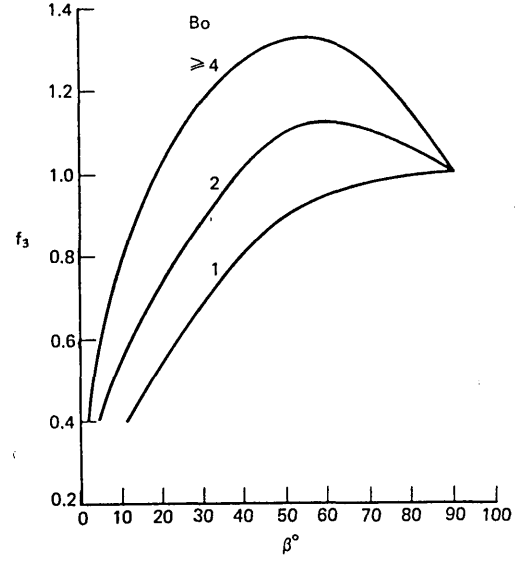

Inclination angle (°)

(b) Variation of function f3 with thermosyphon inclination angle and Bond number

Figure 2.7 The functions f1 and f3 in the correlation for the CCFL (Berenson, 1962)

The observations showed that there were two opposite effects of liquid pool boiling in the evaporator on the operating limit due to flooding : a mild boiling delays the dry-out of the evaporator wall and a violent one promotes it. Taking these effects into consideration, critical heat flux data available for thermosyphons were correlated using new parameters such as the height of the liquid pool and the bubble kinetic energy. O-uchi et al. (1988) observed the boiling heat- transfer and the liquid film breakout occurring on the surface of the evaporator of a thermosyphon. The inside of the evaporator of the thermosyphon was simulated to observe these phenomena : the liquid film occurring on the surface was heated, initiating nucleate boiling in the liquid film. Different surface structures were used to stabilise the nucleate boiling. It was found that for grooved and meshed surfaces, the liquid film was preserved and at the same time the evaporation and the boiling heat transfer increased; however, dry-out also increased. Many other investigators presented the criteria for heat-transport limitations in the thermosyphon. According to Groll et al (1983), film boiling is the dominant heat transfer limit in relatively-short, small-diameter thermosyphons subject to high radial evaporator heat fluxes. For relatively long high-performance thermosyphons subject to small radial evaporator heat fluxes, vapour-liquid flow interaction is the performance-limiting effect. Gross et al. (1986) performed an experimental investigation for reflux film condensation inside a closed tube. A wide range of pressures, heat-flow rates and inclination angles of the thermosyphon were employed. The results indicated that film flow patterns can be achieved in both the laminar and turbulent region. Zuo et al. (1995) conducted a theoretical parametric 'scaling' study to investigate how size reduction affects the steady-state heat-transfer behaviour of the two-phase thermosyphon. A numerical model was developed from first principles to describe the heat-transfer behaviour of the vertical thermosyphon incorporating the performance constraints of dry-out, critical heat flux and flooding limits. Experiments were also conducted with water-charged thermosyphons. They concluded that, normally, dry-out can be avoided if the working fluid inventory is more than a predictable threshold amount. The

actual performance heat-transfer limitation corresponds to the lesser of the critical heat flux and flooding limits. As the thermosyphon becomes smaller, larger magnitude thermal oscillations occur, and the heat-transfer capacity and efficiency can significantly decrease. Fukano et al. (1990) examined reflux condensation inside a closed two-phase vertical thermosyphon experimentally and analytically, with the attention focused on the local heat transfer characteristics. They took into account the effects of the turbulence in the liquid film near the gas-liquid interface which is caused by the wave-like structure of the liquid surface and also by the vapour flow and improves the heat-transfer characteristics in the lower part of the condenser and the deposition of droplets from the vapour core to the liquid film which results in the increase of the film thickness and therefore, reduces the heat-transfer near the top end of the condenser in the proposed theoretical model.

2.3.2 Comparative Studies of Heat Pipes and Thermosyphons

Comparative studies concerning the behaviours of heat pipe and thermosyphon, at the same operating conditions, appear to be very limited. Through the literature survey, only the study of Feldman et al.'s (1978) could be traced. They reported the results of a series of experiments on the performances of gravity-assisted heat pipes with and without circumferential grooves (see Figure 2.8). They measured heat transfer rates and temperature gradients, so that heat pipe conductance and evaporator and condenser heat-transfer coefficients were determined. Such performance data are important since the added cost of manufacturing the grooves is a significant part of the cost of the heat pipe, especially long pipes. According to their results, for a 91.4cm long and 1.27cm outside-diameter heat pipe with 40 grooves per cm, the maximum thermal conductance measured was 22.7W/°C, and the heat transfer coefficients in the evaporator and condenser were 4.7 and 12.0 kW/m^2 °C, respectively. The same size and type of heat pipe without grooves had a thermal conductance of 4.2W/°C, and evaporator and condenser heat transfer coefficients of 1.0 and 1.5 kW/m^2 °C.

* Shematic drawing of experimetal apparatus

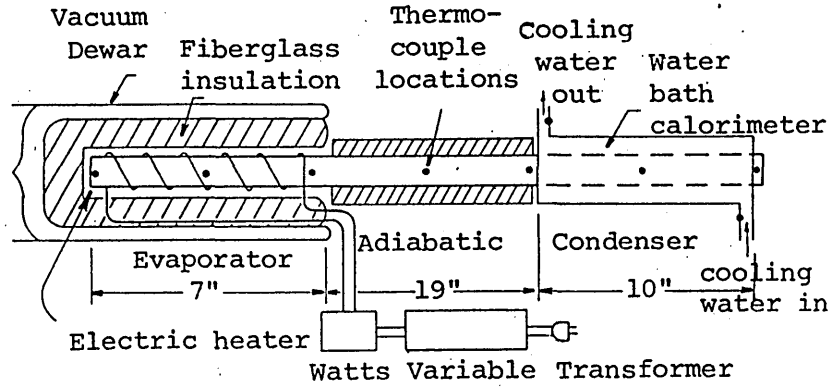

* Summary of experimental results

Type	Wick (grooves/cm)	Heat flux input (W/cm^2)	Conductance (W/°C)	Heat-transfer coefficient ($W/m^2°C$)	
				Evaporator	Condenser
Copper-water	39.4	5	22.7	4,700	11,992
Copper-water	None	1.4	4.2	1,008	1,505

Figure 2.8 Experimental results of thermal performance of heat pipe with and without wicks (Feldman, 1979)

Experiments were also conducted on a 6.4m long and 3.18cm outside-diameter iron/water heat pipe without grooves and on a U-shaped copper water heat pipe with grooves.

2.3.3 Previous Studies on Heat Pipe Heat Exchangers (HPHEs)

Heat pipe heat exchangers (HPHEs) offer many advantages over other types of heat exchangers for the recovery of heat from industrial gaseous waste streams in the low and medium temperature range. Features of HPHEs which are attractive in industrial heat recovery applications are :

- No moving parts and no small external power requirements implying high reliability.
- Cross-contamination is totally eliminated because of a solid wall between the hot and cold gas streams.
- A wide variety of sizes are available, and the unit is in general compact and suitable for all, except the highest temperature, applications.
- The HPHEs are fully reversible (i.e. heat can be transferred in either direction).
- Collection of condensate in the exhaust gases can be arranged.
- The flexibility of using different fin spacings permits easy cleaning if required.

The application of these devices fall into three main categories:

- Heat recovery in air-conditioning systems, normally involving comparatively low temperatures and duties.
- Recovery of heat from a process-exhaust stream to preheat air for space heating.
- Recovery of waste heat from process for reuse in the process (e.g. preheating of combustion air) .

This area of application is the most diverse and can involve a wide range of temperatures and duties. Although HPHEs have been in production for less than a decade, a review of manufacturers' literature and published studies on

their development and use indicate a very wide range of applications in industry. Lee et al. (1978) studied the characteristics of counter-flow heat exchangers units, using heat pipes or two-phase closed thermosyphons as the heat transfer elements experimentally, and developed simple analytical model to predict the performance of HPHEs. They concluded that the maximum heat-transfer rate has a unique functional relationship between the ratio of two streams mass flow rates, and the ratio of heated to cooled lengths of the heat transfer elements. Huang et al. (1985) developed a method of analysis for the thermal performance of HPHEs based on the conductance model. In the analysis, the specific conductance of the heat pipe was obtained from a performance test of a single heat pipe and the well known universal correlations were used to calculate the convective heat-transfer coefficients in tube bank. A computer program, based on the finite-difference technique, was then developed to calculate the thermal performance of HPHEs (see Figure 2.9). For any staggered or alignment arrangement of tubes, a simplified method was developed to predict the thermal performances of the HPHE by Hsieh (1988). The resultant thermal performances were correlated to provide thermal-design data for a HPHE configuration applicable to waste-heat recovery systems. Hsieh (1990) also performed comparative studies on thermal performances and pressure drops of counterflow and parallel-flow HPHEs with aligned/staggered tube rows. The design of HPHEs involves the selection of parameters which influence heat-transport on the outer surfaces of both the condenser and the evaporator. Important external parameters include the heat-pipe temperature, heat-exchange surface areas, heat-transfer coefficients, and flow rates. According to Swanson et al. (1989), the selection of these parameters influences the design of the internal structure of the heat pipe. A constrained optimisation problem has been formulated which minimises the total external heat-exchange surface area as a function of the targeted condenser external outflow temperature. Niro et al. (1992) presented an analytical model to evaluate the thermal performance and the pressure drops of a gas to gas heat exchanger using thermosyphons.

*** Test rig of HPHE**

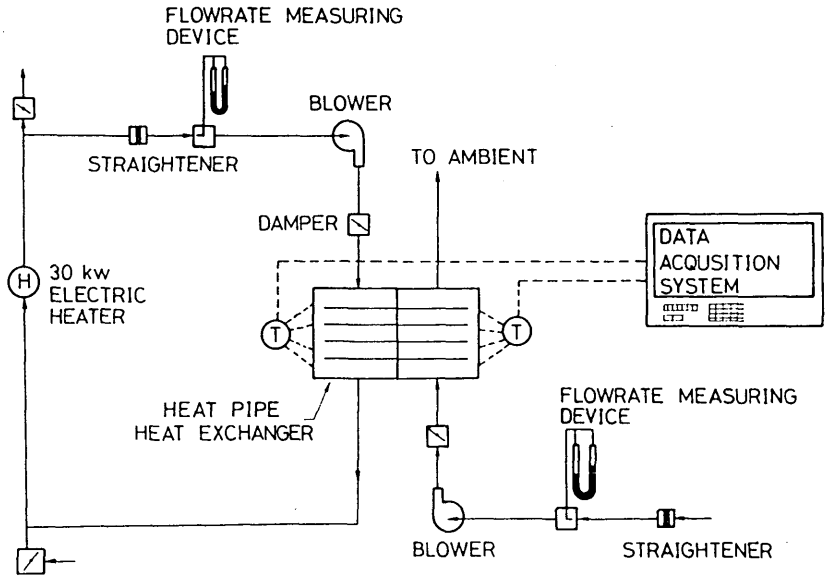

*** Comparison of experiment with theory of HPHE**

Test run No.	Hot air		Cold air		Energy transfer rate, Q (W)	
	Flowrate (SCMM)	Inlet temp., $T_{h,0}$ (°C)	Flowrate (SCMM)	Inlet temp., $T_{c,4}$ (°C)	Experiment	Theory
1	12.9	244.1	13.2	25.1	6290	5920
2	12.8	240.0	13.0	25.2	6050	5770
3	12.6	238.4	13.2	24.6	5870	5750
4	12.2	276.2	12.7	24.8	6750	6520
5	9.10	297.1	10.4	28.8	5710	6020
6	9.10	295.7	10.3	28.7	5640	5990
7	12.3	274.4	7.20	32.0	5660	5480
8	11.8	296.6	6.80	34.7	5720	5710
9	11.5	261.6	7.00	31.7	4720	5080
10	11.3	298.5	7.20	33.0	5700	5820
11	8.20	299.0	7.10	31.3	4880	5320
12	8.20	300.7	7.10	31.4	4940	5350

Figure 2.9 Experimental results of HPHE thermal performance test (Huang, 1985)

They reviewed the correlations to estimate the heat-transfer coefficients both outside and inside thermosyphons, and the gas pressure drops through the exchanger. They derived an analytical correlation to evaluate the gas inlet temperatures to a tube-row as a function of row-effectiveness and heat capacity rates, and then the row effectiveness to the exchanger effectiveness was correlated. They also evaluated the performance of a thermosyphon heat exchanger for a low-temperature waste-heat application. Lukitobudi et al. (1995) designed and constructed an air to air heat exchangers for medium-temperature heat recovery using thermosyphons with water as the working fluid. The constructed heat exchangers were found to be highly effective in recovering heat compared with similar heat exchangers using other working fluids. Wang (1993) applied HPHEs to a reheating furnace for steel rolling. The exchanger had the advantages of high heat-exchange efficiency, compact structure and easy installation. It proved very suitable for the recovery of waste heat at medium and low temperatures and played an important role in energy saving.

Tanisho et al. (1992) studied a heat recovery unit constructed with heat pipes and analysed the influence of the inclination of the heat pipes on the performance of the equipment. The results have shown that there exists an inclination at which the system has a better performance, but for higher inclinations there is no significant increase in the efficiency of the system.

2.4 SUMMARY OF THE REVIEW ON PREVIOUS WORK

Heat pipes and closed two-phase thermosyphons are highly-efficient heat-transfer devices utilising the continuous evaporation and condensation of a suitable working fluid for two-phase heat-transport in a closed system. As one of widely-considered applications of heat pipes and thermosyphons, HPHEs offer many advantages over other types of heat exchangers for the recovery of heat from industrial gaseous waste streams in the low- or medium-temperature ranges. Although the heat pipe is similar in some

respects to thermosyphon, there is an important difference in the mechanism of condensate return. A thermosyphon relies only on gravity, whereas a heat pipe employs several forces, such as the capillary force and centrifugal force, for the condensate return. Therefore, the thermosyphon is ineffective in zero gravity or in case where the condensate has to be returned against gravity. The thermosyphon has the advantages of simplicity in construction, and cheap manufacturing cost compared with heat pipe. It also exhibits relatively high rates of heat transfer. Because of those characteristics, comparative studies concerning the behaviours of heat pipe and thermosyphon, at the same operating condition, are important. Although the thermal performances of single heat pipes (or thermosyphons) have been extensively investigated, these comparative studies appear to be very limited. Through the literature survey, only one such a study could be traced. However, theories of single heat pipes (or thermosyphons) are useful in evaluating the significance of parameters pertinent to thermal performance and thus in devising an experimental research programme. In general, laws of fluid mechanics and heat transfer have been used to establish the theory for predicting heat-transport limitations and other thermal performance phenomena of the heat pipe (or thermosyphon). Main conclusions from previous studies pertinent to research are:

Heat transfer characteristics of heat pipe

- The transfer of heat and the associated temperature drops in a heat pipe can be represented by thermal resistances and an analogous equivalent electric circuit. In this thermal-resistance model, effective thermal conductivities for liquid-saturated wicks in the evaporator and the condenser have to be considered according to the wicks in case of heat pipes. In case of thermosyphon, the condensing heat-transfer coefficient in the condenser and the local heat-transfer coefficients of evaporation and boiling in the evaporator have to be estimated.

- Effective thermal conductivities in the condensing and evaporating part are affected by wick porosity. That porosity of a screen wick is a function of the wire diameter, mesh number, and wick crimping factor, whereas porosity of a grooved wick depends upon the groove width, and groove fin width.
- The grooves in the heat pipe improve the heat-transfer coefficient and a groove wick exhibits a low resistance for heat flow.
- The small thermal resistance associated with vapour flow is a consequence of the Clausius-Clapeyron relationship, which requires a small drop in temperature for a relatively large drop in pressure. For this reason, the thermal resistance for vapour flow can be neglected with little effect on the value of the heat-transfer coefficient for the heat pipe.
- As an analytical model for thermosyphon thermal performance, film condensation along the inside surface of the condenser, and evaporation from a liquid film above the pool and boiling of the liquid pool in the evaporator should be considered as the heat transfer mechanisms, and the effects of the amount and type of the working fluid, the operating pressure and the heat flux can be brought into consideration.
- In case of thermosyphon, the occurrence of nucleate boiling in both the liquid film and the pool side has been confirmed. The nucleate boiling in the liquid film improves the heat-transfer capability of the thermosyphon. However, the occurrence of dry-out conditions has a negative effect on the performance of the system.
- At a certain inclination angle, the mean heat-transfer coefficient of the thermosyphon reaches a maximum value; which is related to the heat-transfer behaviours in both the condenser and evaporator.

Heat transport limitation of heat pipe

- The maximum heat-transport factor for heat pipes can be determined from the values of effective pumping pressures and friction coefficients for liquid and vapour flows.

- A great many heat pipes have been found to have vapour flows within the range of incompressible laminar flow and a friction coefficient for vapour flow that is much smaller than that for liquid flow.
- For the prediction of the maximum heat-transfer rate in a heat pipe, capillary radius, permeability, and porosity should be evaluated. These parameters affect the friction coefficient for the liquid flow.
- The sonic limitation occurs when the vapour velocity at the evaporator exit is sonic and maximum heat transport rate at its sonic limit can be calculated by Levy's equation.
- The entrainment limitation is vapour-dominated and independent of the fluid inventory. This limitation can be evaluated as a function of a critical Weber number.
- Analysis of the boiling limitation involves the theory of nucleate boiling (i.e. the formation of bubbles and the subsequent growth and motion of these bubbles). In the absence of sufficient data, a conservative approach would be to use values of the nucleation radius of 2.54×10^{-5} and 2.54×10^{-4} mm for the gas-loaded and conventional heat pipes, respectively.
- The dry-out limitation usually can be avoided by selecting a sufficient fluid fill charge ratio for the thermosyphon. The dry-out limitation can be determined from a mass flow balance over a control surface in the evaporator, taking into account evaporation and droplet generation due to nucleate boiling inside the condensate film.
- The CCFL heat flux is the functions of f_1, f_2, and f_3, where, f_1 is a function of the Bond number, f_2 is a function of the dimensionless pressure parameter, and f_3 is a function of the inclination angle of the thermosyphon and the Bond number.

The features of heat pipe heat exchangers (HPHEs)

Features of HPHEs which are attractive in industrial heat recovery applications are :

- No moving parts and no external power requirements implying high reliability.

- Cross-contamination is totally eliminated because of a solid wall between the hot and cold gas streams.
- A wide variety of sizes are available, and the unit is in general compact and suitable for all except the highest temperature applications.
- The HPHEs are fully reversible (i.e. heat can be transferred in either direction).
- Collection of condensate in the exhaust gases can be arranged.
- The flexibility of using different fin spacings permits easy cleaning if required.

CHAPTER 3 ANALYTICAL STUDY AND COMPUTER MODELLING OF THE BEHAVIOUR OF HEAT PIPES

This chapter describes the analytical studies adopted for predicting thermal performances of heat pipe and thermosyphon. These analytical studies are utilised for developing the computer model, namely the 'Heat Pipe and Thermosyphon Thermal Performance Model'. The model facilitates the prediction of the temperature distributions along and inside of tubes, heat transport limitations and thermal performances for different type of wicks and pipe specifications.

3.1 ANALYSIS OF THE BEHAVIOUR OF HEAT PIPES

To understand clearly the method adopted for developing the computer model, this part of the work is divided into three sections :

- analysis of thermal performances ;
- analysis of heat transport limitations ; and
- a simple mathematical model for predicting the thermal performances of thermsyphons.

3.1.1 Analysis of Thermal Performances

(a) Steady-state performance

According to Groll et al (1980), the heat pipe and thermosyphon can be treated as a composite thermal conductor of very high thermal conductance. Using an electric analogy and neglecting axial thermal conductance along the wall and wick structure of the heat pipe, the thermal network representation shown in Figure 3.1 can be used for capillary wick heat pipes and closed two-phase thermosyphons.

Figure 3.1. Thermal Resistance Model

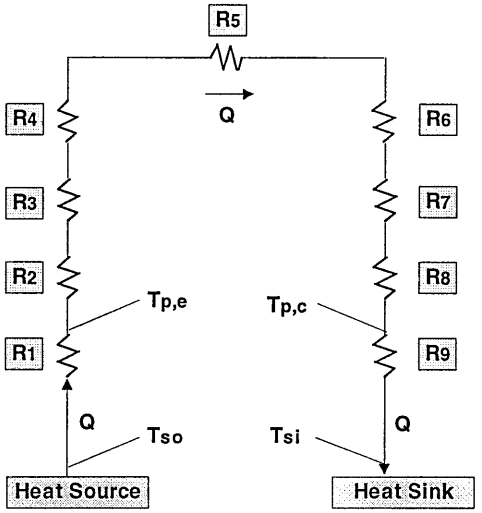

	Heat Pipe	Thermosyphon
R_1	Heat source - Evaporator external surface	Heat source - Evaporator external surface
R_2	Pipe wall in the evaporator	Pipe wall in the evaporator
R_3	Wick in the evaporator	Liquid boilng in the evaporator
R_4	Liquid-vapour interface in the evaporator	Liquid-vapour interface in the evaporator
R_5	Vapour passage	Vapour passage
R_6	Liquid-vapour interface in the condenser	Liquid-vapour interface in the condenser
R_7	Wick in the condenser	Liquid condensing in the conderser
R_8	Pipe wall in the condenser	Pipe wall in the condenser
R_9	Condenser external surface - Heat sink	Condenser external surface - Heat sink

Usually an effective overall thermal conductance C and a thermal resistance R_{tot} are attributed to the heat pipe and thermosyphon, i.e.

$$Q = C\Delta T = \Delta T / R_t \tag{3.1}$$

Two total resistances can be defined:

- R_t is strictly related to the heat pipe and thermosyphon themselves; and
- R'_t incorporating the resistances associated with the coupling of the heat pipe (or thermosyphon) to external heat sources and sinks. The total resistance is given as the sum of the individual resistances,

$$R_t = \sum_{i=2}^{8} R_i = \sum_{i=2}^{8} \Delta T_i / Q \tag{3.2}$$

and

$$R'_t = \sum_{i=1}^{9} R_i = \sum_{i=1}^{9} \Delta T_i / Q \qquad (3.3)$$

The difference between evaporator and condenser surface temperatures is used as the driving temperature difference. Thus

$$Q = \Delta T / R_t \,, \quad \Delta T = T_{p,e} - T_{p,c} \qquad (3.4)$$

If the external resistances between the heat source and the surface, as well as between the surface and the heat sink are considered, the difference between source and sink temperature has to be used as the driving temperature difference:

$$Q = \Delta T' / R'_t \,, \quad \Delta T' = T_{so} - T_{si} \qquad (3.5)$$

Heat pipe

Heat conduction in the pipe wall and in the liquid-saturated wick can be described by the Fourier's law. Heat convection by vapour can be described by the Clausius-Clapeyron relationship. For a cylindrical wall, the thermal resistance against heat conduction through the wall can be expressed as

$$R = \ln (r_2 / r_1) / 2\pi L k \qquad (3.6)$$

Clausius-Clapeyron equation relates the vapour temperature and pressure,

$$T_1 - T_2 = T_v (p_1 - p_2) / (\rho_v \lambda J) \qquad (3.7)$$

Expressions for the individual resistances in the thermal network for a heat pipe are represented in Table 3.1. Asselman et al. (1973) investigated the various thermal resistances in order to provide an indication of their relative magnitudes. They concluded that the thermal resistances R_4, R_5, and R_6 are usually extremely small and, therefore, can be neglected. Table 4.2 indicates some approximate values for a water heat pipe. Thus, the temperature difference between evaporator and condenser surfaces can be calculated in terms of R_2, R_3, R_7 and R_8 only :

Table 3.1 Heat Pipe Thermal Resistances
(Groll,1992)

Thermal resistance	Analytical expression
R_1	$1 / (h_e A_e)$
R_2	$\ln (r_o / r_i) / (2\pi L_e k_p)$
R_3	$\ln (r_i / r_v) / (2\pi L_e k_{e,e})$
R_4	$(\lambda^2 \rho_v / T) [M / (2 \pi R T)]^{1/2}$
R_5	$T_v (p_{v,e} - p_{v,c}) / (\rho_v \lambda J Q)$
R_6	$(\lambda^2 \rho_v / T) [M / (2 \pi R T)]^{1/2}$
R_7	$\ln (r_i / r_v) / (2\pi L_e k_{e,c})$
R_8	$\ln (r_o / r_i) / (2\pi L_c K_p)$
R_9	$1 / (h_c A_c)$

$$T_{p,e} - T_{p,c} = Q \{ [\ln (r_o/r_i) / 2\pi L_e k_p] + [\ln(r_i/r_v) / 2\pi L_e k_{e,e}] + [\ln(r_i/r_v) / 2\pi L_e k_{e,c}] + [\ln(r_o/r_i) / 2\pi L_c k_p] \quad (3.8)$$

The effective thermal conductivity k_e of the wick depends on the wick structure. The simplest configurations consist of wick material and liquid either in series or in parallel. Expressions (Gorring et al, 1961) for k_e for these cases are, respectively,

$$k_e = k_l k_w / [\varepsilon k_w + k_l (1-\varepsilon)] \quad (3.9)$$

and

$$k_e = \varepsilon k_l + k_w (1-\varepsilon) \quad (3.10)$$

where, ε is the volume fraction of liquid (i.e. the volume of the liquid divided by the total volume of the liquid-saturated wick). Thermal conductivity for a liquid saturated wick of distributed cylinders has been correlated by the equation.

$$k_e = k_l [(k_l + k_w) - (1- \varepsilon) (k_l - k_w)] / [(k_l + k_w) - (1- \varepsilon) (k_l - k_w)] \quad (3.11)$$

These expressions of effective thermal conductivity can be used for heat pipe wicks. For example, equation (3.10) can be used for the condenser section of rectangular-grooved wicks, and equation (3.11) can be used for wrapped-screen wicks.

Table 3.2 Order of Magnitude of Thermal Resistances for a Water Heat Pipe (Asselman et al , 1973)

Resistance	Magnitude (°C/W)
R_1	10^3 - 10
R_2	10^{-1}
R_3	10
R_4	10^{-5}
R_5	10^{-8}
R_6	10^{-5}
R_7	10
R_8	10^{-1}
R_9	10^3 - 10

Since the porosity for rectangular-grooved wicks is equal to the width of the grooves over the sum of the groove width and the fin width, equation (3.10), when applied to groove wicks at the condenser section, can be rewritten as

$$k_e = (w\, k_l + w_f\, k_w) / (w + w_f) \qquad (3.12)$$

The mode of heat transfer across groove wicks at the evaporator is somewhat different form that at the condenser. Heat travels

- directly through the liquid film ; and
- through a series path consisting of the groove fin and a thin film of liquid adjacent to the tip of the liquid-fin interface.

According to Chi (1971), the value of the effective thermal conductivity for the groove wicks at the evaporator section can be expressed as:

$$k_e = [\, (w_f\, k_l\, k_w\, \delta) + (w\, k_l)\ (0.185\, w_f\, k_w + k_l\, \delta)\,] / [\, (w + w_f)\, (0.185\, w_f\, k_w + k_l\, \delta)\,] \qquad (3.13)$$

Thermosyphon

The main heat and mass transfer processes that take place in a thermosyphon are :

- pool boiling ;
- thin liquid film evaporation ;
- counter-current two-phase flow ; and
- film condensation.

Heat conduction in the thermosyphon wall can be described by the Fourier's law and heat convection by vapour can be described by the Clausius-Clapeyron relationship.

Special care should be devoted to the correct estimation of R_3 and R_7, since these two thermal resistances are the most important ones for many applications. For longer thermosyphons, the change of saturation temperature in the evaporator due to the hydrostatic height of the pool should also be considered. The thermal resistance R_3 of the boiling liquid in the evaporator can be divided two resistances :

- R_{3p} for the heat transfer process in the liquid pool ; and
- R_{3f} for the heat transfer process in the liquid film.

The heat transfer process in the liquid pool is generally considered to be one of nucleate boiling (O-uchi et al,1988). Purely theoretical study of the boiling in the evaporator is not possible due to the complexity of the boiling process. Therefore, the empirical equation of Imura et al (1973) is applied in this study for the heat transfer coefficient, h_p, of pool boiling,

$$h_p = 0.32\ [\ (\rho_l^{0.65} k_l^{0.3} c_{pl}^{0.7} g^{0.2})\ /\ \rho_v^{0.25} \lambda^{0.4} \mu_l^{0.1}\ ]\ (p_v / p_a)^{0.23}\ q_e^{0.4} \qquad (3.14)$$

By assuming that the condensate-film flow is laminar and the film is thin with respect to the radius of curvature of the inside surface, the Nusselt's film condensation theory can be applied in the condenser section (Shiraishi,1982).

$$h_c = \{1.47\ [4q_c L_c / (\lambda \mu_l)\ ]^{-1/3}\ k_l\ \} / (\nu_l^2/g)^{1/3}$$

The heat transfer in the evaporating liquid film has not been investigated fully. However, at low evaporator heat flux, a continuous liquid film was observed (Andros et al. , 1978) and a laminar film evaporation model which bears a strong resemblance of Nusselt's condensation theory can be applied.

$$h_f = \{1.47\ [4q_e L_f / (\lambda \mu_l)\ ]^{-1/3}\ k_l\ \} / (\nu_l^2/g)^{1/3}$$

Dhir et al. (1971) proved that Nusselt's analysis for vertical condition may be used for inclined condition if 'g' is replaced by 'gsinθ'. That is, above two equations can be re-written for inclined condition as

$$h_c = \{1.47\ [4q_c L_c / (\lambda\ \mu_l)\ ]^{-1/3}\ k_l\ \} / (\nu_l^2/g\sin\theta)^{1/3} \quad (3.15)$$

$$h_f = \{1.47\ [4q_e L_f / (\lambda\ \mu_l)\ ]^{-1/3}\ k_l\ \} / (\nu_l^2/ g\sin\theta))^{1/3} \quad (3.16)$$

A high evaporator heat flux, nucleate boiling dominates and a coverage of the liquid film region by a two-phase mixture was observed (Andros et al., 1978) . Therefore, Imura et al's (1973) empirical equation can be applied, i.e.

$$h_f = h_p \quad (3.17)$$

Table 3.3 presents equations and correlations for the different thermal resistances as suggested by the Engineering Sciences Data Unit (ESDU,1981). In this table, R_4, R_5, and R_6 are neglected because they are always small compared with the other resistances.

Table 3.3 Thermosyphon Thermal Resistance
(ESDU , 1981)

Resistance	Analytical Expression
R_1	$1/ (h_e A_e)$
R_2	$\ln (r_o/r_i) / (2\pi L_e k_p)$
R_{3P}	$1/ (\phi\ g^{0.2} Q^{0.4} A_l^{0.6})$ $\phi = [\ \rho_l^{0.65} k_l^{0.3} c_{pl}^{0.7} / (\rho_v^{0.25} \lambda^{0.4} \mu_l^{0.1})\ ]\ (p_v/p_a)^{0.23}$
R_{3f}	$0.345\ Q^{1/3} / [d_e^{4/3} g^{1/3} L_e (\lambda\ k_l^3 \rho_l^2 / \mu_l)^{1/3}]$
R_7	$0.345\ Q^{1/3} / [d_c^{4/3} g^{1/3} L_c (\lambda\ k_l^3 \rho_l^2 / \mu_l)^{1/3}]$
R_8	$\ln (r_o/r_i) / (2\pi L_c K_p)$
R_9	$1 / (h_c A_c)$

(b) Comparison between the heat pipe and thermosyphon

In comparison with the main heat and mass transfer process in thermosyphons, the primary heat transfer mechanisms for heat pipes are :

- heat conduction across the container wall and the liquid-saturated wick at the evaporator section with subsequent evaporation at the liquid-vapour interface of that section ;
- convective transport of latent heat by vapour from the evaporator to condenser ; and

- heat conduction across the saturated wick and the container wall at the condenser section with subsequent condensation at the liquid-vapour interface of that section.

By comparing these processes, the differences in heat-transfer characteristics can be analysed. In case of thermal resistances, we can calculate the differences by comparing the resistances, R_3 and R_7, at the same operating conditions (see Table 3.4). In the present study, Nusselt's film condensation theory and Imura et al 's empirical equation will also be used, for thermosyphons, in order to compare the heat transfer characteristics of heat pipes and thermosyphons.

Table 3.4 Comparison of Thermal Resistances

1. Description

Resistance	Heat Pipe	Thermosyphon
R_3	Liquid-vapour interface in the evaporator	Pool boilng in the evaporator (R_{3P}) Thin liquid film evaporation (R_{3f})
R_7	Liquid-vapour interface in the condenser	Condensing liquid in the condenser (Filmwise condensation)

2. Related equation

Resistance	Heat Pipe	Thermosyphon
R_3	$\ln (r_i / r_v) / (2\pi L_e k_{e,e})$	$1/ [\phi\ g^{0.2} Q^{0.4} A_l^{0.6}]$ $0.345\ Q^{1/3} / [d_e^{4/3} g^{1/3} L_e (\lambda\ k_l^3 \rho_l^2 / \mu_l)^{1/3}]$
R_7	$\ln (r_i / r_v) / (2\pi L_e k_{e,c})$	$0.345\ Q^{1/3} / [d_c^{4/3} g^{1/3} L_c (\lambda\ k_l^3 \rho_l^2 / \mu_l)^{1/3}]$

3.1.2 Analysis of Heat-Transport Limitations

(A) Heat pipe

There are four parameters limiting heat transport in a heat pipe, and they are the capillary limitation, sonic limitation, entrainment limitation, and boiling limitation.

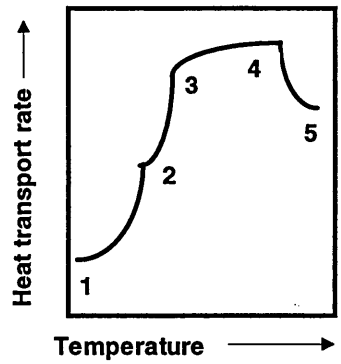

(1-2) : Sonic limitation
(2-3) : Entrainment limitation
(3-4) : Capillary limitation
(4-5) : Boiling limitation

Figure 3.2 Heat-transport limitations of a heat pipe

A possible effect of these limitations on the heat transport capability of a heat pipe is shown in Figure 3.2. The type of limitation restricting the heat transport capability of a heat pipe is determined by the limitation which has the lowest value at the temperature under consideration. The magnitudes of these different limitations are in turn dependent upon various properties of the working fluids, the wick structures, and the heat pipe dimensions.

Capillary limitations

It should be noted that the capillary limitation is the most common of the four limitations and thus, a number of definitions for the heat pipe transport capability have been introduced through the consideration of this limitation. The maximum capillary heat-transport factor $(QL)_{c,max}$ can be defined as (Chi,1972)

$$(QL)_{c,max} = \frac{\text{maximum effective pumping pressure}}{\text{liquid frictional factor} + \text{vapour frictional factor}}$$

$$= \frac{2\sigma/r_c - \Delta p_\perp \pm \rho_l g L_t \sin\theta}{F_l + F_v} \qquad (3.18)$$

where,

$$F_l = \mu_l / K A_w \rho_l \lambda \qquad F_v = (f_v Re_v)\mu_v / 2(r_{h,v})^2 A_v \rho_v \lambda \qquad (3.19)$$

In equation (3.18), the maximum effective pumping pressure consists of maximum capillary pressure $p_{cm} = 2\sigma/r_c$, the normal hydrostatic pressure $\Delta p_{\perp}$ and the axial hydrostatic pressure $\rho_l g L_t \sin\theta$. The axial hydrostatic pressure is '+' for gravity-assisted heat pipe, and '-' for anti-gravity heat pipe. Expressions for the components of maximum effective pumping pressure, liquid frictional factor, and vapour frictional factor as the functions of the geometrical characteristics of the wicks are presented in Table 3.5. It follows, that the capillary limitation on the heat transport rate $Q_{c,max}$ can be derived from the heat transport factor $(QL)_{c,max}$ if the heat flux distribution along the heat pipe is specified. $Q_{c,max}$ and $(QL)_{c,max}$ are related by the equation

$$(QL)_{c,max} = \int_0^{L} Q dx = (0.5 L_c + L_a + 0.5 L_e) Q_{c,max}$$

Consequently, the maximum capillary heat transport limitation $Q_{c,max}$ can be expressed as

$$Q_{c,max} = \frac{(QL)_{c,max}}{0.5 L_c + L_a + 0.5 L_e} \qquad (3.20)$$

Sonic limitation

The sonic limitation has been treated theoretically and experimentally in some detail by Levy (1968), Kemme (1969), and Deverall (1970). There is a similarity between the vapour flow in a heat pipe and the flow of a compressible fluid in a converging-diverging nozzle (Deverall et al, 1970). The sonic limitation occurs when the vapour velocity at the evaporator exit is sonic, i.e. when the Mach number Mv at the evaporator exit is unity. Hence, the sonic limits of a heat pipe $Q_{s,max}$ can be expressed by following equation (Levy, 1968) :

$$Q_{s,max} = A_v \rho_o \lambda \left[\rho_v \mathbf{R}_v T_o / 2 (\gamma_v + 1)\right]^{1/2} \qquad (3.21)$$

where, γ_v is the ratio of specific heats of the vapour (= 5/3, 7/3, or 4/3 for monoatomic, diatomic, or polyatomic vapours, respectively) and $\mathbf{R}_v$ is the vapour gas constant.

Table 3.5 Related Equations for Capillary Limitation (Chi, 1972)

	Wrapped screen wick	Rectangular Grooved wick
Capillary radius	$r_c = 1 / 2N$	$r_c = w$
Maximum capillary pressure	$p_{cm} = 2\sigma/r_c$	$p_{cm} = 2\sigma/r_c$
Normal hydrostatic pressure	$\Delta p_\perp = \rho_l g\, d_v \cos\theta$	$\Delta p_\perp = 0$
Axial hydrostatic pressure	$p_{ah} = \rho_l g\, d_v \sin\theta$	$p_{ah} = \rho_l g\, d_v \sin\theta$
Wick cross sectional area	$A_w = \pi (d_i^2 - d_v^2) / 4$	$A_w = 2\pi r_m \delta$
Wick crimping factor	$s = 1.05$	-
Wick porosity	$\varepsilon = 1 - (\pi s N d / 4)$	$\varepsilon = n w / 2\pi r_m$
Wick permeability	$K = d^2 \varepsilon^2 / 122 (1-\varepsilon)^2$	$K = 2 (r_{h,l})^2 \varepsilon / f_l Re_l$
Groove aspect ratio	-	$\alpha = w / 2\delta$
Groove hydraulic radius	-	$r_{h,l} = 2w\,\delta / (w + 2\delta)$

Entrainment limitation

This entrainment limitation is caused by the shear force at the liquid-vapour interface in the heat pipe. The entrainment limitation is correlated in terms of a critical Weber's number, i.e., the limit begins when Weber's number reaches unity (Kemme, 1967). This Weber's number W_e is defined as

$$W_e = 2\, r_{h,s}\, \rho_v\, V_v^2 / \sigma \qquad (3.22)$$

the vapour velocity V_v is related to the axial heat flux Q by the equation

$$V_v = Q / A_v\, \rho_v \lambda \qquad (3.23)$$

From equations (3.22) and (3.23), the entrainment limitation $Q_{e,max}$ of a heat pipe can be expressed as

$$Q_{e,max} = A_v \lambda [\sigma \rho_v / 2 r_{h,s}]^{1/2} \quad (3.24)$$

In the above equations, the surface pore hydraulic radius, $r_{h,s}$ can be estimated from following expressions.

- Wrapped screen wick : $r_{h,s} = (1/N - d) / 2$ (3.25)
- Rectangular groove : $r_{h,s} = w$ (3.26)

Boiling limitation

Analysis of the boiling limitation involves the theory of nucleate boiling. In nucleate boiling involves two separate processes occur :

- the formation of bubbles (nucleation) ; and
- the subsequent growth and motion of these bubbles.

From the theory of nucleate boiling, an expression for the boiling heat-transport limitation is given by the equation (Chi, 1972).

$$Q_{b,max} = \frac{2\pi L_e k_e T_v}{\lambda \rho_v \ln(r_i/r_v)} (2\sigma/r_n - Pc)$$

$$\cong \frac{2\pi L_e k_e T_v}{\lambda \rho_v \ln(r_i/r_v)} (2\sigma/r_n) \quad (3.27)$$

For a conventional heat pipe, which has been carefully processed to eliminate all noncondensable gases, , the radius vapour bubble, r_n , is equal to 2.54 x 10^{-7} m (Marcus, 1972).

(b) Thermosyphon

In thermosyphons, the three most important performance limitation phenomena are the dry-out, burn-out and counter-current flow limitation (CCFL). The characteristics of those limitations are :

- At comparably low filling ratios (i.e. ratio of working-fluid liquid volume to evaporator volume) a dry-out limitation can occur. The liquid film returning from the condenser to the evaporator is completely vaporised before it reaches the liquid pool.

- The burn-out limitation (or boiling limit) appears under high radial heat fluxes in the evaporator section. The thermo-fluid/dynamic process behind the burn-out limitation is the generation of a more or less stable vapour film between the liquid and the heated wall, which drastically reduces the evaporation heat transfer coefficient.
- If, under high axial heat fluxes, the high-velocity vapour flow from the evaporator to the condenser intensively interacts with the counter-current condensate flow, a counter-current flow limitation (CCFL) can occur. In this case the flow rate of the condensate returning to the evaporator section is reduced to such an extent that comparatively large dry patched are formed.

Dry-Out limitations

The dry-out limitation usually can be avoided by the selection of a sufficient fill ratio for the thermosyphon. From the model results of Takuma et al (1986), they developed an implicit correlation between the radial dry-out heat flux q_{max}, fluid properties, the heated length L_e, and the working fluid fill charge ratio F:

$$F = 1 - \frac{1}{1 + C \{ [q_{max} / \lambda^2) (2\sigma \rho_v)] [3 q_{max} \mu_l L_e) / (\rho l (\rho_l - \rho_v) g \lambda)]^{1/3} \}^{3/4}} \quad (3.28)$$

Burn-Out limitations

A simple correlation for the burn-out limitation was developed by Lienhard et al (1973) :

$$Q_{max} = 0.12 \pi d_e L_e \lambda (\rho_v)^{1/2} [\sigma g (\rho_l - \rho_v)]^{1/4} \quad (3\text{-}29)$$

The above equation applies for pool boiling, i.e. in the lower regions of the evaporator.

CCFL

Regarding CCFL, a large number of analytical models, partly resulting from work on the flooding phenomenon and partly generated in the context of

research on thermosyphon, is available. In the present study, the correlation for the CCFL suggested by ESDU (1981) is employed. This correlation, which is based on experimental data, is also valid for non-vertical orientations.

The CCFL heat flux is :

$$Q_{max} = (\pi d_e^2/4)\ f_1 f_2 f_3 \lambda (\rho_v)^{1/2} [\sigma g (\rho_l - \rho_v)]^{1/4} \quad (3.30)$$

where f_1 is a function of the Bond number according to Figure 2.7 (a) , f_2 as a function of the dimensionless pressure parameter K_p :

$$f_2 = K_p^{-0.17} \quad \text{if} \quad K_p < 4 \times 10^4$$

$$f_2 = 0.165 \quad \text{if} \quad K_p \geq 4 \times 10^4 \quad (3.31)$$

and f_3 is a function of the inclination angle of the thermosyphon and the Bond number according to Figure 2.7 (b).

The, Bond number B_o is defined as

$$B_o = d_i^2 [g (\rho_l - \rho_v) / \sigma] \quad (3.32)$$

and the dimensionless pressure parameter K_p can be expressed as,

$$K_p = p_v / [g (\rho_l - \rho_v) \sigma]^{1/2} \quad (3.33)$$

3.1.3 The Simple Mathematical Model for Thermosyphons

In addition to the thermal resistance model, a simple mathematical model was developed by Shiraishi (1981) by employing experimentally-determined heat-transfer coefficients. This simple mathematical model is suitable for predicting thermal performances of thermosyphons. The predicted overall thermal performance is quite close to that estimated by employing the thermal-resistance model, providing that all properties are evaluated at the same temperatures. The following assumption were adopted for this model :

- The axial conduction through the tube wall is negligible.
- The wall temperature of the condenser section is constant along its length. Heat is supplied uniformly to the evaporator section.
- The steady state operating condition is established and all the heat added at the evaporator section is removed at the condenser section.

- Change of liquid pool level in the evaporator due to the boiling action is negligible.

The change of saturation temperature in the evaporator due to the hydrostatic height of the pool should also be considered. That is, the saturation pressure-temperature relationship of the working fluid is applicable in the liquid pool as well as in the vapour space and this relationship is expressed as:

$$T = f\ (p) \tag{3.34}$$

The primary parameters which are possible to control during the operation of a thermosyphon are the heat-transfer rate (or the heat flux $q=q_e=q_c$), and the vapour-temperature T_v. Once these parameters are given, the pressure distribution within the liquid pool can be calculated as :

$$p(x) = p_v + \rho\ g\ (L_p - x) \tag{3.35}$$

The inside temperature distribution $T_i(x)$ can then be expressed as

$$T_i\ (x) = f\ (p(x)\ ), \qquad 0 \le x \le L_p \tag{3.36}$$

$$T_i\ (x) = f\ (p_v) = T_v, \qquad x < L_p \tag{3.37}$$

and the wall axial temperature distribution can be estimated as

$$\begin{aligned} T_w\ (x) &= T_i\ (x) + q_e / h_p && 0 \le x \le L_p \\ T_w\ (x) &= T_i\ (x) + q_e / h_f && L_p \le x \le L_e \\ T_w\ (x) &= T_i\ (x) && L_e < x \le L_e + L_a \\ T_w\ (x) &= T_i\ (x) - q_c / h_c && L_e + L_a < x \end{aligned} \tag{3.38}$$

3.2 HEAT PIPE AND THERMOSYPHON THERMAL-PERFORMANCE COMPUTER MODEL

The above theoretical analyses for thermal performance, heat transport limitations were employed for developing the Heat Pipe and Thermosyphon Thermal Performance Model. The model predicts temperature distribution, thermal resistances, heat-transfer coefficients and heat-transport limitation for different pipe specification and wick types. The main aim of this computer

program is to enable designers of waste-heat recovery systems to select the most appropriate heat pipe and thermosyphon for a particular application. This computer program was compiled in Visual Basic. Visual basic is an object-oriented/event-driven programming language that is easy enough for a non-programmer. Visual Basic runs in Windows environment and it takes just a few clicks of the mouse to include standard Windows objects such as buttons, list box, scroll bars, and icons. It not only provides an easy-to-use graphical interface, referred to as a GUI, with which a user can interact but also facilitates access to data stored in databases. That is, Visual Basic allows the user to move from record to record and display data from each record in bound controls.

3.2.1 Computer Program Design

Figure 3.3 and Figure 3.4 show the flow chart and example for Heat Pipe and Thermosyphon Thermal Performance Model. This computer program is designed to read working fluid properties, i.e. saturated water properties (see Table 3.6), wick and container material properties when it is run by binding those properties to the program through the database file. It is easily designed to input pipe specification and operating conditions by using standard Windows object and all of information on heat pipe and thermosyphon thermal performance can be calculated in consecutive order by just a few clicks. Because this computer program has not only its own command such as exit, print, connection to other computer program but also menus and dialogue boxes, it is convenient to operate the program under its own environment. This application is also connect with graphic mode, which shows the differences of thermal performances between heat pipes and thermosyphons easily as shown in Figure 3.5 without inputting pipe specifications and operating conditions separately. This program is designed to transfer the results of Heat Pipe and Thermosyphon Thermal Performance Model to graphic mode and Heat Pipe Heat Exchangers Design Model.

Figure 3.3 Flow chart for Heat Pipe and Thermosyphon Thermal Peformance Model

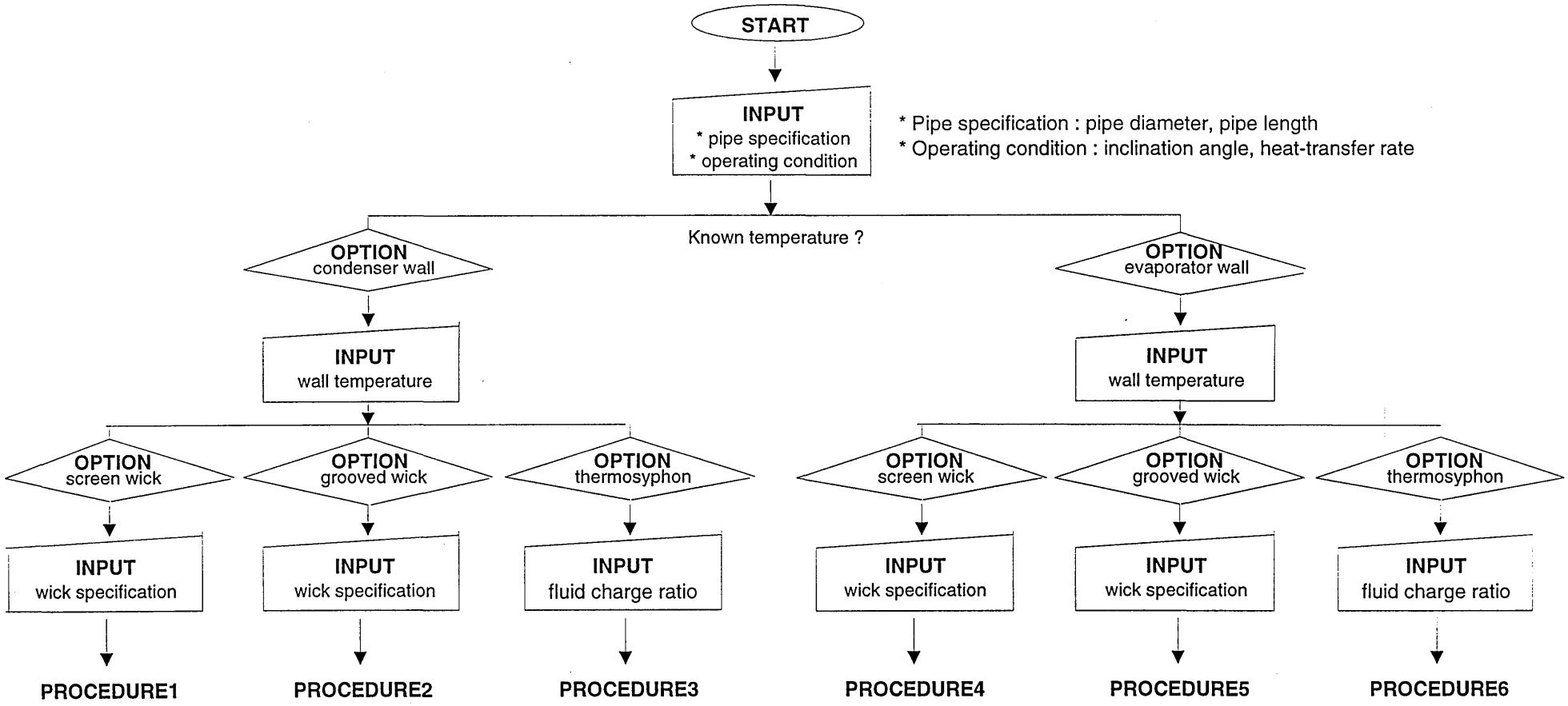

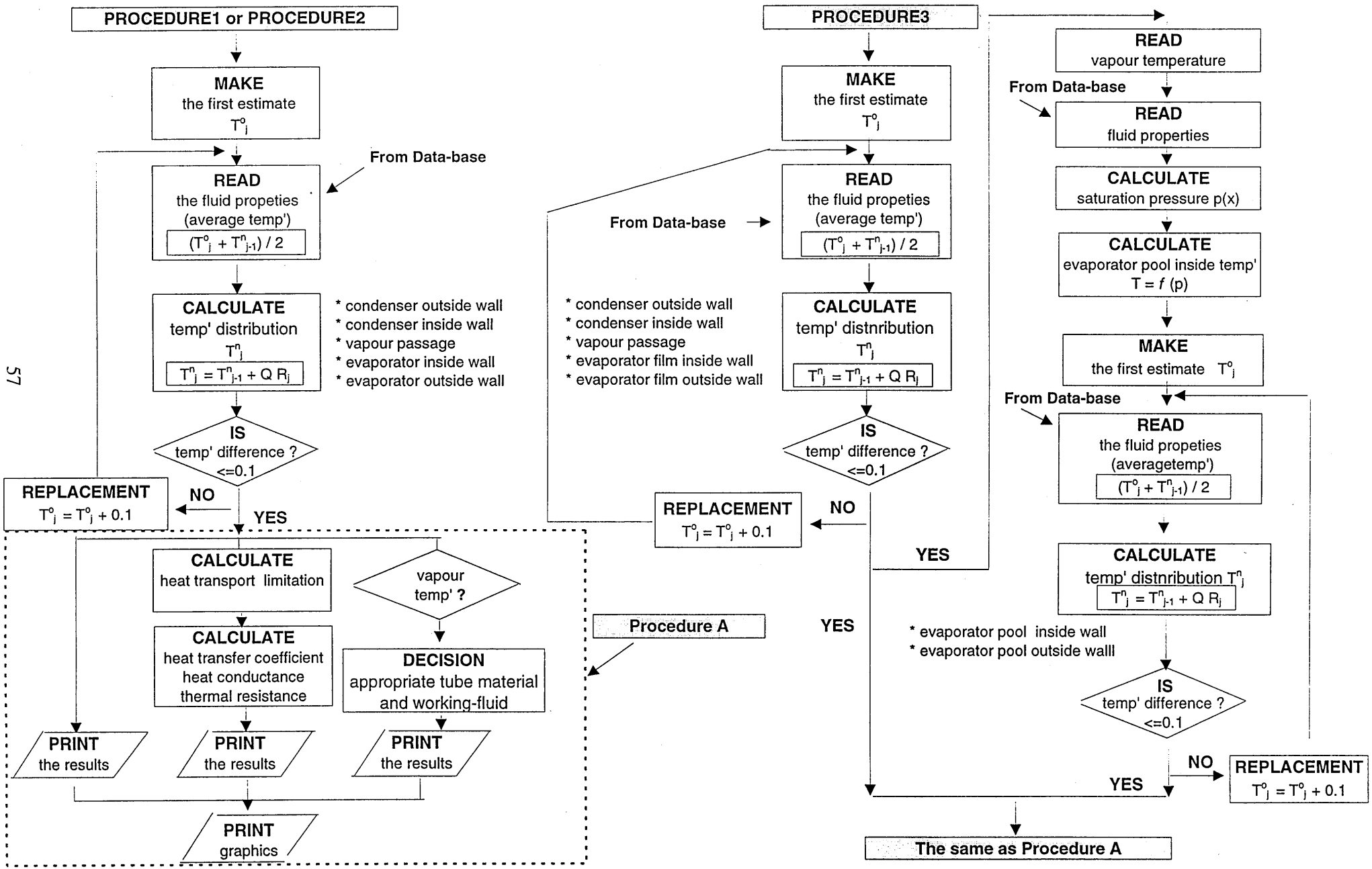
PROCEDURE1 or PROCEDURE2
MAKE
the first estimate
T^o_j
From Data-base
READ
the fluid propeties
(average temp')
$(T^o_j + T^n_{j-1}) / 2$
CALCULATE
temp' distribution
T^n_j
$T^n_j = T^n_{j-1} + Q R_j$
* condenser outside wall
* condenser inside wall
* vapour passage
* evaporator inside wall
* evaporator outside wall
IS
temp' difference ?
<=0.1
NO
REPLACEMENT
$T^o_j = T^o_j + 0.1$
YES
CALCULATE
heat transport limitation
CALCULATE
heat transfer coefficient
heat conductance
thermal resistance
vapour
temp' ?
DECISION
appropriate tube material
and working-fluid
PRINT
the results
PRINT
the results
PRINT
the results
PRINT
graphics
PROCEDURE3
MAKE
the first estimate
T^o_j
From Data-base
READ
the fluid propeties
(average temp')
$(T^o_j + T^n_{j-1}) / 2$
* condenser outside wall
* condenser inside wall
* vapour passage
* evaporator film inside wall
* evaporator film outside wall
CALCULATE
temp' distnribution
T^n_j
$T^n_j = T^n_{j-1} + Q R_j$
IS
temp' difference ?
<=0.1
NO
REPLACEMENT
$T^o_j = T^o_j + 0.1$
YES
Procedure A
READ
vapour temperature
From Data-base
READ
fluid properties
CALCULATE
saturation pressure p(x)
CALCULATE
evaporator pool inside temp'
$T = f(p)$
MAKE
the first estimate T^o_j
From Data-base
READ
the fluid propeties
(averagetemp')
$(T^o_j + T^n_{j-1}) / 2$
CALCULATE
temp' distnribution T^n_j
$T^n_j = T^n_{j-1} + Q R_j$
* evaporator pool inside wall
* evaporator pool outside walll
IS
temp' difference ?
<=0.1
NO
REPLACEMENT
$T^o_j = T^o_j + 0.1$
YES
The same as Procedure A

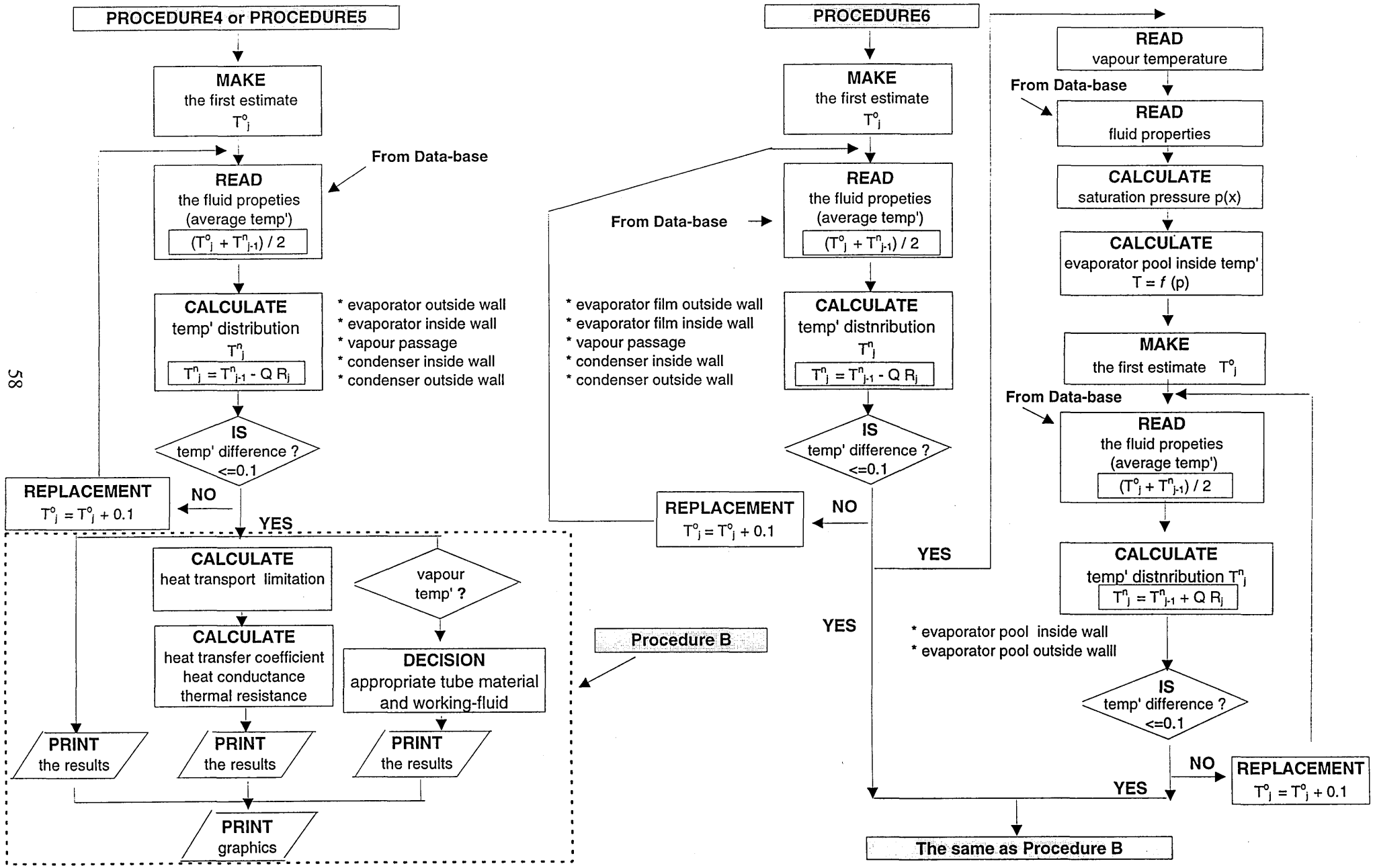
PROCEDURE4 or PROCEDURE5
MAKE
the first estimate
T^o_j
From Data-base
READ
the fluid propeties
(average temp')
$(T^o_j + T^n_{j-1}) / 2$
CALCULATE
temp' distribution
T^n_j
$T^n_j = T^n_{j-1} - Q R_j$
* evaporator outside wall
* evaporator inside wall
* vapour passage
* condenser inside wall
* condenser outside wall
IS
temp' difference ?
<=0.1
NO
REPLACEMENT
$T^o_j = T^o_j + 0.1$
YES
CALCULATE
heat transport limitation
CALCULATE
heat transfer coefficient
heat conductance
thermal resistance
vapour
temp' ?
DECISION
appropriate tube material
and working-fluid
PRINT
the results
PRINT
the results
PRINT
the results
PRINT
graphics
Procedure B
PROCEDURE6
MAKE
the first estimate
T^o_j
From Data-base
READ
the fluid propeties
(average temp')
$(T^o_j + T^n_{j-1}) / 2$
* evaporator film outside wall
* evaporator film inside wall
* vapour passage
* condenser inside wall
* condenser outside wall
CALCULATE
temp' distnribution
T^n_j
$T^n_j = T^n_{j-1} - Q R_j$
IS
temp' difference ?
<=0.1
NO
REPLACEMENT
$T^o_j = T^o_j + 0.1$
YES
READ
vapour temperature
From Data-base
READ
fluid properties
CALCULATE
saturation pressure p(x)
CALCULATE
evaporator pool inside temp'
T = f (p)
MAKE
the first estimate T^o_j
From Data-base
READ
the fluid propeties
(average temp')
$(T^o_j + T^n_{j-1}) / 2$
CALCULATE
temp' distnribution T^n_j
$T^n_j = T^n_{j-1} + Q R_j$
* evaporator pool inside wall
* evaporator pool outside walll
IS
temp' difference ?
<=0.1
NO
REPLACEMENT
$T^o_j = T^o_j + 0.1$
YES
YES
The same as Procedure B

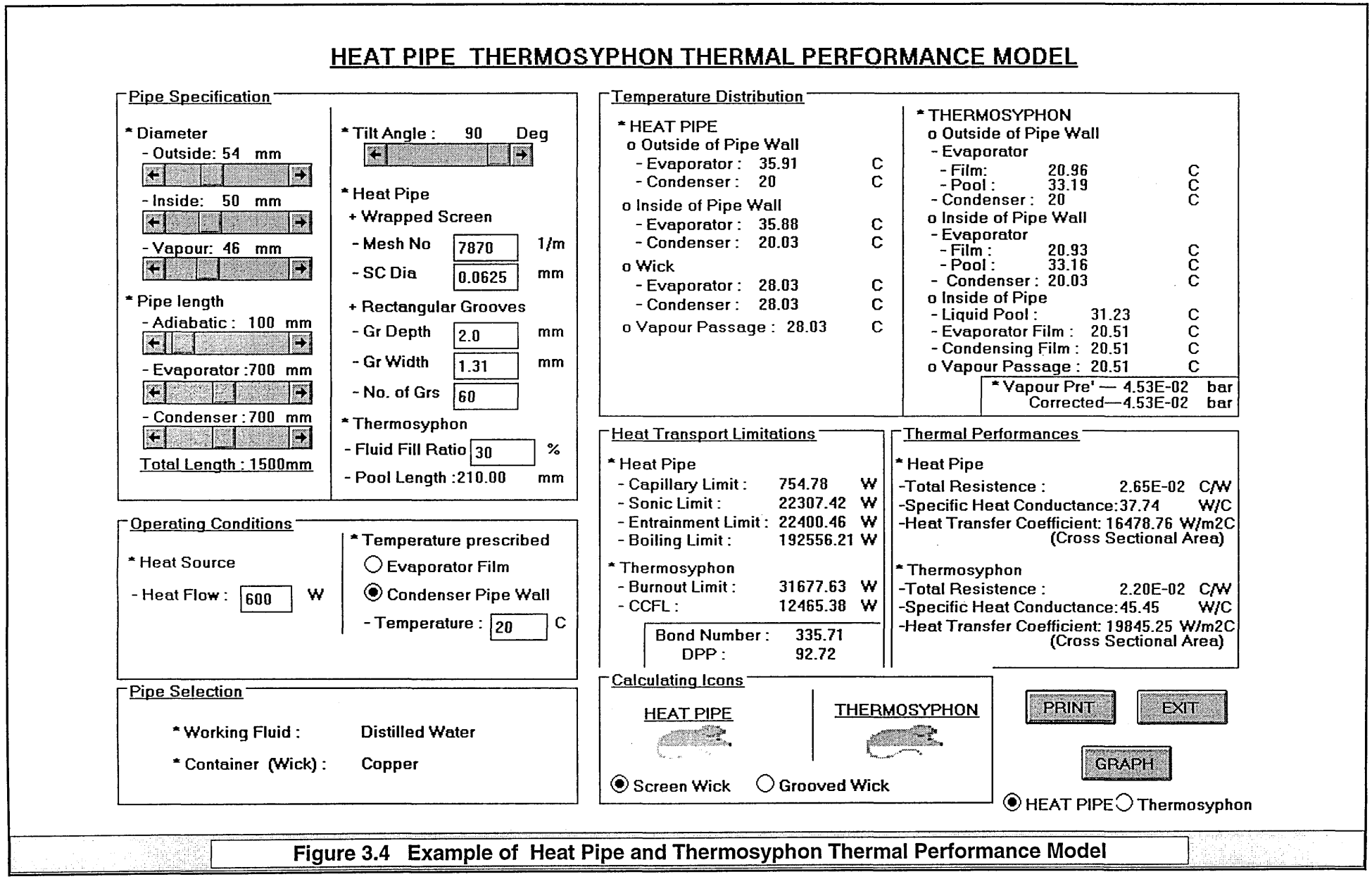

Figure 3.4 Example of Heat Pipe and Thermosyphon Thermal Performance Model

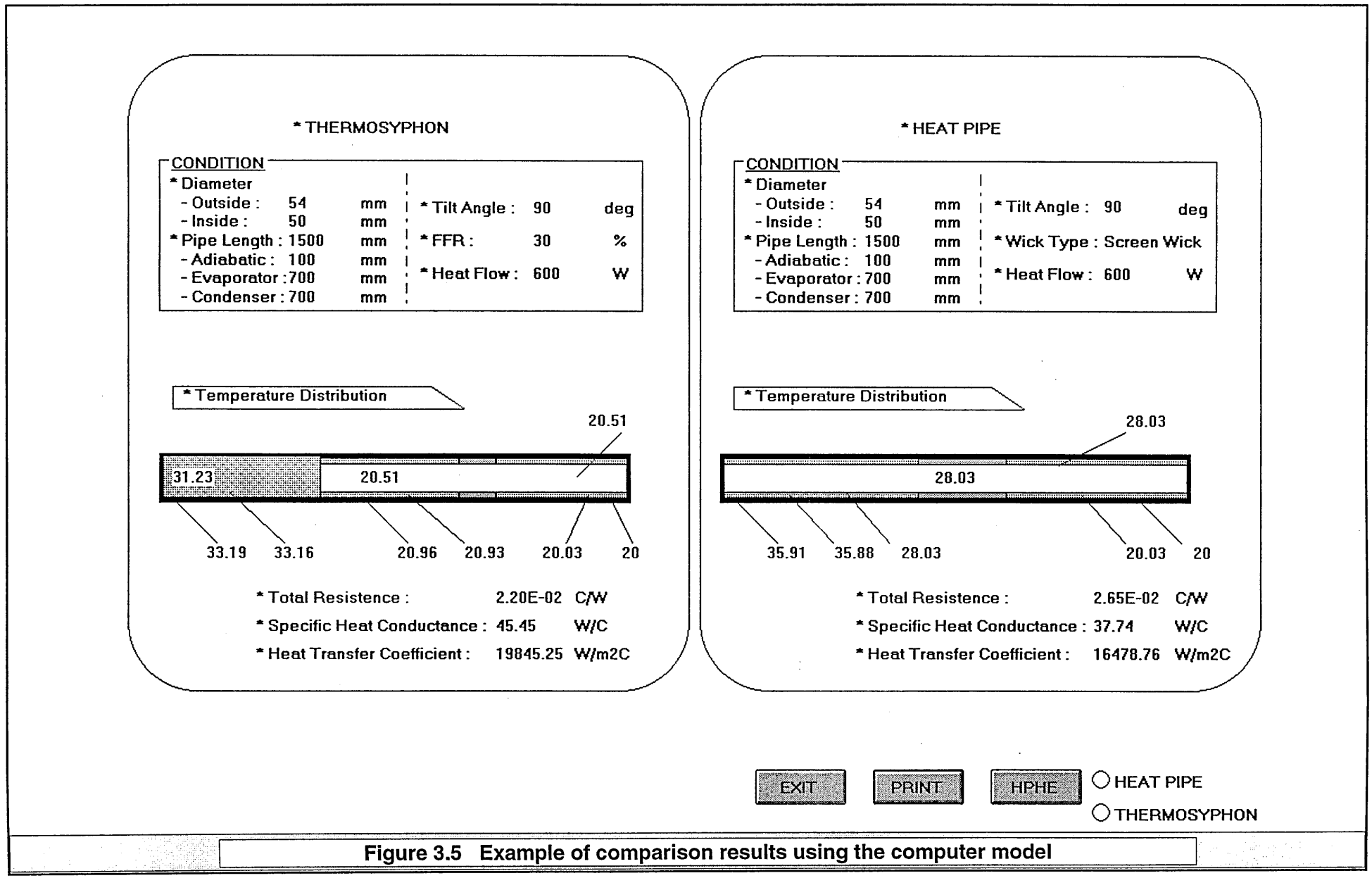

Figure 3.5 Example of comparison results using the computer model

3.2.2 Computer Program Notes

(a) The data-base file with working-fluid properties, wick and tube material properties can be incorporated.

(b) The program structure is as follows :

- This program is divided into two parts according to the known temperature (i.e. either evaporator or condenser outside wall temperature). The first option is prediction for temperature from condenser to evaporator, whereas the second option is from evaporator to condenser
- Each part above has three options (i.e. the selection for screen wick, grooved wick and thermosyphon). Each option predicts temperature distributions, heat-transport limitations, heat-transfer coefficients, heat conductance and thermal resistances.
- To solve the temperature distributions, thermal resistance model is employed. All properties are evaluated at average temperate between two point of thermal network (i.e. condenser outside wall and inside wall, condenser inside wall and vapour passage, vapour passage and evaporator inside wall, evaporator inside wall and outside wall). Figure 3.3 shows this procedure employing iteration technique for evaluating all properties at average temperature between two point, where the superscripts, n and o, represent the new and old value, respectively, during iteration.
- According to the temperature of vapour passage, appropriate tube and wick material and compatible working fluid can be selected.
- For predicting temperature distributions in the thermosyphon, the sequential order to thermal resistance model is different. The sequential order from condenser is condenser outside wall, condenser inside wall, vapour flow passage. From this point, one loop goes to evaporator film inside wall, evaporator film outside wall, and the other loop goes to evaporator pool inside, evaporator pool inside wall, evaporator pool outside wall. Whereas, the sequential order from evaporator is evaporator film outside wall, evaporator film inside wall, vapour flow passage. From

this point, one loop goes to condenser inside wall, condenser outside wall, and the other loop goes to evaporator pool inside, evaporator pool inside wall, evaporator pool outside wall.

- For calculating the inside temperature of evaporator pool in the thermosyphon, this program reads the calculated vapour temperature and change that temperature to correspondent vapour pressure in the database. After computing the equation (3.35), it scans corresponding saturation temperature according to the depth in the database.
- This computer program is directly connected to graphic mode to be able to compare thermal behaviours of heat pipe and thermosyphon easily.

(c) The equations used in this computer program for calculating thermal performances and heat transport limitations of heat pipe and thermosyphon are as follows :

- To predict temperature distributions (equation 3.1) , thermal resistance model presented in table 3.1 is used. In this program, total thermal resistance is calculated using equation (3.4), where, R_4, R_5, and R_6 are neglected because they are usually extremely small.
- The effective thermal conductivity of heat pipe is calculated by using equation (3.11) for wrapped-screen wick and equation (3.12) and (3.13) for condenser section and evaporator section of rectangular-grooved wick, respectively. In equation (3.11), wick porosity (ε) is calculated by the expression presented in Table 3.5.
- In case of thermosyphon, one program is developed by employing Table 3.3 for thermal resistances, and the other program is developed by using equation (3.14), (3.15), (3.16) and (3.17). In equation (3.14), 'g' is replaced by '$g \sin\theta$' for inclined thermosyphon tube. These equations can be expressed as the function of R using the relationship, $R = 1/(hA)$. For predicting inside temperature of evaporator pool, equation (3.34), (3.35), and (3.36) are used for each program.
- To model the capillary limitations, equation (3.18), (3.19), (3.20), and Table 3.5 are used. Frictional coefficient is computed by Figure 2.6 which is

changed from graph to numerical function for coding. For computing sonic limitation, equation (3.21) is used. In that equation, specific heat ratio (γ_v), molecular weight are applied 4/3, 18, respectively for water. Equation (3.24) and (3.27) are used for predicting entrainment limitation and boiling limitation. In those equations, the surface pore hydraulic radius, $r_{h,s}$, is applied by the equation (3.25), and (3.26) for wrapped-screen wick and rectangular-grooved wick, respectively, and the radius vapour bubble, r_n, is applied by 2.54×10^{-4} mm.

- To calculate the dry-out and burn-out limitation, equation (3.28) and (3.29) are used, respectively. In case of CCFL, equation (3.30) with f_1 as the function of the Bond number (see Figure 2.7 (a)), f_2 as a function of the dimensionless pressure parameter K_p (see equation 3.31), and f_3 as a function of the inclination angle of the thermosyphon and the Bond number (see Figure 2.7 (b)) is employed. Figure 2.7(a), and (b) are changed from graph to numerical function for coding.

CHAPTER 4 EXPERIMENTAL SET-UP AND PROCEDURE

In this chapter detailed design information about the test rig is provided, including specifications of the cooling assembly and the heat-supplying loop. The instrumentation for measuring temperatures and other control parameters, as well as the data acquisition system are detailed. The experimental procedure and measuring techniques for the present study are also presented.

4.1 DESIGN OF TEST APPARATUS

The general layout of test rig used for the present investigation is similar to that of El-Genk et al. (1995), which was employed for studying the transient behaviour of an inclined copper-water heat pipe. Figures 4.1 and 4.2 present a schematic diagram and a photograph of the experimental set-up, respectively. The main components of the test apparatus are the inclination test tube (i.e. the thermosyphon), an electric heater, a water chiller, a cooling-water jacket, an angle adjusting support frame and instrumentation for measuring temperatures, cooling-water mass flow rate, and electric power input. The specification of each component described in Table 4.1. As a working fluid,under the temperature characteristics of the present study, water or methanol is suitable. However, water has a better liquid transport and conductance properties than methanol. Compatible materials for water are copper,nickel and stainless steel but copper has superior conductance characteristic at the temperature range of interest. Copper is therefore selected as the material for container. The one end of the test tube is closed while the other end is equipped with a vacuum seal valve which provided connections to a mechanical vacuum pump and charging line of the working fluid.

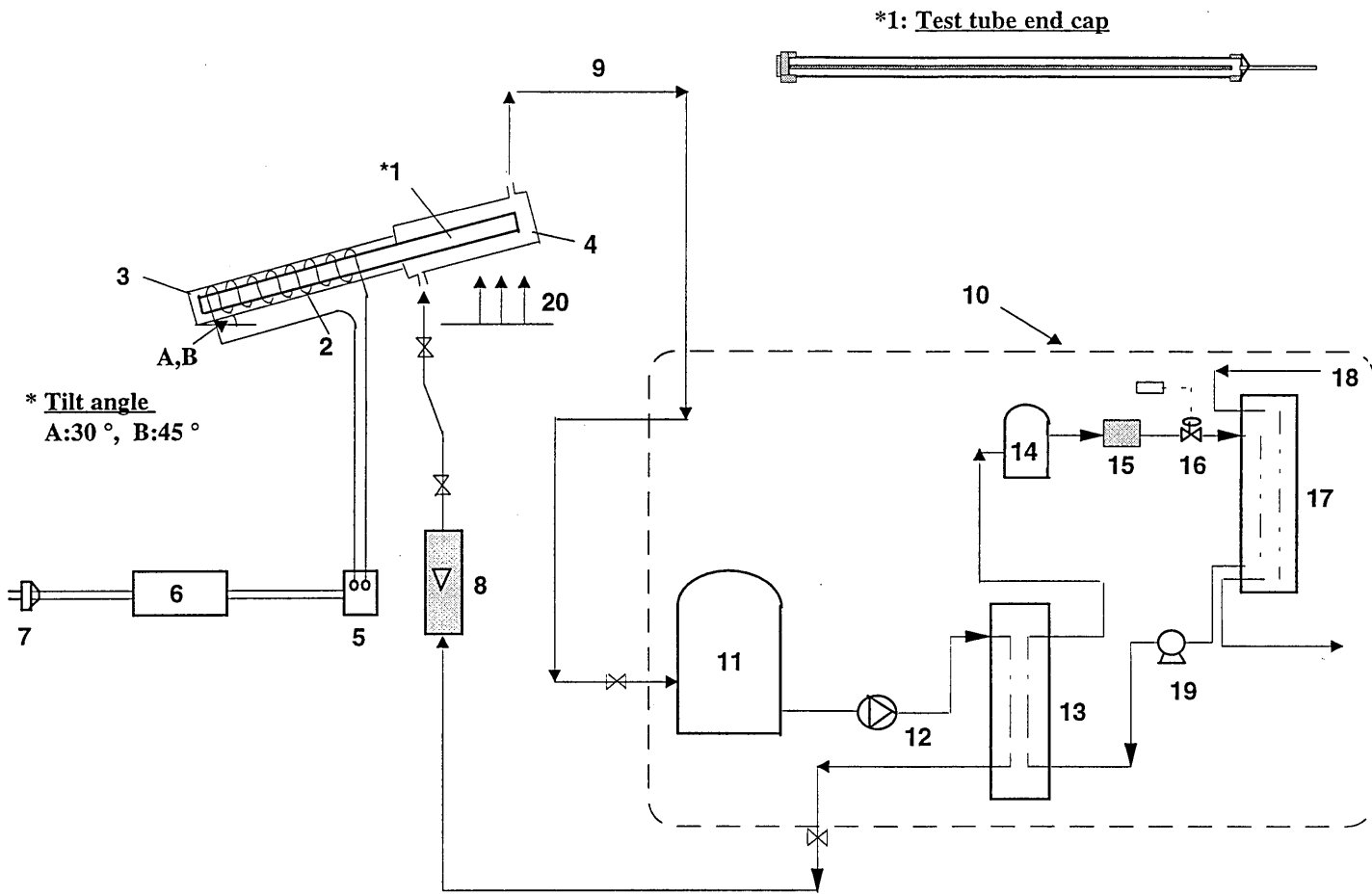

No	Description
1	Thermosyphon
2	Heater Tape
3	Thermal Insulation
4	Water Jacket
5	Watt Meter
6	Variable Transformer
7	Electric Plug
8	Rotameter
9	Cooling Water Pipe
10	Water Chiller
11	Water Tank
12	Cooling Water Pump
13	Heat Exchanger
14	Liquid Receiver
15	Filter / Dryer
16	Expansion Valve (TCV)
17	Heat Exchanger
18	Surrounding Water Circuit
19	Compressor
20	Angle Adjustment Support Frame

Figure 4.1 Schematic drawing of the experimental apparatus

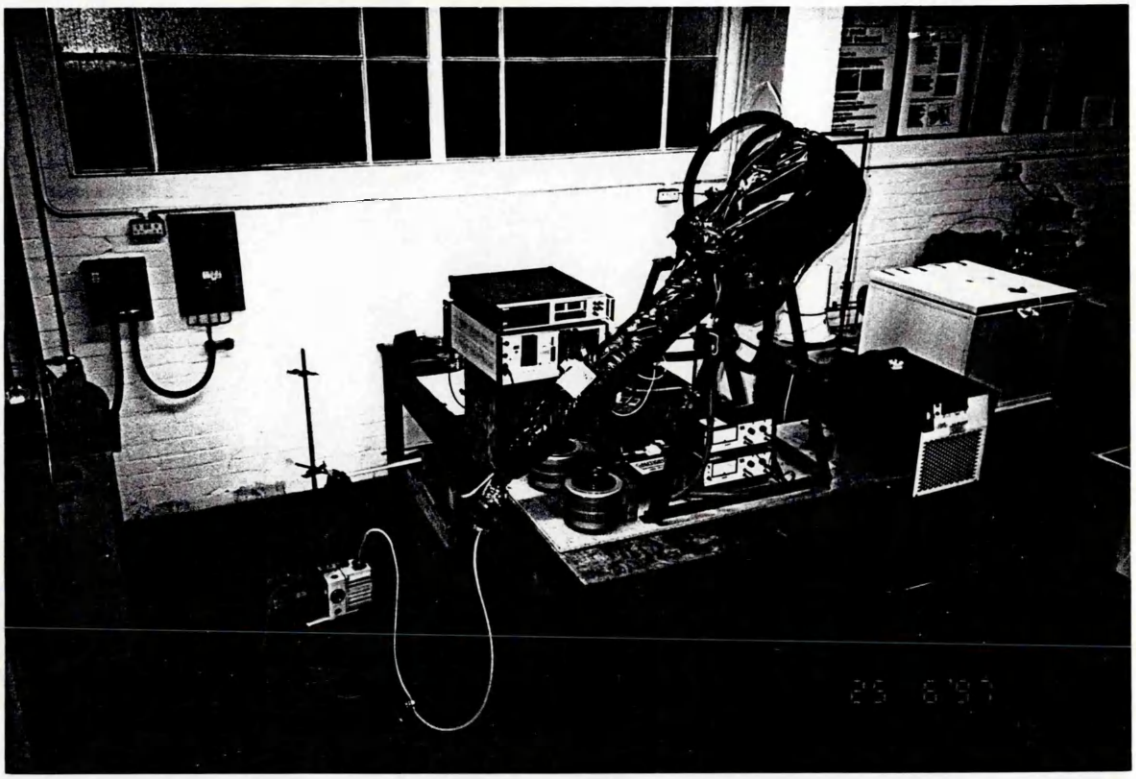

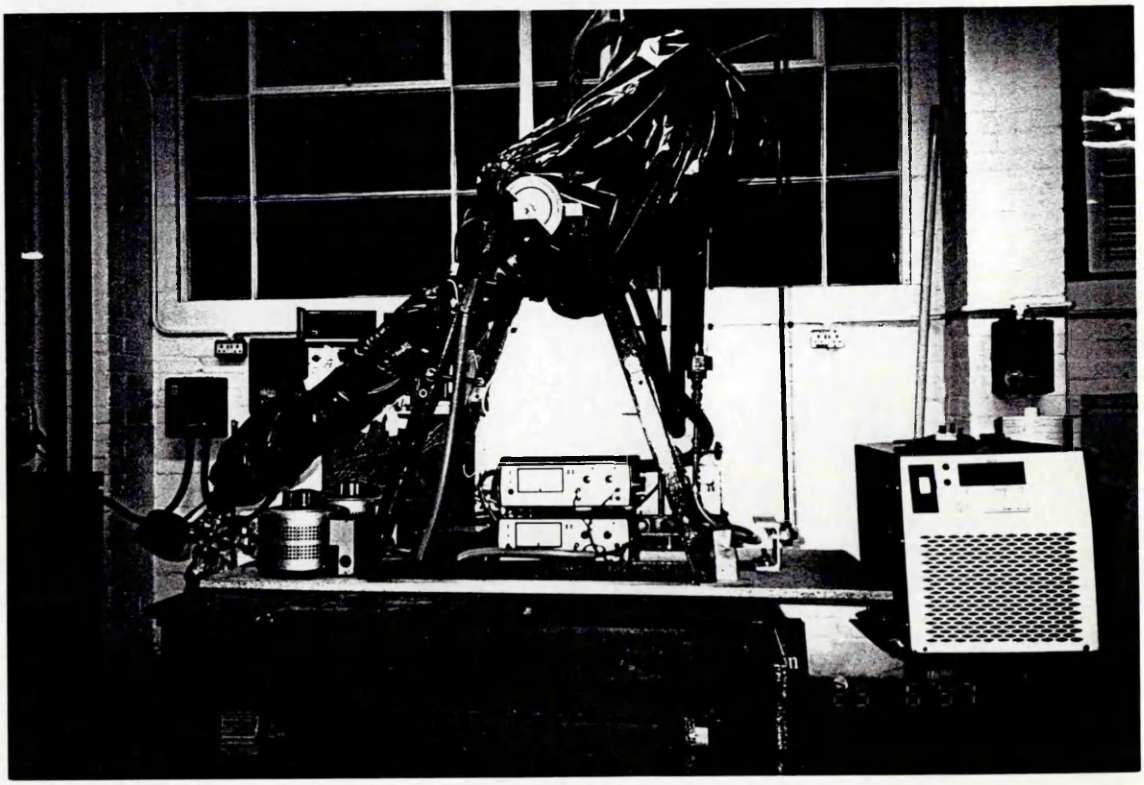

Figure 4.2 Photograph of the experimental apparatus

According to equation (3.28) for dry-out limitation, equation (3.29) for the burn-out limitation and equation (3.30) for the CCFL, this thermosyphon can be operated within electric power input, range from 200 to 600Watt.

Figure 4.3 presents the detailed design specification of the thermosyphon test tube. The evaporator section is much longer than the condenser section in order to allow accurate measurements of the axial vapour temperature distribution which are needed for the computer model verification.

The evaporator section is uniformly heated using a flexible, electric-heater tape, which is covered with silicon rubber insulation and capable of maintaining the test tube surface temperature at up to 80°C. To eliminate the heat losses, the main heater is carefully insulated by two layers of 6-mm thick ceramic-fibre blanket and then a guard heater tape is installed outside of the insulation to supplement for any heat losses. The guard heater tape is covered by three layers of the ceramic-fibre blanket. The electric-power input to the main and guard heaters are regulated by variable transformers.

Table 4.1 Specification for Test Apparatus

Description	Part No	Specification
Test Tube	1	* Outside Diameter : 54mm * Inside Diameter : 50mm * Wall Thickness : 2.0 mm * Total Length : 1350mm - Evaporator:850mm - Adiabatic section:100mm - Condenser:400mm * Working Fluid : Distilled Water * Container Material : Copper
Electric Heater Tape	2	* Thermal Output : 42 Watt/M (Flexible Tape) - Main heater : 16 meter - Guard heater : 4 meter
Watt Meter	5	* Measuring Range - Main heater:1000watt - Guard heater:200watt
Rotameter	8	* Mesuring range : 1363 litres/hour at 100% opening * Inlet & Outlet Diameter : 20mm
Cooling Water Pipe Line	9	* Diameter : 20mm * Material : Steel & Flexible tube
Water Chiller	10	
Cooling Capacity	-	* 20,290 KJ/h
Compressor	19	* 1.5 kW
Water Pump	12	* 0.37 kW
Pump Capacity	12	* 50 Litre/min at 1.5 bar
Tank Capacity	11	* 12 Litres

(Unit : mm)

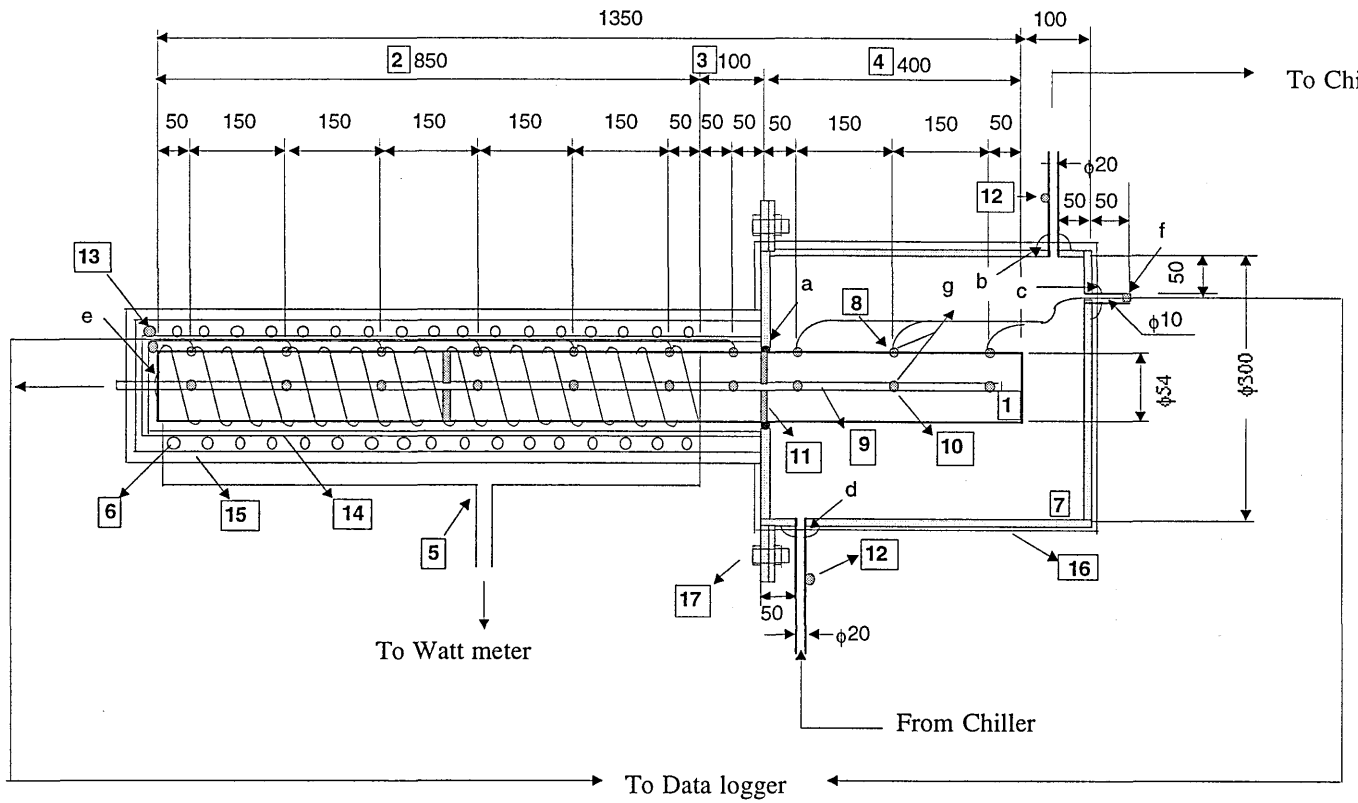

No	Description
1	Test Thermosyphon
2	Evaporating Section
3	Adiabatic Section
4	Condensing Section
5	Heater Tape
6	Guard Heater
7	Water Jacket
8	Wall Thermocouples
9	Vapour-Temperature Probe
10	Vapour Thermocouples
11	Probe Support Arm
12	Cooling Water Thermocouples
13	Thermocouples for Auxiliary Heating
14	Insulation (2 Layers of Blanket)
15	Insulation (3 Layers of Blanket)
16	Insulation (1 Layer of Blanket)
17	Flange
a	Adapter Flange
b	Welding
c	Welding
d	Welding
e	Sealing (Sealants)
f	Sealing (Sealants)
g	Soldering

Figure 4.3 Thermosyphon test apparatus

Figure 4.4 details the cross section of the evaporator. The heat transported from the evaporator is removed at the condenser by a cooling water jacket. A water chiller is used to control the cooling-temperature. The chiller is a self contained unit which provides cooling water at a constant temperature under varying load conditions and consists of two separate systems (i.e. the primary-refrigeration and chiller-water circuits), which are coupled through a heat exchanger. The instrumented test tube is mounted on a specially devised support frame with a special arrangement for adjusting its inclination angle.

4.2 INSTRUMENTATION

The vapour temperature is measured along the centre-line of the thermosyphon by using a special probe made of a thin-wall, brass tube of 6.35mm outside diameter, an contain 10 T-type thermocouples (see Figure 4.5). The thermocouples, T_{v1}-T_{v10}, in the probe are used to measure the vapour temperature at different axial locations of the thermosyphon. The thermocouples were inserted into the probe shell and pulled out through small holes along the probe wall. The thermocouples were then soldered on the outer surface of the probe wall, but their ends were kept about 0.1mm above the probe wall surface to directly measure the vapour temperature. An additional 10 thermocouples are attached to the outer surface of the thermosyphon tube to measure its temperature at the same axial locations as the vapour temperature thermocouples.

Two T-type thermocouples are employed for measuring the inlet and outlet temperature of cooling water in the water jacket. Two other T-type thermocouples are placed in the ceramic fibre blanket insulation of the evaporator section to determine the surface heat losses by natural convection to ambient. The temperature deviation between two thermocouples is directly measured by a microprocessor voltmeter which operates the guard heater.

(Unit : mm)

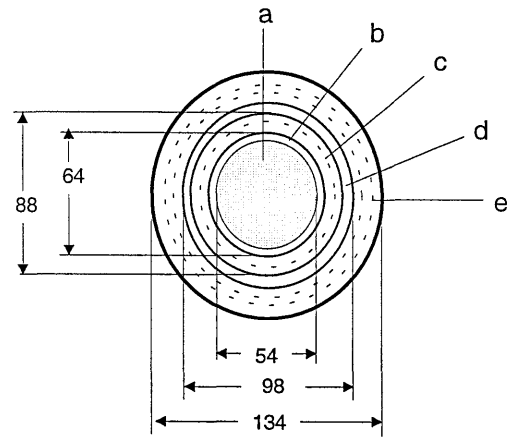

a: Thermosyphon
b: Main heater tape (t:5mm)
c: Ceramic-fibre blanket (2 layers)
d: Guard heater tape
e: Ceramic fibre blanket (3 layers)

Figure 4.4 Cross section of evaporator

(Unit : mm)

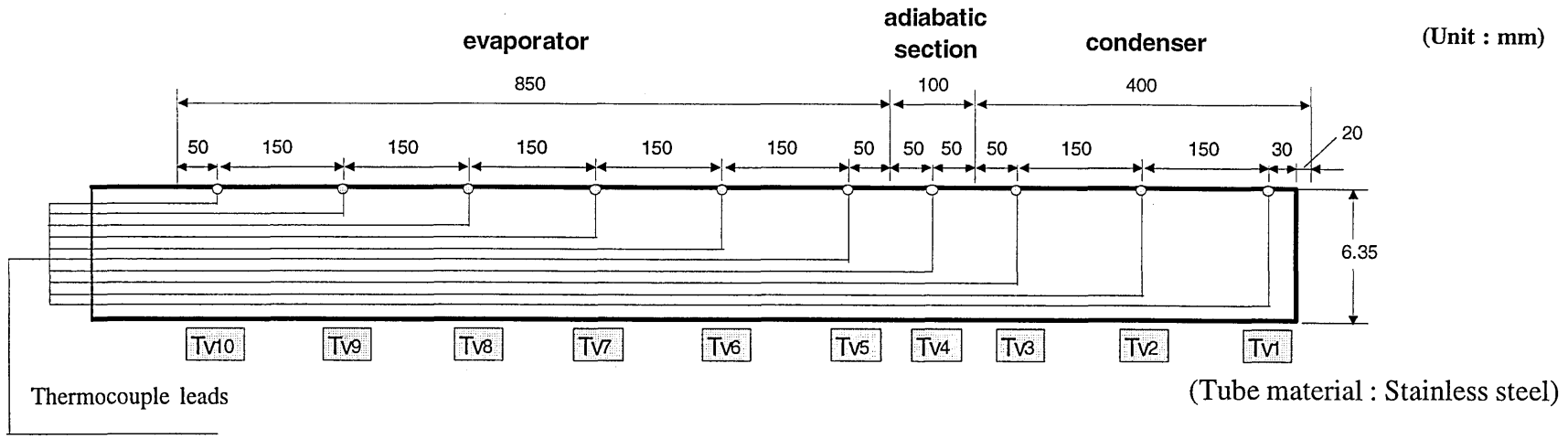

Figure 4.5 Longitudinal cross section of the vapour temperature probe

To monitor the 22 thermocouples readings above, a data logger, Fluke Model 2200B is used. Temperature measurement is assigned to an interval scan mode, which allows the single scan sequence to be repeated at a programmed time interval. The time interval of 5 minutes was programmed to allow also studying the transient behaviour of the thermosyphon.

The electric power inputs to the heaters of the evaporator section are measured using wattmeters and regulated by variable transformers. Full-scale reading of the wattmeters for main and guard heaters were adjusted to 1000Watt and 200Watt, respectively. The mass flow rate of the cooling water flowing through the water jacket, surrounding the condenser section of the thermosyphon, is measured by a rotameter which has a full scale of 1363 litre/hour.

The overall energy transfer rate by the thermosyphon test tube can be measured either by measuring the rate of energy added by the main electric heater tape or by measuring the rate of energy removed by the cooling water.

4.3. EXPERIMENTAL PROCEDURE

Figure 4.6 Schematic drawing for test tube evacuation and filling

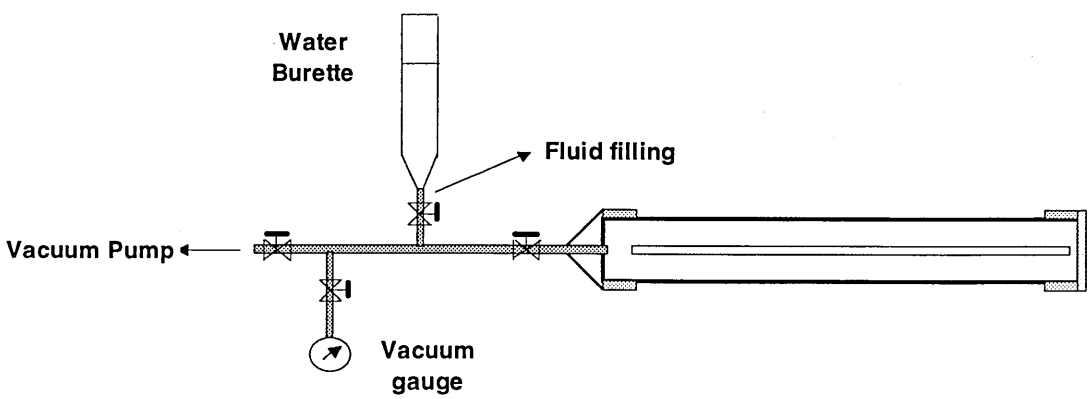

Before starting the actual testing, the thermosyphon tube was cleaned and rinsed with water. A leak test was then performed under vacuum. After the system has been evacuated, the thermosyphon was charged the necessary

amount of the working fluid (i.e. distilled water) for the required fill-charge ratio (see Figure 4.6). In order to examine that no non- condensible gases exist in the tube, the thermosyphon was operated, with the electric heater at a suitable power level, and measurements of the inside axial temperature distribution examined. In this study, the fluid fill charge ratio (FFCR) is defined as the volume of the working fluid in the tube to the inside volume of the evaporator section.

Experimental procedure for present study is described in Table 4.2. The thermosyphon tube which was charged with 30% of FFCR of distilled water was carefully tilted to 30 degree from the horizontal position. At that inclination angle, electric heater power was applied to the evaporator and controlled power input at 200Watt. Condenser cooling water was adjusted to obtain 20°C by controlling water chiller and temperature measurement was assigned to an interval scan mode, the time interval of 5 minutes.

Table 4.2 Experimental Procedure

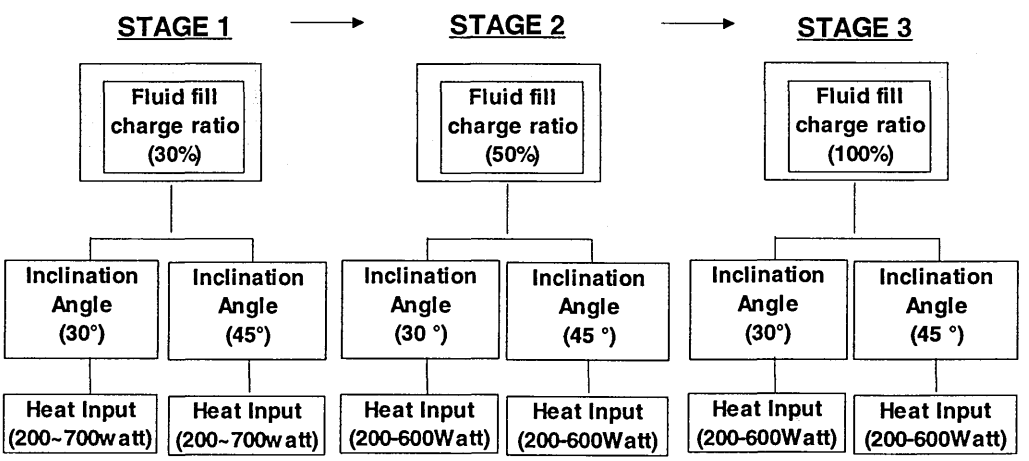

*** Operating Conditions**

Fluid Fill Charge Ratio (%)	Input Electric Power (Watt)	Inclination Angle (Deg)	Cooling Water Temperature (°C)
30 , 50 100	200 - 600	30 45	20

Once steady state operating conditions were reached, cooling water flow rate was measured.

The same experiments were repeated at 300Watt, 400Watt, 500Watt, and 600Watt of electric power input. After all of data were measured at 30 degree of inclination angle for each experiment, the test tube was tilted to 45 degree. At that tilted angle, the same experiments were repeated at 200Watt, 300Watt, 400Watt, 500Watt, and 600Watt of electric power input.

The same procedures were performed at 50% and 100% of FFCR of distilled water and the same data were checked for each experiment.

CHAPTER 5 EXPERIMENTAL RESULTS AND DISCUSSION

In this chapter, the results of the experimental investigation of the steady-state behaviour of the thermosyphon are presented. These results are compared with the corresponding predictions of the computer model developed. The influences of the fluid fill charge ratio (FFCR), heat-supply rate to the evaporator, inclination angle, and the hydrostatic pressure in the pool are discussed.

5.1 EXPERIMENTAL RESULTS

The behaviour of the thermosyphon tested was investigated for FFCRs of 30, 50 and 100%, heat supply-rate to the evaporator in the range of 200 to 600W, and inclination angles of 30 and 45°. The overall heat-transfer rate through the tube was measured as the rate of energy added by the main electric heater to the evaporator or the rate of energy removed by the cooling water flowing through the jacket surrounding the condenser. It was observed that the deviations between these two values are measured within $\pm$ 5%.

Figure 5.1 and 5.2 present the working-fluid and outside-wall temperature variations. The value of the temperature at any location along the thermosyphon is the mean value of 4 recordings (with 5minutes interval) after the steady state operating conditions were reached (see Table 5.1). The results show that :

- Vapour temperature distributions are almost uniform, particularly at high heat-supply rate ($Q \geq 500W$). The fluctuations in vapour temperature are more apparent with the increase in the inclination angle from 30 to 45°.
- Saturation temperatures are varied due to hydrostatic height in the evaporator pool.

- For the 30 and 50% FFCRs, the outside wall temperature peaked within the evaporator-film section of the thermosyphon.

Figure 5.3 shows the experimentally-determined heat-transfer coefficients at the condenser, evaporator film, and evaporator pool sections of the thermoshphon tested. These coefficients were determined by employing the mean temperature difference between the working-fluid and the wall of the tube in the sections considered. The lines represent the least-square best fit of the experimental points. These results indicated that :

- The highest heat-transfer coefficients were achieved in the condenser, whereas the worst heat-transfer coefficients occurred in the evaporator-film section of the thermosyphon.
- The highest overall heat transfer coefficient can be achieved under 30% FFCR and 600W heat-supply rate to the evaporator.

Figure 5.1 (a) Working-Fluid Temperature Variations

(Fluid fill charge ratio : 30% , Tilt angle : 30°)

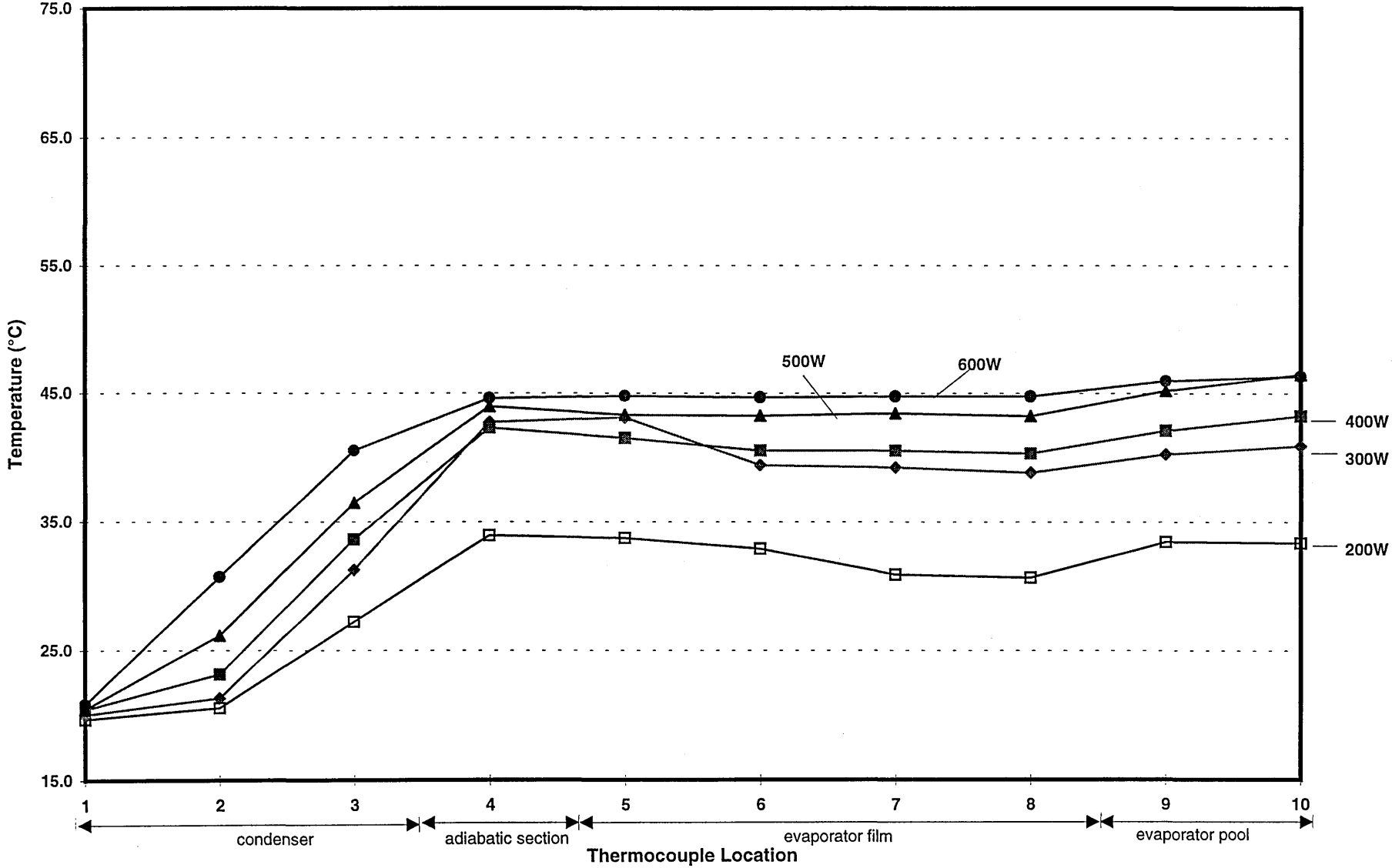

Figure 5.1 (b) Working-Fluid Temperature Variations
(Fluid fill charge ratio : 30% , Tilt angle : 45°)

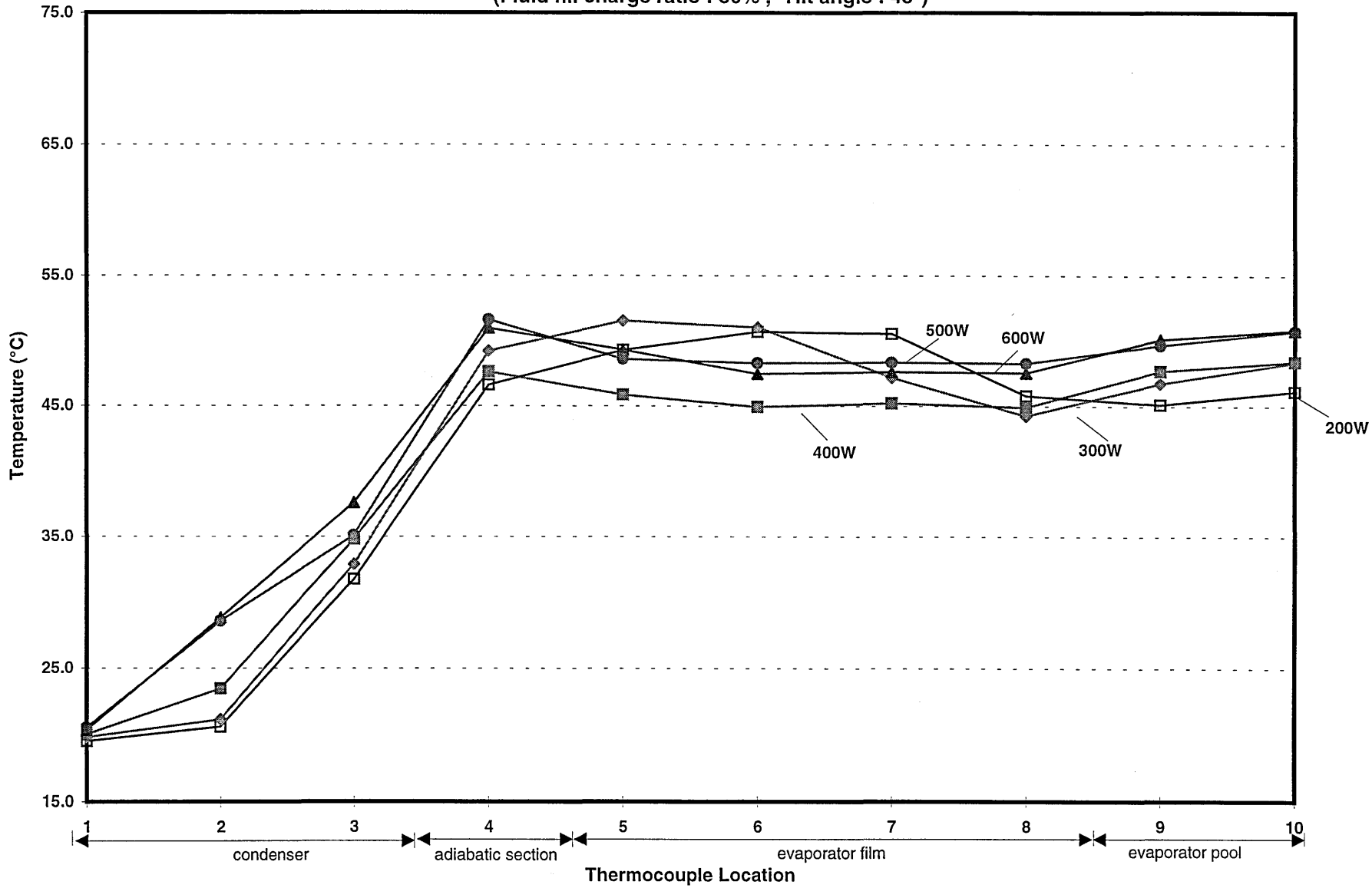

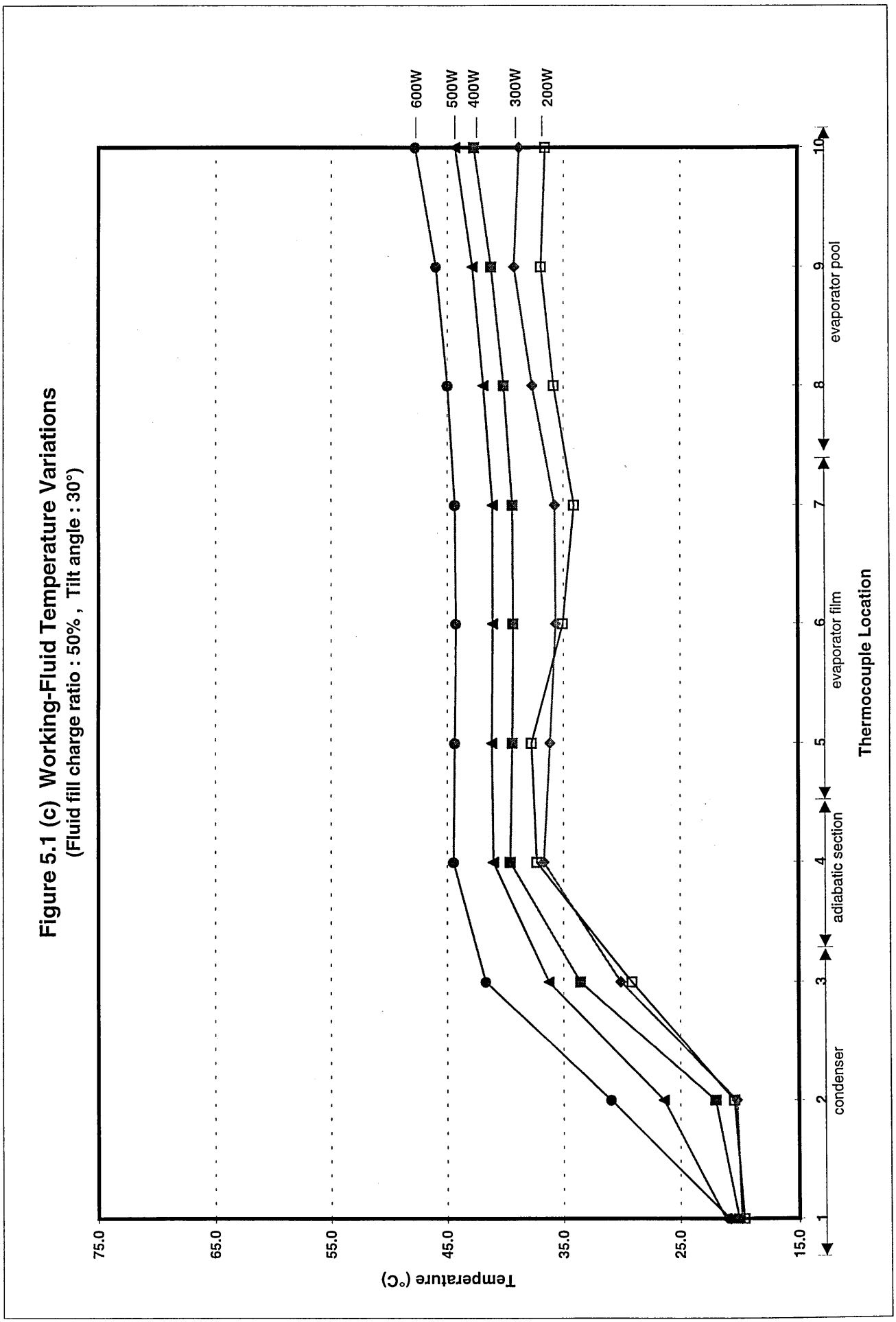
Figure 5.1 (c) Working-Fluid Temperature Variations
(Fluid fill charge ratio : 50% , Tilt angle : 30°)
600W
500W
400W
300W
200W
75.0
65.0
55.0
45.0
35.0
25.0
15.0
Temperature (°C)
1
2
3
4
5
6
7
8
9
10
condenser
adiabatic section
evaporator film
evaporator pool
Thermocouple Location

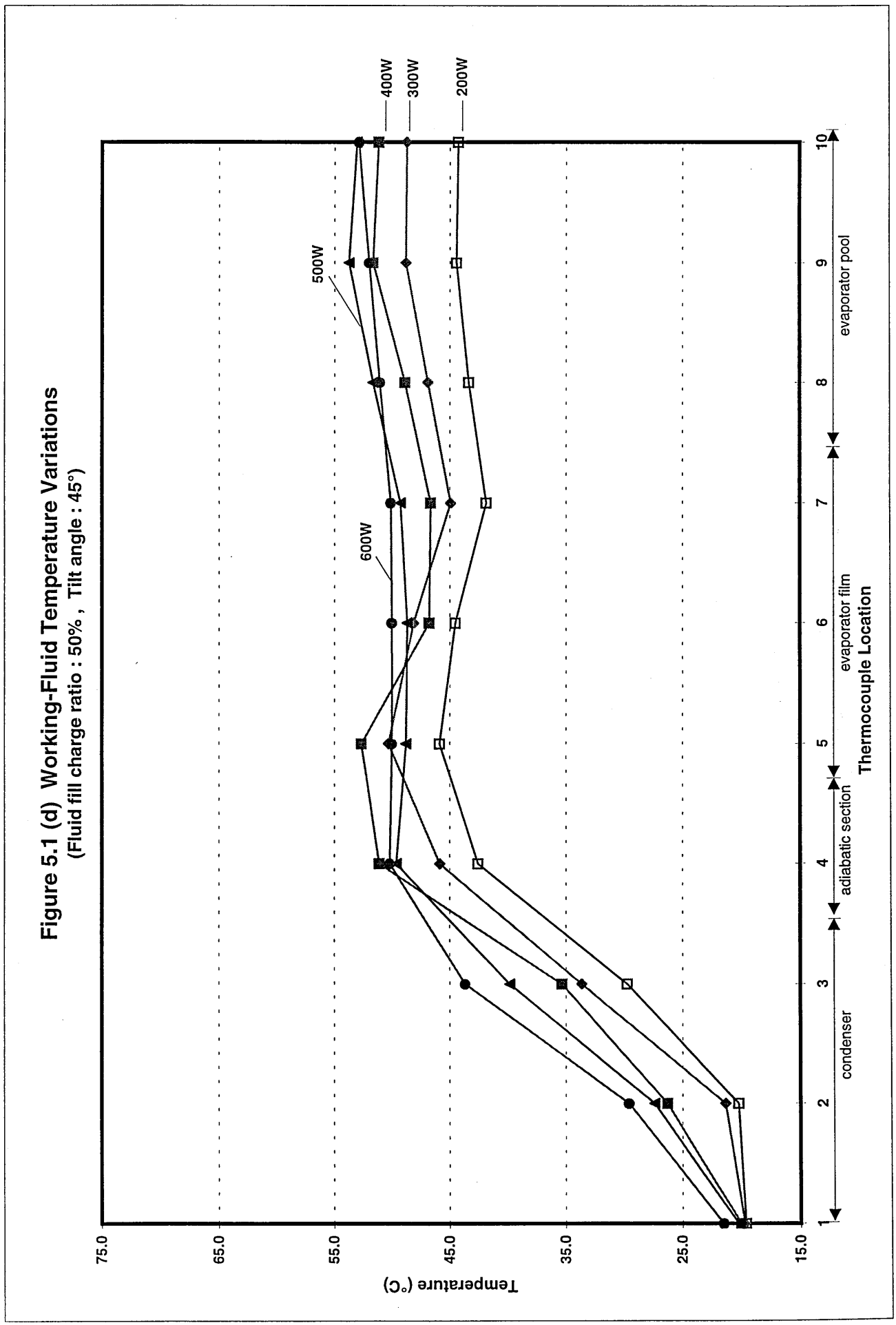
Figure 5.1 (d) Working-Fluid Temperature Variations
(Fluid fill charge ratio : 50% , Tilt angle : 45°)
400W
300W
200W
500W
600W
75.0
65.0
55.0
45.0
35.0
25.0
15.0
Temperature (°C)
1
2
3
4
5
6
7
8
9
10
condenser
adiabatic section
evaporator film
evaporator pool
Thermocouple Location

Figure 5.1 (e) Working-Fluid Temperature Variations
(Fluid fill charge ratio : 100% , Tilt angle : 30°)

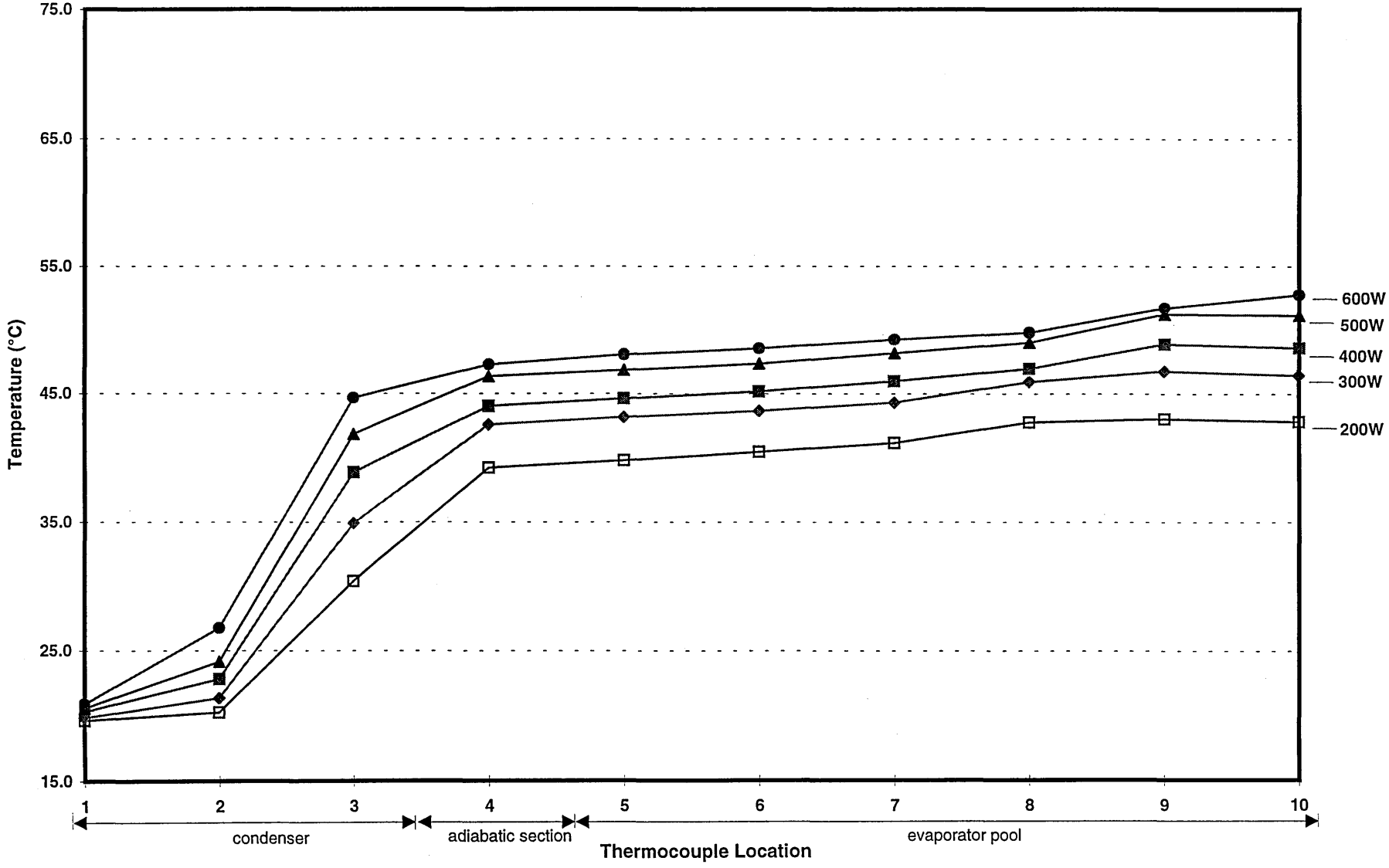

Figure 5.1 (f) Working-Fluid Temperature Variations
(Fluid fill charge ratio : 100% , Tilt angle : 45°)

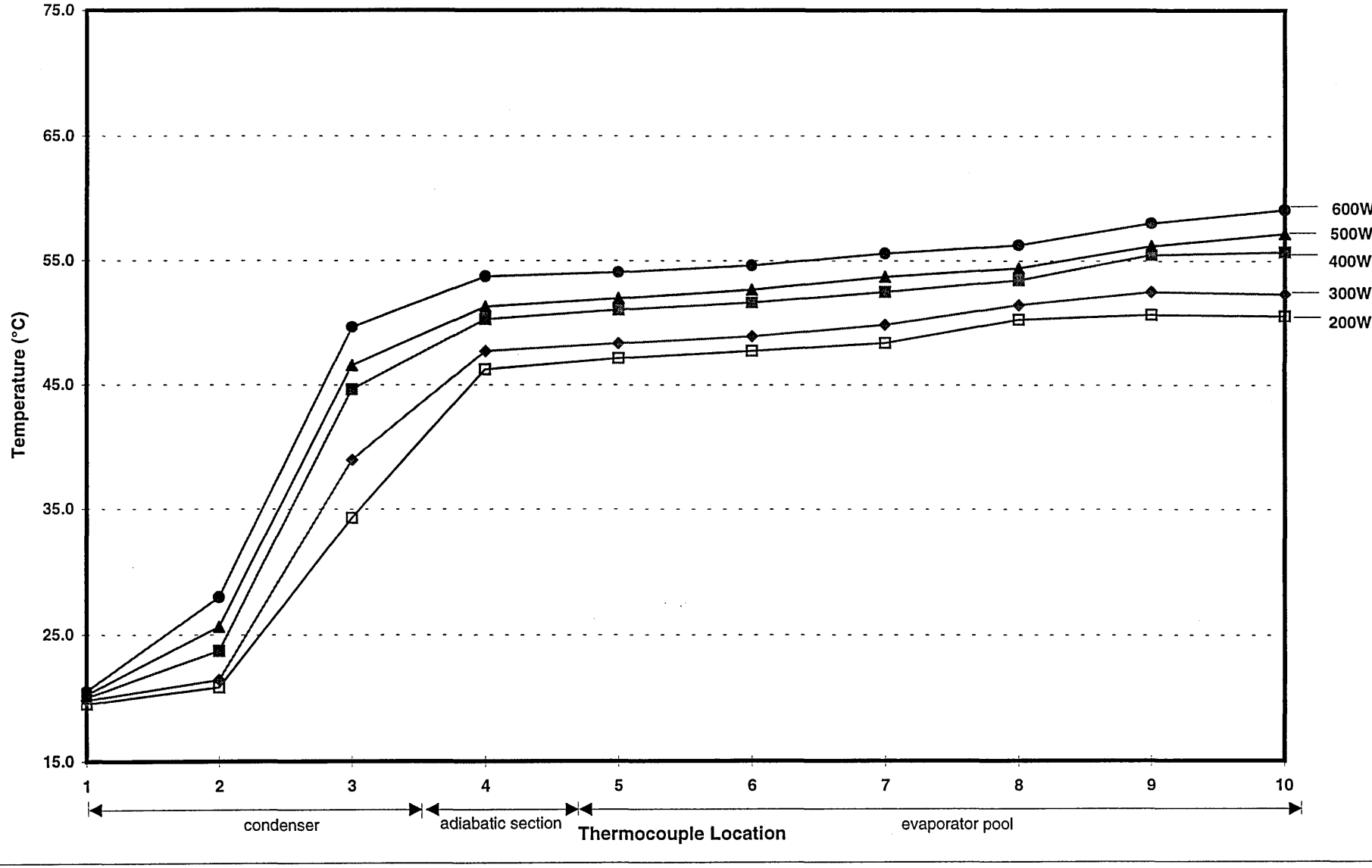

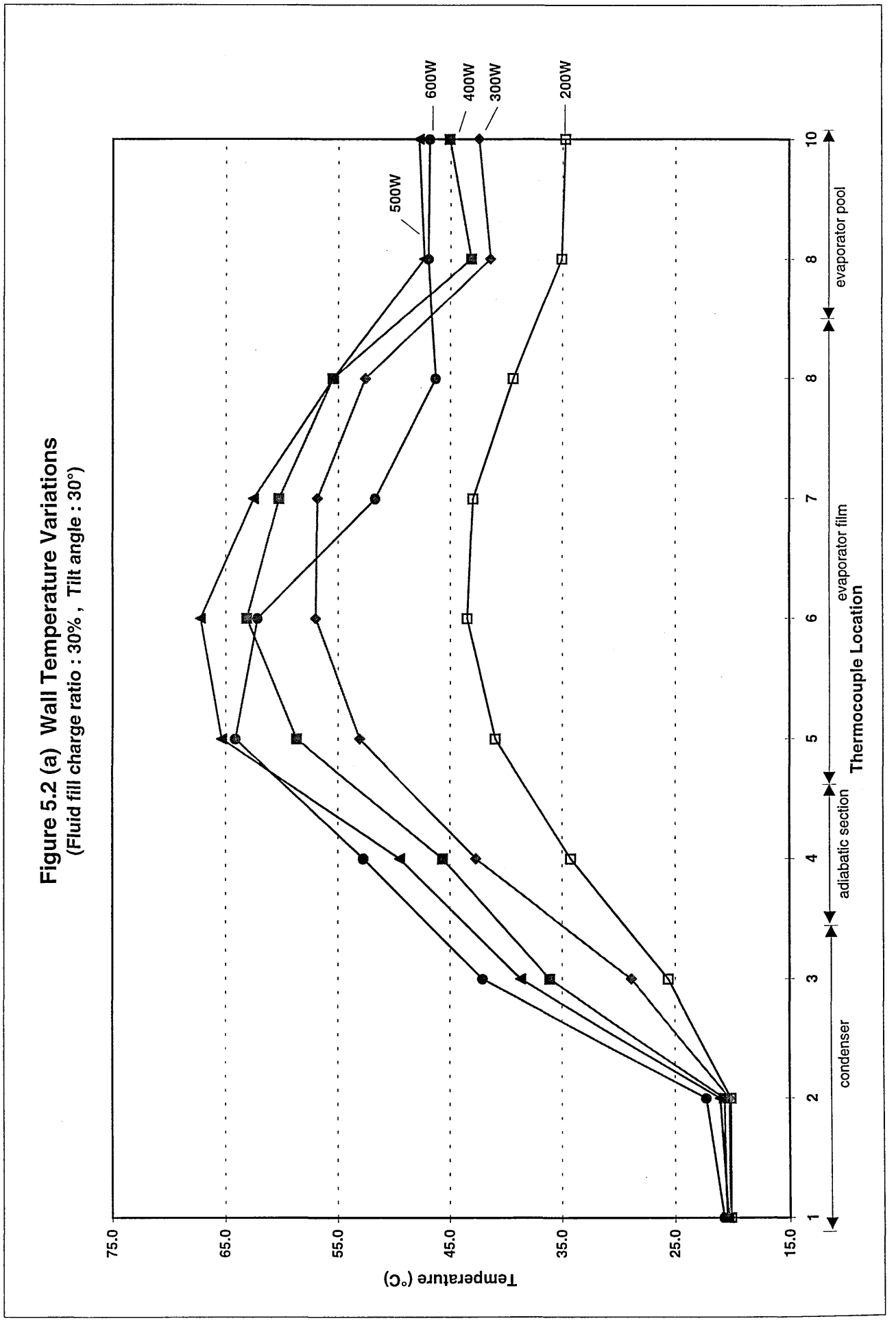

Figure 5.2 (a) Wall Temperature Variations
(Fluid fill charge ratio : 30% , Tilt angle : 30°)

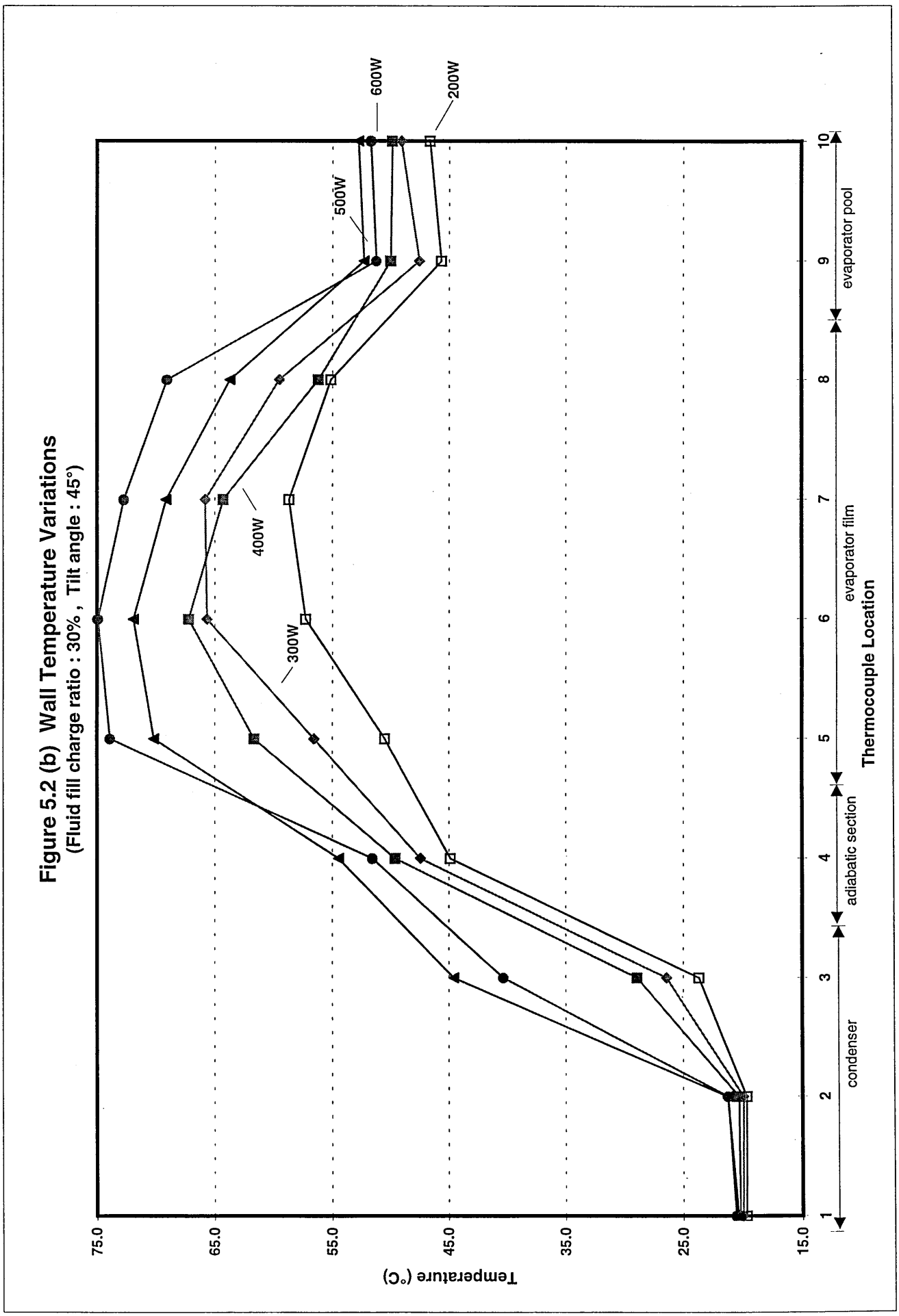
Figure 5.2 (b) Wall Temperature Variations
(Fluid fill charge ratio : 30% , Tilt angle : 45°)
600W
500W
400W
300W
200W
Temperature (°C)
75.0
65.0
55.0
45.0
35.0
25.0
15.0
1
2
3
4
5
6
7
8
9
10
condenser
adiabatic section
evaporator film
evaporator pool
Thermocouple Location

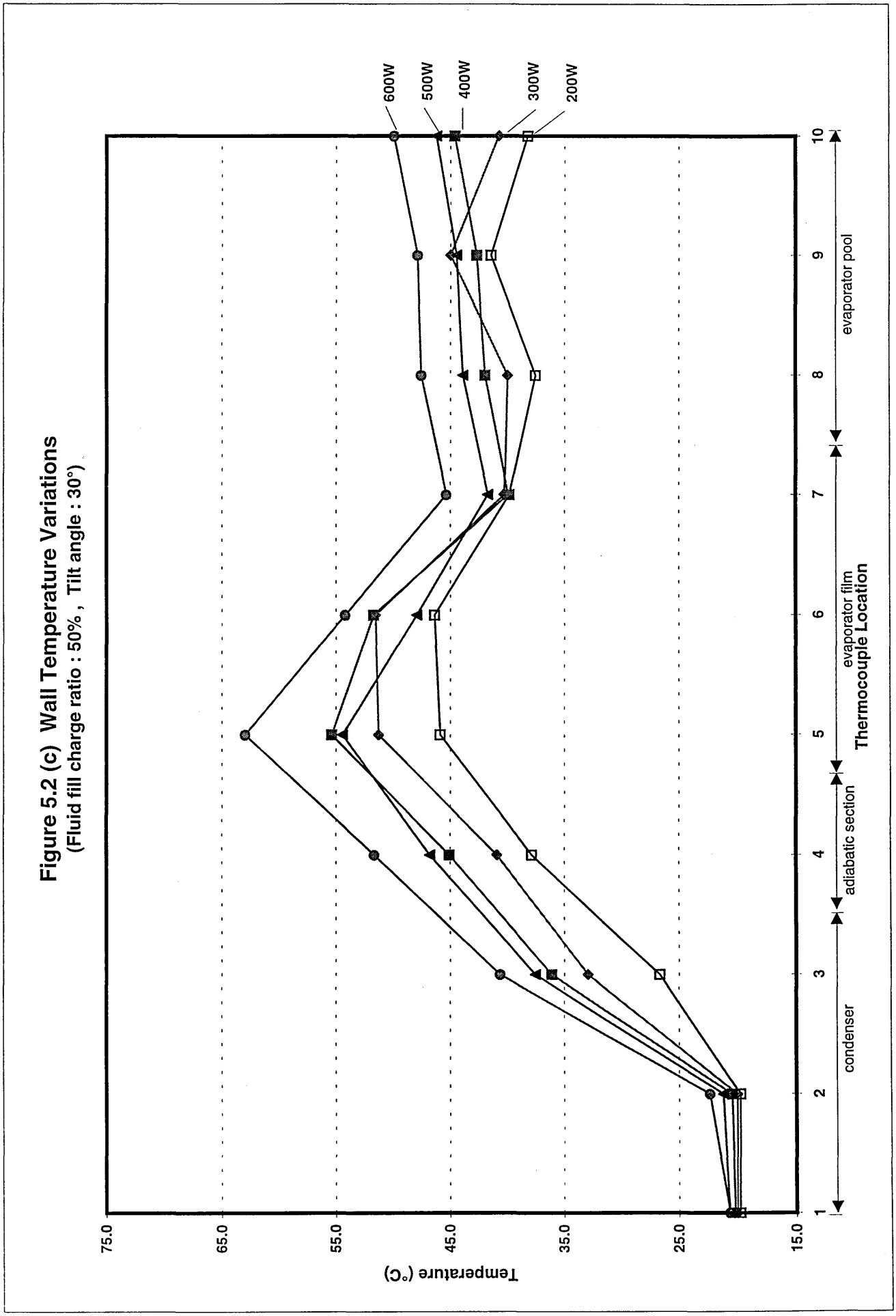

Figure 5.2 (c) Wall Temperature Variations
(Fluid fill charge ratio : 50%, Tilt angle : 30°)

Figure 5.2 (d) Wall Temperature Variations
(Fluid fill charge ratio : 50% , Tilt angle : 45°)

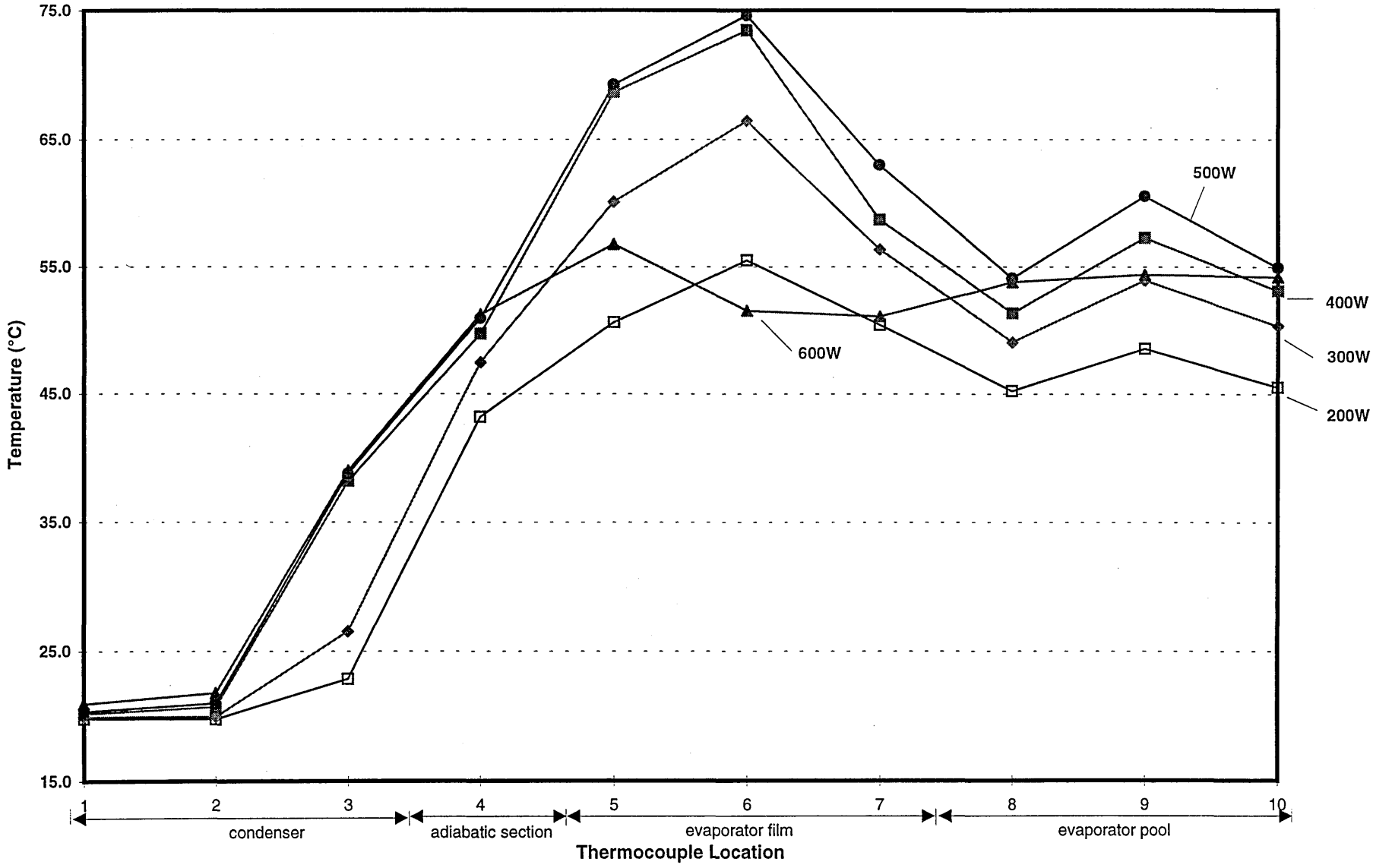

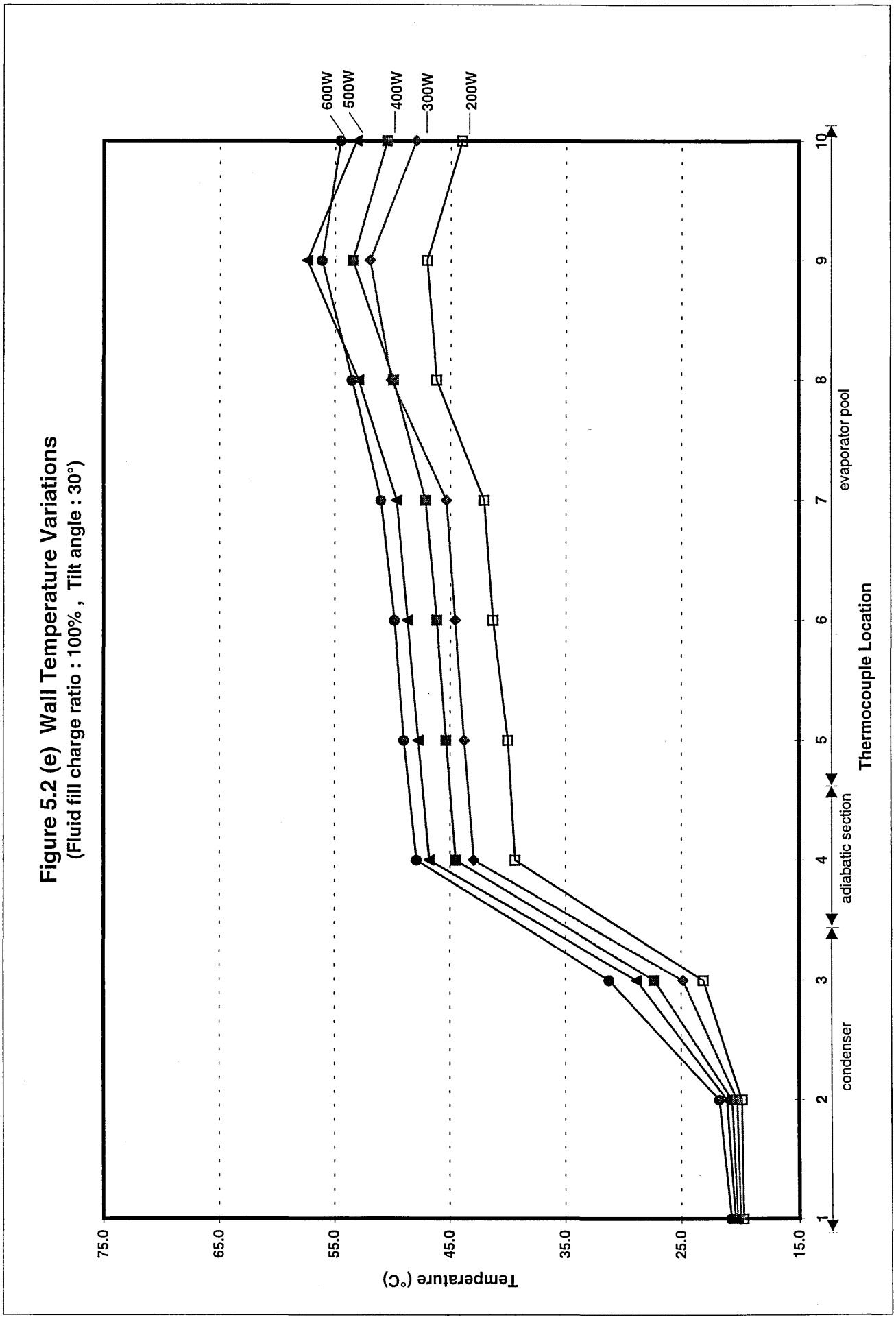

Figure 5.2 (e) Wall Temperature Variations
(Fluid fill charge ratio : 100% , Tilt angle : 30°)

Figure 5.2 (f) Wall Temperature Variations
(Fluid fill charge ratio : 100% , Tilt angle : 45°)

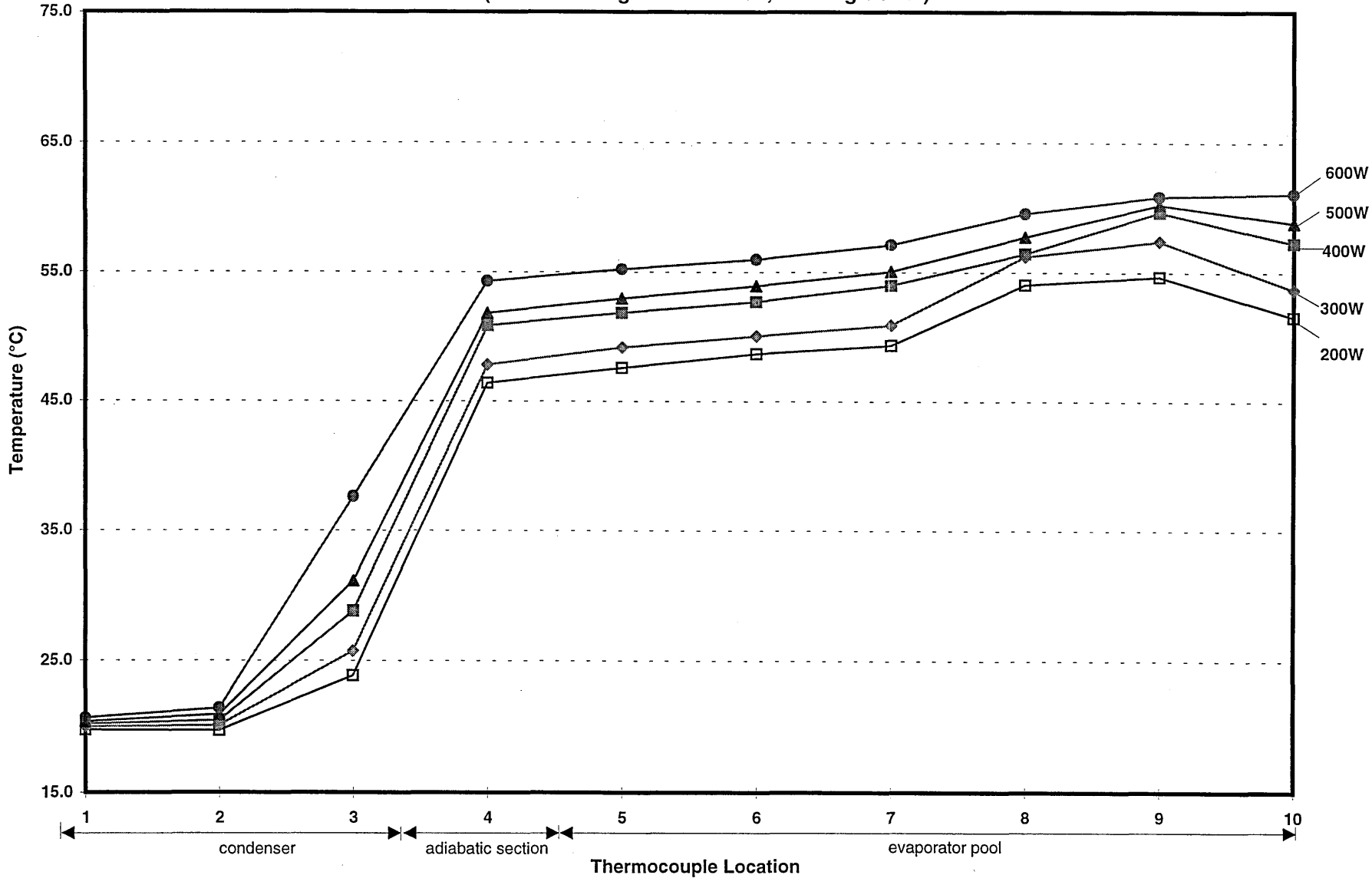

Figure 5.3 (a) Heat Transfer Coefficient in the Condenser
(Tilt Angle : 30°)

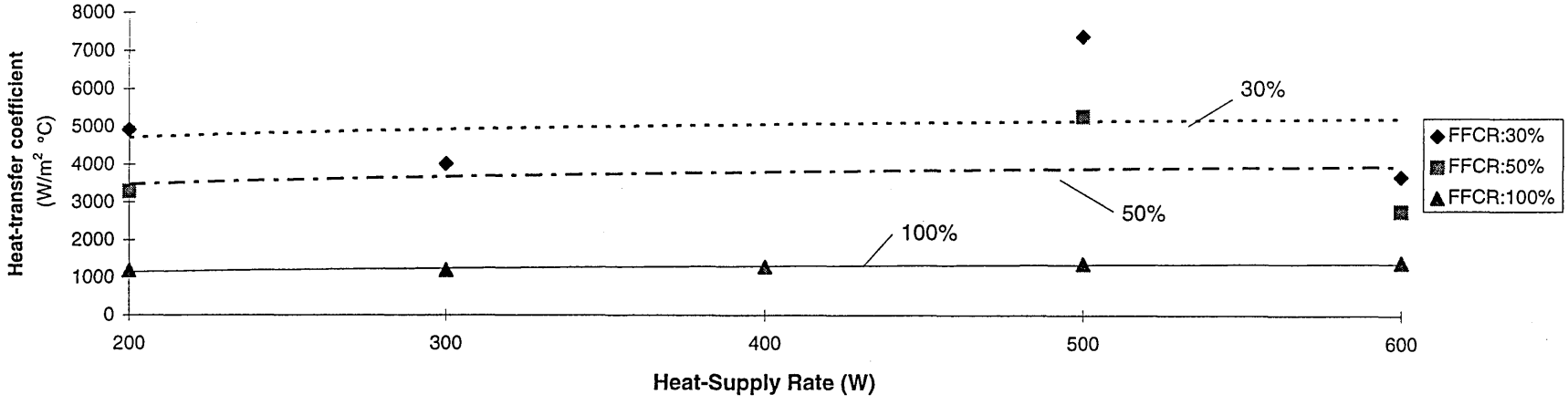

Figure 5.3 (b) Heat Transfer Coefficient in the Condenser
(Tilt Angle : 45°)

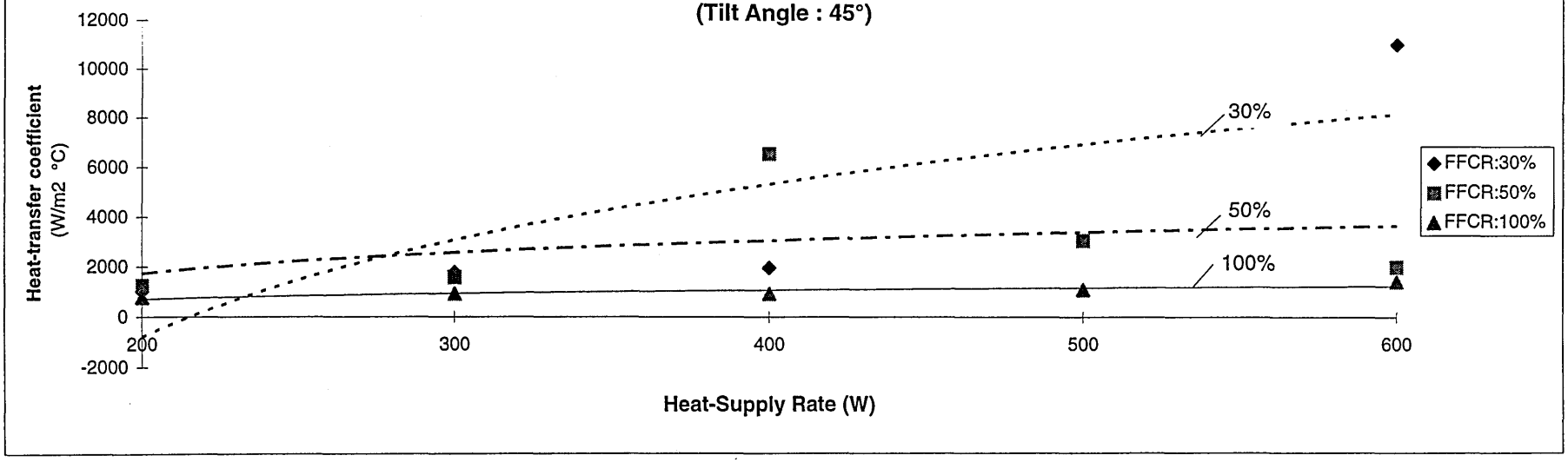

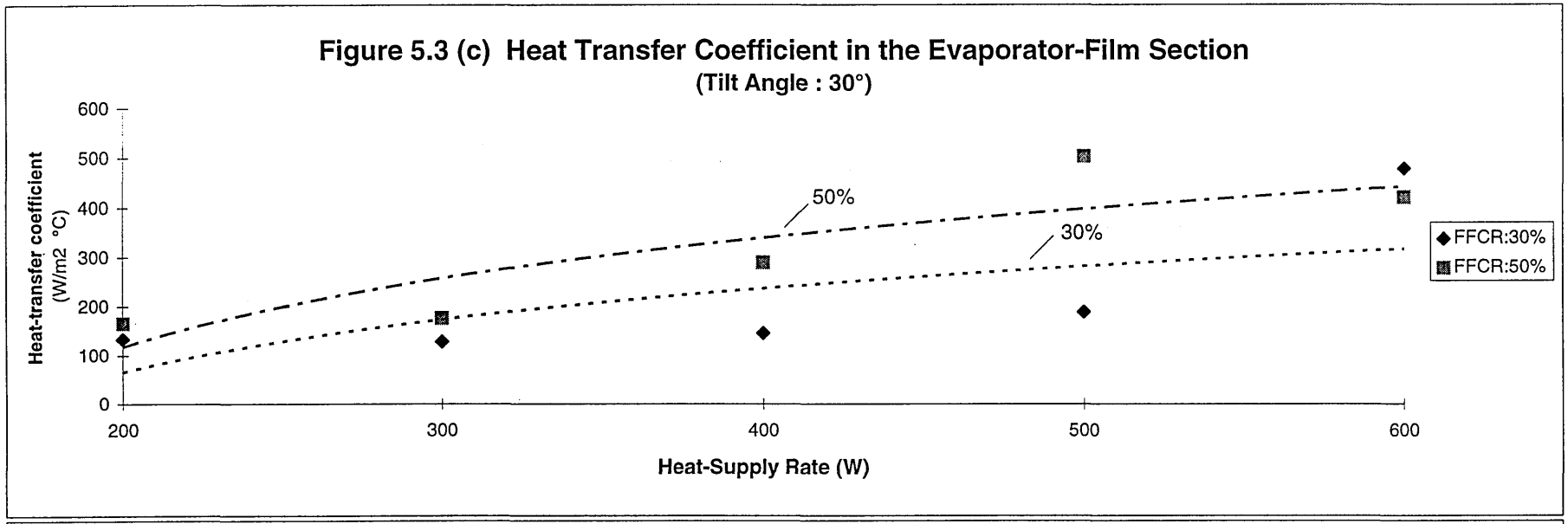
Figure 5.3 (c) Heat Transfer Coefficient in the Evaporator-Film Section
(Tilt Angle : 30°)
Heat-transfer coefficient (W/m2 °C)
600
500
400
300
200
100
0
50%
30%
FFCR:30%
FFCR:50%
200
300
400
500
600
Heat-Supply Rate (W)

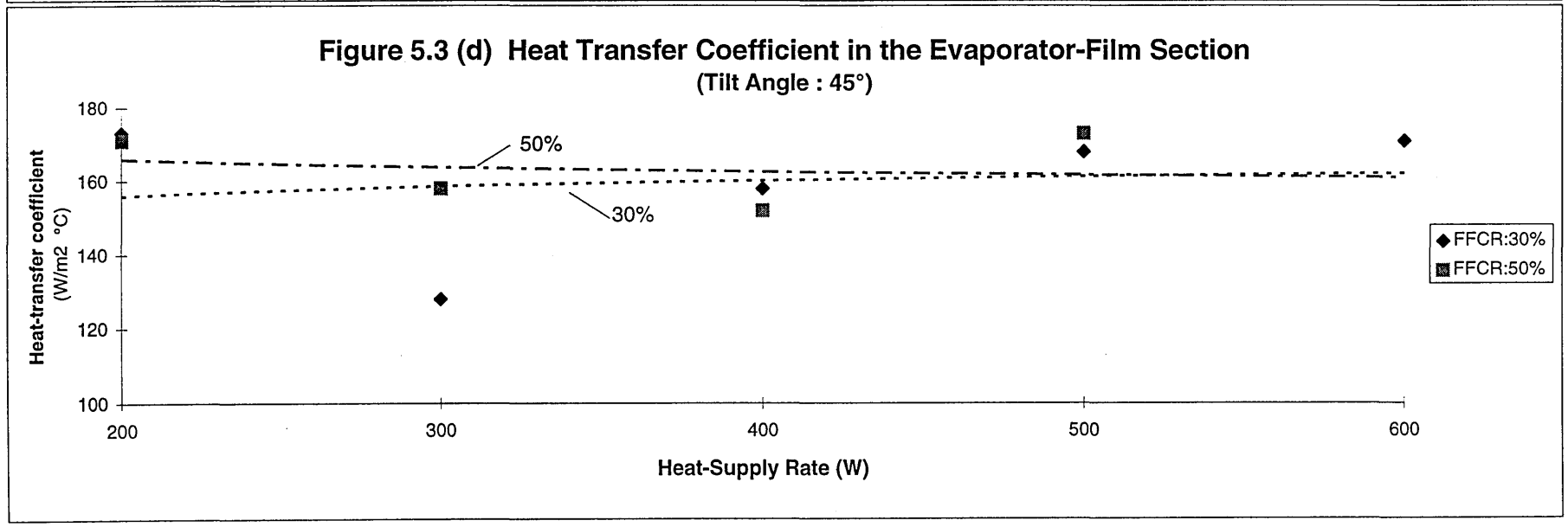
Figure 5.3 (d) Heat Transfer Coefficient in the Evaporator-Film Section
(Tilt Angle : 45°)
Heat-transfer coefficient (W/m2 °C)
180
160
140
120
100
50%
30%
FFCR:30%
FFCR:50%
200
300
400
500
600
Heat-Supply Rate (W)

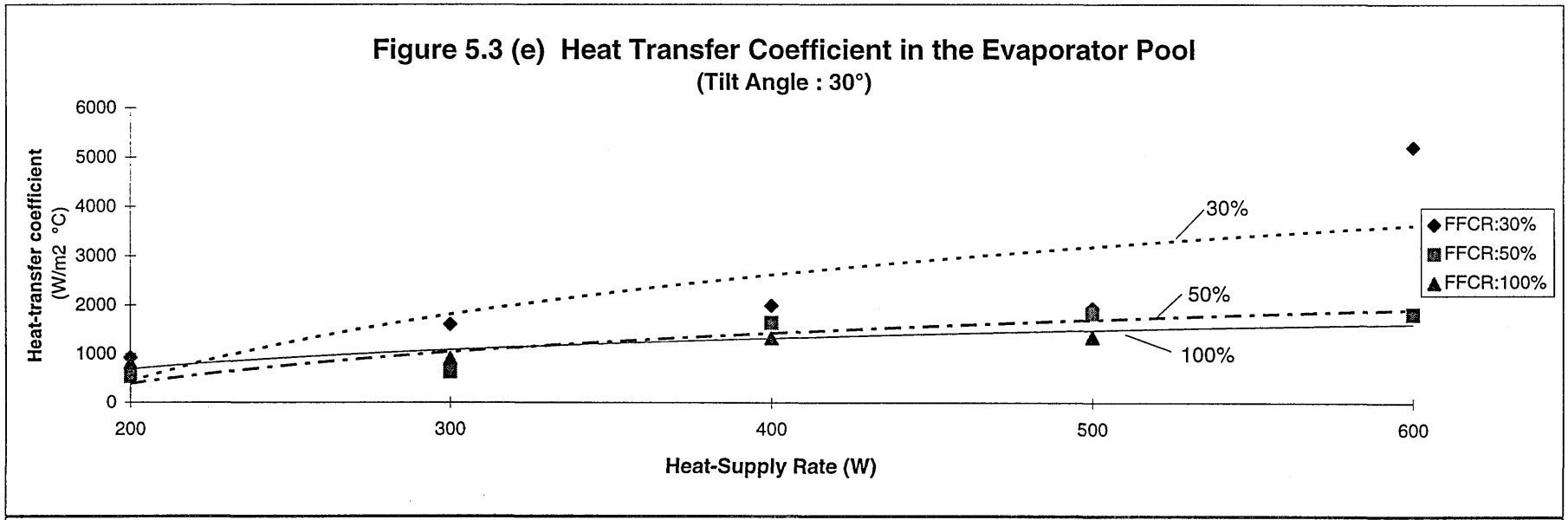
Figure 5.3 (e) Heat Transfer Coefficient in the Evaporator Pool
(Tilt Angle : 30°)
Heat-transfer coefficient (W/m2 °C)
6000
5000
4000
3000
2000
1000
0
200
300
400
500
600
Heat-Supply Rate (W)
30%
50%
100%
FFCR:30%
FFCR:50%
FFCR:100%

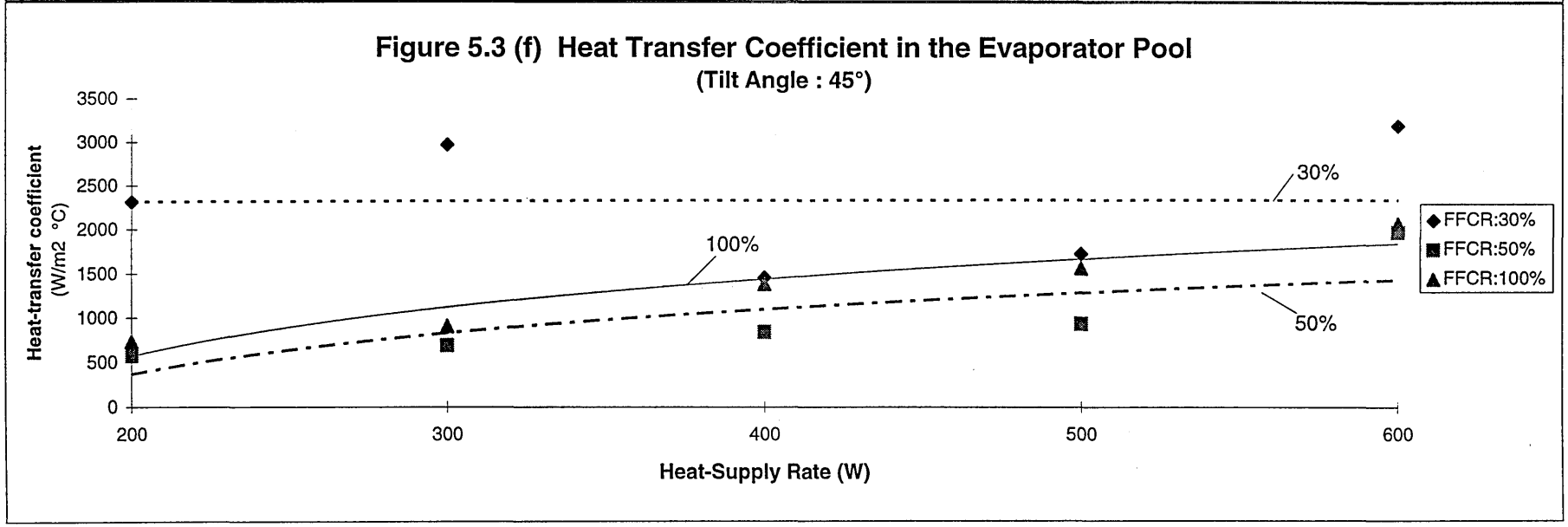
Figure 5.3 (f) Heat Transfer Coefficient in the Evaporator Pool
(Tilt Angle : 45°)
Heat-transfer coefficient (W/m2 °C)
3500
3000
2500
2000
1500
1000
500
0
200
300
400
500
600
Heat-Supply Rate (W)
30%
100%
50%
FFCR:30%
FFCR:50%
FFCR:100%

5.2. COMPARISON BETWEEN EXPERIMENTAL RESULTS AND ANALYTICAL PREDICTIONS

Figure 5.4 presents comparisons between the experimentally-determined and analytically-predicted heat transfer coefficients in the condenser, evaporator film and evaporator pool of the thermosyphon considered. For analytical predictions, equation (3.14), (3.15) and (3.16) were employed.

In equation (3.14), 'g' is replaced by 'g sinθ' for inclined thermosyphon tube.

There are large discrepancies between predicted and experimentally-obtained values of the heat-transfer coefficients in the condenser and especially in the evaporator-film sections of the thermosyphon. However, there is a relatively better match between the predicted and experimentally-determined heat-transfer coefficients in the evaporator pool, particularly at high rates of heat supply.

Figure 5.5 presents a comparison for the thermal resistances of the various sections of the thermosyphon tested between experimental results and analytical predictions (see Table 3.3) suggested by the Engineering Sciences Data Unit (1981). Again, there are large deviations between two values especially for the evaporator-film section.

Figure 5.4 (a) Comparison between Experimental Results and Analytical Predictions for the Heat-Transfer Coefficient in the Condenser

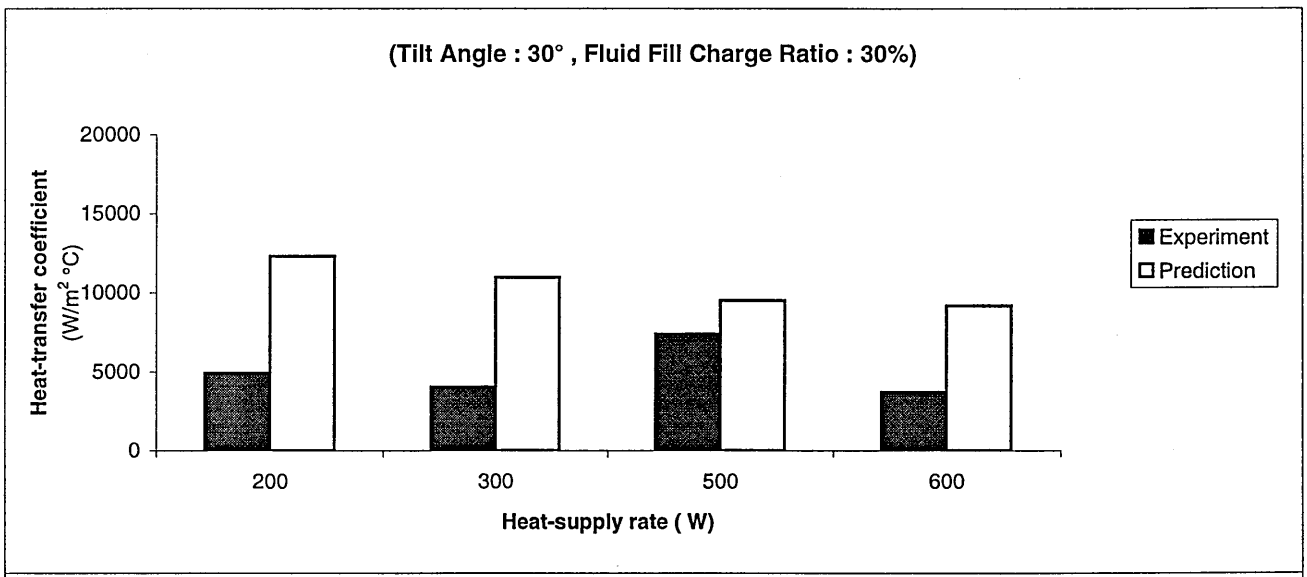

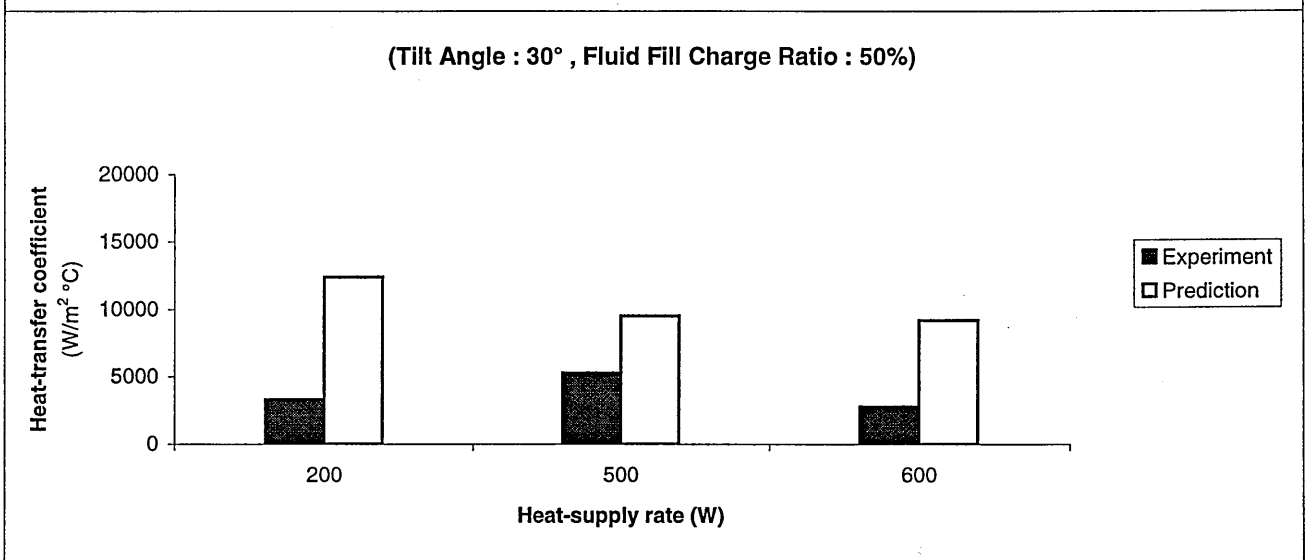

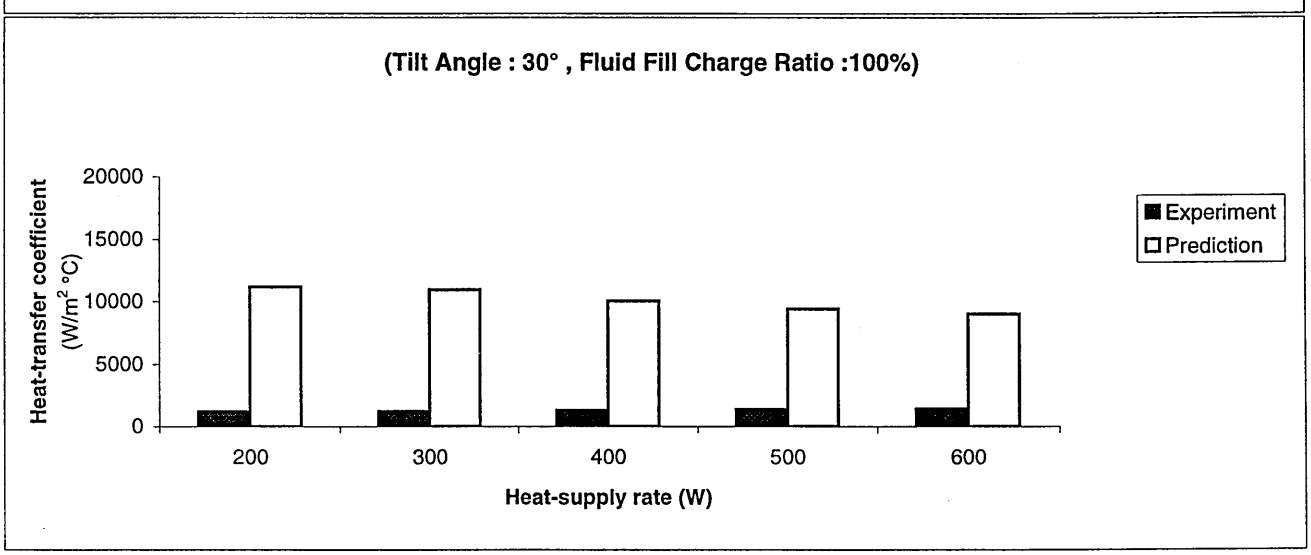

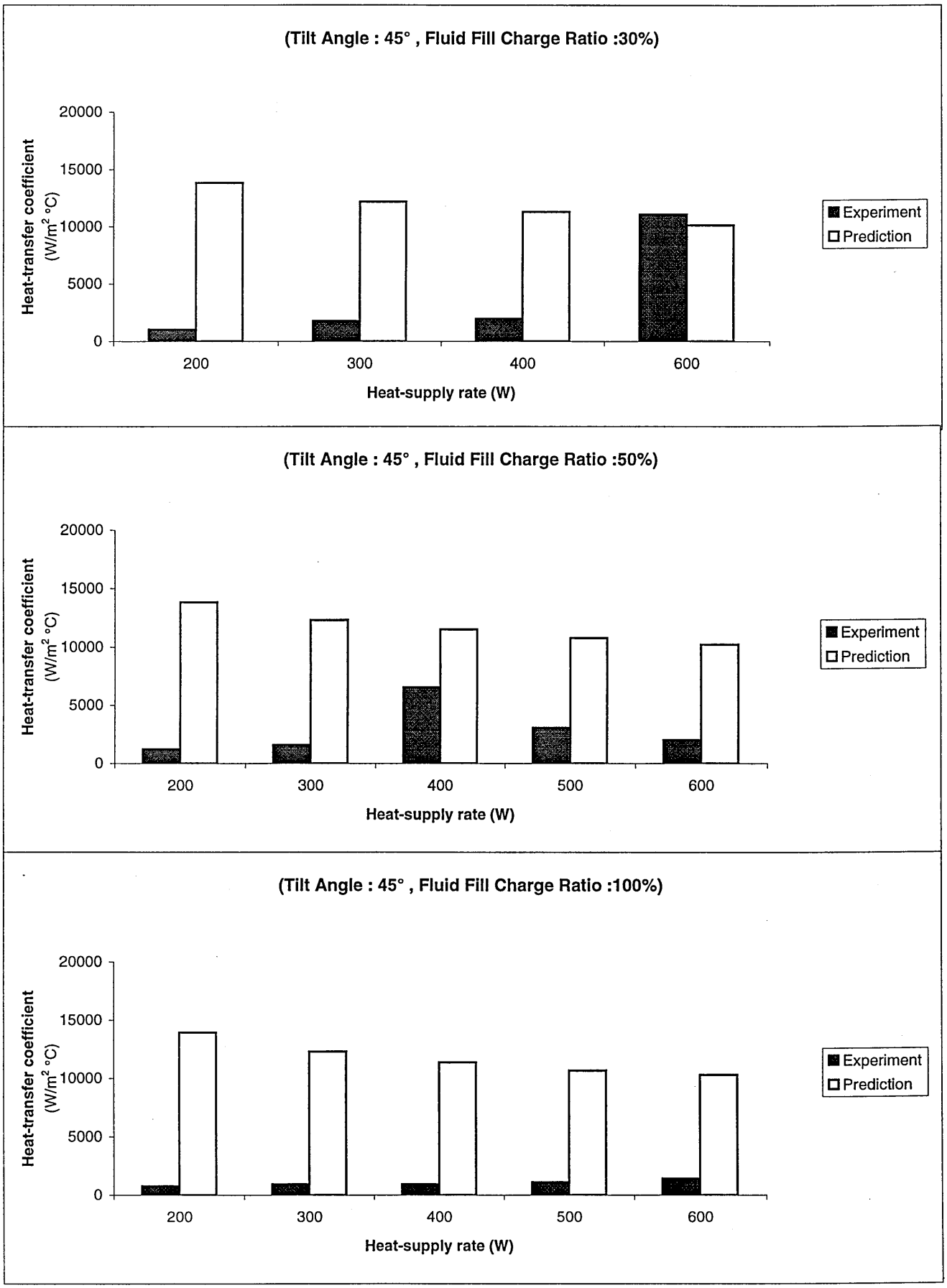
(Tilt Angle : 45° , Fluid Fill Charge Ratio :30%)
Heat-transfer coefficient (W/m² °C)
20000
15000
10000
5000
0
200
300
400
600
Heat-supply rate (W)
Experiment
Prediction
(Tilt Angle : 45° , Fluid Fill Charge Ratio :50%)
Heat-transfer coefficient (W/m² °C)
20000
15000
10000
5000
0
200
300
400
500
600
Heat-supply rate (W)
Experiment
Prediction
(Tilt Angle : 45° , Fluid Fill Charge Ratio :100%)
Heat-transfer coefficient (W/m² °C)
20000
15000
10000
5000
0
200
300
400
500
600
Heat-supply rate (W)
Experiment
Prediction

Figure 5.4 (b) Comparison between Experimental Results and Analytical Predictions for the Heat-Transfer Coefficient in the Evaporator-Film Section

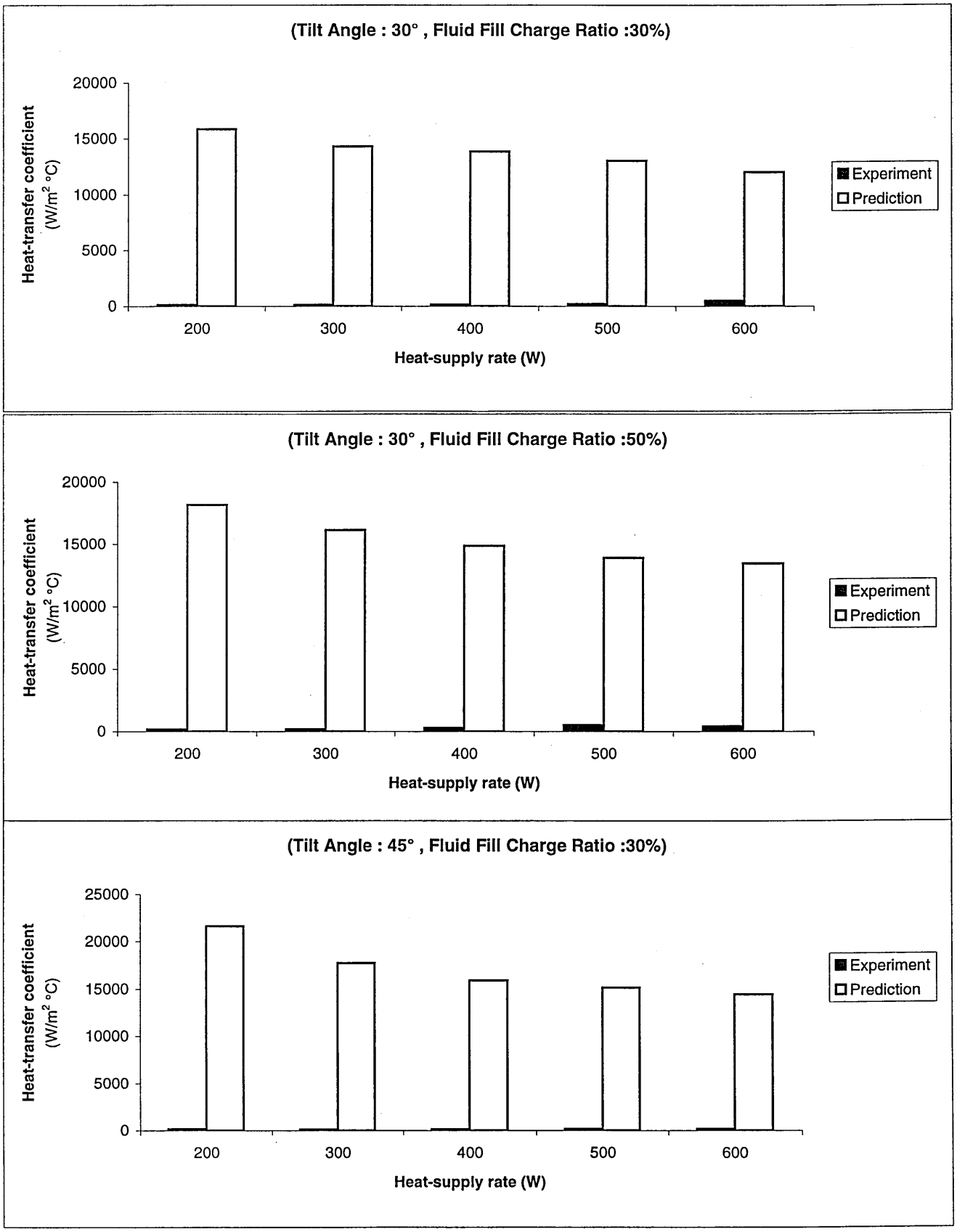

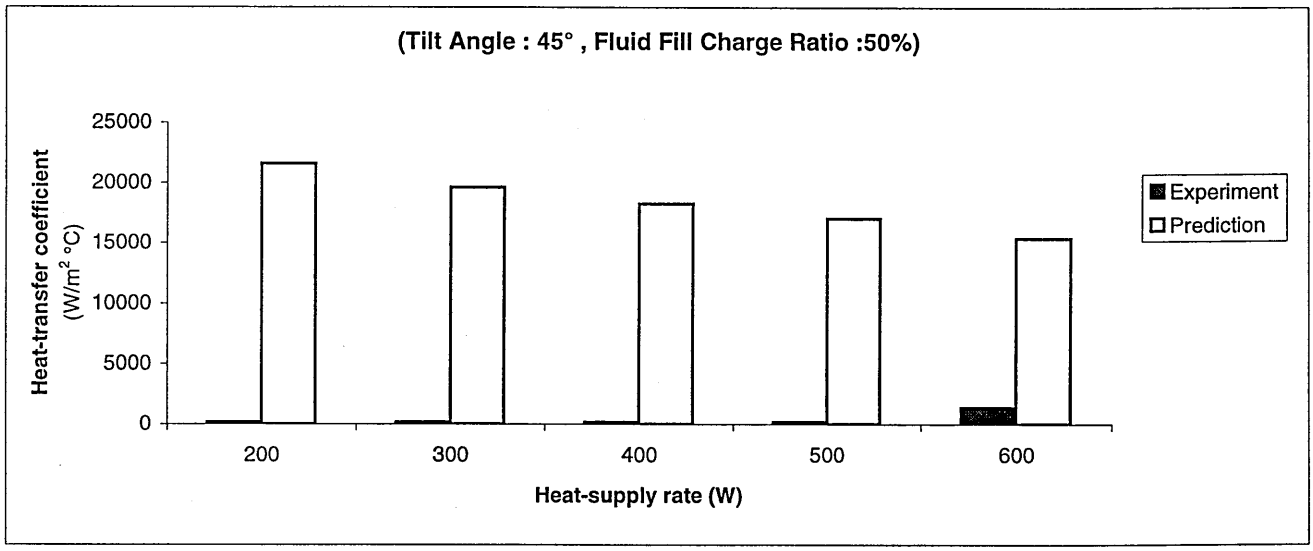

Figure 5.4 (c) Comparison between Experimental Results and Analytical Predictions for the Heat-Transfer Coefficient in the Evaporator Pool

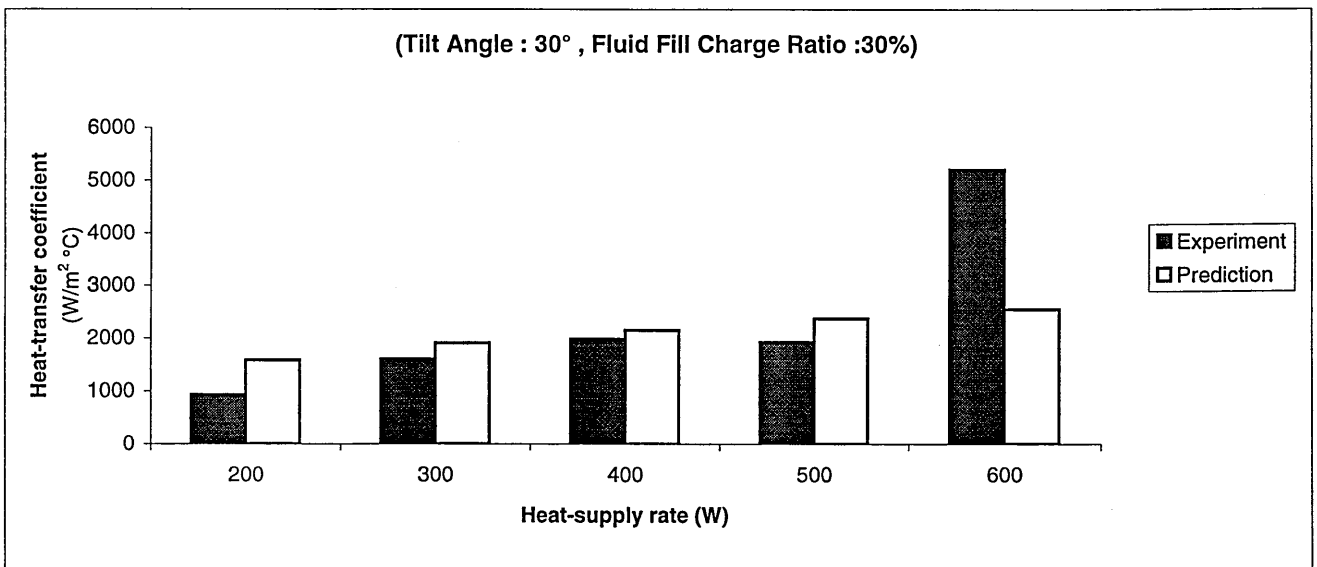

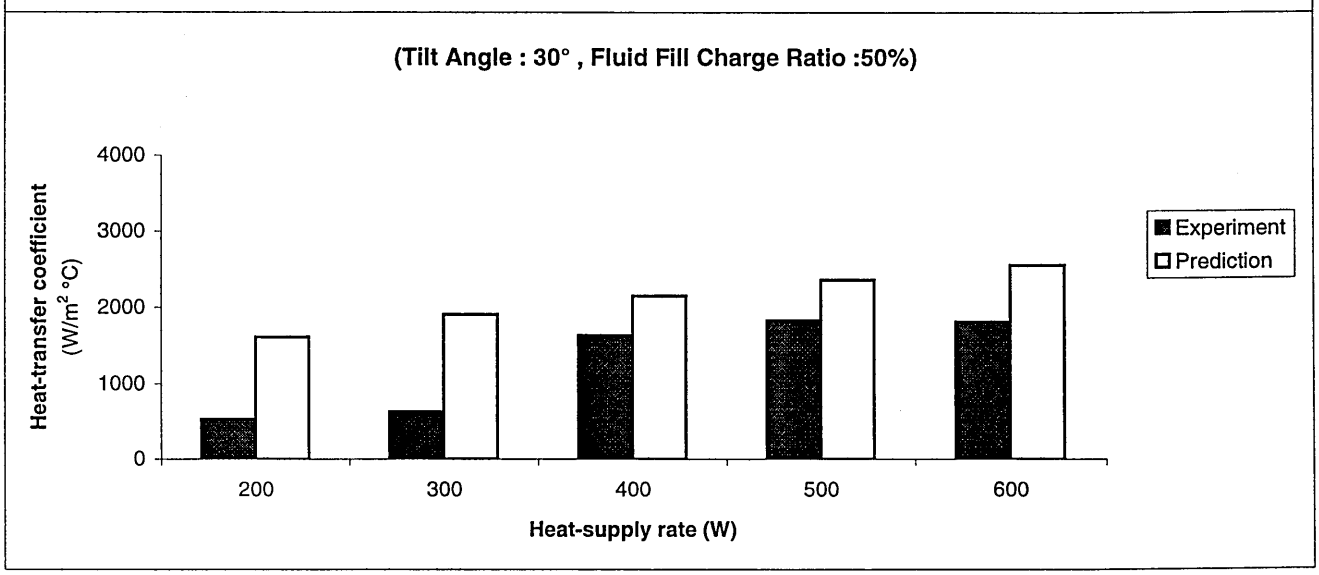

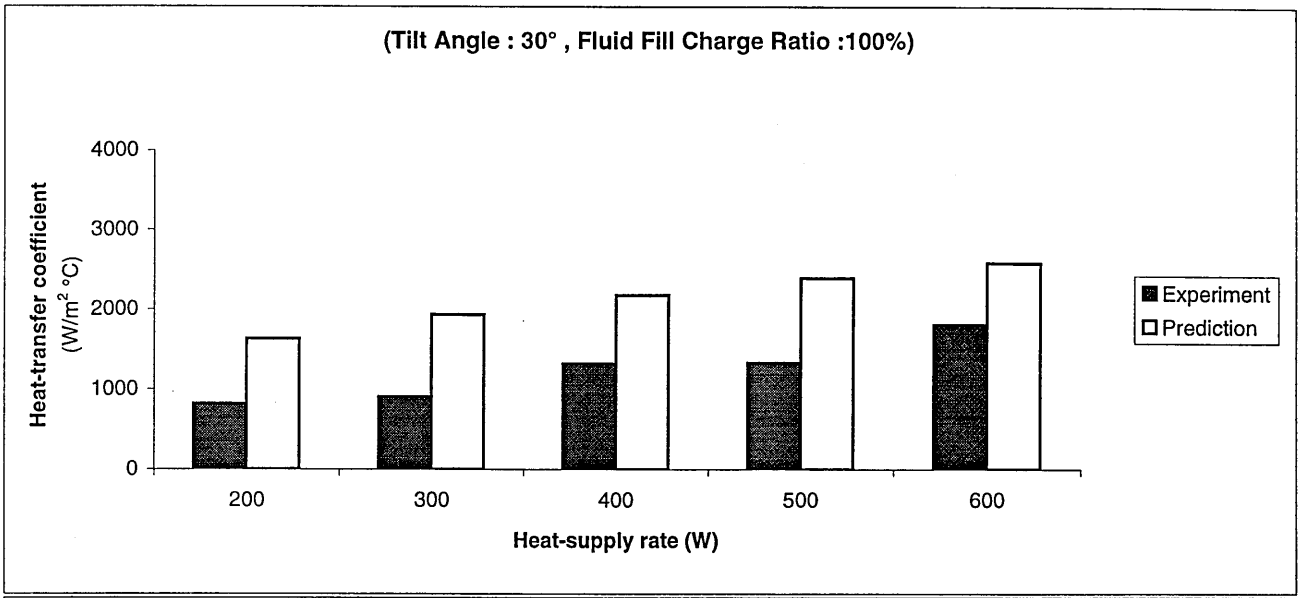
(Tilt Angle : 30° , Fluid Fill Charge Ratio :100%)
Heat-transfer coefficient (W/m² °C)
4000
3000
2000
1000
0
200
300
400
500
600
Heat-supply rate (W)
Experiment
Prediction

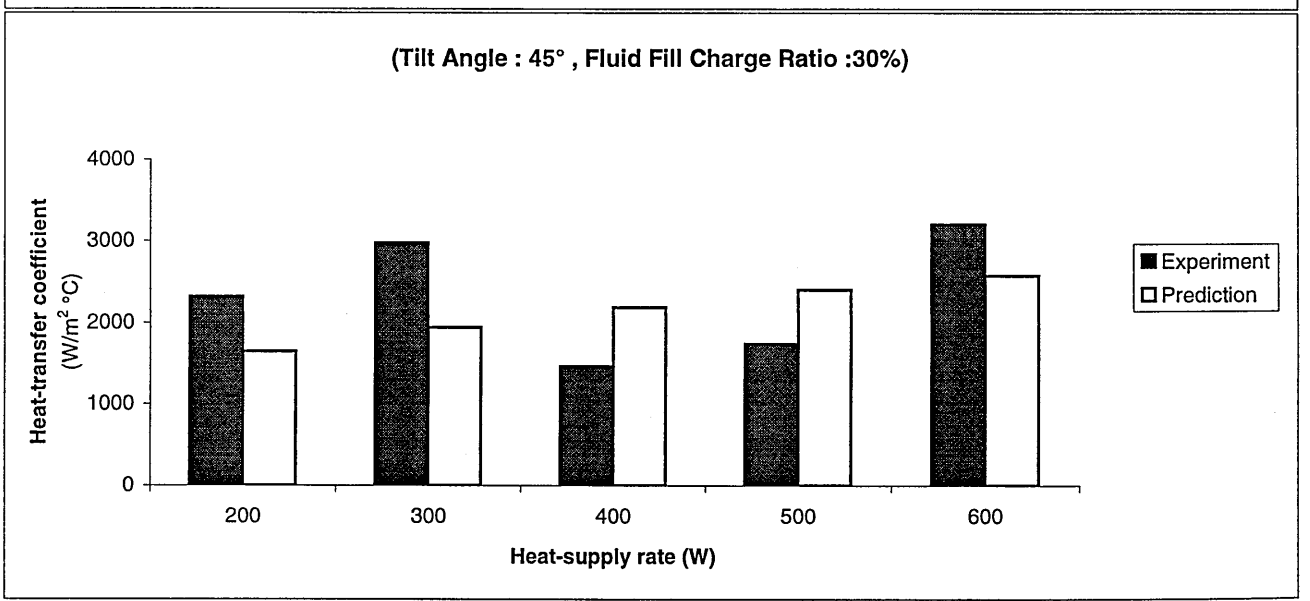
(Tilt Angle : 45° , Fluid Fill Charge Ratio :30%)
Heat-transfer coefficient (W/m² °C)
4000
3000
2000
1000
0
200
300
400
500
600
Heat-supply rate (W)
Experiment
Prediction

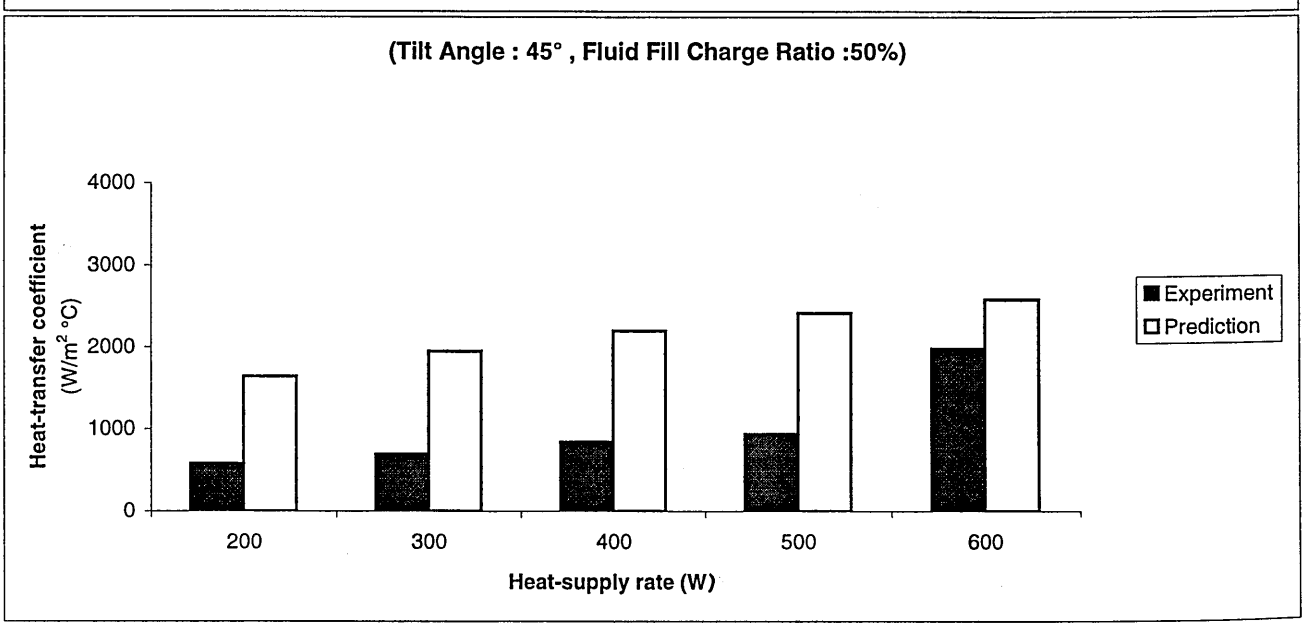
(Tilt Angle : 45° , Fluid Fill Charge Ratio :50%)
Heat-transfer coefficient (W/m² °C)
4000
3000
2000
1000
0
200
300
400
500
600
Heat-supply rate (W)
Experiment
Prediction

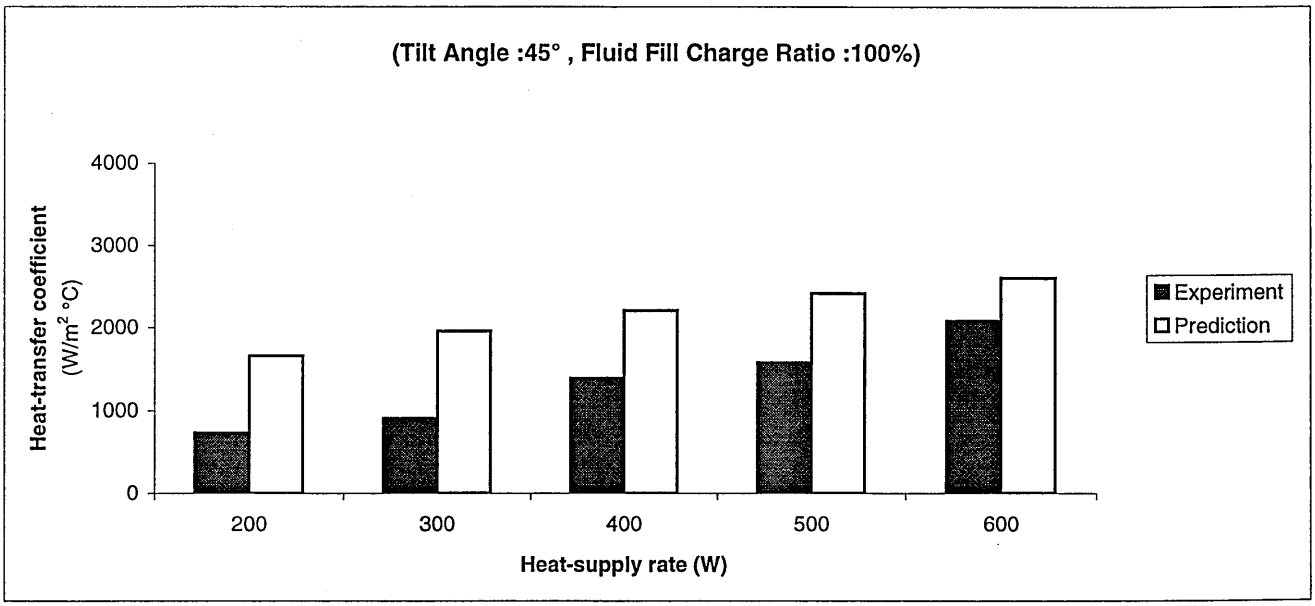
(Tilt Angle :45° , Fluid Fill Charge Ratio :100%)
Heat-transfer coefficient (W/m² °C)
4000
3000
2000
1000
0
200
300
400
500
600
Heat-supply rate (W)
Experiment
Prediction

Figure 5.5 (a) Comparison between Experimental Results and Analytical Precictions for the Thermal Resistance in the Condenser

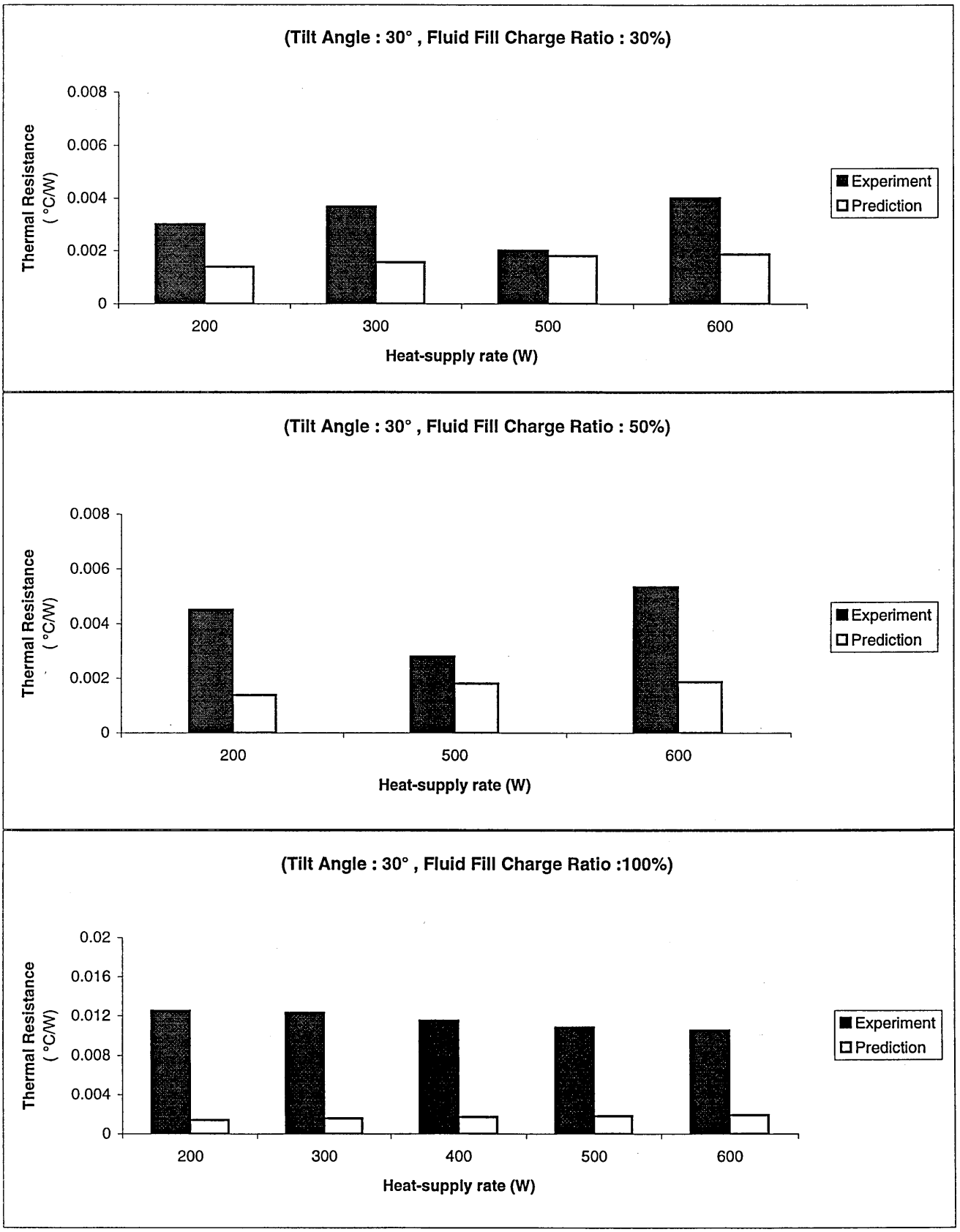

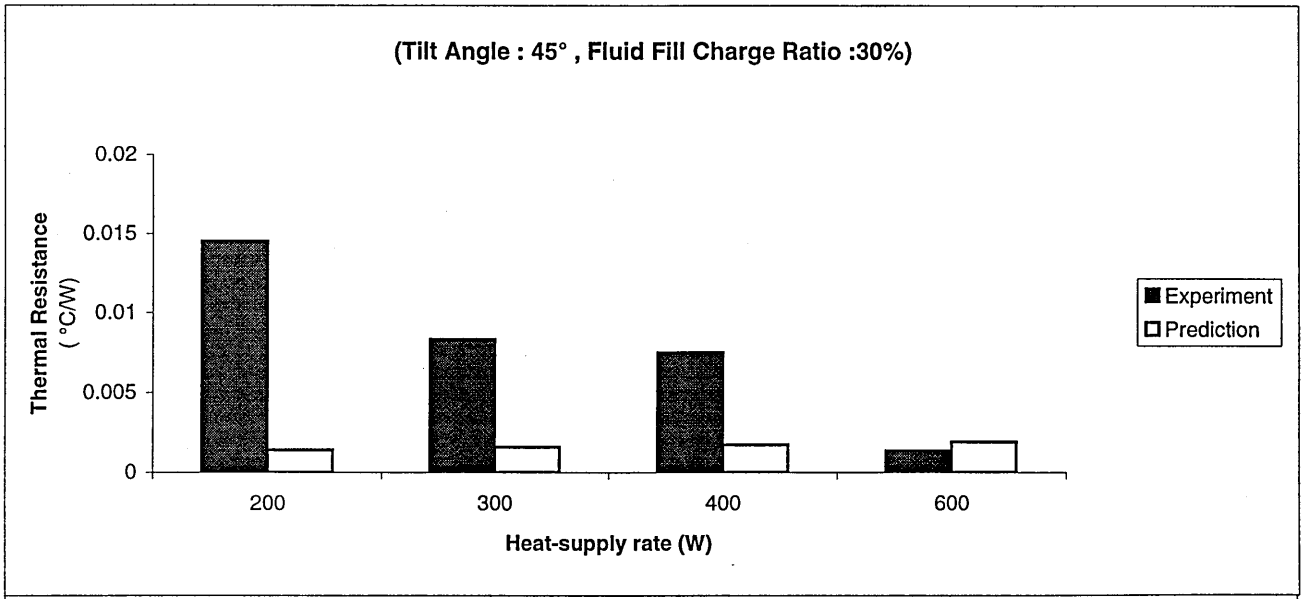
(Tilt Angle : 45° , Fluid Fill Charge Ratio :30%)
Thermal Resistance (°C/W)
0.02
0.015
0.01
0.005
0
200
300
400
600
Heat-supply rate (W)
Experiment
Prediction

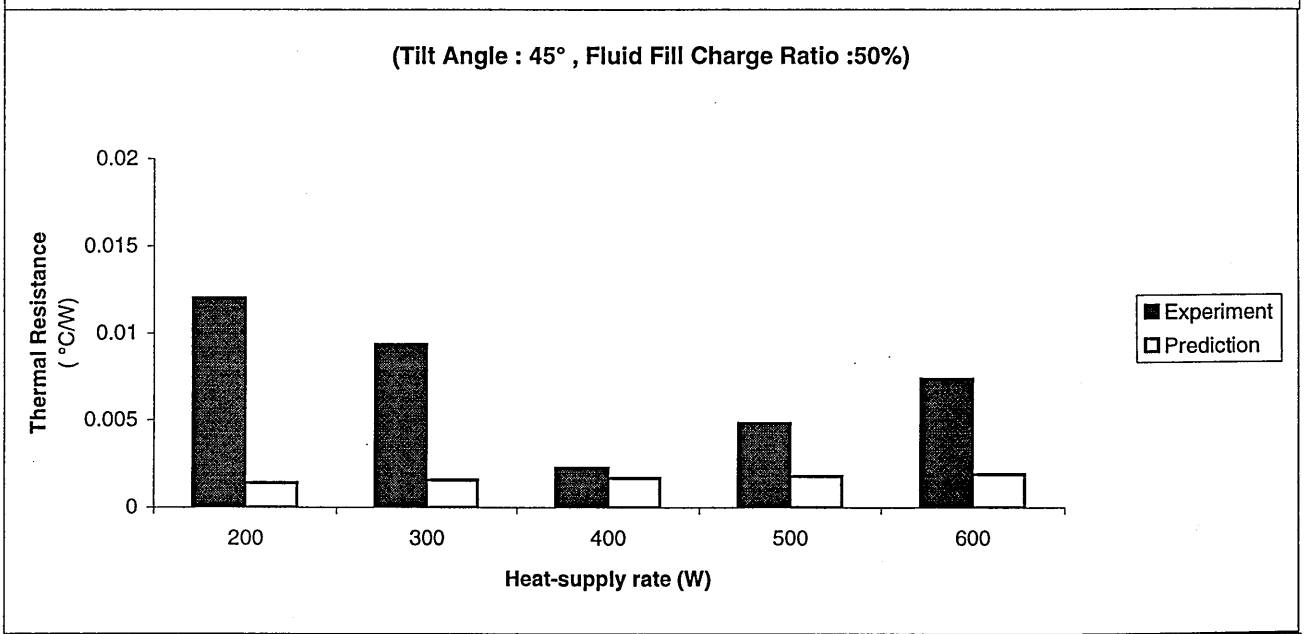
(Tilt Angle : 45° , Fluid Fill Charge Ratio :50%)
Thermal Resistance (°C/W)
0.02
0.015
0.01
0.005
0
200
300
400
500
600
Heat-supply rate (W)
Experiment
Prediction

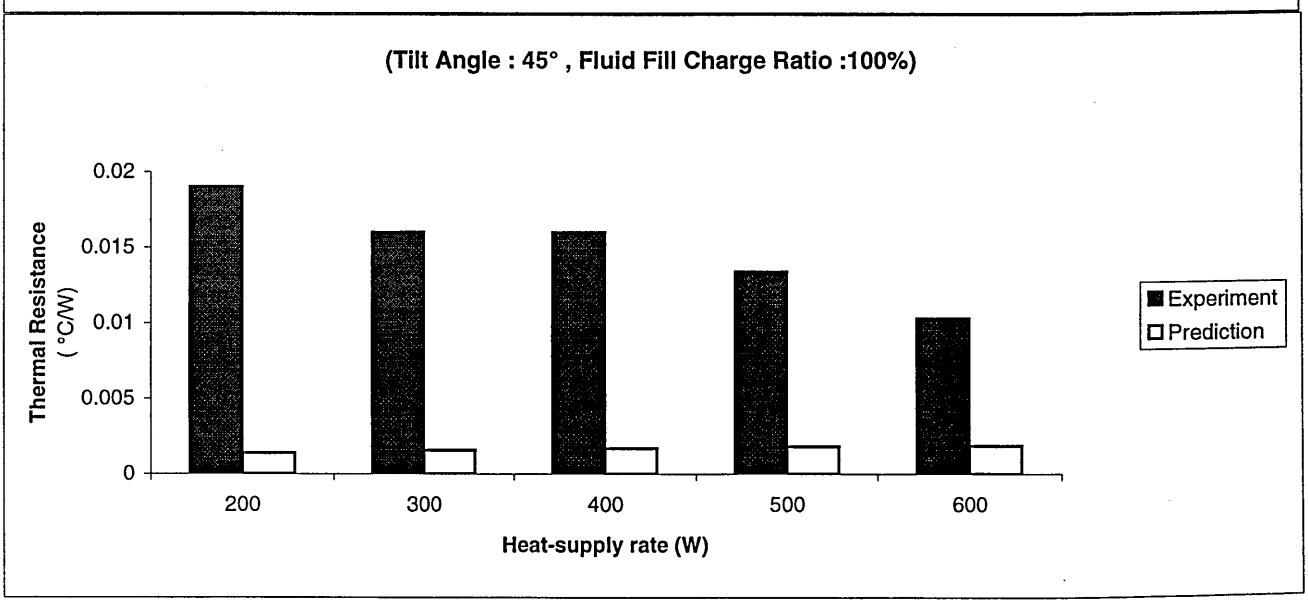
(Tilt Angle : 45° , Fluid Fill Charge Ratio :100%)
Thermal Resistance (°C/W)
0.02
0.015
0.01
0.005
0
200
300
400
500
600
Heat-supply rate (W)
Experiment
Prediction

Figure 5.5 (b) Comparison between Experimental Results and Analytical Precictions for the Thermal Resistance in the Evaporator-Film Section

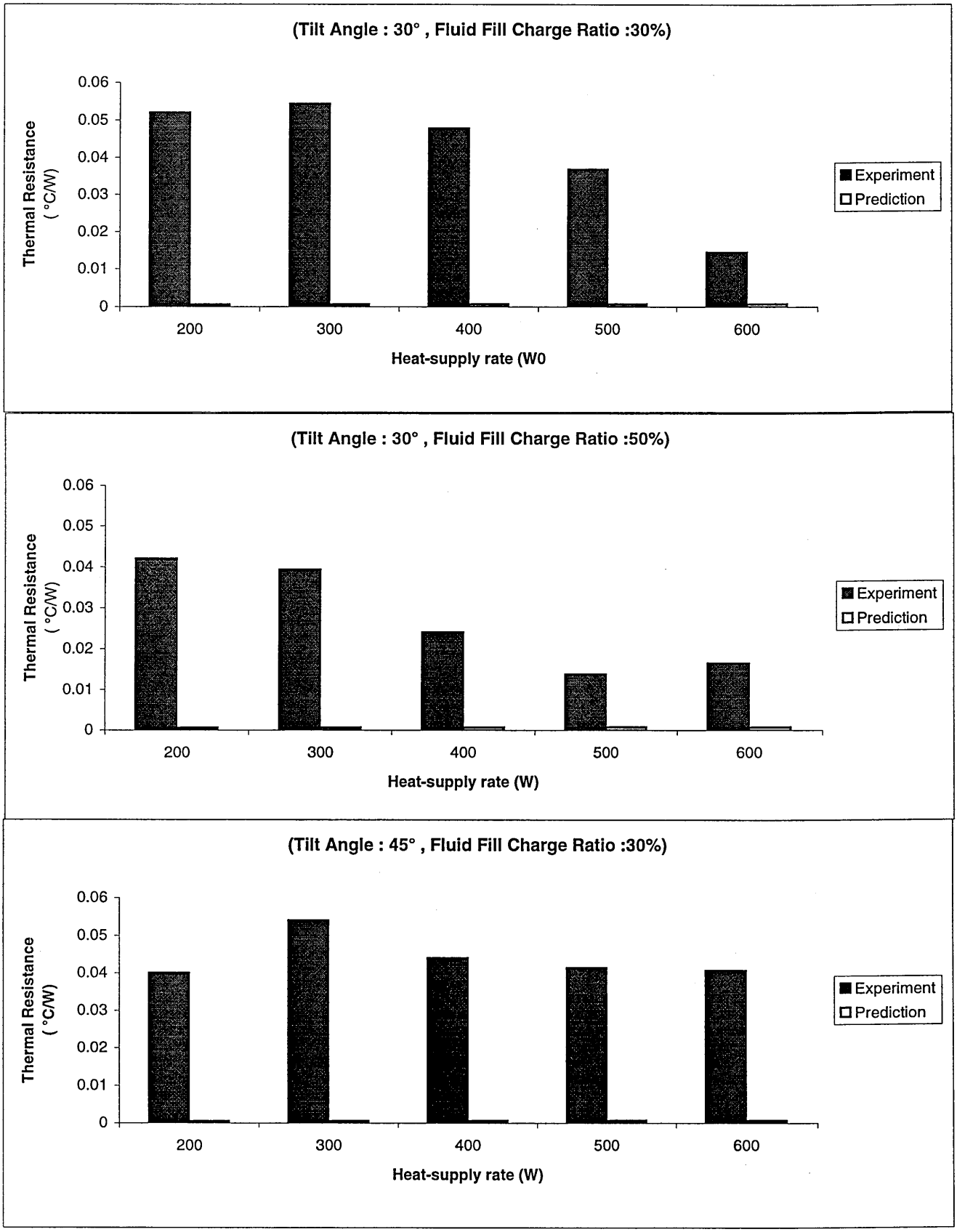

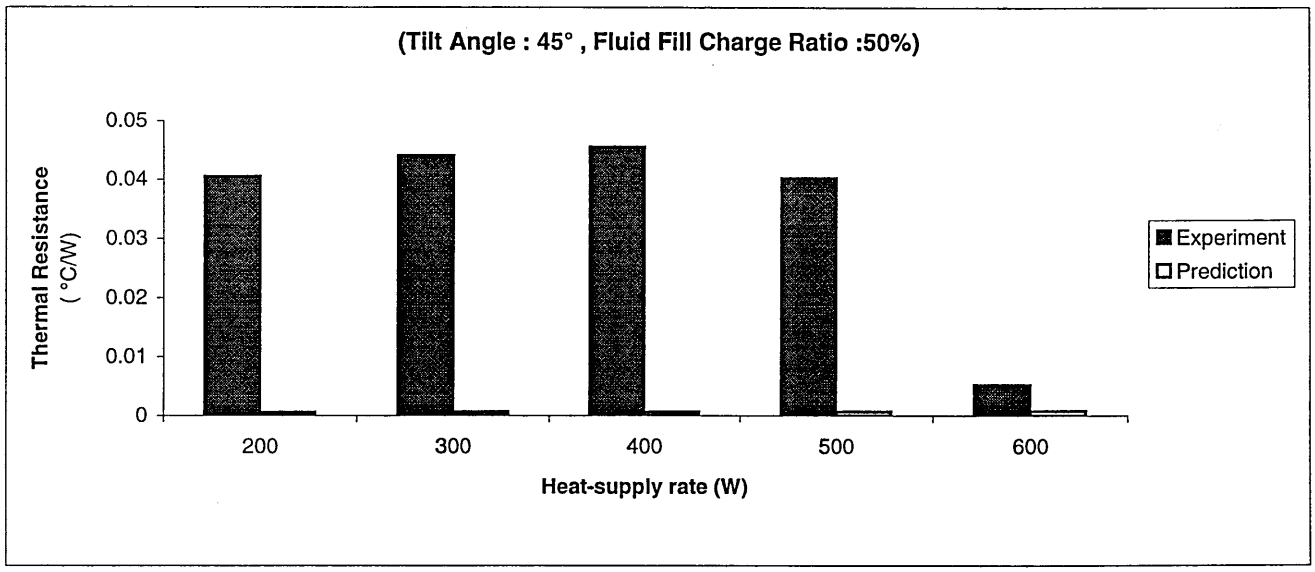

Figure 5.5 (c) Comparison between Experimental Results and Analytical Precictions for the Thermal Resistance in the Evaporator-Pool

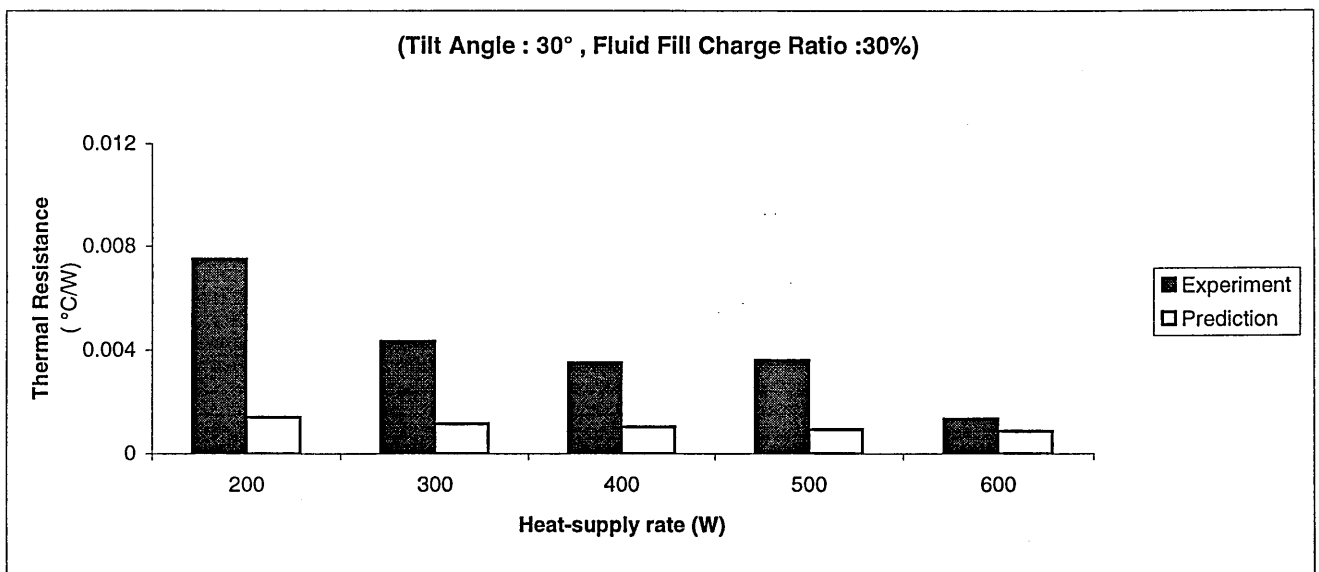

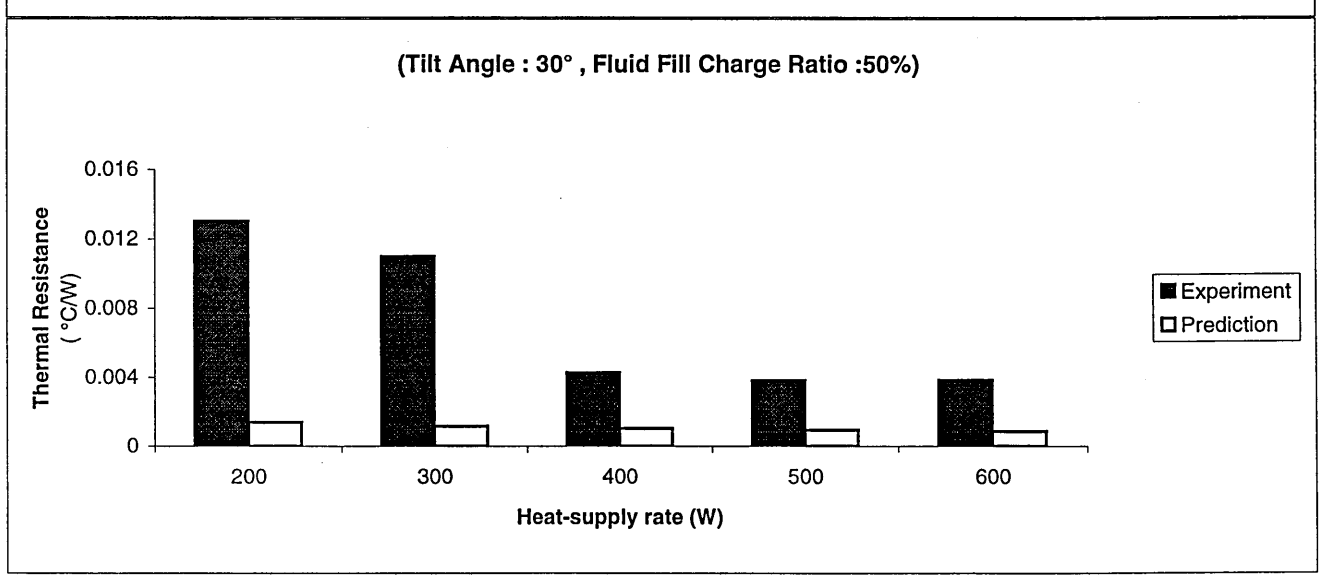

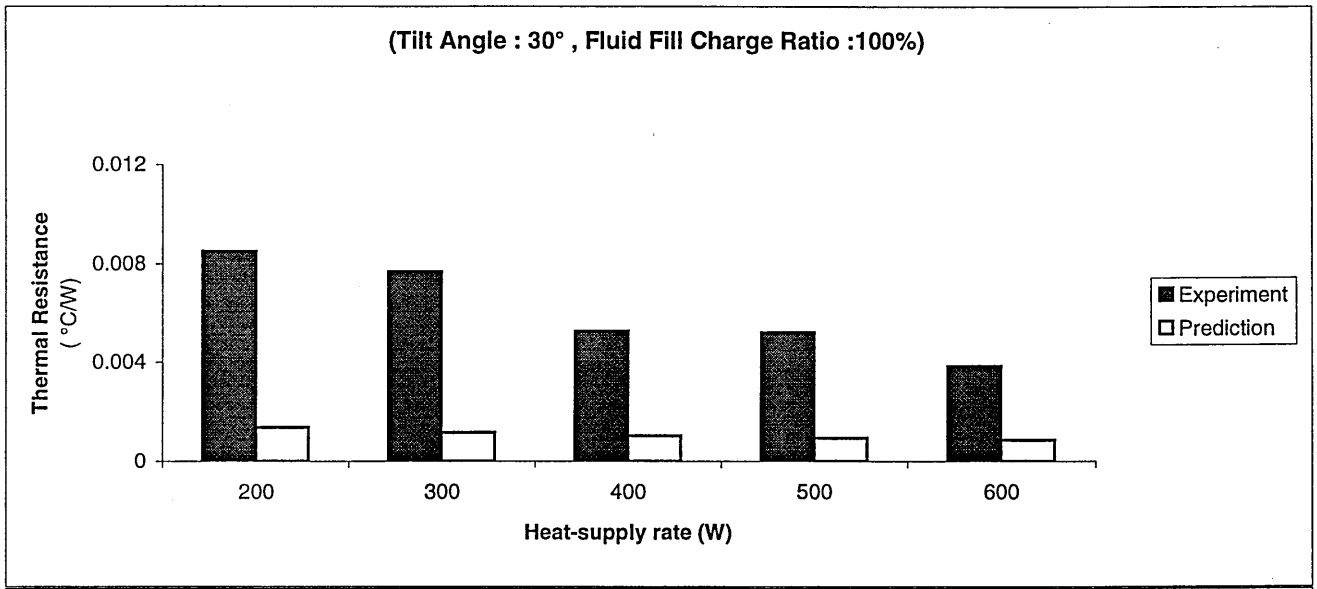
(Tilt Angle : 30° , Fluid Fill Charge Ratio :100%)
Thermal Resistance (°C/W)
0.012
0.008
0.004
0
200
300
400
500
600
Heat-supply rate (W)
Experiment
Prediction

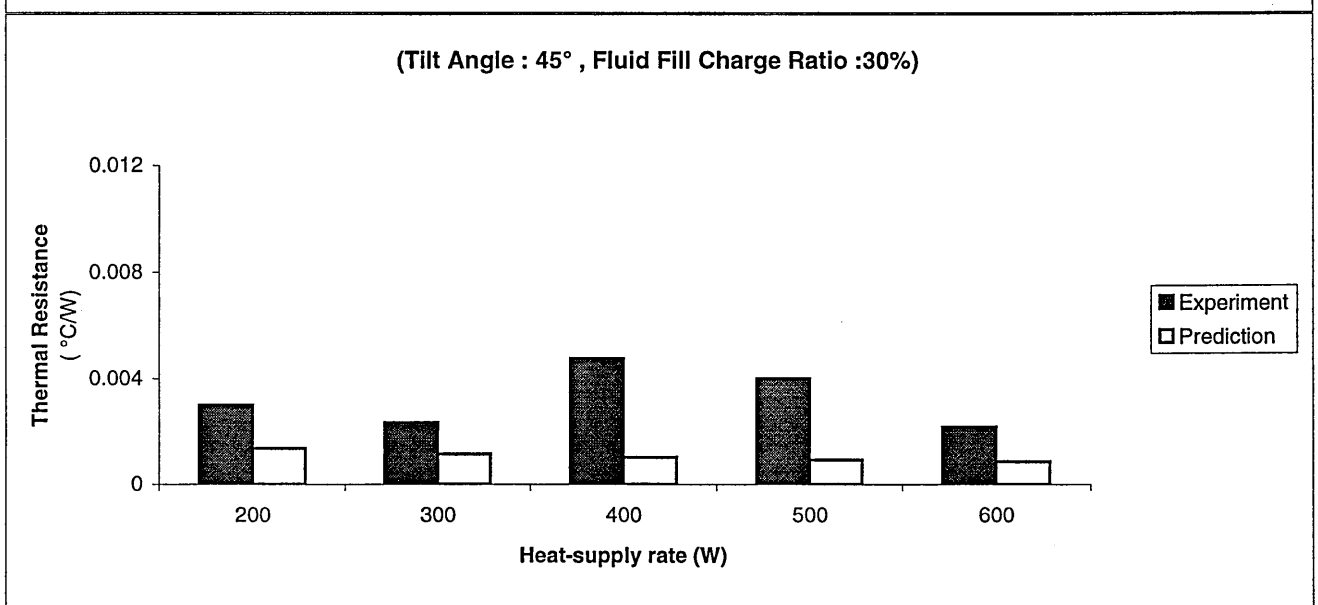
(Tilt Angle : 45° , Fluid Fill Charge Ratio :30%)
Thermal Resistance (°C/W)
0.012
0.008
0.004
0
200
300
400
500
600
Heat-supply rate (W)
Experiment
Prediction

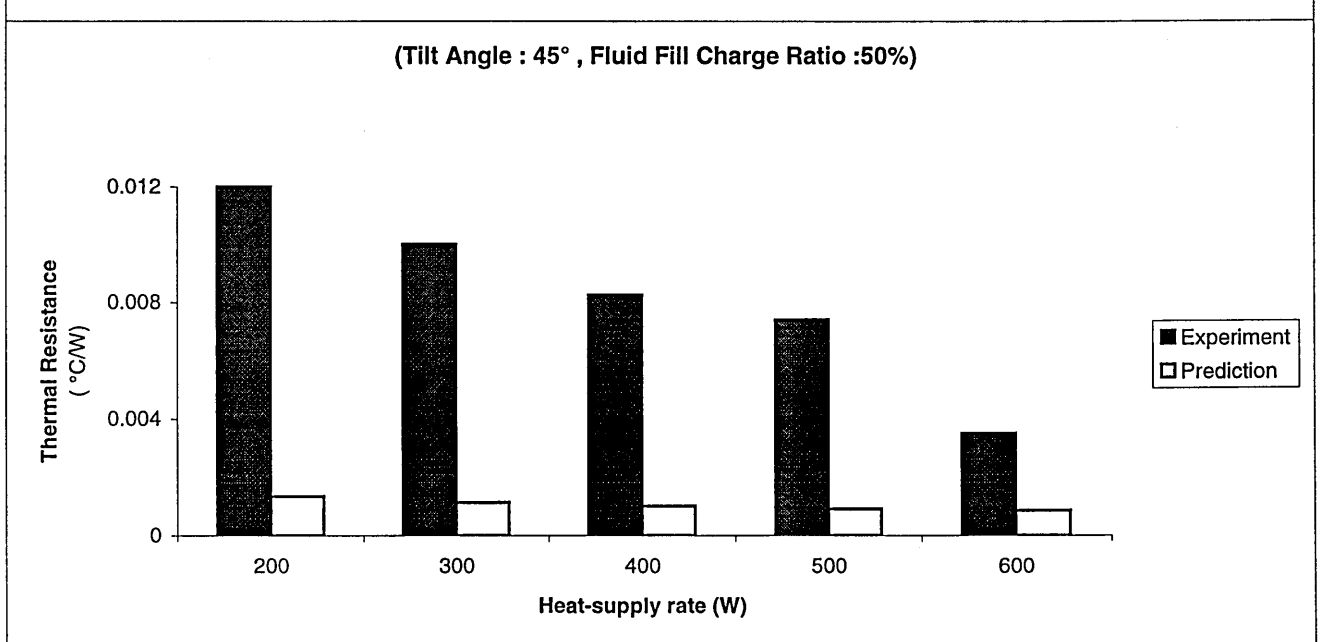
(Tilt Angle : 45° , Fluid Fill Charge Ratio :50%)
Thermal Resistance (°C/W)
0.012
0.008
0.004
0
200
300
400
500
600
Heat-supply rate (W)
Experiment
Prediction

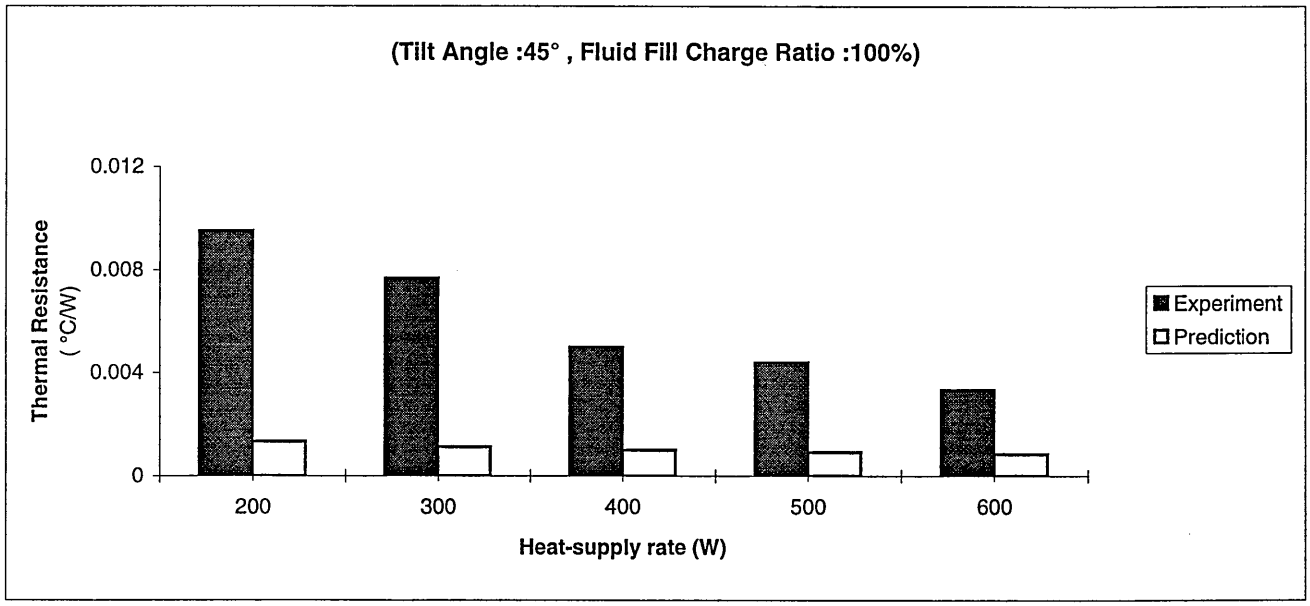
(Tilt Angle :45° , Fluid Fill Charge Ratio :100%)
Thermal Resistance (°C/W)
0.012
0.008
0.004
0
200
300
400
500
600
Heat-supply rate (W)
Experiment
Prediction

5.3 DISCUSSION

5.3.1 Condenser and Evaporator Film

In the present study, heat-transfer coefficients in the evaporator film and condenser of the thermosyphon were analytically predicted by employing Nusselt's film condensation theory. This theory applies for a continuous liquid film on a vertical plate. Shiraishi. et al (1985) predicted heat-transfer coefficients at the evaporator film and condenser of a vertical two-phase closed thermosyphon by employing this theory. Their experimental results when using ethanol and R-113 as working-fluids indicated deviations within only ±30%. The results of the present study indicates that Nusselt's film condensation theory could not be applied for inclined copper-water thermosyphons. Such a large discrepancy may be attributed to two facts.

- Firstly, the actual condensation and film evaporation processes in the inclined thermosyphons can not be exactly described by the Nusselt's film condensation theory, due to the possibility of the breakdown or non-existence of the smooth continuous liquid film on a large percentage of the surface area of the inclined tube
- Secondly, the thermocouples employed to monitor outside wall temperatures were located at upper side of thermosyphon tube. This is the side where the non-existence of a continuous liquid film is more probable.

5.3.2 Evaporator Pool

According to the measured temperature distribution of the working fluid in the liquid pool, the change of saturation temperature due to the hydrostatic height of the pool should be considered. Figure 5.6 shows the good agreement between experimental results and analytical predictions for the working-fluid temperature distributions .

Figure 5.6 The effects of Hydrostatic Pressure in the Evaporator Pool (Heat-Supply Rate : 600W, FFCR:100%)

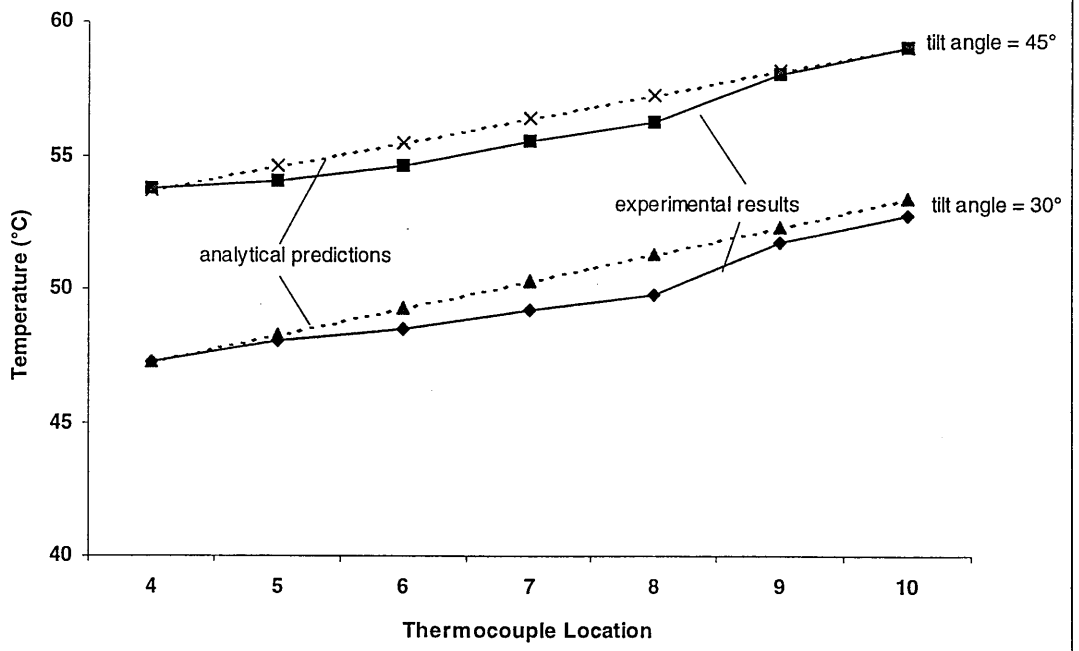

5.4 VALIDATION OF THE COMPUTER MODEL

According to the experimental results, Nusselt's film theory for continuous liquid film could not be employed for predicting thermal performances in the condenser and evaporator film region of inclined thermosyphons. Figure 5.7 shows comparisons between the present computer model, Heat Pipe and Thermosyphon Thermal Performance Model, and reference, at the same operating condition and specification. The behaviour of the thermosyphon tested of reference (Kikuchi et al., 1985) was investigated for FFCRs of 50 and 100%, heat supply-rate to the evaporator at 1346W, and inclination angle of 90°. There is a relatively better match between the computer model and reference in the evaporator-film section, particularly in the condenser and evaporator pool. This means that liquid film can only be maintained circumferentially in vertical thermosyphon tubes, even though might not the smooth continuous liquid film, and the computer model is still valid when it is applied to vertical thermosyphons. In the evaporator-pool region, Imura's equation (i.e. equation 3.14) can be employed for predicting thermal performance in the inclined thermosyphon if 'g' is replaced by 'g $\sin\theta$'.

Figure 5.7 Comparison between Reference (Kikuchi, 1985) and the Computer Model

(a) Heat-Transfer Cofficients

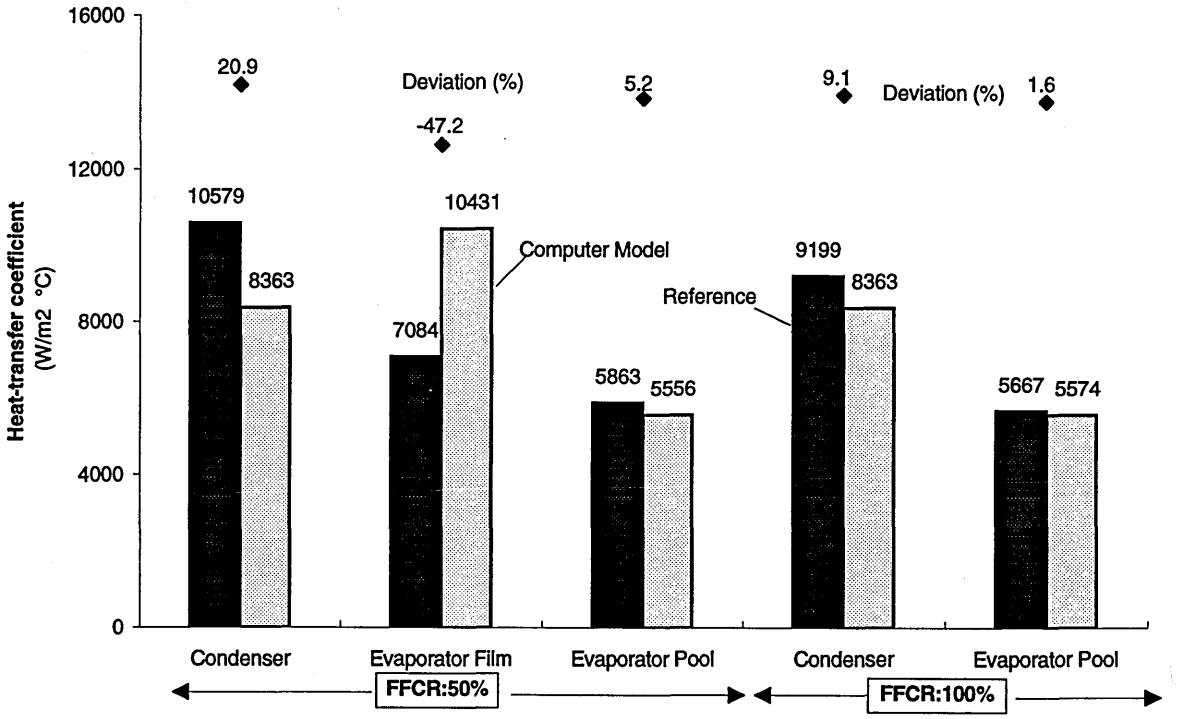

(b) Overall Thermal Resistance

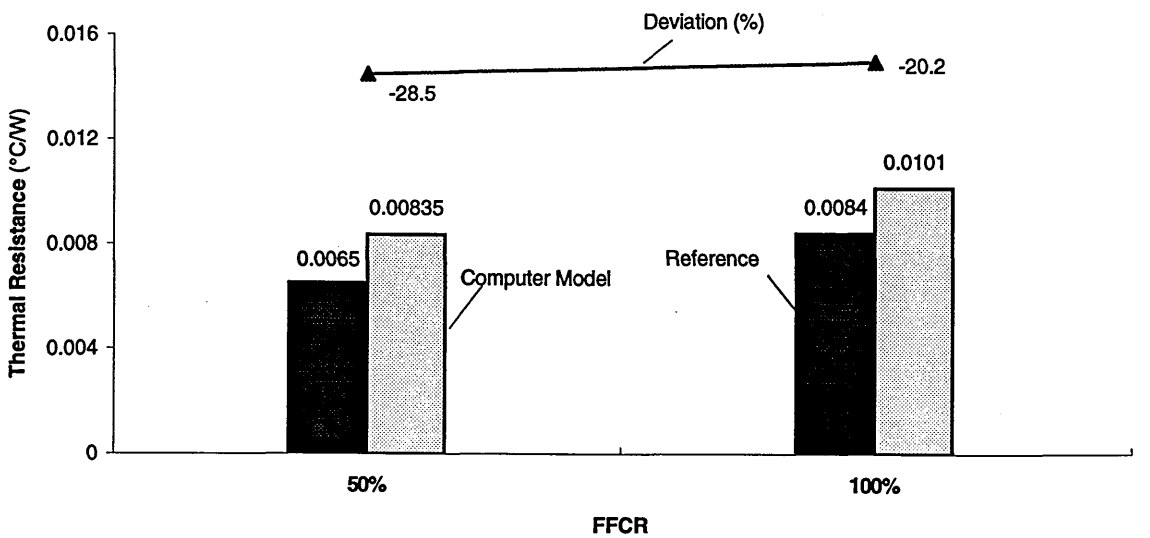

* Reference data reading : from graph
* Deviation = [(experimental value-computer model value) / experimental value]

CHAPTER 6 HEAT PIPE HEAT EXCHANGERS

The study of the behaviours of heat pipes and thermosyphons was undertaken to facilitate both the design and the prediction of performances of HPHEs. The results of the former study were utilised to develop a 'Heat Pipe Heat Exchangers Design Model'. This model should enable the designers of waste-heat recovery systems to choose the most appropriate type of heat-transfer elements and optimise the design parameters of a HPHE for a given application.

6.1 THERMAL PERFORMANCES OF HPHES

In process plants, cross-flow heat exchangers are often used (see Figure 6.1). Under steady-state operating conditions the rate of heat exchange Q_j between the hot and the cold streams flowing across the jth row of heat pipes (or thermosyphons) can be estimated as (Huang et al., 1985) :

$$Q_j = \dot{m}_h c_{ph} (T_{h,j-1} - T_{h,j}) \quad (6.1)$$

$$Q_j = \dot{m}_c c_{pc} (T_{c,j} - T_{c,j-1}) \quad (6.2)$$

$$Q_j = n_j (AU)_j (\overline{T}_{h,j} - \overline{T}_{c,j}) \quad (6.3)$$

$\dot{m}_h$ and $\dot{m}_c$ are the mass flow rates of the hot and cold flow respectively, n_j is the number of pipes in jth row, and $\overline{T}_{h,j}$, $\overline{T}_{c,j}$ are defined as

$$\overline{T}_{h,j} = (T_{h,j-1} + T_{h,j}) / 2$$

$$\overline{T}_{c,j} = (T_{c,j-1} + T_{c,j}) / 2$$

These are considered positive for the flow directions shown in Figure 6.1. Equation (6.3) can be re-written as

$$Q_j = n_j (1/R_j) (\overline{T}_{h,j} - \overline{T}_{c,j}) \quad (6.4)$$

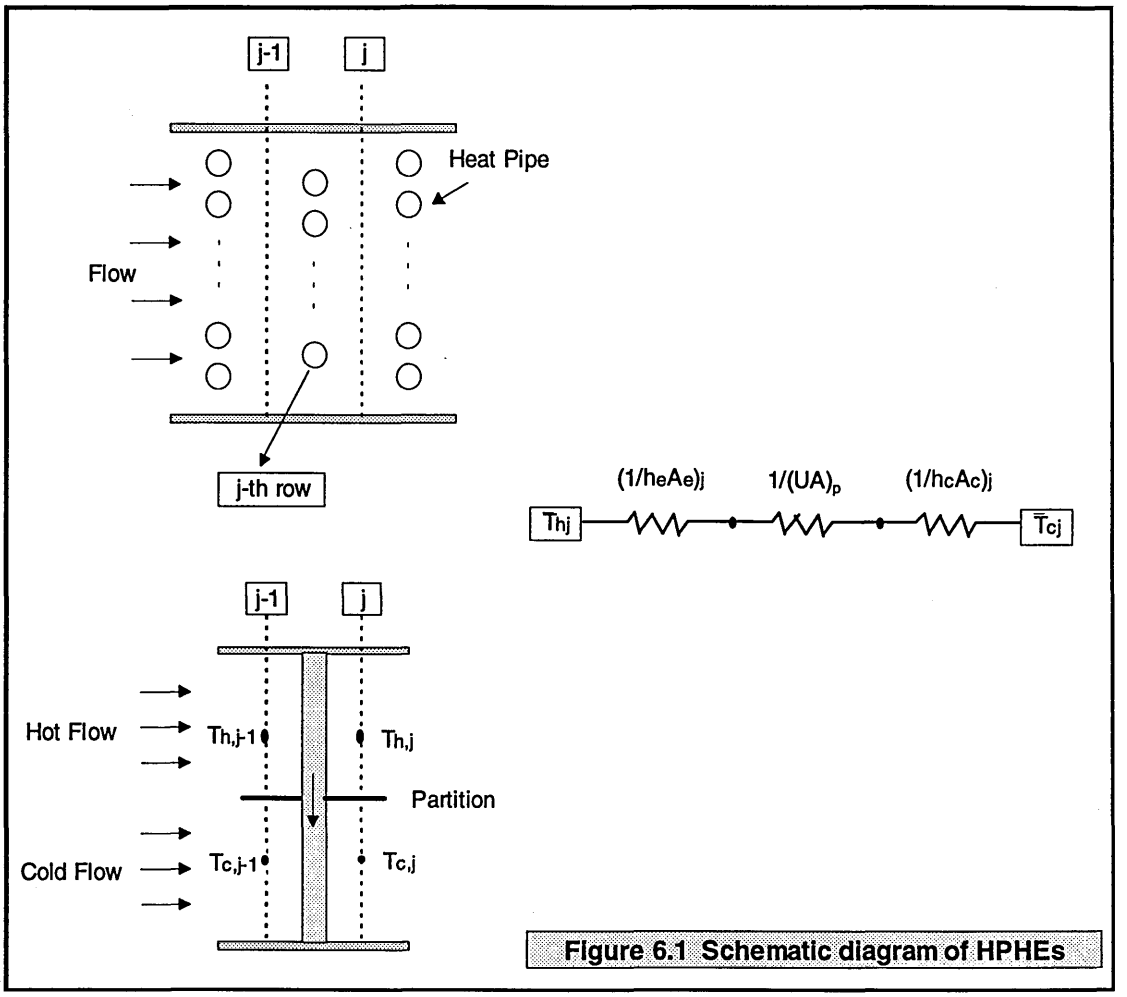

Figure 6.1 Schematic diagram of HPHEs

Where Rj is the overall heat-transfer resistance from the hot flow to the cold flow for a pipe in the jth row, and can be expressed as

$$R_j=(1/h_eA_e)_j+(1/UA)_p+(1/h_cA_c)_j \qquad (6.5)$$

where h_e and h_c are the convective heat-transfer coefficients between the pipe wall and the hot and cold flow, respectively ; A_e and A_c are the outside surface areas of the evaporating and the condensing sections ; and $(1/UA)_p$ is the thermal resistance of the heat pipe (or thermosyphon). The total heat-transfer rate delivered a HPHE, in which the pipes are arranged in N rows normal to the flow direction, can, then, be calculated as

$$Q = \sum_{j=1}^{N} Q_j \qquad (6.6)$$

It is necessary to calculate the temperature distributions in the hot and cold flows before calculating the total heat-transfer rate via equations (6.4) to

(6.6). By substituting equation (6.4) into equations (6.1) and (6.2), the temperature changes in the flows across the jth row of pipes can be expressed as

$$T_{h,j-1}-T_{h,j} = n_j (1/R_j) (\bar{T}_{h,j} - \bar{T}_{c,j}) / \dot{m}_h c_{ph} \quad (6.7)$$

$$T_{c,j}-T_{c,j-1} = n_j (1/R_j) (\bar{T}_{h,j} - \bar{T}_{c,j}) / \dot{m}_c c_{pc} \quad (6.8)$$

According to equations (6.7) and (6.8), the temperature distributions can be obtained, by employing the following iteration technique:

$$T^n_{h,j} = [1/(1+K_{hj})]\, T^o_{h,j-1} - \{ [K_{hj}/(1+K_{hj})] (T^o_{h,j-1}-T^o_{c,j}-T^o_{c,j-1}) \} \quad (6.9)$$

$$T^n_{c,j} = [1/(1+K_{cj})]\, T^o_{c,j-1} - \{ [K_{cj}/(1+K_{cj})] (T^o_{c,j-1}-T^o_{h,j}-T^o_{h,j-1}) \} \quad (6.10)$$

where the superscripts, n and o, represent the new and the old value corresponding of the temperature, respectively. The parameters K_{hj} , K_{cj} can be expressed as

$$K_{hj}=n_j / (2 \dot{m}_h c_{ph} R_j)$$

$$K_{cj}=n_j / (2 \dot{m}_c c_{pc} R_j) \quad (6.11)$$

Equation (6.9) and (6.10) can be used for parallel-flow design in cross-flow heat exchangers. However, equation (6.10) should be changed for counter-flow design because cold flow direction is reverse of parallel-flow. For counter-flow design, the following equations are used for employing iteration technique.

$$T^n_{h,j} = [1/(1+K_{hj})]\, T^o_{h,j-1} - \{ [K_{hj}/(1+K_{hj})] (T^o_{h,j-1}-T^o_{c,j}-T^o_{c,j-1}) \} \quad (6.12)$$

$$T^n_{c,j-1} = \{[K_{cj} /(K_{cj} - 1)] (T^o_{h,j} + T^o_{h,j-1} - T^o_{c,j})\} - \{ [1 /(K_{cj} - 1)]\, T^o_{c,j} \} \quad (6.13)$$

As shown Figure 6.2, most cross-flow tube banks have geometries that can be classified as either

- in-line arrays, in which tubes in successive (transverse) rows are in line in the direction of fluid flow, or
- staggered arrays, in which successive tube rows are staggered so that the tubes in any given row occupy a position in line with the midpoint of the gap between tubes in the previous row.

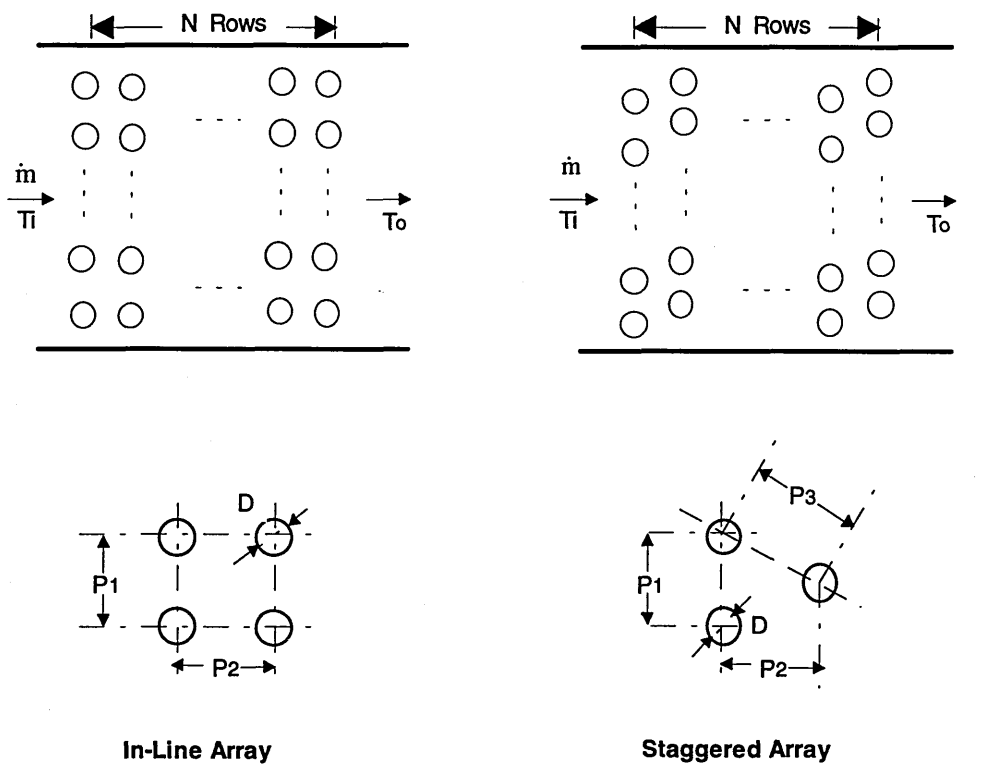

Figure 6.2 Geometry of Cross-flow Tube Arrays

To calculate the convective heat transfer coefficients h_e and h_c in cross-flow heat exchangers, the universal correlations proposed by the Engineering Science Data Unit (ESDU, 1973) are used, i.e. :

$$\overline{Nu_D} = hD/k = a\,(Re_{D,max})^m\ Pr^{0.34}\ F_1\ F_2 \qquad (6.14)$$

In equation (6.12) , all fluid properties are to be calculated at its bulk mean temperature. The correlation constants a and m are given in Table 6.1 as functions of the cross flow Reynolds number $Re_{D,max}$, which is defined as

$$Re_{D,max} = \rho\, V_{max}\, D / \mu \qquad (6.15)$$

where, V_{max} is the maximum flow velocity, calculated for the minimum flow area between tubes, normal to the local flow direction. Equations for the calculation of V_{max} for specific tube arrays are given in Table 6.2. In establishing the equations for V_{max} it has been assumed that the sum of the spaces between tubes in a given transverse row is equal to the sum of tube

diameters in a row. This implies, for instance, that in an in-line square array the gap at each edge of the bundle is equal to half the transverse tube spacing. In staggered arrays the gap between the end tube and the wall is larger and allowance must be made for this in calculating S_{min}. An approximate correction can be made by adding 0.5 to n_t if corbels or dummy half tubes are present, or 1.0 if they are not.

The correction factor F_1 accounts for surface-to-fluid bulk physical property variations and can be calculated as

$$F_1 = (Pr / Pr_w)^{0.26} \tag{6.16}$$

where Pr_w is the Prandtl number of the fluid at the wall temperature.

Figure 6.3 shows a plot of $(Nu_D / Pr^{0.34} F_1 F_2)$ as a function of $Re_{D,max}$. The factor F_2 corrects for the influence of the number of rows, N, on the average Nusselt number (see Figure 6.4). For N>10, F_2 is close to unity.

Table 6.1 Values of a and m (ESDU,1973)

$Re_{D,max}$	In-Line Banks		Staggered Banks	
	a	m	a	m
$10 - 3 \times 10^2$	0.742	0.431	1.309	0.360
$3 \times 10^2 - 2 \times 10^5$	0.211	0.651	0.273	0.635
$2 \times 10^5 - 2 \times 10^6$	0.116	0.700	0.124	0.700

Description	Layout Sketch	Range of Validity of Equation (2.218)	Formula for Calculating V_{max}
In-line square pitch (use a and m values for in-line bundle, Table 2.5)	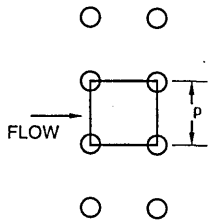	$1.2 < p/D < 4$ p = tube pitch D = tube diameter	$V_{max} = \frac{W}{\rho n_t (p - D) L}$ W = mass rate of fluid flow n_t = number of tubes in transverse row ρ = fluid density L = tube length
Rotated square pitch (use a and m values for staggered bundles, Table 2.5)	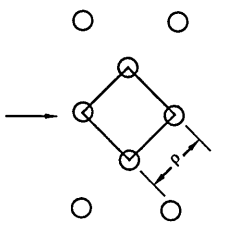	$1 < p/D < 2.8$	$V_{max} = \frac{W}{2\rho n_t (p - D) L}$, $p/D < 1.71$ $V_{max} = \frac{W}{\rho n_t (1.414\, p - D) L}$, $p/D > 1.71$
Triangular pitch (use a and m values for staggered bundles Table 2.5)	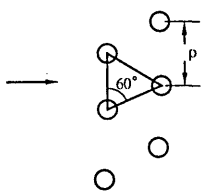	$1 < p/D < 4$	$V_{max} = \frac{W}{\rho n_t (p - D) L}$
Rotated triangular pitch (use a and m values for staggered bundles Table 2.5)	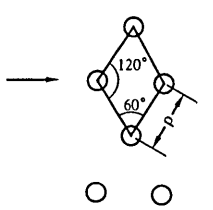	$1 < p/D < 2.3$	$V_{max} = \frac{W}{2\rho n_t (p - D) L}$, $p/D < 3.73$ $V_{max} = \frac{W}{\rho n_t (1.732 p - D) L}$, $p/D > 3.73$

Table 6.2 Tube Arrays Commly Used in Heat Exchangers (ESDU , 1973)

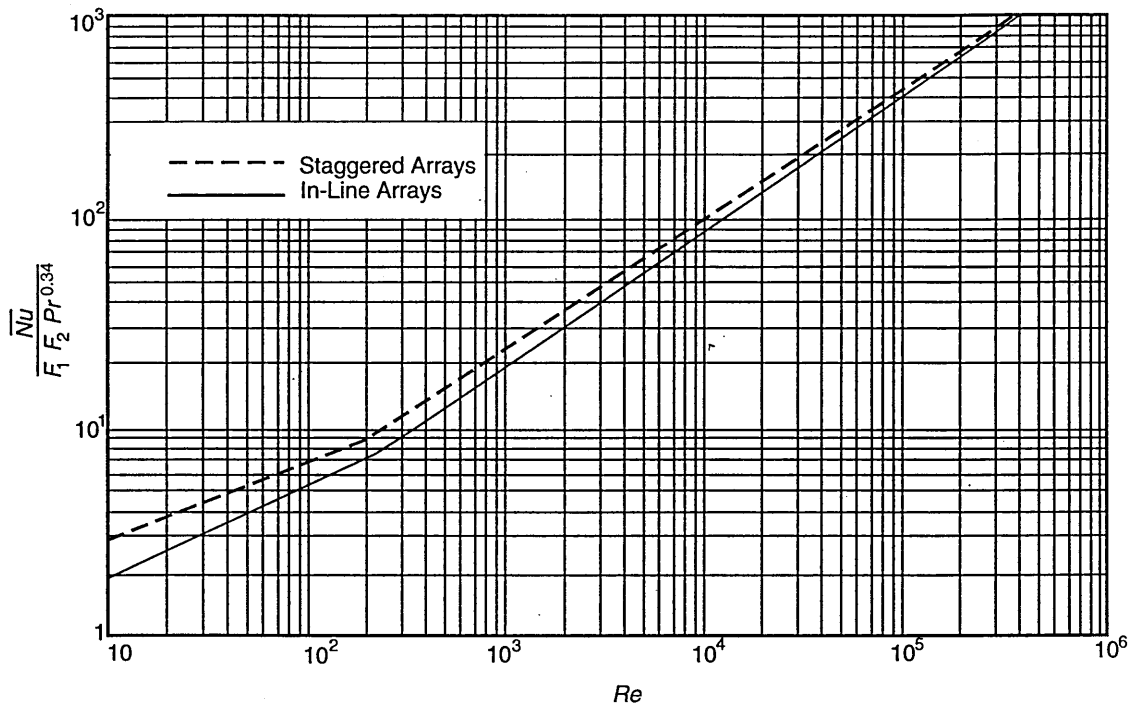

Figure 6.3 Variation of average Nusselt number with Reynolds number for in-line and staggered tube banks (ESDU, 1973)

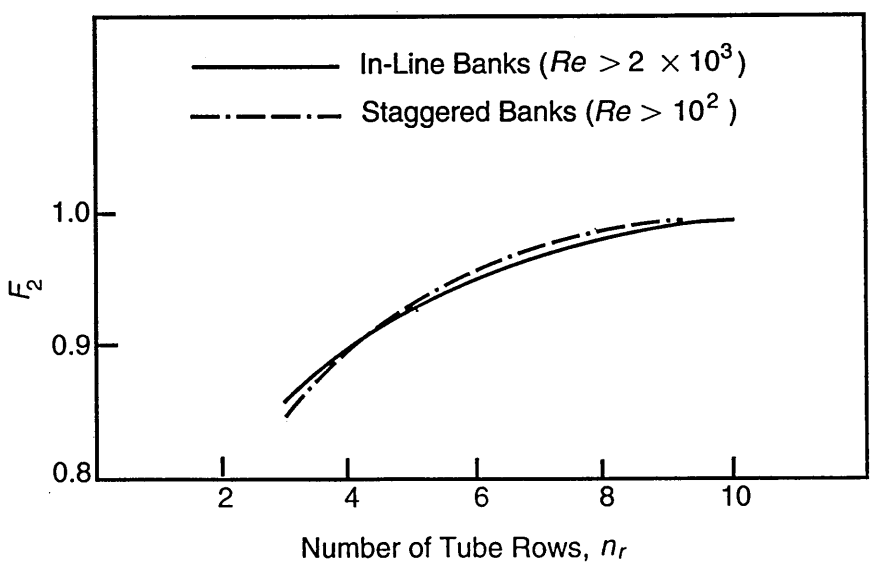

Figure 6.4 Correction factor F_2 (ESDU, 1973)

6.2 HPHE DESIGN MODEL

The above analysis was employed to develop a Visual Basic computer routine for designing cross-flow HPHEs. For given design specifications, the program predicts temperature distributions of the hot and cold streams at each transverse row of tubes and total heat-transfer rate. Consequently, it can be employed for optimising the design parameters and selecting the most appropriate type of heat pipe (or thermosyphon) for a specific waste-heat recovery system.

6.2.1 Computer Program Design

Figures 6.5 and 6.6 show the flow chart and input/output sheet for the 'HPHEs Design Model' developed. This computer program is designed to read input/output data of 'Heat Pipe and Thermosyphon Thermal Performance Model', i.e. diameter, pipe length and overall thermal resistance, by binding single heat pipe (or thermosyphon) data to this model.
It is also designed to read energy-transfer fluid properties (i.e. air properties (see Table 6.3)) by binding those properties to this model through the database file. It is easily designed to input HPHE specifications (i.e. number of rows, number of tubes in each row and geometry) and operating conditions (i.e. energy-transfer fluid temperature and mass flow rate) by using standard Windows object. Temperature distributions of the hot and cold streams at each transverse row of tubes and total heat-transfer rate can be calculated in consecutive order by just a few clicks. Because this computer model has not only its own command such as exit, print, connection to other computer program but also menus and dialogue boxes, it is convenient to operate the program under its own environment.

6.2.2 Computer Program Notes

(a) The program structure is as follows :

- It is connected with input/output data of Heat Pipe and Thermosyphon Thermal Performance Model.

- The data-base file with air properties can be incorporated.
- This program is divided into two parts according to the geometry of HPHEs (i.e. either in line array or the staggered array). The staggered array has three options according to the type of that array (i.e. rotated square pitch, triangular pitch, and rotated triangular pitch (see Table 6.2)). Each type has two options according to the presence of corbels or dummy half tubes.
- Each option goes to corresponding procedure and each procedure predicts temperature distributions of the hot and cold streams at each transverse row of tubes for parallel flow direction or counter flow direction of cross-flow heat exchanger.
- To solve the temperature distributions, iteration technique is employed. Figure 6.5 shows this procedure within 0.05°C temperature deviation between new value and old value.
- After the temperature distributions are calculated, total heat transfer-rate of HPHEs are estimated by the sequential order.

(b) The equations used in this computer program are as follows :

- To predict temperature distributions of the hot and cold streams at each transverse row of tubes by iteration technique, one pair of equation (6.9) and (6.10) and the other pair of equation (6.12) and (6.13) are employed for parallel-flow design and counter-flow design, respectively.
- To model the convetive heat transfer coefficient, equation (6.14) and (6.15) are used. The maximum flow velocity (V_{max}) is computed by Table 6.2 according to geometry of HPHE. Approximate correction for number of tubes in transverse row is made by the existence of corbels or dummy half tubes for calculating V_{max}. Correction constants a and m are coded by Table 6.1, and correction factors F_1 and F_2 are estimated by equation (6.16) and Figure 6.4, respectively. Figure 6.4 is changed from graph to numerical function for coding.
- After temperature distributions are calculated at each row, total heat transfer rate is computed by equation (6.6).

Figure 6.5 Flow chart for HPHEs Design Model

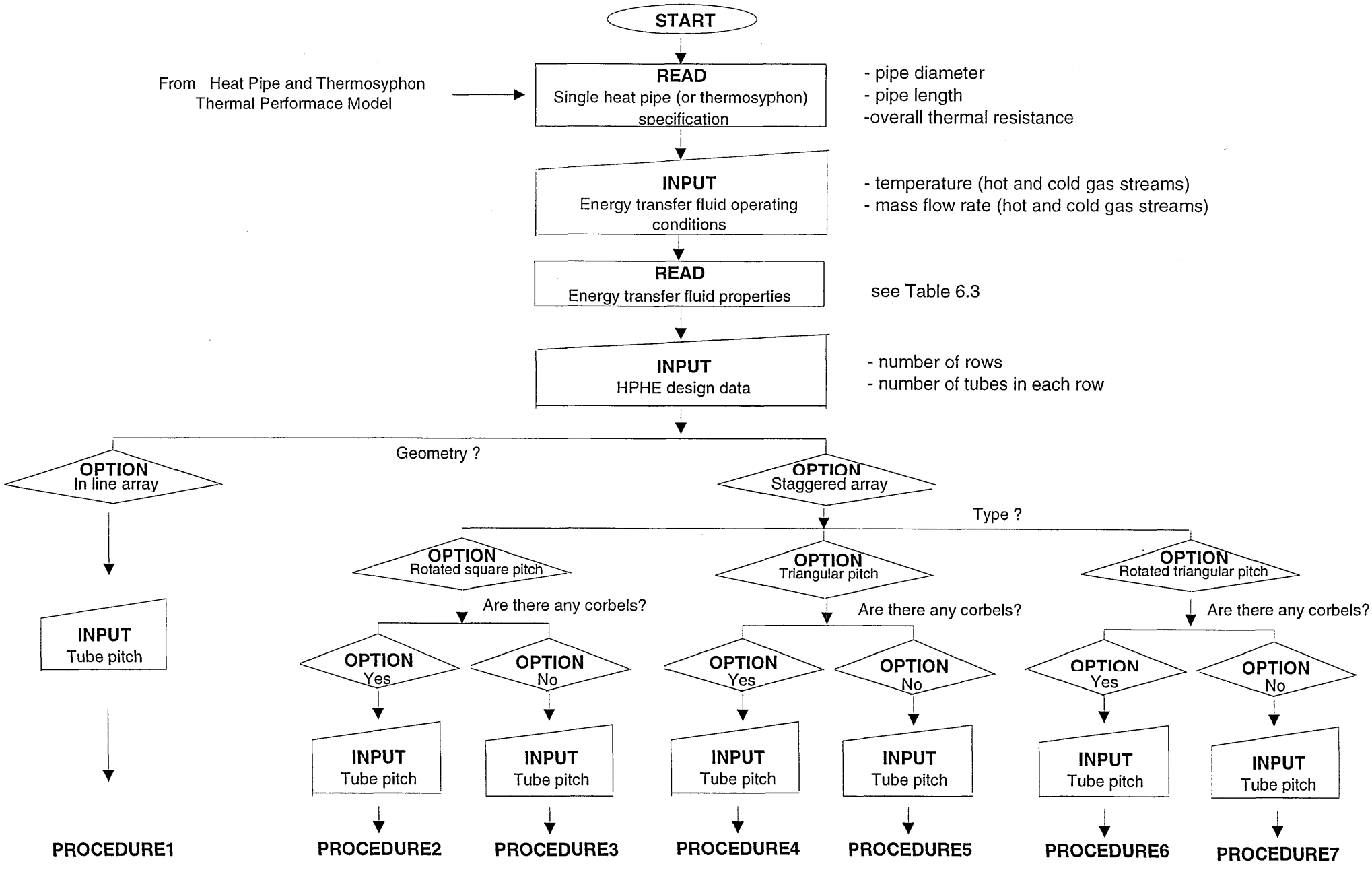

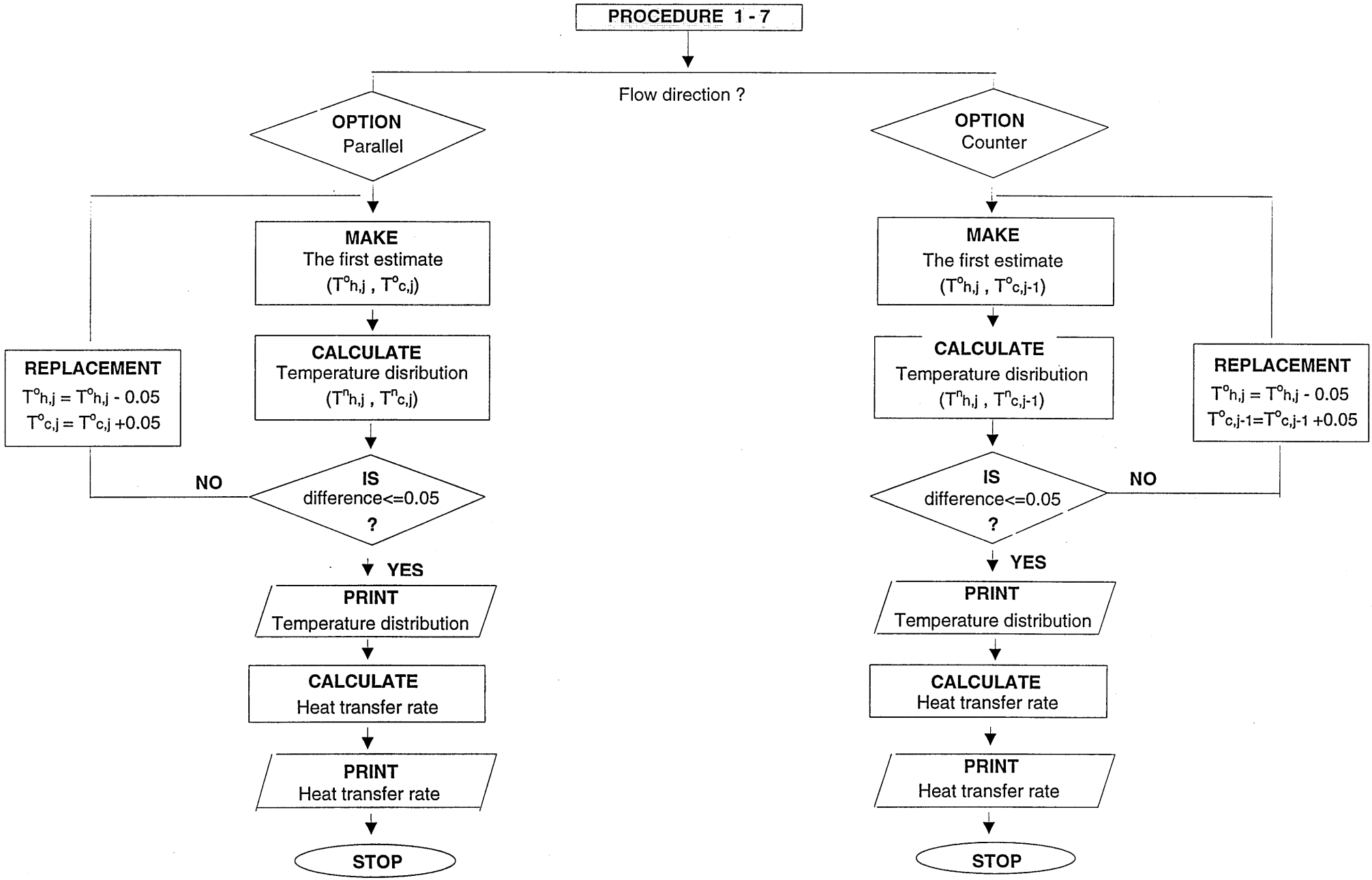
PROCEDURE 1 - 7
Flow direction ?
OPTION
Parallel
MAKE
The first estimate
($T^{o}_{h,j}$, $T^{o}_{c,j}$)
CALCULATE
Temperature disribution
($T^{n}_{h,j}$, $T^{n}_{c,j}$)
IS
difference<=0.05
?
NO
REPLACEMENT
$T^{o}_{h,j} = T^{o}_{h,j} - 0.05$
$T^{o}_{c,j} = T^{o}_{c,j} +0.05$
YES
PRINT
Temperature distribution
CALCULATE
Heat transfer rate
PRINT
Heat transfer rate
STOP
OPTION
Counter
MAKE
The first estimate
($T^{o}_{h,j}$, $T^{o}_{c,j-1}$)
CALCULATE
Temperature disribution
($T^{n}_{h,j}$, $T^{n}_{c,j-1}$)
IS
difference<=0.05
?
NO
REPLACEMENT
$T^{o}_{h,j} = T^{o}_{h,j} - 0.05$
$T^{o}_{c,j-1} = T^{o}_{c,j-1} +0.05$
YES
PRINT
Temperature distribution
CALCULATE
Heat transfer rate
PRINT
Heat transfer rate
STOP

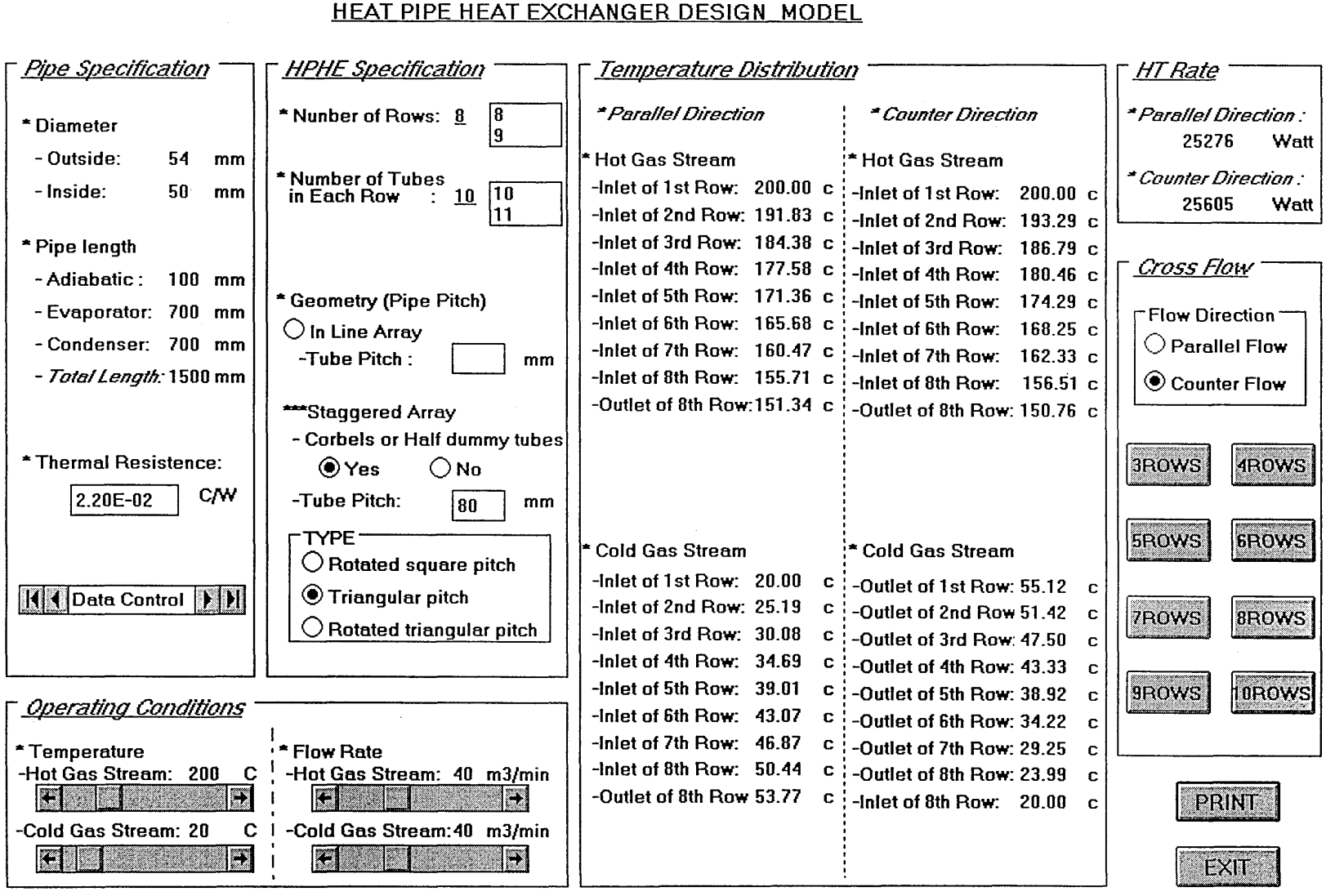

Figure 6.6 Example for the HPHEs Design Model

6.2.3 Case Study

Figure 6.7 presents the case study using HPHE Design Model. In that case study, total heat transfer rates of rectangular grooved wick HPHE are 25,943W and 26,304W for parallel-direction and counter-direction of cross-flow heat exchangers, respectively. Whereas, thermosyphon heat exchanger shows 25,276W and 25,605W for parallel-direction and counter-direction of cross-flow heat exchangers, respectively.

Figure 6.7 The case study of HPHEs Design model
(a) Heat pipe cross-flow heat exchangers

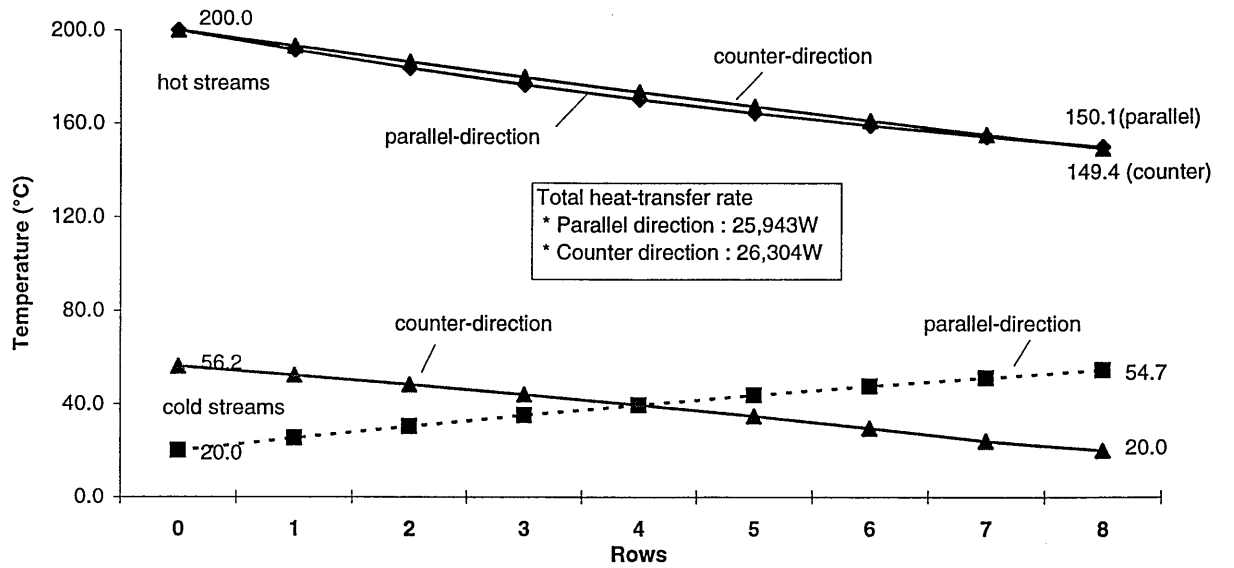

(b) Thermosyphon cross-flow heat exchagners

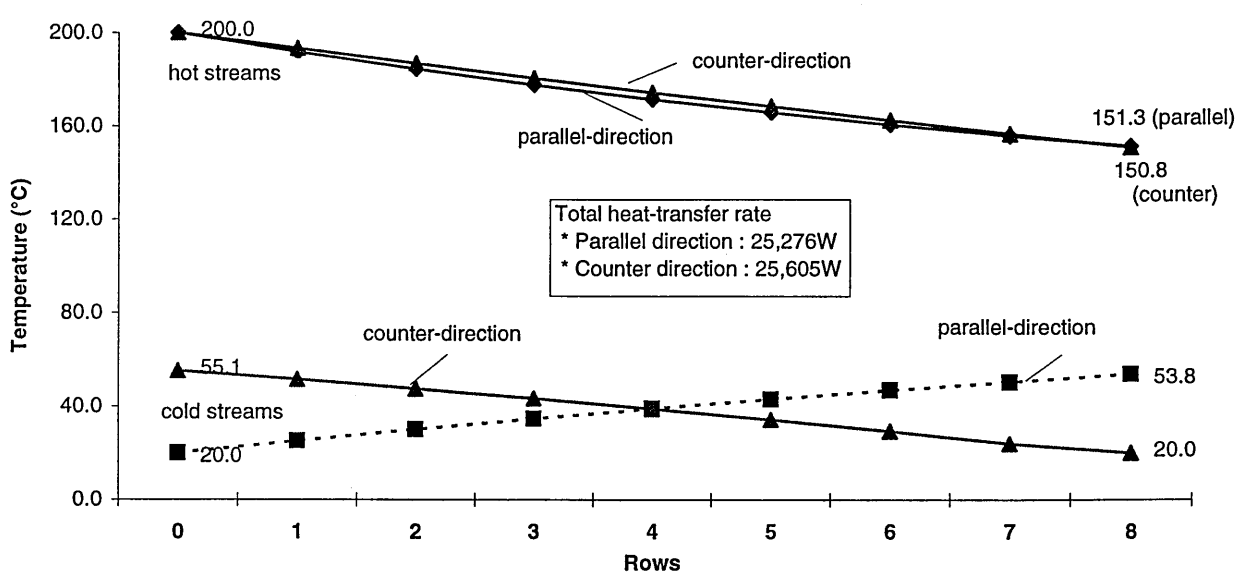

Single pipe specification		HPHE specification	Air operating condition
Heat-Pipe (Grooved wick)	* Diameter (mm) -Outside: 54, -Inside :50 * Pipe length (mm) -Adiabatic:100, -Evaporator:700 -Condenser:700 * Overall thermal resistance: 0.00680	* Number of Rows: 8 * Number of tubes in each row :10 * Geometry - Staggered array (Triangular pitch) - Tube pitch : 80mm - Corbels	* Temperature (°C) - Cold air stream : 20 - Hot air stream : 200 * Mass flow rate (m3/min) - Cold air stream : 40 - Hot air stream : 40
Thermo-syphon	* Diameter (mm) -Outside: 54, -Inside :50 * Pipe length (mm) -Adiabatic:100, -Evaporator:700 -Condenser:700 * Overall thermal resistance: 0.0220 °C/W		

CHAPTER 7 CONCLUSIONS AND RECOMMENDATIONS FOR FURTHER WORK

7.1 CONCLUSIONS

Heat pipes and closed two-phase thermosyphons are highly efficient heat transfer devices utilising the continuous evaporation and condensation of a suitable working fluid for two-phase heat transport in a closed system. As one of widely considered applications of heat pipes and thermosyphons, heat pipe heat exchangers (HPHEs) offer many advantages over other types of heat exchangers for the recovery of heat from industrial gaseous waste streams in the low and medium temperature ranges. Results of a thermal-performance comparative study between heat pipes and thermosyphons in HPHEs are presented in Figure 7.1. These were obtained at the same operating conditions by utilising the 'Heat Pipe and Thermosyphon Thermal Performance Model' and 'Heat Pipe Heat Exchangers Design Model' developed. The study indicates that thermosyphon exhibits relatively high rates of heat transfer as compared to conventional type of heat pipe (i.e. with a wrapped screen wick), whereas, it is clear that the overall heat-transfer coefficient for a grooved-wick heat pipe is better than that of a thermosyphon. However, the superior thermal performances of heat pipes with grooved wicks does not lead to a proportional decrease in the number of tubes in the design of HPHEs (see Figure 7.2) . The total heat transfer rate of rectangular grooves HPHE with 8rows-9tubes/row is almost same as thermosyphon heat exchangers with 8rows-10tubes/row in cross flow- counter HPHE.

These are important features associated with the present studies on heat-transfer characteristics of HPHEs for low and medium temperature recovery through comparison studies between thermosyphon and heat pipe, at the same operating conditions. On that point of view, it is concluded that two computer models is very useful for the field application.

Figure 7.1 Comparison between thermal performances of thermosyphon and heat pipes in HPHEs

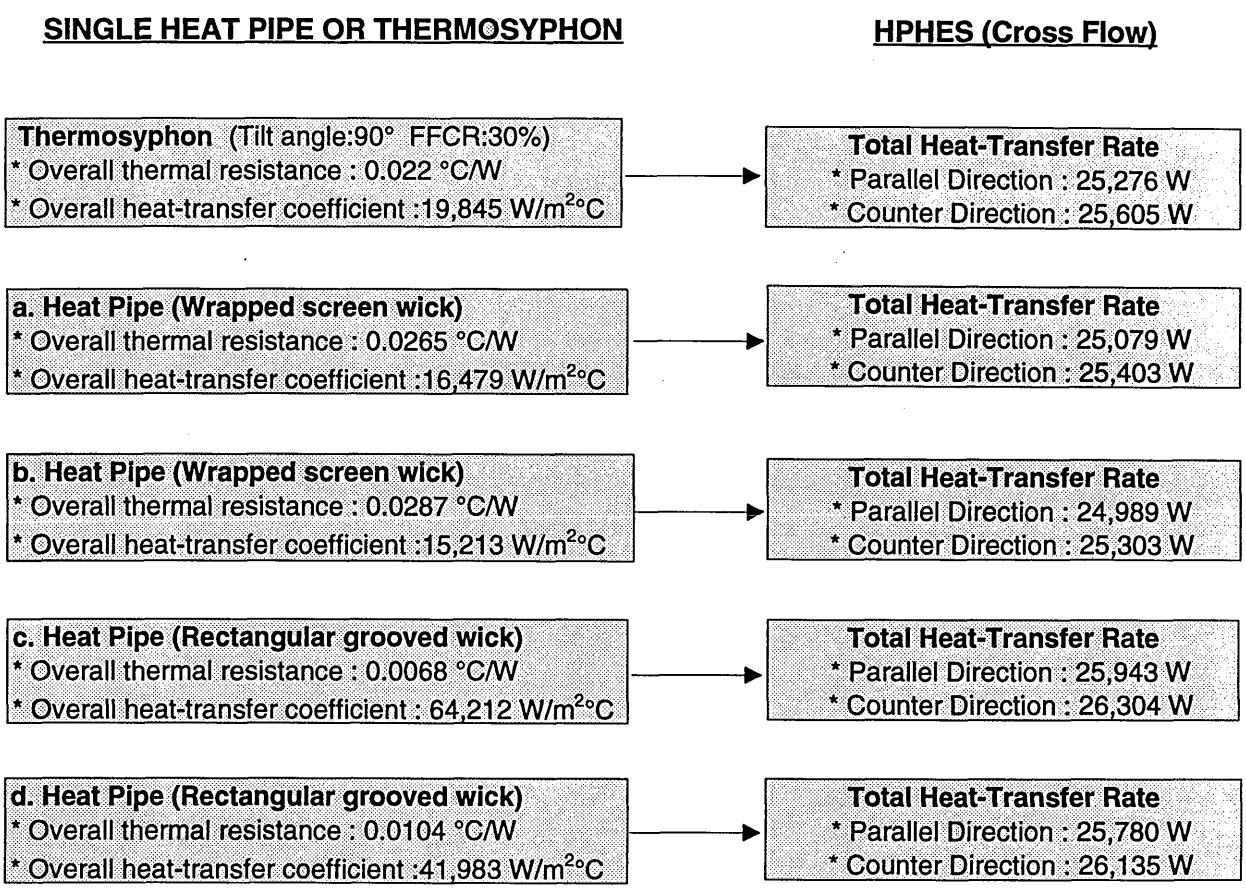

* Overall heat-tranfer coefficient : based upon the pipe cross-sectional area

Pipe Specification
- Outside diameter : 54 mm
- Inside diameter : 50 mm
- Vapour diameter :46 mm
- Pipe Length :1500 mm
  * Adiabatic section : 100 mm
  * Evaporator : 700 mm
  * Condenser : 700 mm

Wick Specification for Heat Pipes

a Mesh Number :200 in-1
Screen wire diameter : 0.0625 mm

b Mesh Number :100 in-1
Screen wire diameter : 0.1143 mm

c. Groove depth : 2.0 mm
Groove width : 1.31 mm
Number of grooves : 60

d. Groove depth : 2.0 mm
Groove width : 2.182 mm
Number of grooves : 36

HPHE Specification
- Number of rows :8
- Number of tubes in each row : 10
- Stagger array (Triangular pitch)
- Tube pitch :80 mm

Operating Condition
- Energy transfer fluid : air
- Hot gas streams
  * Temperature : 200°C
  * Flow rate : 40 m^3/min
- Cold gas streams
  * Temperature :20°C
  * Flow rate : 40 m3/min

Figure 7.2 The effect of thermal performances of a single thermosyphon and grooved-wick heat pipe on the overall performances of HPHEs

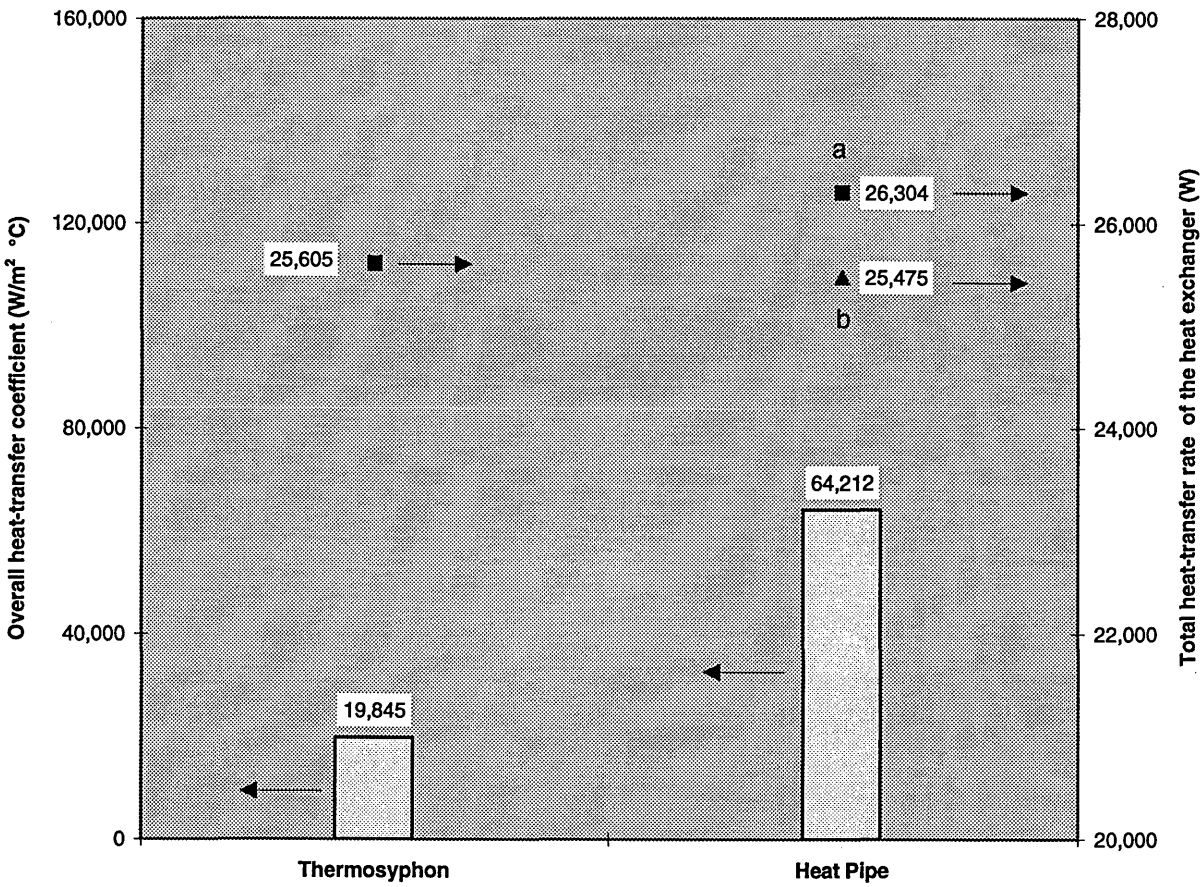

Specifications of the thermosyphon are as shown in Figure 7.1.
Those for the grooved-wick heat pipe are presented in Figure 7.1 c

	Thermosyphon	Grooved-Wick Heat Pipe	
HPHEs Specification	8 Rows - 10 tubes/row	**a**	8 Rows - 10 tubes/row
		b	8 Rows - 9 tubes/row

Operating conditions are the same as in Figure 7.1

7.2 EXPERIMENTAL INVESTIGATION

According to the experimental results, Nusselt's film theory for continuous liquid film could not be employed for predicting thermal performances in the condenser and evaporator film region of inclined thermosyphons. Liquid film could only be maintained circumferentially in vertical thermosyphon tubes, even though might not the smooth continuous film. In the evaporator pool region, the change in saturation temperature due to the hydrostatic height of the pool should be considered for predicting the axial temperature distributions. According to experimental results, Imura's equation (i.e. equation 3.14) could be employed for predicting thermal performance of the evaporator pool in the inclined thermosyphon if 'g' is replaced by 'g sinθ'.

7.3 SUGGESTIONS FOR FUTURE WORK

Whereas the present work is a contribution to research on heat transfer characteristics of heat pipe heat exchangers for low and medium temperature recovery, it should be realised that there is much work remaining to be done before it is accepted as a standard item to designers. It is hoped that the following suggestions may provoke new ideas for further investigations :

- In this study, experiments on thermal behaviour of thermosyphon were carried out at various FFCR, heat-supply rate to the evaporator, and inclination angle. However, accurate assessment of thermal performance of the inclined thermosyphon could not be achieved because of thermocouple locations on the upper-side of the thermosyphon tube. A continuos liquid film does not occur in the condenser and evaporator film region in case of the inclined thermosyphon. For further studies on inclined thermosyphon, it is recommended that thermocouples should be located circumferentially in the condenser and evaporator-film regions.
- No experimental investigations for the behaviours of heat pipes, at the same operating conditions, were carried out during this study. Only

analytical techniques were developed to evaluate their heat-transfer characteristics. Experimental validation of the computer model for heat pipes is needed. It is suggested that experimental testing of heat pipes should be done at the same operating conditions as for thermosyphon to facilitate a 'true' comparison.

- In this study, finned tubes for heat exchangers were not considered in Heat Pipe Heat Exchangers Design Model. For field applications, this arrangement should be considered.

REFERENCES

Al-Farah,M.; Kaviany,M.; Marshall,H. "Analysis of Film Condensation in Tilted Thermosyphon", ASME (Papers), Newyork, p.1-11, 1991

Ambrose,J.H.; Chow,L.C.; Ponnappan,R. "Boiling Heat Transfer Correlation for Heat Pipes", SAE Technical Paper Series, Warrebdale, PA, USA, 851326, p.7, 1985

Andros,F.E.; Florschuetz,L.W. "The Two-Phase Closed Thermosyphon: An Experimental Study with Flow Visualisation" Two-Phase Transport and Reactor Safety, Vol.4, Hemisphere Publishing Co., Washington DC, p.1231-1267, 1978

Asselman,G.; Green.D.B. "Heat Pipes", Phillips Tech. Rev., Vol.53, No.4, p.104-113, 1973

Bartsch,G.; Brito,J. "Heat Transfer Coefficient of Pool Boiling within the Heating Zone of a Two-Phase Closed Thermosyphon", ASME, Heat Transfer Division, Vol.140, New York, p.99-104, 1990

Berenson,P.J. "Experiment on Pool Boiling Heat Transfer", International Journal of Heat and Mass Transfer, Vol.5, p.985-999, 1962

Bezrodnyi,M.K.; Alekseenhi,D.B. "Investigation of the Critical Region of Heat and Mass Transfer in Low Temperature Wickless Heat Pipes", High Temperature, Vol.15, p.309-313, 1977

Binert,W.B. "Heat Pipes for Temperature Control", Proc.4th Intersoc. Energy Conversion Engineering Conference, Washington DC, p.1043-1041, September, 1969

Casarosa,C. ; Dobran,F. "Experimental Investigation and Analytical Modelling of a Closed Two-Phase Thermosyphon with Imposed Convection Boundary Conditions", International Journal of Heat and Mass Transfer, Vol. 31, No.9, p.1815-1833, 1988

Cheng,K.C. ; Rovang,G.W. "Heat Transfer Characteristics of a Closed-Loop Two-Phase Thermosyphon System for Low Grade Waste Heat Recovery from Liquid Heat Sources", ASME, Heat Transfer Division,vol.44, New York, p.53-61, 1985

Chi,S.W. "Heat Pipe Theory and Practice", Hemisphere Publishing.Co., McGraw-Hill Book Co., 1976

Chi,S.W. "Mathematical Modelling of High and Low Temperature Heat Pipes", GW University Rept. to NASA, Grant No. NGR 09-010-070, 1971

Cotter,T.P. "Theory of Heat Pipes", Los Alamos Scientific Laboratory, Rept. No. LA-3246-MS, 1965

Coyne-Pregner,P. ; Kemme,J.E. "Performance Limits of Gravity Assist Heat Pipes with Simple Wick Structures", Proceedings of the 4th International Heat Pipe Conference, London, Pergamon Press, Oxford,1981

Deverall,J.E. ; Kemme,J.E. ; Florschuetz,L.W. "Sonic Limitations and Start-up Problems of Heat Pipes, Los Alamos Scientific Laboratory, Rept.No. LA-4578, 1970

Dhir,V.K.; Lienhard,J.H. "Laminar Film Condensation on Plane and Axisymmetric Bodies in Non-Uniform Gravity", Journal of Heat Transfer, Vol.93, p.97, 1971

Dobran,F. "Steady-State Characteristics and Stability Thresholds of a Closed Two-Phase Thermosyphon", International Journal of Heat and Mass Transfer, Vol.28, No.5, p.949-957, 1985

Dunn,P.D.; Reay,D.A. "Heat Pipes" (4th Ed.), Oxford, Pergamon 1994

El-Genk,M. ; Huang,L. ; Tournier,J. "Transient Experiments of an Inclined Copper-Water Heat Pipe", Journal of Thermophysics and Heat Transfer, Vol. 9, No.1, p.109-116,1995

Feldman,K.T. ; Munje,S. "Experiments with Gravity-Assisted Heat Pipes with and without Circumferential Grooves", Journal of Energy, Vol.3, No. 4, 1979.

Fukano,T. ; Kadoguchi,K.; Tien,C. "Experimental Study on the Critical Heat-Flux at the Operating Limit of a Closed Two-Phase Thermosyphon", Heat Transfer-Japanese Research, Vol.17, No.5, p.43-60, 1988

Fukano,T. ; Kadoguchi,K. "Local Heat Transfer in a Reflux Condensation inside Closed Two-Phase Thermosyphon", Nippon Kikai Gakkai Ronbunshu, Vol.56, No.525, p.1475-1482, 1990

Gorring,R.L. ; Churchill,S.W. "Thermal Conductivity of Heterogeneous Materials Physical Principles of Heat Pipes", Chem.Eng.Prog., Vol.57, No.7, p. 53-59, 1961

Grakovich,L.P. ; Khrustalev,D.K. ; Ustok,K. "Overall Characteristics of Axial Grooved Heat Pipes", Heat Transfer-Soviet Research, Vol.20, No.5, p.702-708, 1988

Griffith,P. ; Wallis,J.D. "The Role of Surface Conditions in Nucleate Boiling", ASME-AIChE Heat Transfer Conference, August, 1959

Groll,M. ; Brost,O.; Heine,D. "Heat Transfer, Vapour-Liquid Flow Interaction and Materials Compatibility in Two-Phase Thermosyphons", Commission of the European Communities, Report EUR 8434, D.Reidel Publishing Co., p. 66-81, 1983

Groll,M. "Heat Pipe Research and Development in Western Europe", Heat recovery systems & CHP, Vol.9, No.1, p.19-66, 1989

Groll,M. ; Rosler,S. "Operation Principles and Performance of Heat Pipes and Closed Two-Phase Thermosyphons", Journal of Non-Equilibrium Thermodynamics , Vol .17, 1992

Gross,U.;Hahne.E. "Reflux Condensation Inside a Two-Phase Thermosyphon at Pressures up to the Critical", Proceedings of the 8th International Heat Transfer Conference, Hemisphere Publishing Co., Washington DC,USA, p. 1613-1620, 1986

Hsieh,S. ; Huang,D. "Comparisons of Thermal Performances and Pressure Drop of Counterflow and Parallel-Flow Heat Pipe Heat exchangers with Aligned/Staggered Tube Rows", Energy Conversion and Management, Vol.30, No.4, p 357-368, 1990

Hsieh,S. ; Liauh,C. ; Han,W. "Thermal Performances of Heat exchangers Applicable to Waste-Heat Recovery Systems", Applied Energy, Vol.29, No.3, p 191-200, 1988

Holman,J.P. "Heat Transfer" (7th Ed.), McGraw-Hill Book Co., 1990

Huang,B.J. ; Tsuei.J.T. "Method of Analysis for Heat Pipe Heat Exchangers", International Journal of Heat and Mass Transfer, Vol.28, No.3, p.553-562, 1985

Imura,H.; Kusuda,H.; Ogata,J. "Heat Transfer in the Two-Phase Closed Thermosyphon", Trans.of Japan Soc. Mech. Engrs., Vol.45, p.712-722, 1973

Imura,H.; Kozai,H.; Hayashida,S. "Heat Transfer Characteristics in Screen Wick Heat Pipes", Nippon Kikai Gakkai Ronbunshu, Vol.53, No.491, p.2143-2152, 1987

Ikeda,Y. "Effective Thermal Conductivity of Screen Wicks", ASME, Heat Transfer Division, ASME, Newyork, Vol.96, p.717-722, 1988

Kays,W.M. "Convective Heat and Mass Transfer", McGraw-Hill Book Co., Newyork, 1976

Kemme,J.E. "Theoretical Investigation of Heat Pipes Operating at Low Vapour Pressure", Los Alamos Scientific Laboratory, Rept. No. LA-4221-MS, 1969

Kemme,J.E. "High Performance Heat Pipes", 1967 Thermionic conversion specialist conference, Palo Alto, California, October 1967

Khrustalev,D. ; Faghri,A. "Heat Transfer during Evaporation on Capillary-Grooved Structure of Heat Pipes", Journal of Heat Transfer, Vol.117, No.3, p.740-747, 1995

Kozai,H.; Imura,H.; Ikeda,Y. "Effective Pore Radius of Screen Wicks", Nippon Kikai Gakkai Ronbunshu, Vol.56, No.521, p.168-174, 1990

Kuramae,M.; Matsumoto,M. "Dry-Out Characteristics", Heat Transfer-Japanese Research, Vol.14, No.3, p.84-99. 1985

Larkin,B.S. "An Experimental Study of the Temperature Profiles and Heat-Transfer Coefficients in a Heat Pipe for a Heat Exchangers", Proceedings of the 4th International Heat Pipe Conference, London, Pergamon Press, Oxford, p.177-191, 1981

Lee,Y. ; Bedrossian,A. "The Characteristics of Heat Exchangers Using Heat Pipes or Thermosyphons", International Journal of Heat and Mass Transfer, Vol.21, p. 221-229, 1978

Leidenfrost,W. ; Modrei,P. "Flow Conditions and Heat Transfer in a Two-Phase Closed Loop Thermosyphon", ASME, Fluids Engineering Division, ASME, New York, Vol.61, p.185-192, 1987

Levy,E.K. "Theoretical Investigation of Heat Pipes Operating at Low Vapour Pressure", Journal of Engineering for Industry, Vol.90, p. 547-552, 1968

Li,X. ; Wen,J.; Shan,Y "Condensing Heat Transfer in an Advanced Two-Phase Closed Thermosyphon", Chinese Journal of Chemical Engineering, Vol.4, No.1, p.85-89, 1996

Lienhard,J.H. ; Dhir, V.K. "Extended Hydrodynamic Theory of the Peak and Minimum Pool Boiling Heat Fluxes", NASA CR 2270, 1973

Lukitobudi,A.R. ; Akbarzadeh, A. "Desigh,Construction and Testing of a Thermosyphon Heat Exchanger for Medium Temperature Heat Recovery in Bakeries", Heat Recovery & CHP, Vol.15, No.5, p.481-491, 1995

Marcus,B.D. "Theory and Design of Variable Conductance Heat Pipes", NASA, CR-2018, 1972

Miyasaka,A. "Heat Transport Characteristics of Capillary Looped Pipes", Nippon Kikai Gakkai Ronbunshu, Vol.61, No.582, p.665-671, 1995

Mohamed,S.; Lianmin H. "Transient Experiments of an Inclined Copper-Boiling Regimes in a Closed Two-Phase Thermosyphon", International Journal of Heat and Mass Transfer, Vol.33, No.10, p.2099-2110, 1990

Niro,A.; Beretta,G "Boiling Regimes in a Closed Two-Phase Thermosyphon", International Journal of Heat and Mass Transfer, Vol.33, No.10, p.2099-2110, 1990

Niro,A.; Beretta,G "Analytical Model for the Design of Wickless Heat-Pipe Heat Exchangers", Heat Pipes and Thermosyphons of ASME, Heat Transfer Division, Vol.221, ASME, New York, p.61-68,1992

Noda,H.; Yoshioka,K.; Hamatake,T "Model for the Heat Transfer Limit of a Screen Wick Heat Pipe", Nippon Kikai Gakkai Ronbunshu, Vol.53, No.494, p.3118-3123, 1987

Noda,H.; Yoshioka,K.; Hamatake,T "Experimental Study on the Permeability of Screen Wicks", Nippon Kikai Gakkai Ronbunshu, Vol.57, No.542, p.3537-3542, 1991

O-uchi,M.; Takamori,Y. ; Izumi,M. "Boiling Heat Transfer of a Liquid Film Formed in the Evaporator of a Thermosyphon", Nippon Kikai Gakkai Ronbunshu, Vol.54, No.507, p.3227-3231, 1988

Pande,D.P.; Dhar,P.L.; Agarwal,R.S. "Thermal Hydraulic During Boiling in Thermosyphon Evaporators", Nuclear Technology, Vol.92, No.2, p.269-281, 1990

Peterson,G.P.; Bage,B.K. "Entrainment Limitatiions in Thermosyphons and Heat Pipes", Journal of Energy Resources Technology, Vol.113, No.3, p.147-153, 1991

Pioro,I.L. "Correlation of Experimental Data on the Maximum Heat and Mass Transfer in Two-Phase Thermosyphons", Heat Transfer-Soviet Research, Vol.17, No. 5, p.75-83, 1985

Pioro,.I.L..; Vorontsova,M.V. "Calculation of the Limiting Heat Flux for a Liquid Boiling in a Two-Phase Thermal-syphon", Journal of Engineering Physics, Vol.53, No.3, p.1003-1008, 1987

Reed,J.G.; Tien,C.L. "Modelling of the Two-Phase Thermosyphon", Journal of Heat Transfer, Vol.109, No.3, p.722-730, 1987

Rosenfeld,J.H. "Modelling of Heat Transfer into a Heat Pipe for a Localised Heat Input Zone", AIChE Symposium Series No.257, Vol.83 p.71-76, 1987

Rosenhow,W.M. "A Method of Correlating Heat Transfer Data for Surface Boiling of Saturated Liquids", ASME-AIChe Heat transfer symposium, Louisville, 1955

Shiraishi,M. ; Kikuchi,K. ; Yamanishi,T. "Investigation of Heat Transfer Characteristics of a Two-Phase Closed Thermosyphon", Proceedings of the 4th International Heat Pipe Conference, London, Pergamon Press, Oxford, p.95 - 104, 1981

Shishido,I. ; Matsuda,T. ; Iida,T. ; Ohtani,S "Measurement of Working Fluid Distribution within Heat Pipes", Energy Developments in Japan (Chicago), Vol.3, No 4, p.357-368, 1985

Silverstein,C.C. "Correlation of Heat Pipe Heat Transport Limits with Vapour Pressure", AIAA Paper, New York, USA, AIAA-85-0939, p5, 1985

Stephan,P.C. ; Busse,C.A. "Analysis of the Heat Transfer Coefficients of Grooved Heat Pipe Evaporator Walls", International Journal of Heat and Mass Transfer, Vol.35, No. 3, p.383-391, 1992

Swanson,L. ; Zillmann,W. "Optimal External Parameter Selection for Heat Pipe Heat Exchangers", AIChe Symposium Series, Vol.85, No.269, AIChe, Newyork, p.318, 1989

Takuma,M. ; Rosler,S. ; Maezawa,S. "Heat Transfer Characteristics of the Evaporator Section of the Annular Two-Phase Thermosyphons", Proceedings of International Heat Pipe Symposium, Osaka,1986

Tanisho,P.M. ; Murcia,N. "Experimental Analysis of Heat Recoveries with Heat Pipes in Low Inclination Angle", ECOS '92 International Syposium, ASME, Newyork, p.537-541, 1992

Terdtoon.P. "Investigation of Effect of Inclination Angle on Heat Transfer Characteristics of Closed Two-Phase Thermosyphons", Paper B9P, Proceedings of the 7th International Heat Pipe Conference, Minsk, May 1990

Tien,C.L. ; Chung,K.S. "Entrainment limits in heat pipes", AIAA Paper 78-382, Proceedings of the 3rd International Heat Pipe Conference, Palo Alto, AIAA Rept. CP784, Newyork,1978

Tu,C.; Xie.G; Gao,Z. "Two Phase Closed Thermosyphon - An Experimental Study with Flow Pattern and Optimum Fill Charge", Hemisphere Publishing Co., Washington DC, USA, p.395-405,1985

Vasilev,L.L. ; Grakovich,L.P. ; Khrustalev,D.K. "Low temperature axially grooved heat pipes", Proceedings of the 4th International Heat Pipe Conference, London, Pergamon Press, Oxford,1981

Vasilev,L.L. ; Grakovich,L.P. ; Khrustalev,D.K. "Limiting Characteristics of Inclined Thermosyphons and Heat Pipes with Excess Heat-Transfer Agent", Journal of Engineering Physics, Vol.46, No.5, p. 505-510, 1984

Yiwei,M. ; Wang,J.; Jifu,L.; Yi,F. "Theoretical and Experimental Studies on Condensation Heat Transfer inside Vertical and Inclined Thermosyphons", ASME, Heat Transfer Division, ASME, Newyork, Vol.108, p.111-116, 1989

Zuo,Z.J. ; Gunnerson,F.S. "Numerical Modelling of the Steady-State Two-Phase Closed Thermosyphon", International Journal of Heat and Mass Transfer, Vol.37, No.17, p. 2715-2722, 1994

Zuo,Z.J. ; Gunnerson,F.S. "Heat Transfer Analysis of an Inclined Two-Phase Closed Thermosyphon", Journal of Heat Transfer, Transactions ASME Vol.117, No.5, p. 1073-1075, 1995

Zuo,Z.J. ; Gunnerson,F.S. "Effect of Thermosyphon Size Reduction on Heat Transfer Performance", ASME/JSME Thermal Engineering Joint Conference - Proceedings Vol.2, ASME, New York, p.51-59, 1995

Table 3.6 Thermophysical Properties of Saturated Water (Liley, 1984)

T °C	λ kJ/kg	ρ_l kg/m^3	ρ_v kg/m^3	k_l W/m·K	μ_l 10^{-3} N·s/m^2	μ_v 10^{-5} N·s/m^2	p_v bars	c_{pv} kJ/kg·K	c_{pl} kJ/kg·K	σ_l 10^{-2} N/m	Pr_l -
0	2502.0	1000.0	0.005	0.569	1.750	0.802	0.00611	1.854	4.217	7.55	12.99
1	2499.5	1000.0	0.005	0.572	1.701	0.806	0.00654	1.855	4.214	7.54	12.61
2	2497.0	1000.0	0.006	0.574	1.652	0.809	0.00697	1.855	4.211	7.53	12.22
3	2494.6	1000.0	0.006	0.576	1.606	0.813	0.00756	1.856	4.208	7.52	11.83
4	2492.2	1000.0	0.006	0.577	1.560	0.817	0.00814	1.856	4.206	7.51	11.44
5	2489.8	1000.0	0.007	0.579	1.514	0.821	0.00873	1.857	4.203	7.50	11.04
6	2487.4	1000.0	0.007	0.580	1.468	0.825	0.00931	1.858	4.201	7.49	10.65
7	2485.0	1000.0	0.008	0.582	1.422	0.829	0.00990	1.858	4.198	7.48	10.26
8	2482.6	1000.0	0.008	0.584	1.383	0.833	0.01069	1.859	4.196	7.47	9.97
9	2480.2	1000.0	0.009	0.585	1.343	0.837	0.01149	1.859	4.194	7.46	9.68
10	2477.8	1000.0	0.009	0.587	1.304	0.841	0.01228	1.860	4.193	7.45	9.39
11	2475.4	1000.0	0.010	0.588	1.264	0.845	0.01308	1.860	4.191	7.44	9.10
12	2473.0	1000.0	0.010	0.590	1.225	0.849	0.01387	1.861	4.189	7.43	8.81
13	2470.6	999.8	0.011	0.592	1.196	0.853	0.01493	1.862	4.188	7.42	8.56
14	2468.2	999.6	0.012	0.593	1.167	0.857	0.01599	1.862	4.187	7.41	8.31
15	2465.8	999.3	0.013	0.595	1.138	0.861	0.01705	1.863	4.186	7.39	8.06
16	2463.4	999.0	0.013	0.596	1.109	0.865	0.01811	1.863	4.185	7.38	7.81
17	2461.0	999.0	0.014	0.598	1.080	0.869	0.01917	1.864	4.184	7.37	7.56
18	2458.6	998.8	0.015	0.600	1.056	0.873	0.02057	1.865	4.183	7.35	7.37
19	2456.2	998.6	0.016	0.601	1.032	0.877	0.02197	1.866	4.183	7.33	7.18
20	2453.8	998.4	0.017	0.603	1.007	0.881	0.02337	1.866	4.182	7.31	7.00
21	2451.4	998.2	0.018	0.604	0.983	0.885	0.02477	1.867	4.182	7.29	6.81
22	2449.0	998.0	0.019	0.606	0.959	0.889	0.02617	1.868	4.181	7.27	6.62
23	2446.8	997.8	0.021	0.607	0.938	0.893	0.02800	1.869	4.181	7.25	6.46
24	2444.6	997.6	0.022	0.609	0.917	0.897	0.02983	1.870	4.180	7.23	6.30
25	2442.4	997.4	0.023	0.610	0.897	0.901	0.03165	1.870	4.180	7.21	6.15
26	2440.2	997.2	0.024	0.612	0.876	0.905	0.03348	1.871	4.179	7.19	5.99
27	2438.0	997.0	0.026	0.613	0.855	0.909	0.03531	1.872	4.179	7.17	5.83
28	2435.6	996.6	0.028	0.614	0.838	0.913	0.03767	1.875	4.179	7.15	5.70
29	2433.2	996.2	0.030	0.616	0.821	0.917	0.04003	1.878	4.179	7.14	5.58
30	2430.8	995.8	0.032	0.617	0.803	0.921	0.04240	1.881	4.178	7.12	5.45
31	2428.4	995.4	0.034	0.619	0.786	0.925	0.04476	1.884	4.178	7.11	5.33
32	2426.0	995.0	0.036	0.620	0.769	0.929	0.04712	1.887	4.178	7.09	5.20
33	2423.6	994.6	0.037	0.622	0.754	0.933	0.05014	1.886	4.178	7.07	5.08
34	2421.2	994.2	0.039	0.623	0.739	0.937	0.05316	1.885	4.178	7.05	4.97

T °C	λ kJ/kg	ρ_l kg/m^3	ρ_v kg/m^3	k_l W/m·K	μ_l 10^{-3} N·s/m^2	μ_v 10^{-5} N·s/m^2	p_v bars	c_{pv} kJ/kg·K	c_{pl} kJ/kg·K	σ_l 10^{-2} N/m	Pr_l -
35	2418.8	993.8	0.040	0.625	0.725	0.941	0.05617	1.884	4.178	7.04	4.85
36	2416.4	993.4	0.042	0.626	0.710	0.945	0.05919	1.883	4.178	7.02	4.74
37	2414.0	993.0	0.044	0.628	0.695	0.949	0.06221	1.882	4.178	7.00	4.62
38	2411.6	992.8	0.046	0.629	0.682	0.953	0.06603	1.883	4.178	6.98	4.53
39	2409.2	992.6	0.049	0.630	0.669	0.957	0.06985	1.884	4.178	6.97	4.44
40	2406.8	992.5	0.051	0.632	0.657	0.961	0.07368	1.886	4.179	6.95	4.34
41	2404.4	992.3	0.054	0.633	0.644	0.965	0.07750	1.887	4.179	6.94	4.25
42	2402.0	992.1	0.056	0.634	0.631	0.969	0.08132	1.888	4.179	6.92	4.16
43	2399.6	991.5	0.059	0.635	0.620	0.973	0.08612	1.889	4.179	6.87	4.08
44	2397.2	990.9	0.062	0.636	0.609	0.977	0.09091	1.891	4.179	6.83	4.00
45	2394.8	990.3	0.065	0.638	0.599	0.981	0.09571	1.892	4.180	6.78	3.93
46	2392.4	989.7	0.068	0.639	0.588	0.985	0.10050	1.894	4.180	6.73	3.85
47	2390.0	989.1	0.072	0.640	0.577	0.989	0.10530	1.895	4.18	6.68	3.77
48	2387.6	988.7	0.075	0.641	0.567	0.993	0.11126	1.897	4.180	6.70	3.70
49	2385.2	988.3	0.079	0.642	0.557	0.997	0.11722	1.898	4.181	6.71	3.63
50	2382.8	988.0	0.083	0.643	0.548	1.001	0.12318	1.900	4.181	6.72	3.56
51	2380.4	987.6	0.087	0.644	0.538	1.005	0.12914	1.901	4.182	6.74	3.49
52	2378.0	987.2	0.090	0.645	0.528	1.009	0.13510	1.903	4.182	6.75	3.42
53	2375.6	986.6	0.095	0.646	0.520	1.013	0.14246	1.905	4.182	6.73	3.37
54	2373.2	986.0	0.100	0.647	0.512	1.017	0.14982	1.906	4.183	6.71	3.31
55	2370.8	985.4	0.104	0.648	0.505	1.021	0.15718	1.908	4.183	6.70	3.26
56	2368.4	984.8	0.109	0.649	0.497	1.025	0.16454	1.909	4.184	6.68	3.20
57	2366.0	984.3	0.113	0.650	0.489	1.029	0.17190	1.911	4.184	6.66	3.15
58	2363.6	983.9	0.119	0.651	0.482	1.033	0.18086	1.913	4.184	6.64	3.10
59	2361.2	983.5	0.124	0.652	0.475	1.037	0.18982	1.915	4.185	6.63	3.04
60	2358.8	983.1	0.130	0.654	0.467	1.041	0.19878	1.916	4.185	6.61	2.99
61	2356.4	982.7	0.135	0.655	0.460	1.045	0.20774	1.918	4.186	6.60	2.93
62	2354.0	982.3	0.141	0.656	0.453	1.049	0.21670	1.920	4.186	6.58	2.88
63	2351.6	981.7	0.148	0.657	0.446	1.053	0.22762	1.922	4.186	6.56	2.84
64	2349.2	981.2	0.154	0.658	0.440	1.057	0.23854	1.924	4.187	6.54	2.79
65	2346.8	980.6	0.161	0.658	0.433	1.061	0.24946	1.926	4.187	6.53	2.75
66	2344.4	980.0	0.168	0.659	0.427	1.065	0.26038	1.928	4.188	6.51	2.70
67	2342.0	979.4	0.174	0.660	0.420	1.069	0.27130	1.930	4.188	6.49	2.66
68	2339.4	978.9	0.182	0.662	0.414	1.073	0.28448	1.932	4.189	6.47	2.62
69	2336.8	978.3	0.190	0.663	0.408	1.077	0.29766	1.934	4.189	6.46	2.58
70	2334.2	977.7	0.198	0.665	0.401	1.081	0.31084	1.937	4.190	6.44	2.53
71	2331.6	977.1	0.206	0.666	0.395	1.085	0.32402	1.939	4.190	6.43	2.49
72	2329.0	976.6	0.214	0.668	0.389	1.089	0.33720	1.941	4.191	6.41	2.45

T °C	λ kJ/kg	ρ_l kg/m^3	ρ_v kg/m^3	k_l W/m·K	μ_l 10^{-3} N·s/m^2	μ_v 10^{-5} N·s/m^2	p_v bars	c_{pv} kJ/kg·K	c_{pl} kJ/kg·K	σ_l 10^{-2} N/m	Pr_l -
73	2326.6	977.2	0.223	0.668	0.384	1.093	0.35302	1.944	4.192	6.39	2.42
74	2324.2	977.8	0.232	0.668	0.379	1.097	0.36884	1.946	4.193	6.37	2.39
75	2321.8	978.5	0.241	0.668	0.375	1.101	0.38466	1.949	4.193	6.36	2.35
76	2319.4	979.1	0.251	0.668	0.370	1.105	0.40048	1.951	4.194	6.34	2.32
77	2317.0	979.7	0.260	0.668	0.365	1.109	0.41630	1.954	4.195	6.32	2.29
78	2314.4	977.9	0.271	0.669	0.361	1.113	0.43504	1.957	4.196	6.30	2.26
79	2311.8	976.2	0.282	0.669	0.356	1.117	0.45378	1.960	4.197	6.28	2.23
80	2309.2	974.4	0.293	0.670	0.352	1.121	0.47252	1.962	4.197	6.27	2.20
81	2306.6	972.6	0.304	0.670	0.347	1.125	0.49126	1.965	4.198	6.25	2.17
82	2304.0	970.9	0.315	0.671	0.343	1.129	0.51000	1.968	4.199	6.23	2.14
83	2301.4	970.1	0.327	0.672	0.339	1.133	0.53218	1.971	4.200	6.21	2.12
84	2298.8	969.4	0.340	0.672	0.335	1.137	0.55436	1.974	4.201	6.19	2.09
85	2296.2	968.6	0.353	0.673	0.332	1.141	0.57654	1.977	4.201	6.18	2.07
86	2293.6	967.9	0.365	0.673	0.328	1.145	0.59872	1.980	4.202	6.16	2.04
87	2291.0	967.1	0.378	0.674	0.324	1.149	0.62090	1.983	4.203	6.14	2.02
88	2288.4	966.4	0.393	0.675	0.320	1.153	0.64700	1.986	4.204	6.12	2.00
89	2285.8	965.6	0.408	0.675	0.317	1.157	0.67310	1.989	4.205	6.10	1.98
90	2283.2	964.9	0.423	0.676	0.313	1.161	0.69920	1.993	4.207	6.09	1.95
91	2280.6	964.1	0.437	0.676	0.310	1.165	0.72530	1.996	4.208	6.07	1.93
92	2278.0	963.4	0.452	0.677	0.306	1.169	0.75140	1.999	4.209	6.05	1.91
93	2275.4	962.8	0.469	0.677	0.303	1.173	0.78192	2.003	4.210	6.03	1.89
94	2272.8	962.3	0.486	0.678	0.299	1.177	0.81244	2.006	4.211	6.01	1.87
95	2270.2	961.7	0.503	0.678	0.296	1.181	0.84296	2.010	4.212	5.99	1.84
96	2267.6	961.2	0.520	0.679	0.292	1.185	0.87348	2.013	4.213	5.97	1.82
97	2265.0	960.6	0.537	0.679	0.289	1.189	0.90400	2.017	4.214	5.95	1.80
98	2262.4	959.9	0.557	0.679	0.286	1.193	0.93950	2.021	4.215	5.93	1.78
99	2259.8	959.1	0.577	0.680	0.283	1.197	0.97500	2.025	4.216	5.91	1.76
100	2257.2	958.4	0.596	0.680	0.280	1.201	1.01050	2.028	4.218	5.90	1.74
101	2254.6	957.7	0.616	0.681	0.277	1.205	1.04600	2.032	4.219	5.88	1.72
102	2252.0	956.9	0.635	0.681	0.274	1.209	1.08150	2.036	4.22	5.86	1.70
103	2249.4	956.2	0.658	0.681	0.271	1.213	1.12258	2.040	4.221	5.84	1.68
104	2246.8	955.5	0.680	0.682	0.268	1.217	1.16366	2.044	4.222	5.82	1.66
105	2244.2	954.7	0.703	0.682	0.266	1.221	1.20474	2.049	4.224	5.80	1.65
106	2241.6	954.0	0.725	0.683	0.263	1.225	1.24582	2.053	4.225	5.78	1.63
107	2239.0	953.3	0.748	0.683	0.260	1.229	1.28690	2.057	4.226	5.76	1.61
108	2236.2	952.6	0.773	0.683	0.258	1.233	1.33418	2.062	4.227	5.74	1.59
109	2233.4	951.8	0.799	0.684	0.255	1.237	1.38146	2.066	4.228	5.72	1.58
110	2230.6	951.1	0.824	0.684	0.253	1.241	1.42874	2.071	4.230	5.70	1.56

T °C	λ kJ/kg	ρ_l kg/m^3	ρ_v kg/m^3	k_l W/m·K	μ_l 10^{-3} N·s/m^2	μ_v 10^{-5} N·s/m^2	p_v bars	c_{pv} kJ/kg·K	c_{pl} kJ/kg·K	σ_l 10^{-2} N/m	Pr_l -
111	2227.8	950.4	0.850	0.685	0.250	1.245	1.47602	2.075	4.231	5.68	1.55
112	2225.0	949.7	0.875	0.685	0.248	1.249	1.52330	2.080	4.232	5.66	1.53
113	2222.4	948.8	0.904	0.685	0.246	1.253	1.57744	2.085	4.233	5.64	1.52
114	2219.8	947.9	0.933	0.685	0.244	1.257	1.63158	2.090	4.235	5.62	1.51
115	2217.2	947.0	0.962	0.686	0.241	1.261	1.68572	2.094	4.236	5.60	1.49
116	2214.6	946.1	0.991	0.686	0.239	1.265	1.73986	2.099	4.238	5.58	1.48
117	2212.0	945.2	1.020	0.686	0.237	1.269	1.79400	2.104	4.239	5.56	1.47
118	2209.1	944.4	1.055	0.686	0.235	1.273	1.86010	2.109	4.241	5.54	1.46
119	2206.2	943.6	1.090	0.686	0.233	1.276	1.92620	2.115	4.242	5.52	1.44
120	2203.3	942.8	1.125	0.687	0.231	1.280	1.99230	2.120	4.244	5.50	1.43
121	2200.4	942.0	1.159	0.687	0.229	1.283	2.05840	2.126	4.246	5.48	1.42
122	2197.5	941.2	1.194	0.687	0.227	1.287	2.12450	2.131	4.248	5.46	1.41
123	2194.6	940.4	1.229	0.687	0.225	1.291	2.19060	2.136	4.249	5.44	1.39
124	2191.7	939.6	1.264	0.687	0.223	1.294	2.25670	2.142	4.251	5.42	1.38
125	2188.8	938.8	1.298	0.688	0.221	1.298	2.32280	2.147	4.253	5.40	1.37
126	2185.9	938.0	1.333	0.688	0.219	1.301	2.38890	2.153	4.254	5.38	1.35
127	2183.0	937.2	1.368	0.688	0.217	1.305	2.45500	2.158	4.256	5.36	1.34
128	2180.0	936.3	1.419	0.688	0.215	1.309	2.53970	2.164	4.258	5.34	1.33
129	2177.0	935.5	1.470	0.688	0.214	1.312	2.62440	2.171	4.260	5.32	1.32
130	2174.0	934.6	1.520	0.688	0.212	1.316	2.70910	2.177	4.263	5.30	1.31
131	2171.0	933.7	1.571	0.688	0.210	1.320	2.79380	2.183	4.265	5.28	1.30
132	2168.0	932.9	1.622	0.688	0.209	1.324	2.87850	2.190	4.267	5.26	1.29
133	2165.0	932.0	1.673	0.688	0.207	1.327	2.96320	2.196	4.269	5.23	1.28
134	2162.0	931.1	1.724	0.688	0.205	1.331	3.04790	2.202	4.271	5.21	1.27
135	2159.0	930.2	1.775	0.688	0.203	1.335	3.13260	2.208	4.274	5.19	1.26
136	2156.0	929.4	1.825	0.688	0.202	1.338	3.21730	2.215	4.276	5.17	1.25
137	2153.0	928.5	1.876	0.688	0.200	1.342	3.30200	2.221	4.278	5.15	1.24
138	2150.0	927.6	1.924	0.688	0.199	1.346	3.40880	2.228	4.280	5.13	1.23
139	2147.0	926.6	1.972	0.688	0.197	1.349	3.51560	2.235	4.283	5.11	1.22
140	2144.0	925.7	2.019	0.688	0.196	1.353	3.62240	2.242	4.285	5.09	1.22
141	2141.0	924.8	2.067	0.688	0.194	1.357	3.72920	2.249	4.288	5.07	1.21
142	2138.0	923.8	2.115	0.688	0.193	1.361	3.83600	2.256	4.290	5.05	1.20
143	2135.0	922.9	2.162	0.688	0.191	1.364	3.94280	2.263	4.292	5.02	1.19
144	2132.0	921.9	2.210	0.688	0.190	1.368	4.04960	2.270	4.295	5.00	1.18
145	2129.0	921.0	2.258	0.688	0.188	1.372	4.15640	2.277	4.297	4.98	1.18
146	2126.0	920.1	2.305	0.688	0.187	1.375	4.26320	2.284	4.300	4.96	1.17
147	2123.0	919.1	2.353	0.688	0.185	1.379	4.37000	2.291	4.302	4.94	1.16
148	2119.8	918.2	2.420	0.688	0.184	1.383	4.50290	2.299	4.305	4.92	1.15

T °C	λ kJ/kg	ρ_l kg/m^3	ρ_v kg/m^3	k_l W/m·K	μ_l 10^{-3} N·s/m^2	μ_v 10^{-5} N·s/m^2	p_v bars	c_{pv} kJ/kg·K	c_{pl} kJ/kg·K	σ_l 10^{-2} N/m	Pr_l -
149	2116.6	917.3	2.487	0.687	0.183	1.386	4.63580	2.307	4.308	4.90	1.15
150	2113.4	916.4	2.553	0.687	0.181	1.390	4.76870	2.314	4.311	4.87	1.14
151	2110.2	915.4	2.620	0.687	0.180	1.393	4.90160	2.322	4.314	4.85	1.13
152	2107.0	914.5	2.687	0.687	0.179	1.397	5.03450	2.330	4.317	4.83	1.13
153	2103.8	913.6	2.754	0.686	0.178	1.400	5.16740	2.338	4.319	4.81	1.12
154	2100.6	912.7	2.821	0.686	0.177	1.404	5.30030	2.346	4.322	4.79	1.11
155	2097.4	911.8	2.887	0.686	0.175	1.407	5.43320	2.353	4.325	4.76	1.10
156	2094.2	910.8	2.954	0.685	0.174	1.411	5.56610	2.361	4.328	4.74	1.10
157	2091.0	909.9	3.021	0.685	0.173	1.414	5.69900	2.369	4.331	4.72	1.09
158	2087.8	909.0	3.102	0.685	0.172	1.418	5.86240	2.378	4.334	4.70	1.09
159	2084.6	908.1	3.183	0.684	0.171	1.421	6.02580	2.387	4.337	4.68	1.08
160	2081.4	907.2	3.264	0.684	0.170	1.425	6.18920	2.396	4.340	4.66	1.08
161	2078.2	906.3	3.345	0.684	0.169	1.428	6.35260	2.405	4.343	4.64	1.07
162	2075.0	905.4	3.426	0.684	0.168	1.432	6.51600	2.415	4.346	4.62	1.07
163	2071.8	904.5	3.507	0.683	0.166	1.436	6.67940	2.424	4.348	4.59	1.06
164	2068.6	903.6	3.588	0.683	0.165	1.439	6.84280	2.433	4.351	4.57	1.06
165	2065.4	902.7	3.669	0.683	0.164	1.443	7.00620	2.442	4.354	4.55	1.05
166	2062.2	901.8	3.750	0.682	0.163	1.446	7.16960	2.451	4.357	4.53	1.05
167	2059.0	900.9	3.831	0.682	0.162	1.450	7.33300	2.460	4.36	4.51	1.04
168	2055.5	899.9	3.929	0.682	0.161	1.454	7.53160	2.470	4.364	4.49	1.04
169	2052.0	898.8	4.038	0.681	0.160	1.457	7.73020	2.480	4.368	4.47	1.03
170	2048.5	897.8	4.160	0.681	0.159	1.461	7.92880	2.490	4.372	4.44	1.03
171	2045.0	896.7	4.293	0.680	0.158	1.464	8.12740	2.500	4.376	4.42	1.02
172	2041.5	895.7	4.438	0.680	0.157	1.468	8.32600	2.510	4.380	4.40	1.02
173	2038.0	894.6	4.594	0.680	0.156	1.471	8.52460	2.520	4.384	4.38	1.01
174	2034.5	893.6	4.763	0.679	0.155	1.475	8.72320	2.530	4.388	4.36	1.01
175	2031.0	892.6	4.943	0.679	0.154	1.478	8.92180	2.540	4.392	4.33	1.00
176	2027.5	891.5	5.135	0.678	0.153	1.482	9.12040	2.550	4.396	4.31	1.00
177	2024.0	890.5	4.808	0.678	0.152	1.485	9.31900	2.560	4.4	4.29	0.99
178	2020.5	891.2	4.926	0.678	0.151	1.488	9.55810	2.572	4.404	4.27	0.99
179	2017.0	891.9	5.044	0.677	0.150	1.492	9.79720	2.584	4.408	4.25	0.98
180	2013.5	892.6	5.162	0.677	0.149	1.495	10.03630	2.596	4.412	4.22	0.98
181	2010.0	893.3	5.280	0.676	0.148	1.499	10.27540	2.608	4.416	4.20	0.97
182	2006.5	894.0	5.398	0.676	0.148	1.502	10.51450	2.620	4.420	4.18	0.97
183	2003.0	894.7	5.516	0.675	0.147	1.505	10.75360	2.632	4.424	4.16	0.97
184	1999.5	895.4	5.634	0.675	0.146	1.509	10.99270	2.644	4.428	4.14	0.96
185	1996.0	896.1	5.752	0.674	0.145	1.512	11.23180	2.656	4.432	4.11	0.96
186	1992.5	896.8	5.870	0.674	0.144	1.516	11.47090	2.668	4.436	4.09	0.95

T °C	λ kJ/kg	ρ_l kg/m^3	ρ_v kg/m^3	k_l W/m·K	μ_l 10^{-3} N·s/m^2	μ_v 10^{-5} N·s/m^2	p_v bars	c_{pv} kJ/kg·K	c_{pl} kJ/kg·K	σ_l 10^{-2} N/m	Pr_l -
187	1989.0	897.5	5.988	0.673	0.143	1.519	11.71000	2.680	4.44	4.07	0.95
188	1985.2	894.6	6.124	0.672	0.142	1.523	11.99400	2.691	4.444	4.05	0.95
189	1981.4	891.6	6.261	0.672	0.142	1.526	12.27800	2.702	4.448	4.03	0.94
190	1977.6	888.7	6.397	0.671	0.141	1.530	12.56200	2.713	4.452	4.00	0.94
191	1973.8	885.7	6.534	0.671	0.140	1.533	12.84600	2.724	4.456	3.98	0.94
192	1970.0	882.8	6.670	0.670	0.140	1.537	13.13000	2.735	4.460	3.96	0.94
193	1966.2	879.8	6.807	0.669	0.139	1.540	13.41400	2.746	4.464	3.94	0.93
194	1962.4	876.9	6.943	0.669	0.138	1.544	13.69800	2.757	4.468	3.92	0.93
195	1958.6	873.9	7.080	0.668	0.137	1.547	13.98200	2.768	4.472	3.89	0.93
196	1954.8	871.0	7.216	0.668	0.137	1.551	14.26600	2.779	4.476	3.87	0.92
197	1951.0	868.1	7.353	0.667	0.136	1.554	14.55000	2.790	4.48	3.85	0.92
198	1947.1	866.9	7.519	0.666	0.135	1.557	14.88500	2.805	4.485	3.83	0.92
199	1943.2	865.8	7.684	0.666	0.135	1.561	15.22000	2.820	4.490	3.80	0.91
200	1939.3	864.7	7.850	0.665	0.134	1.564	15.55500	2.835	4.495	3.78	0.91
201	1935.4	863.6	8.015	0.664	0.133	1.568	15.89000	2.850	4.500	3.76	0.91
202	1931.5	862.5	8.181	0.664	0.133	1.571	16.22500	2.865	4.505	3.74	0.91
203	1927.6	861.4	8.347	0.663	0.132	1.574	16.56000	2.880	4.510	3.71	0.90
204	1923.7	860.2	8.512	0.662	0.131	1.578	16.89500	2.895	4.515	3.69	0.90
205	1919.8	859.1	8.678	0.661	0.130	1.581	17.23000	2.910	4.520	3.67	0.90
206	1915.9	858.0	8.843	0.661	0.130	1.585	17.56500	2.925	4.525	3.64	0.89
207	1912.0	856.9	9.009	0.660	0.129	1.588	17.90000	2.940	4.53	3.62	0.89
208	1907.8	855.7	9.193	0.659	0.129	1.592	18.29300	2.956	4.536	3.60	0.89
209	1903.6	854.4	9.376	0.658	0.128	1.595	18.68600	2.972	4.542	3.57	0.89
210	1899.4	853.2	9.560	0.657	0.128	1.599	19.07900	2.988	4.548	3.55	0.88
211	1895.2	852.0	9.744	0.656	0.127	1.602	19.47200	3.004	4.554	3.53	0.88
212	1891.0	850.7	9.928	0.656	0.127	1.606	19.86500	3.020	4.560	3.51	0.88
213	1886.8	849.5	10.111	0.655	0.126	1.609	20.25800	3.036	4.566	3.48	0.88
214	1882.6	848.3	10.295	0.654	0.126	1.613	20.65100	3.052	4.572	3.46	0.88
215	1878.4	847.1	10.479	0.653	0.125	1.616	21.04400	3.068	4.578	3.44	0.87
216	1874.2	845.8	10.662	0.652	0.125	1.620	21.43700	3.084	4.584	3.41	0.87
217	1870.0	844.6	10.846	0.651	0.124	1.623	21.83000	3.100	4.59	3.39	0.87
218	1865.5	843.3	11.067	0.650	0.123	1.627	22.28700	3.117	4.597	3.37	0.87
219	1861.0	841.9	11.288	0.649	0.123	1.630	22.74400	3.134	4.604	3.34	0.87
220	1856.5	840.6	11.509	0.648	0.122	1.634	23.20100	3.151	4.611	3.32	0.87
221	1852.0	839.3	11.730	0.647	0.122	1.637	23.65800	3.168	4.618	3.30	0.87
222	1847.5	837.9	11.951	0.647	0.121	1.641	24.11500	3.185	4.625	3.28	0.87
223	1843.0	836.6	12.171	0.646	0.120	1.645	24.57200	3.202	4.632	3.25	0.86
224	1838.5	835.3	12.392	0.645	0.120	1.648	25.02900	3.219	4.639	3.23	0.86

T °C	λ kJ/kg	ρ_l kg/m^3	ρ_v kg/m^3	k_l W/m·K	μ_l 10^{-3} N·s/m^2	μ_v 10^{-5} N·s/m^2	p_v bars	c_{pv} kJ/kg·K	c_{pl} kJ/kg·K	σ_l 10^{-2} N/m	Pr_l -
225	1834.0	833.9	12.613	0.644	0.119	1.652	25.48600	3.236	4.646	3.21	0.86
226	1829.5	832.6	12.834	0.643	0.119	1.655	25.94300	3.253	4.653	3.18	0.86
227	1825.0	831.3	13.055	0.642	0.118	1.659	26.40000	3.270	4.66	3.16	0.86
228	1820.4	830.0	13.334	0.641	0.118	1.663	26.92600	3.290	4.668	3.14	0.86
229	1815.8	828.7	13.614	0.640	0.117	1.666	27.45200	3.310	4.676	3.11	0.86
230	1811.2	827.4	13.893	0.639	0.117	1.670	27.97800	3.330	4.684	3.09	0.86
231	1806.6	826.1	14.172	0.638	0.116	1.673	28.50400	3.350	4.692	3.07	0.86
232	1802.0	824.8	14.452	0.637	0.116	1.677	29.03000	3.370	4.700	3.05	0.86
233	1797.4	823.5	14.731	0.635	0.115	1.681	29.55600	3.390	4.708	3.02	0.85
234	1792.8	822.2	15.010	0.634	0.115	1.684	30.08200	3.410	4.716	3.00	0.85
235	1788.2	820.9	15.289	0.633	0.114	1.688	30.60800	3.430	4.724	2.98	0.85
236	1783.6	819.6	15.569	0.632	0.114	1.691	31.13400	3.450	4.732	2.95	0.85
237	1779.0	818.3	15.848	0.631	0.113	1.695	31.66000	3.470	4.74	2.93	0.85
238	1774.1	816.9	16.168	0.630	0.113	1.699	32.26400	3.493	4.750	2.91	0.85
239	1769.2	815.4	16.488	0.629	0.112	1.703	32.86800	3.516	4.760	2.88	0.85
240	1764.3	814.0	16.808	0.628	0.112	1.706	33.47200	3.539	4.770	2.86	0.85
241	1759.4	812.5	17.128	0.627	0.111	1.710	34.07600	3.562	4.780	2.83	0.85
242	1754.5	811.1	17.448	0.626	0.111	1.714	34.68000	3.585	4.790	2.81	0.85
243	1749.6	809.6	17.768	0.625	0.110	1.718	35.28400	3.608	4.800	2.79	0.84
244	1744.7	808.2	18.088	0.624	0.110	1.722	35.88800	3.631	4.810	2.76	0.84
245	1739.8	806.8	18.408	0.623	0.109	1.725	36.49200	3.654	4.820	2.74	0.84
246	1734.9	805.3	18.728	0.622	0.109	1.729	37.09600	3.677	4.830	2.71	0.84
247	1730.0	803.9	19.048	0.621	0.108	1.733	37.70000	3.700	4.84	2.69	0.84
248	1724.9	802.3	19.390	0.620	0.108	1.737	38.38800	3.726	4.851	2.67	0.84
249	1719.8	800.8	19.733	0.618	0.107	1.741	39.07600	3.752	4.862	2.64	0.84
250	1714.7	799.3	20.075	0.617	0.107	1.745	39.76400	3.778	4.873	2.62	0.84
251	1709.6	797.8	20.418	0.616	0.106	1.749	40.45200	3.804	4.884	2.59	0.84
252	1704.5	796.3	20.760	0.615	0.106	1.753	41.14000	3.830	4.895	2.57	0.85
253	1699.4	794.7	21.102	0.613	0.106	1.756	41.82800	3.856	4.906	2.55	0.85
254	1694.3	793.2	21.445	0.612	0.105	1.760	42.51600	3.882	4.917	2.52	0.85
255	1689.2	791.7	21.787	0.611	0.105	1.764	43.20400	3.908	4.928	2.50	0.85
256	1684.1	790.2	22.130	0.609	0.104	1.768	43.89200	3.934	4.939	2.47	0.85
257	1679.0	788.6	22.472	0.608	0.104	1.772	44.58000	3.960	4.95	2.45	0.85

Table 5.1 Experimental Results of Steady-State Temperature Distribution

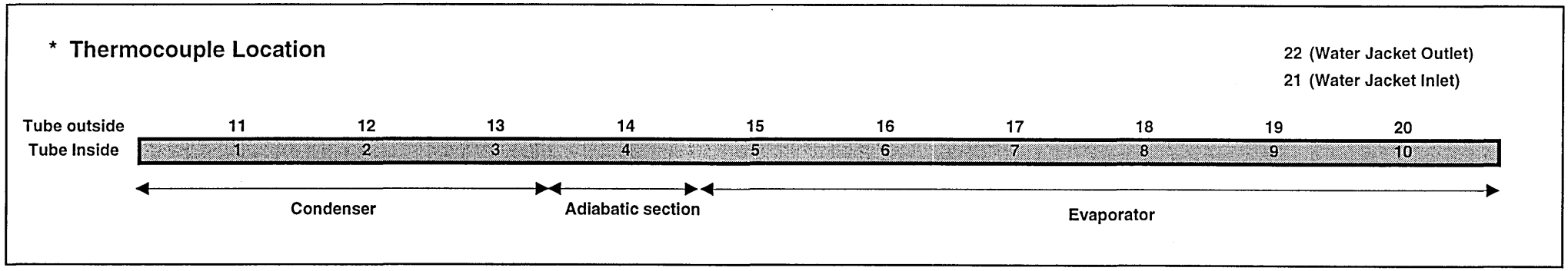

Fluid fill charge ratio:30% , Tilt angle:30°

* Heat-supply rate = 200W

	Temperature at the stated location (°C)																					
TEST	1	2	3	4	5	6	7	8	9	10	11	12	13	14	15	16	17	18	19	20	21	22
A	19.6	20.5	27.6	34.3	35.4	32.4	31.1	30.9	32.0	33.1	20.1	20.1	26.2	34.5	41.2	43.7	43.1	38.6	32.6	34.6	19.7	20.1
B	19.6	20.5	27.2	34.5	35.1	33.8	30.9	30.6	33.8	33.2	20.1	20.1	25.7	34.3	41.1	43.6	43.0	39.2	35.6	34.7	19.6	20.1
C	19.7	20.5	26.9	33.8	33.1	33.2	30.7	30.5	34.6	33.5	20.1	20.1	25.1	34.1	40.8	43.4	43.1	40.5	37.4	34.9	19.6	20.0
D	19.6	20.5	27.2	33.1	31.3	32.2	30.8	30.6	33.3	33.6	20.1	20.1	25.4	34.0	40.7	43.2	42.7	39.2	34.7	34.8	19.6	20.0
mean value	19.6	20.5	27.2	33.9	33.7	32.9	30.9	30.7	33.4	33.4	20.1	20.1	25.6	34.2	41.0	43.5	43.0	39.4	35.1	34.8	19.6	20.1

* Heat-supply rate = 300W

	Temperature at the stated location (°C)																					
TEST	1	2	3	4	5	6	7	8	9	10	11	12	13	14	15	16	17	18	19	20	21	22
A	20.0	21.3	31.6	43.0	44.1	40.3	39.5	38.9	40.2	41.0	20.2	20.2	29.2	42.8	53.4	57.4	57.4	53.0	41.6	42.6	19.6	20.2
B	19.9	21.2	31.3	42.8	43.5	39.5	39.2	38.9	40.2	40.9	20.2	20.2	28.9	42.7	53.1	57.1	57.0	52.9	41.4	42.5	19.5	20.2
C	20.0	21.3	31.3	42.6	42.6	38.9	39.1	38.8	40.3	40.9	20.2	20.2	29.0	42.6	52.9	56.7	56.6	52.3	41.4	42.4	19.5	20.2
D	20.0	21.3	30.7	42.6	42.2	38.9	39.1	38.7	40.3	40.8	20.2	20.2	28.3	42.5	52.8	56.8	56.4	52.1	41.3	42.3	19.6	20.1
mean value	20.0	21.3	31.2	42.8	43.1	39.4	39.2	38.8	40.3	40.9	20.2	20.2	28.9	42.7	53.1	57.0	56.9	52.6	41.4	42.5	19.6	20.2

* Heat-supply rate = 400W

TEST	Temperature at the stated location (°C)																					
	1	2	3	4	5	6	7	8	9	10	11	12	13	14	15	16	17	18	19	20	21	22
A	20.4	22.4	31.7	40.4	40.2	40.1	40.2	40.0	41.9	43.2	20.5	20.5	33.1	45.3	57.6	60.4	58.8	54.0	42.7	44.7	19.7	20.4
B	20.3	23.7	36.9	42.2	41.2	41.0	41.0	40.8	42.4	43.3	20.4	20.9	38.6	46.0	59.2	64.4	60.2	55.9	43.2	45.2	19.5	20.4
C	20.4	22.4	30.9	41.7	40.5	40.3	40.4	40.1	42.0	43.1	20.5	20.6	34.1	45.4	58.3	62.9	62.7	56.5	42.9	44.9	19.5	20.4
D	20.4	24.0	35.0	44.9	44.1	40.7	40.5	40.4	42.1	43.4	20.5	20.7	38.6	45.8	59.6	64.8	59.4	55.4	43.7	45.4	19.5	20.4
mean value	20.4	23.1	33.6	42.3	41.5	40.5	40.5	40.3	42.1	43.3	20.5	20.7	36.1	45.6	58.7	63.1	60.3	55.5	43.1	45.1	19.6	20.4

* Heat-supply rate = 500W

TEST	Temperature at the stated location (°C)																					
	1	2	3	4	5	6	7	8	9	10	11	12	13	14	15	16	17	18	19	20	21	22
A	20.4	26.2	38.2	44.0	43.4	43.3	43.5	43.3	45.2	46.9	20.4	21.2	40.8	49.6	66.8	66.9	64.1	59.8	46.2	48.6	19.2	20.3
B	20.4	29.8	37.3	44.3	44.3	44.2	44.3	44.2	45.3	46.2	20.3	21.6	41.6	50.4	64.1	63.3	54.5	45.6	46.0	46.6	19.3	20.3
C	20.4	23.2	34.5	43.6	42.5	42.5	42.8	42.5	45.6	46.3	20.4	20.5	34.1	48.8	64.9	70.4	68.6	61.1	51.4	48.0	19.2	20.3
D	20.4	25.4	35.9	44.0	43.0	43.0	43.1	42.9	44.7	46.4	20.3	20.8	38.2	49.0	65.6	68.3	63.0	55.2	45.7	48.0	19.3	20.3
mean value	20.4	26.2	36.5	44.0	43.3	43.3	43.4	43.2	45.2	46.5	20.4	21.0	38.7	49.5	65.4	67.2	62.6	55.4	47.3	47.8	19.3	20.3

* Heat-supply rate = 600W

TEST	Temperature at the stated location (°C)																					
	1	2	3	4	5	6	7	8	9	10	11	12	13	14	15	16	17	18	19	20	21	22
A	20.7	30.1	38.8	44.5	44.7	44.6	44.8	44.8	46.0	46.3	20.6	22.1	41.5	53.2	64.5	62.2	51.9	46.4	46.7	46.8	19.2	20.5
B	20.7	30.4	42.8	44.5	44.8	44.7	44.7	44.7	45.9	46.3	20.7	22.3	42.5	52.4	63.1	61.0	50.1	46.5	46.8	46.8	19.3	20.5
C	20.9	31.6	39.6	44.5	44.8	44.7	44.7	44.7	45.9	46.5	20.8	22.2	42.2	52.6	64.4	62.4	52.1	45.9	47.5	47.1	19.2	20.5
D	20.8	30.7	40.9	44.9	44.8	44.7	44.8	44.8	46.0	46.2	20.7	22.4	42.1	52.6	64.6	63.1	52.7	46.4	46.9	46.7	19.2	20.5
mean value	20.8	30.7	40.5	44.6	44.8	44.7	44.8	44.8	46.0	46.3	20.7	22.3	42.1	52.7	64.2	62.2	51.7	46.3	47.0	46.9	19.2	20.5

Fluid fill charge ratio:30% , Tilt angle:45°

* Heat-supply rate = 200W

TEST	Temperature at the stated location (°C)																					
	1	2	3	4	5	6	7	8	9	10	11	12	13	14	15	16	17	18	19	20	21	22
A	19.5	20.5	31.7	46.9	49.5	50.8	50.6	45.8	45.1	46.2	19.6	19.6	23.8	44.9	50.6	57.4	58.9	55.3	45.7	46.7	19.1	19.6
B	19.5	20.6	31.6	46.5	49.2	50.7	50.6	45.8	45.1	46.1	19.7	19.7	23.7	44.9	50.5	57.3	58.7	55.1	45.7	46.7	19.2	19.6
C	19.5	20.6	31.8	46.7	49.4	50.7	50.5	45.8	45.3	46.2	19.6	19.6	23.5	44.8	50.4	57.2	58.6	55.0	45.6	46.6	19.2	19.6
D	19.5	20.6	31.9	46.3	49.0	50.6	50.5	45.8	45.0	46.1	19.7	19.6	23.6	44.9	50.5	57.2	58.5	55.1	45.6	46.6	19.2	19.7
mean value	19.5	20.6	31.8	46.6	49.3	50.7	50.6	45.8	45.1	46.2	19.7	19.6	23.7	44.9	50.5	57.3	58.7	55.1	45.7	46.7	19.2	19.6

* Heat-supply rate = 300W

TEST	Temperature at the stated location (°C)																					
	1	2	3	4	5	6	7	8	9	10	11	12	13	14	15	16	17	18	19	20	21	22
A	19.8	21.1	32.9	49.3	51.9	51.8	50.4	44.2	46.7	48.4	19.9	19.9	26.7	47.5	56.7	66.0	66.1	59.5	47.6	49.2	19.2	19.9
B	19.8	21.1	33.0	49.3	51.7	51.2	47.6	44.3	46.7	48.3	20.0	19.9	26.1	47.4	56.6	65.8	65.8	59.2	47.5	49.1	19.2	19.9
C	19.8	21.2	32.8	49.2	51.5	51.1	45.7	44.3	46.7	48.4	19.9	19.9	26.0	47.4	56.5	65.6	65.9	59.8	47.6	49.1	19.3	19.9
D	19.8	21.1	32.9	49.0	51.0	50.1	45.1	44.2	46.9	48.4	19.9	19.9	26.8	47.4	56.4	65.3	65.5	59.6	47.5	49.1	19.3	19.9
mean value	19.8	21.1	32.9	49.2	51.5	51.1	47.2	44.3	46.8	48.4	19.9	19.9	26.4	47.4	56.6	65.7	65.8	59.5	47.6	49.1	19.3	19.9

* Heat-supply rate = 400W

TEST	Temperature at the stated location (°C)																					
	1	2	3	4	5	6	7	8	9	10	11	12	13	14	15	16	17	18	19	20	21	22
A	20.0	23.9	35.3	48.0	46.3	45.2	45.4	45.2	47.7	48.5	20.1	20.4	34.3	49.9	61.8	67.7	65.4	57.2	48.8	50.1	19.2	20.0
B	20.0	23.8	35.4	47.7	45.9	45.0	45.2	44.8	47.2	48.0	20.2	20.3	25.3	49.5	61.4	65.2	59.9	51.2	50.0	49.1	19.2	20.1
C	20.0	22.9	34.0	46.1	45.3	45.0	45.2	44.9	46.9	49.0	20.2	20.2	27.8	49.6	61.8	68.8	67.0	59.4	48.6	50.4	20.0	20.0
D	20.0	23.2	34.5	48.6	45.9	44.6	45.1	44.7	49.0	48.2	20.2	20.2	28.2	49.4	61.6	67.3	64.9	57.0	52.6	50.0	19.2	20.1
mean value	20.0	23.5	34.8	47.6	45.9	45.0	45.2	44.9	47.7	48.4	20.2	20.3	28.9	49.6	61.7	67.3	64.3	56.2	50.0	49.9	19.4	20.1

* Heat-supply rate = 500W

TEST	Temperature at the stated location (°C)																					
	1	2	3	4	5	6	7	8	9	10	11	12	13	14	15	16	17	18	19	20	21	22
A	20.4	28.9	37.2	52.6	50.8	47.4	47.5	47.5	50.2	51.2	20.3	21.1	45.2	54.8	72.4	73.6	69.5	64.2	52.4	53.0	19.2	20.3
B	20.3	29.3	37.0	51.5	50.1	47.6	47.7	47.6	49.9	50.9	20.3	21.3	43.7	54.4	69.9	71.6	68.7	64.0	52.2	53.0	19.1	20.2
C	20.3	28.6	38.0	50.7	48.8	47.6	47.8	47.7	50.2	50.7	20.3	21.4	45.1	54.4	69.2	71.2	69.5	62.8	52.6	52.8	19.1	20.2
D	20.3	28.4	38.1	49.0	47.5	47.3	47.5	47.4	50.2	50.5	20.3	21.1	44.3	54.2	69.2	71.3	68.9	63.9	51.9	52.3	19.2	20.3
mean value	20.3	28.8	37.6	51.0	49.3	47.5	47.6	47.6	50.1	50.8	20.3	21.2	44.6	54.5	70.2	71.9	69.2	63.7	52.3	52.8	19.2	20.3

* Heat-supply rate = 600W

TEST	Temperature at the stated location (°C)																					
	1	2	3	4	5	6	7	8	9	10	11	12	13	14	15	16	17	18	19	20	21	22
A	20.5	28.6	34.5	51.3	48.5	48.3	48.3	48.2	49.6	50.9	20.5	21.2	41.5	51.6	73.4	73.7	72.6	68.8	51.4	51.8	19.2	20.5
B	20.5	28.8	34.7	51.3	48.7	48.4	48.5	48.4	49.8	50.8	20.5	21.3	40.7	51.7	74.6	75.6	73.1	69.0	51.3	51.9	19.2	20.5
C	20.5	28.1	35.6	52.4	48.7	48.2	48.3	48.2	49.7	50.7	20.5	21.1	40.2	51.5	73.9	75.0	73.4	69.9	51.2	51.6	19.2	20.4
D	20.5	28.8	35.6	51.4	48.5	48.3	48.3	48.3	49.6	50.7	20.5	21.2	38.9	51.4	73.7	75.5	71.9	68.6	51.1	51.6	19.1	20.5
mean value	20.5	28.6	35.1	51.6	48.6	48.3	48.4	48.3	49.7	50.8	20.5	21.2	40.3	51.6	73.9	75.0	72.8	69.1	51.3	51.7	19.2	20.5

Fluid fill charge ratio:50% , Tilt angle:30°

* Heat-supply rate = 200W

	Temperature at the stated location (°C)																					
TEST	**1**	**2**	**3**	**4**	**5**	**6**	**7**	**8**	**9**	**10**	**11**	**12**	**13**	**14**	**15**	**16**	**17**	**18**	**19**	**20**	**21**	**22**
A	19.6	20.4	29.1	37.3	37.6	35.0	34.0	35.7	37.1	36.7	19.8	19.8	25.8	37.9	45.9	46.3	39.9	37.7	41.7	38.3	19.2	19.7
B	19.6	20.4	29.1	37.3	37.8	35.1	34.1	36.0	36.9	36.6	19.8	19.7	26.9	37.9	45.9	46.3	39.5	37.1	41.4	38.2	19.2	19.7
C	19.6	20.4	29.1	37.3	37.8	34.9	34.1	35.8	36.9	36.6	19.7	19.7	27.2	37.8	45.8	46.4	39.8	37.9	41.4	38.2	19.2	19.7
D	19.6	20.4	29.1	37.3	37.8	35.2	34.1	35.9	36.9	36.6	19.8	19.8	26.8	37.8	45.9	46.5	40.2	37.5	41.4	38.2	19.1	19.8
mean value	19.6	20.4	29.1	37.3	37.8	35.1	34.1	35.9	37.0	36.6	19.8	19.8	26.7	37.9	45.9	46.4	39.9	37.6	41.5	38.2	19.2	19.7

* Heat-supply rate =300W

	Temperature at the stated location (°C)																					
TEST	**1**	**2**	**3**	**4**	**5**	**6**	**7**	**8**	**9**	**10**	**11**	**12**	**13**	**14**	**15**	**16**	**17**	**18**	**19**	**20**	**21**	**22**
A	19.8	20.4	30.3	36.9	36.5	35.7	35.8	37.8	39.4	39.0	20.0	20.0	33.6	41.1	51.3	50.7	40.8	39.9	45.0	40.9	19.3	19.9
B	19.8	20.2	30.2	36.8	36.2	35.7	35.8	37.7	39.3	38.9	20.0	20.0	32.1	40.9	51.2	51.5	41.1	40.8	45.1	40.8	19.3	19.8
C	19.8	20.1	29.8	36.7	36.0	35.6	35.7	37.6	39.3	38.9	20.0	20.0	33.9	41.0	51.6	51.7	38.8	39.8	45.1	40.8	19.2	19.8
D	19.8	20.1	29.8	36.4	35.9	35.7	35.7	37.7	39.1	38.7	20.0	20.0	32.0	40.7	51.0	52.3	40.4	39.5	44.8	40.6	19.2	19.9
mean value	19.8	20.2	30.0	36.7	36.2	35.7	35.8	37.7	39.3	38.9	20.0	20.0	32.9	40.9	51.3	51.6	40.3	40.0	45.0	40.8	19.3	19.9

* Heat-supply rate = 400W

	Temperature at the stated location (°C)																					
TEST	**1**	**2**	**3**	**4**	**5**	**6**	**7**	**8**	**9**	**10**	**11**	**12**	**13**	**14**	**15**	**16**	**17**	**18**	**19**	**20**	**21**	**22**
A	20.0	22.1	31.5	39.3	39.4	39.3	39.3	40.1	41.3	42.8	20.2	20.3	35.1	44.8	53.8	48.7	39.8	41.9	42.6	44.7	19.1	20.1
B	20.1	22.5	35.5	39.8	39.5	39.5	39.6	40.3	41.3	42.8	20.2	20.6	36.7	45.4	56.6	54.2	40.1	42.1	42.9	44.7	19.1	20.1
C	20.0	21.3	31.7	39.5	39.2	39.2	39.1	40.0	41.1	42.8	20.2	20.3	35.7	44.9	55.2	50.9	39.8	41.8	42.6	44.7	19.3	20.2
D	20.0	22.0	35.4	39.7	39.4	39.4	39.5	40.2	41.3	42.6	20.2	20.6	36.9	45.2	55.9	53.0	40.1	42.1	42.8	44.4	19.2	20.1
mean value	20.0	22.0	33.5	39.6	39.4	39.4	39.4	40.2	41.3	42.8	20.2	20.5	36.1	45.1	55.4	51.7	40.0	42.0	42.7	44.6	19.2	20.1

* Heat-supply rate = 500W

	Temperature at the stated location (°C)																					
TEST	**1**	**2**	**3**	**4**	**5**	**6**	**7**	**8**	**9**	**10**	**11**	**12**	**13**	**14**	**15**	**16**	**17**	**18**	**19**	**20**	**21**	**22**
A	22.7	25.7	35.4	41.3	41.5	41.4	41.4	42.4	43.2	44.5	21.1	21.1	37.8	45.0	48.3	42.5	42.1	44.3	44.8	45.9	19.3	20.4
B	20.3	27.2	35.5	41.0	41.1	41.0	40.9	41.7	42.6	44.4	20.4	21.3	37.3	48.7	60.9	55.0	41.5	43.7	44.2	46.7	19.2	20.3
C	20.9	28.2	37.2	41.0	41.3	41.3	41.3	42.0	42.9	44.2	20.6	21.2	37.3	46.3	51.8	42.4	41.9	43.9	44.6	46.0	19.2	20.3
D	20.6	24.4	36.9	40.8	40.7	40.7	40.8	41.5	42.7	44.3	20.5	21.2	37.8	47.1	56.7	51.8	41.4	43.7	44.3	46.3	19.1	20.3
mean value	21.1	26.4	36.3	41.0	41.2	41.1	41.1	41.9	42.9	44.4	20.7	21.2	37.6	46.8	54.4	47.9	41.7	43.9	44.5	46.2	19.2	20.3

* Heat-supply rate = 600W

TEST	Temperature at the stated location (°C)																					
	1	2	3	4	5	6	7	8	9	10	11	12	13	14	15	16	17	18	19	20	21	22
A	20.7	30.0	41.1	44.3	44.1	44.0	44.1	44.7	45.8	47.8	20.6	22.1	40.6	50.9	64.3	58.0	45.1	47.3	47.7	50.0	19.1	20.5
B	20.5	31.4	41.6	44.6	44.2	44.1	44.1	44.8	45.9	48.0	20.6	22.5	40.8	52.5	65.3	57.1	45.4	47.5	48.1	50.3	19.2	20.5
C	21.1	31.5	42.2	44.5	44.8	44.7	44.8	45.5	46.3	47.6	20.7	22.7	41.3	51.3	59.8	47.9	45.6	47.9	47.9	49.6	19.1	20.5
D	20.8	30.6	41.8	44.4	44.2	44.2	44.3	44.9	45.9	47.7	20.6	22.1	39.9	51.8	62.4	53.8	45.3	47.5	47.9	49.9	19.2	20.5
mean value	20.8	30.9	41.7	44.5	44.3	44.3	44.3	45.0	46.0	47.8	20.6	22.4	40.7	51.6	63.0	54.2	45.4	47.6	47.9	50.0	19.2	20.5

Fluid fill charge ratio:50% , Tilt angle:45°

* Heat-supply rate =200W

TEST	Temperature at the stated location (°C)																					
	1	2	3	4	5	6	7	8	9	10	11	12	13	14	15	16	17	18	19	20	21	22
A	19.6	20.2	29.7	42.6	45.9	44.5	41.9	43.4	44.6	44.4	19.8	19.7	22.7	43.2	50.6	55.6	50.9	45.3	48.6	45.6	19.3	19.7
B	19.6	20.2	29.9	42.6	45.9	44.4	41.9	43.4	44.3	44.3	19.8	19.7	23.0	43.2	50.7	55.6	49.9	45.0	48.6	45.5	19.2	19.7
C	19.6	20.2	29.5	42.5	45.8	44.5	41.8	43.3	44.5	44.2	19.7	19.7	22.7	43.1	50.5	55.4	50.5	45.6	48.6	45.5	19.3	19.7
D	19.6	20.2	29.8	42.5	45.9	44.7	41.8	43.4	44.3	44.2	19.8	19.8	23.0	43.2	50.6	55.5	50.3	45.0	48.4	45.5	19.2	19.7
mean value	19.6	20.2	29.7	42.6	45.9	44.5	41.9	43.4	44.4	44.3	19.8	19.7	22.9	43.2	50.6	55.5	50.4	45.2	48.6	45.5	19.3	19.7

* Heat-supply rate = 300W

TEST	Temperature at the stated location (°C)																					
	1	2	3	4	5	6	7	8	9	10	11	12	13	14	15	16	17	18	19	20	21	22
A	19.7	21.3	33.8	45.9	50.4	48.1	45.0	46.9	48.5	48.8	19.9	19.9	27.6	47.6	60.2	66.5	56.1	49.4	53.9	50.4	19.2	19.9
B	19.7	21.3	33.5	45.8	50.4	48.2	44.8	46.8	48.8	48.7	19.9	19.9	26.0	47.4	60.2	66.5	56.4	48.9	54.1	50.3	19.1	19.8
C	19.7	21.3	33.6	45.8	50.3	48.0	44.9	47.0	49.1	48.7	19.9	19.9	26.2	47.5	60.1	66.5	56.6	49.0	53.9	50.3	19.2	19.8
D	19.7	21.3	33.7	45.9	50.0	48.2	45.0	46.9	48.8	48.7	19.9	19.9	26.3	47.4	60.0	66.3	56.4	48.9	53.9	50.3	19.2	19.8
mean value	19.7	21.3	33.7	45.9	50.3	48.1	44.9	46.9	48.8	48.7	19.9	19.9	26.5	47.5	60.1	66.5	56.4	49.1	54.0	50.3	19.2	19.8

* Heat-supply rate = 400W

TEST	Temperature at the stated location (°C)																					
	1	2	3	4	5	6	7	8	9	10	11	12	13	14	15	16	17	18	19	20	21	22
A	20.0	24.2	33.4	51.3	52.2	46.4	46.5	48.7	51.7	51.3	20.2	20.4	32.8	49.5	68.7	73.9	57.4	51.1	57.2	53.2	19.3	20.1
B	20.0	27.5	36.0	51.3	52.4	46.8	46.8	49.0	51.6	51.2	20.1	20.8	40.3	49.9	68.6	71.4	58.4	51.4	57.4	53.2	19.3	20.1
C	20.0	27.3	37.2	50.9	53.0	46.8	46.8	49.0	51.6	51.1	20.1	20.8	39.9	49.8	68.9	73.1	58.4	51.3	57.2	53.0	19.2	20.1
D	20.0	26.1	34.8	50.8	52.9	47.1	46.5	48.8	51.7	51.1	20.1	20.7	39.7	49.6	68.5	75.4	60.6	51.6	57.4	53.1	19.2	20.1
mean value	20.0	26.3	35.4	51.1	52.6	46.8	46.7	48.9	51.7	51.2	20.1	20.7	38.2	49.7	68.7	73.5	58.7	51.4	57.3	53.1	19.3	20.1

* Heat-supply rate = 500W

TEST	Temperature at the stated location (°C)																					
	1	2	3	4	5	6	7	8	9	10	11	12	13	14	15	16	17	18	19	20	21	22
A	20.3	27.7	37.0	49.0	48.8	48.7	48.7	50.8	53.5	52.8	20.3	21.0	40.4	50.6	68.5	73.8	63.2	54.2	60.6	54.9	19.2	20.2
B	20.1	29.7	38.4	51.9	49.2	48.9	49.0	51.3	54.2	53.7	20.3	21.1	37.5	52.1	72.9	73.8	61.2	54.3	60.4	55.1	19.1	20.2
C	20.2	24.0	34.7	48.8	48.4	48.4	48.3	50.5	53.3	52.7	20.3	20.5	34.4	50.9	69.5	75.1	63.1	54.0	60.4	54.7	19.1	20.2
D	20.2	28.1	49.2	48.7	48.7	48.7	51.0	54.0	54.0	53.0	20.3	21.1	42.7	50.1	66.1	75.8	64.5	53.9	60.8	55.1	19.1	20.2
mean value	20.2	27.4	39.8	49.6	48.8	48.7	49.3	51.7	53.8	53.1	20.3	20.9	38.8	50.9	69.3	74.6	63.0	54.1	60.6	55.0	19.1	20.2

* Heat-supply rate = 600W

TEST	Temperature at the stated location (°C)																					
	1	2	3	4	5	6	7	8	9	10	11	12	13	14	15	16	17	18	19	20	21	22
A	21.4	28.6	42.5	50.5	49.8	50.0	50.4	51.1	51.8	52.8	20.7	21.7	31.7	51.4	52.5	51.1	51.1	53.9	54.5	54.0	19.2	20.5
B	22.1	28.9	42.8	50.1	49.9	49.9	49.8	50.8	51.8	52.7	21.5	21.6	37.5	50.2	58.1	53.4	51.3	53.7	54.0	54.0	19.3	20.5
C	21.3	29.6	45.3	49.8	50.1	50.0	49.9	51.0	52.0	52.8	20.7	21.7	46.3	50.9	58.5	50.5	50.6	53.6	54.8	54.3	19.2	20.5
D	21.1	31.1	44.0	50.3	50.1	50.1	50.3	51.3	52.3	53.2	20.7	21.9	40.4	52.4	58.0	51.1	51.3	54.0	54.3	54.5	19.2	20.5
mean value	21.5	29.6	43.7	50.2	50.0	50.0	50.1	51.1	52.0	52.9	20.9	21.7	39.0	51.2	56.8	51.5	51.1	53.8	54.4	54.2	19.2	20.5

Fluid fill charge ratio:100% , Tilt angle:30°

* Heat-supply rate =200W

TEST	Temperature at the stated location (°C)																					
	1	2	3	4	5	6	7	8	9	10	11	12	13	14	15	16	17	18	19	20	21	22
A	19.6	20.2	30.7	39.2	39.8	40.4	41.1	42.8	43.0	42.8	19.7	19.9	23.2	39.5	40.1	41.3	42.0	46.3	47.1	44.0	19.2	19.7
B	19.6	20.3	30.7	39.2	39.8	40.5	41.2	42.4	43.1	42.9	19.7	19.8	23.4	39.4	40.0	41.4	42.0	46.1	47.0	44.0	19.1	19.6
C	19.6	20.1	30.2	39.2	39.9	40.6	41.3	42.7	43.1	42.8	19.7	19.8	23.1	39.4	40.0	41.5	42.2	46.1	47.0	44.0	19.2	19.6
D	19.6	20.3	29.9	39.3	39.7	40.4	41.0	43.2	43.0	42.8	19.7	19.8	22.7	39.2	39.9	41.1	42.1	46.3	47.1	44.0	19.2	19.6
mean value	19.6	20.2	30.4	39.2	39.8	40.5	41.2	42.8	43.1	42.8	19.7	19.8	23.1	39.4	40.0	41.3	42.1	46.2	47.1	44.0	19.2	19.6

* Heat-supply rate = 300W

TEST	Temperature at the stated location (°C)																					
	1	2	3	4	5	6	7	8	9	10	11	12	13	14	15	16	17	18	19	20	21	22
A	19.9	21.4	34.3	42.8	43.1	43.6	44.2	45.7	46.7	46.3	19.9	20.2	24.4	42.9	43.7	44.5	45.2	50.6	52.0	48.0	19.1	19.8
B	19.8	21.2	35.4	42.4	43.2	43.8	44.4	46.2	46.9	46.6	19.9	20.2	25.6	42.9	43.7	44.6	45.5	49.9	52.0	48.0	19.2	19.8
C	19.8	21.2	35.2	42.4	43.3	43.6	44.3	45.9	46.8	46.5	20.0	20.3	24.9	43.1	43.8	44.5	45.3	49.6	52.0	48.0	19.2	19.8
D	19.8	21.5	34.7	42.7	43.1	43.6	44.3	45.9	46.7	46.4	20.0	20.2	24.5	42.9	43.9	44.8	45.4	50.3	52.0	48.0	19.2	19.9
mean value	19.8	21.3	34.9	42.6	43.2	43.7	44.3	45.9	46.8	46.5	20.0	20.2	24.9	43.0	43.8	44.6	45.4	50.1	52.0	48.0	19.2	19.8

* Heat-supply rate = 400W

TEST	Temperature at the stated location (°C)																				
	1	2	3	4	5	6	7	8	9	10	11	12	13	14	15	16	17	18	19	20	21	22
A	20.3	23.1	39.5	43.9	44.8	45.2	46.1	46.7	48.8	48.5	20.2	20.6	27.6	44.7	45.5	46.3	47.4	49.1	53.8	50.5	19.2	20.1
B	20.2	23.0	38.1	44.0	44.7	45.2	46.1	47.3	48.8	48.5	20.1	20.7	27.8	44.5	45.3	46.1	47.3	49.7	52.6	50.4	19.1	20.0
C	20.3	22.9	38.0	44.1	44.4	45.0	45.6	46.8	49.2	48.9	20.3	20.7	26.7	44.2	45.3	45.9	46.6	51.1	54.3	50.7	19.1	20.1
D	20.3	22.2	39.8	44.1	44.6	45.3	46.1	47.0	48.7	48.5	20.2	20.6	27.1	44.6	45.3	46.4	47.3	49.8	53.2	50.4	19.2	20.0
mean value	20.3	22.8	38.9	44.0	44.6	45.2	46.0	47.0	48.9	48.6	20.2	20.7	27.3	44.5	45.4	46.2	47.2	49.9	53.5	50.5	19.2	20.1

* Heat-supply rate =500W

TEST	Temperature at the stated location (°C)																				
	1	2	3	4	5	6	7	8	9	10	11	12	13	14	15	16	17	18	19	20	21	22
A	20.6	24.5	41.3	46.4	46.9	47.5	48.5	49.2	51.3	51.3	20.5	21.2	28.1	47.3	48.0	49.0	50.0	51.8	56.6	53.2	19.1	20.2
B	20.5	24.1	41.6	46.3	46.7	47.2	48.1	48.8	51.3	51.1	20.4	21.2	27.2	46.6	47.7	48.6	49.4	53.4	57.6	53.3	19.2	20.3
C	20.5	23.9	41.8	46.4	46.7	47.1	47.8	49.1	51.1	51.3	20.4	21.0	29.2	46.5	47.5	48.4	49.3	54.9	58.0	53.2	19.1	20.3
D	20.6	24.1	42.6	46.3	47.1	47.6	48.3	48.9	51.3	50.9	20.3	20.9	30.8	46.8	47.8	48.8	49.8	51.7	57.4	52.9	19.2	20.2
mean value	20.6	24.2	41.8	46.4	46.9	47.4	48.2	49.0	51.3	51.2	20.4	21.1	28.8	46.8	47.8	48.7	49.6	53.0	57.4	53.2	19.2	20.3

* Heat-supply rate = 600W

TEST	Temperature at the stated location (°C)																				
	1	2	3	4	5	6	7	8	9	10	11	12	13	14	15	16	17	18	19	20	21	22
A	20.7	27.8	45.6	47.4	48.4	48.8	49.5	50.1	51.2	52.6	20.7	21.6	32.6	48.0	49.1	49.9	50.8	53.6	55.2	54.5	19.2	20.5
B	20.8	27.8	44.4	47.3	48.0	48.5	49.2	49.8	51.6	52.7	20.7	21.8	29.7	48.2	49.1	49.8	50.8	53.5	56.4	54.7	19.3	20.5
C	21.2	26.4	43.7	47.3	47.8	48.3	49.1	49.6	52.1	53.0	20.8	21.8	31.2	47.7	48.8	49.8	51.5	53.5	54.9	54.0	19.2	20.5
D	20.7	25.0	44.9	47.1	48.0	48.5	49.1	49.6	52.0	52.7	20.7	21.7	31.2	47.7	48.9	49.8	50.9	53.4	58.0	54.9	19.2	20.4
mean value	20.9	26.8	44.7	47.3	48.1	48.5	49.2	49.8	51.7	52.8	20.7	21.7	31.2	47.9	49.0	49.8	51.0	53.5	56.1	54.5	19.2	20.5

Fluid fill charge ratio:100% , Tilt angle:45°

* Heat-supply rate = 200W

TEST	Temperature at the stated location (°C)																				
	1	2	3	4	5	6	7	8	9	10	11	12	13	14	15	16	17	18	19	20	21	22
A	19.5	20.7	34.4	46.0	47.1	47.7	48.3	50.3	50.8	50.5	19.7	19.7	24.2	46.4	47.6	48.7	49.3	54.0	54.7	51.5	19.2	19.6
B	19.5	20.9	34.2	46.4	47.2	47.7	48.4	50.0	50.6	50.6	19.7	19.7	23.6	46.6	47.7	48.6	49.3	54.0	54.7	51.6	19.1	19.7
C	19.5	20.9	34.2	46.2	47.1	47.7	48.2	50.1	50.6	50.6	19.7	19.7	23.7	46.4	47.5	48.8	49.4	54.0	54.7	51.6	19.2	19.7
D	19.5	20.8	34.4	46.3	47.1	47.8	48.5	50.6	50.6	50.5	19.7	19.6	23.9	46.2	47.5	48.6	49.3	54.1	54.5	51.5	19.2	19.7
mean value	19.5	20.8	34.3	46.2	47.1	47.7	48.4	50.3	50.7	50.6	19.7	19.7	23.9	46.4	47.6	48.7	49.3	54.0	54.7	51.6	19.2	19.7

* Heat-supply rate = 300W

TEST	Temperature at the stated location (°C)																					
	1	2	3	4	5	6	7	8	9	10	11	12	13	14	15	16	17	18	19	20	21	22
A	19.8	21.5	39.3	47.8	48.4	49.1	49.8	51.0	52.5	52.3	20.0	20.2	26.0	48.0	49.1	50.0	51.0	56.2	57.4	53.6	19.3	19.9
B	19.8	21.3	39.8	47.8	48.4	48.8	49.7	51.7	52.5	52.3	20.0	20.0	25.7	47.8	49.2	50.2	51.0	56.4	57.4	53.6	19.2	19.9
C	19.8	21.4	38.4	47.6	48.2	48.8	50.1	51.3	52.5	52.2	19.9	20.0	25.7	47.6	49.1	50.0	50.9	56.1	57.3	53.6	19.2	19.8
D	19.8	21.4	38.2	47.6	48.3	48.9	49.7	51.7	52.5	52.5	19.9	20.0	25.5	47.8	49.2	50.0	50.7	56.2	57.5	53.9	19.2	19.9
mean value	19.8	21.4	38.9	47.7	48.3	48.9	49.8	51.4	52.5	52.3	20.0	20.1	25.7	47.8	49.2	50.1	50.9	56.2	57.4	53.7	19.2	19.9

* Heat-supply rate = 400W

TEST	Temperature at the stated location (°C)																					
	1	2	3	4	5	6	7	8	9	10	11	12	13	14	15	16	17	18	19	20	21	22
A	20.0	23.8	44.7	50.3	51.0	51.7	52.5	53.4	55.2	55.8	20.2	20.5	28.8	50.8	51.6	52.7	54.4	56.5	59.3	57.4	19.3	20.1
B	20.0	24.0	44.8	50.4	51.0	51.6	52.4	53.6	56.0	55.9	20.1	20.4	27.8	50.8	51.7	52.5	54.0	56.9	59.9	57.4	19.1	20.1
C	20.0	23.6	44.2	50.2	51.0	51.6	52.5	53.1	55.4	55.7	20.2	20.4	30.1	51.2	52.2	52.7	53.9	56.1	59.9	57.3	19.2	20.1
D	20.0	23.5	44.8	50.2	51.1	51.6	52.5	53.6	55.3	55.4	20.1	20.4	28.4	50.5	51.8	52.9	53.6	56.3	59.5	57.0	19.1	20.1
mean value	20.0	23.7	44.6	50.3	51.0	51.6	52.5	53.4	55.5	55.7	20.2	20.4	28.8	50.8	51.8	52.7	54.0	56.5	59.7	57.3	19.2	20.1

* Heat-supply rate = 500W

TEST	Temperature at the stated location (°C)																					
	1	2	3	4	5	6	7	8	9	10	11	12	13	14	15	16	17	18	19	20	21	22
A	20.2	25.7	46.5	51.4	51.9	52.9	53.4	54.4	55.8	57.0	20.3	20.9	32.3	51.9	53.0	53.8	54.7	57.4	59.3	58.8	19.2	20.3
B	20.3	25.9	45.9	51.4	52.1	52.7	53.9	54.5	56.4	57.3	20.3	20.9	32.2	51.8	53.2	54.2	54.9	57.3	59.7	58.3	19.2	20.3
C	20.2	25.4	47.5	51.2	51.9	52.4	53.7	54.3	56.1	57.2	20.3	20.8	28.7	51.6	52.6	53.7	55.2	58.9	61.3	59.1	19.2	20.3
D	20.2	25.6	46.3	51.1	51.9	52.6	53.8	54.4	56.5	57.2	20.4	20.9	31.2	51.9	53.0	54.0	55.4	57.4	60.6	59.1	19.2	20.3
mean value	20.2	25.7	46.6	51.3	52.0	52.7	53.7	54.4	56.2	57.2	20.3	20.9	31.1	51.8	53.0	53.9	55.1	57.8	60.2	58.8	19.2	20.3

* Heat-supply rate = 600W

TEST	Temperature at the stated location (°C)																					
	1	2	3	4	5	6	7	8	9	10	11	12	13	14	15	16	17	18	19	20	21	22
A	20.5	27.7	49.8	53.4	54.1	54.5	55.6	56.2	57.9	59.0	20.6	21.4	31.3	54.3	55.1	55.9	57.1	59.5	60.9	61.1	19.2	20.4
B	20.5	28.1	50.0	53.5	54.1	54.8	55.7	56.5	57.8	59.3	20.6	21.4	32.5	54.1	55.2	56.2	57.2	60.0	61.0	61.1	19.2	20.4
C	20.5	28.0	49.8	53.4	54.1	54.6	55.5	56.1	58.3	59.1	20.6	21.2	53.1	54.1	55.1	55.9	57.1	59.5	60.7	61.0	19.2	20.4
D	20.5	28.1	48.9	54.6	53.9	54.5	55.5	56.2	58.1	59.0	20.6	21.4	33.5	54.6	55.4	55.9	57.1	59.2	60.8	61.1	19.3	20.5
mean value	20.5	28.0	49.6	53.7	54.1	54.6	55.6	56.3	58.0	59.1	20.6	21.4	37.6	54.3	55.2	56.0	57.1	59.6	60.9	61.1	19.2	20.4

Table 6.3 Thermophysical Properties of Air (Liley, 1984)

T °C	ρ kg/m^3	c_p kJ/kg·K	μ 10^5 kg /m·s	ν 10^6 m^2/s	k_l W/m·K	Pr_l -
-23	1.3947	1.0060	1.5960	11.440	0.0223	0.720
-22	1.3900	1.0060	1.6010	11.529	0.0224	0.720
-21	1.3854	1.0060	1.6060	11.618	0.0225	0.719
-20	1.3807	1.0061	1.6110	11.707	0.0225	0.719
-19	1.3760	1.0061	1.6160	11.796	0.0226	0.719
-18	1.3714	1.0061	1.6210	11.885	0.0227	0.719
-17	1.3667	1.0061	1.6260	11.974	0.0228	0.718
-16	1.3620	1.0061	1.6310	12.063	0.0229	0.718
-15	1.3574	1.0062	1.6360	12.152	0.0229	0.718
-14	1.3527	1.0062	1.6410	12.241	0.0230	0.718
-13	1.3480	1.0062	1.6460	12.330	0.0231	0.717
-12	1.3434	1.0062	1.6510	12.419	0.0232	0.717
-11	1.3387	1.0062	1.6560	12.508	0.0233	0.717
-10	1.3340	1.0063	1.6610	12.597	0.0233	0.717
-9	1.3294	1.0063	1.6660	12.686	0.0234	0.716
-8	1.3247	1.0063	1.6710	12.775	0.0235	0.716
-7	1.3200	1.0063	1.6760	12.864	0.0236	0.716
-6	1.3154	1.0063	1.6810	12.953	0.0237	0.716
-5	1.3107	1.0064	1.6860	13.042	0.0237	0.715
-4	1.3060	1.0064	1.6910	13.131	0.0238	0.715
-3	1.3014	1.0064	1.6960	13.220	0.0239	0.715
-2	1.2967	1.0064	1.7010	13.309	0.0240	0.715
-1	1.2920	1.0064	1.7060	13.398	0.0241	0.714
0	1.2874	1.0065	1.7110	13.487	0.0241	0.714
1	1.2827	1.0065	1.7160	13.576	0.0242	0.714
2	1.2781	1.0065	1.7210	13.665	0.0243	0.713
3	1.2734	1.0065	1.7260	13.754	0.0244	0.713
4	1.2687	1.0065	1.7310	13.843	0.0245	0.713
5	1.2641	1.0066	1.7360	13.932	0.0245	0.713
6	1.2594	1.0066	1.7410	14.021	0.0246	0.712
7	1.2547	1.0066	1.7460	14.110	0.0247	0.712
8	1.2501	1.0066	1.7510	14.199	0.0248	0.712
9	1.2454	1.0066	1.7560	14.288	0.0249	0.712
10	1.2407	1.0067	1.7610	14.377	0.0249	0.711
11	1.2361	1.0067	1.7660	14.466	0.0250	0.711
12	1.2314	1.0067	1.7710	14.555	0.0251	0.711
13	1.2267	1.0067	1.7760	14.644	0.0252	0.711
14	1.2221	1.0067	1.7810	14.733	0.0253	0.710
15	1.2174	1.0068	1.7860	14.822	0.0253	0.710
16	1.2127	1.0068	1.7910	14.911	0.0254	0.710
17	1.2081	1.0068	1.7960	15.000	0.0255	0.710
18	1.2034	1.0068	1.8010	15.089	0.0256	0.709
19	1.1987	1.0068	1.8060	15.178	0.0257	0.709
20	1.1941	1.0069	1.8110	15.267	0.0257	0.709
21	1.1894	1.0069	1.8160	15.356	0.0258	0.709
22	1.1847	1.0069	1.8210	15.445	0.0259	0.708
23	1.1801	1.0069	1.8260	15.534	0.0260	0.708
24	1.1754	1.0069	1.8310	15.623	0.0261	0.708
25	1.1707	1.0070	1.8360	15.712	0.0261	0.708
26	1.1661	1.0070	1.8410	15.801	0.0262	0.707
27	1.1614	1.0070	1.8460	15.890	0.0263	0.707
28	1.1581	1.0070	1.8507	15.991	0.0264	0.707

T	ρ	c_p	μ	ν	k_l	Pr_l
°C	kg/m³	kJ/kg·K	10^5 kg /m·s	10^6 m²/s	W/m·K	-
29	1.1547	1.0071	1.8554	16.091	0.0264	0.707
30	1.1514	1.0071	1.8602	16.192	0.0265	0.707
31	1.1481	1.0072	1.8649	16.292	0.0266	0.706
32	1.1448	1.0072	1.8696	16.393	0.0267	0.706
33	1.1414	1.0072	1.8743	16.494	0.0267	0.706
34	1.1381	1.0073	1.8790	16.594	0.0268	0.706
35	1.1348	1.0073	1.8838	16.695	0.0269	0.706
36	1.1314	1.0074	1.8885	16.795	0.0270	0.706
37	1.1281	1.0074	1.8932	16.896	0.0270	0.706
38	1.1248	1.0074	1.8979	16.997	0.0271	0.705
39	1.1215	1.0075	1.9026	17.097	0.0272	0.705
40	1.1181	1.0075	1.9074	17.198	0.0273	0.705
41	1.1148	1.0076	1.9121	17.298	0.0273	0.705
42	1.1115	1.0076	1.9168	17.399	0.0274	0.705
43	1.1082	1.0076	1.9215	17.500	0.0275	0.705
44	1.1048	1.0077	1.9262	17.600	0.0276	0.705
45	1.1015	1.0077	1.9310	17.701	0.0276	0.704
46	1.0982	1.0078	1.9357	17.801	0.0277	0.704
47	1.0948	1.0078	1.9404	17.902	0.0278	0.704
48	1.0915	1.0078	1.9451	18.003	0.0279	0.704
49	1.0882	1.0079	1.9498	18.103	0.0279	0.704
50	1.0849	1.0079	1.9546	18.204	0.0280	0.704
51	1.0815	1.0080	1.9593	18.304	0.0281	0.704
52	1.0782	1.0080	1.9640	18.405	0.0282	0.703
53	1.0749	1.0080	1.9687	18.506	0.0282	0.703
54	1.0715	1.0081	1.9734	18.606	0.0283	0.703
55	1.0682	1.0081	1.9782	18.707	0.0284	0.703
56	1.0649	1.0082	1.9829	18.807	0.0285	0.703
57	1.0616	1.0082	1.9876	18.908	0.0285	0.703
58	1.0582	1.0082	1.9923	19.009	0.0286	0.703
59	1.0549	1.0083	1.9970	19.109	0.0287	0.703
60	1.0516	1.0083	2.0018	19.210	0.0288	0.702
61	1.0482	1.0084	2.0065	19.310	0.0288	0.702
62	1.0449	1.0084	2.0112	19.411	0.0289	0.702
63	1.0416	1.0084	2.0159	19.512	0.0290	0.702
64	1.0383	1.0085	2.0206	19.612	0.0291	0.702
65	1.0349	1.0085	2.0254	19.713	0.0291	0.702
66	1.0316	1.0086	2.0301	19.813	0.0292	0.702
67	1.0283	1.0086	2.0348	19.914	0.0293	0.701
68	1.0250	1.0086	2.0395	20.015	0.0294	0.701
69	1.0216	1.0087	2.0442	20.115	0.0294	0.701
70	1.0183	1.0087	2.0490	20.216	0.0295	0.701
71	1.0150	1.0088	2.0537	20.316	0.0296	0.701
72	1.0116	1.0088	2.0584	20.417	0.0297	0.701
73	1.0083	1.0088	2.0631	20.518	0.0297	0.701
74	1.0050	1.0089	2.0678	20.618	0.0298	0.700
75	1.0017	1.0089	2.0726	20.719	0.0299	0.700
76	0.9983	1.0090	2.0773	20.819	0.0300	0.700
77	0.9950	1.0090	2.0820	20.920	0.0300	0.700
78	0.9925	1.0091	2.0864	21.030	0.0301	0.700
79	0.9900	1.0092	2.0908	21.140	0.0302	0.700
80	0.9876	1.0093	2.0951	21.249	0.0303	0.699
81	0.9851	1.0094	2.0995	21.359	0.0303	0.699
82	0.9826	1.0095	2.1039	21.469	0.0304	0.699
83	0.9801	1.0096	2.1083	21.579	0.0305	0.699
84	0.9777	1.0097	2.1127	21.689	0.0306	0.699

T °C	ρ kg/m^3	c_p kJ/kg·K	μ 10^5 kg /m·s	ν 10^6 m^2/s	k_l W/m·K	Pr_l -
85	0.9752	1.0098	2.1170	21.798	0.0306	0.698
86	0.9727	1.0099	2.1214	21.908	0.0307	0.698
87	0.9702	1.0100	2.1258	22.018	0.0308	0.698
88	0.9677	1.0101	2.1302	22.128	0.0309	0.698
89	0.9653	1.0102	2.1346	22.238	0.0309	0.698
90	0.9628	1.0103	2.1389	22.347	0.0310	0.697
91	0.9603	1.0104	2.1433	22.457	0.0311	0.697
92	0.9578	1.0105	2.1477	22.567	0.0312	0.697
93	0.9554	1.0106	2.1521	22.677	0.0312	0.697
94	0.9529	1.0107	2.1565	22.787	0.0313	0.697
95	0.9504	1.0108	2.1608	22.896	0.0314	0.696
96	0.9479	1.0109	2.1652	23.006	0.0315	0.696
97	0.9454	1.0110	2.1696	23.116	0.0315	0.696
98	0.9430	1.0111	2.1740	23.226	0.0316	0.696
99	0.9405	1.0112	2.1784	23.336	0.0317	0.696
100	0.9380	1.0113	2.1827	23.445	0.0318	0.695
101	0.9355	1.0114	2.1871	23.555	0.0318	0.695
102	0.9331	1.0115	2.1915	23.665	0.0319	0.695
103	0.9306	1.0116	2.1959	23.775	0.0320	0.695
104	0.9281	1.0117	2.2003	23.885	0.0321	0.695
105	0.9256	1.0118	2.2046	23.994	0.0321	0.694
106	0.9231	1.0119	2.2090	24.104	0.0322	0.694
107	0.9207	1.0120	2.2134	24.214	0.0323	0.694
108	0.9182	1.0121	2.2178	24.324	0.0324	0.694
109	0.9157	1.0122	2.2222	24.434	0.0324	0.694
110	0.9132	1.0123	2.2265	24.543	0.0325	0.693
111	0.9107	1.0124	2.2309	24.653	0.0326	0.693
112	0.9083	1.0125	2.2353	24.763	0.0327	0.693
113	0.9058	1.0126	2.2397	24.873	0.0327	0.693
114	0.9033	1.0127	2.2441	24.983	0.0328	0.693
115	0.9008	1.0128	2.2484	25.092	0.0329	0.692
116	0.8984	1.0129	2.2528	25.202	0.0330	0.692
117	0.8959	1.0130	2.2572	25.312	0.0330	0.692
118	0.8934	1.0131	2.2616	25.422	0.0331	0.692
119	0.8909	1.0132	2.2660	25.532	0.0332	0.692
120	0.8884	1.0133	2.2703	25.641	0.0333	0.691
121	0.8860	1.0134	2.2747	25.751	0.0333	0.691
122	0.8835	1.0135	2.2791	25.861	0.0334	0.691
123	0.8810	1.0136	2.2835	25.971	0.0335	0.691
124	0.8785	1.0137	2.2879	26.081	0.0336	0.691
125	0.8761	1.0138	2.2922	26.190	0.0336	0.690
126	0.8736	1.0139	2.2966	26.300	0.0337	0.690
127	0.8711	1.0140	2.3010	26.410	0.0338	0.690
128	0.8692	1.0141	2.3051	26.530	0.0339	0.690
129	0.8672	1.0143	2.3092	26.649	0.0339	0.690
130	0.8653	1.0144	2.3134	26.769	0.0340	0.690
131	0.8633	1.0146	2.3175	26.888	0.0341	0.690
132	0.8614	1.0147	2.3216	27.008	0.0342	0.690
133	0.8594	1.0148	2.3257	27.128	0.0342	0.690
134	0.8575	1.0150	2.3298	27.247	0.0343	0.689
135	0.8556	1.0151	2.3340	27.367	0.0344	0.689
136	0.8536	1.0153	2.3381	27.486	0.0344	0.689
137	0.8517	1.0154	2.3422	27.606	0.0345	0.689
138	0.8497	1.0155	2.3463	27.726	0.0346	0.689
139	0.8478	1.0157	2.3504	27.845	0.0346	0.689
140	0.8459	1.0158	2.3546	27.965	0.0347	0.689

T °C	ρ kg/m^3	c_p kJ/kg·K	μ 10^5 kg /m·s	ν 10^6 m^2/s	k_l W/m·K	Pr_l -
141	0.8439	1.0160	2.3587	28.084	0.0348	0.689
142	0.8420	1.0161	2.3628	28.204	0.0349	0.689
143	0.8400	1.0162	2.3669	28.324	0.0349	0.689
144	0.8381	1.0164	2.3710	28.443	0.0350	0.689
145	0.8361	1.0165	2.3752	28.563	0.0351	0.689
146	0.8342	1.0167	2.3793	28.682	0.0351	0.688
147	0.8323	1.0168	2.3834	28.802	0.0352	0.688
148	0.8303	1.0169	2.3875	28.922	0.0353	0.688
149	0.8284	1.0171	2.3916	29.041	0.0353	0.688
150	0.8264	1.0172	2.3958	29.161	0.0354	0.688
151	0.8245	1.0174	2.3999	29.280	0.0355	0.688
152	0.8226	1.0175	2.4040	29.400	0.0356	0.688
153	0.8206	1.0176	2.4081	29.520	0.0356	0.688
154	0.8187	1.0178	2.4122	29.639	0.0357	0.688
155	0.8167	1.0179	2.4164	29.759	0.0358	0.688
156	0.8148	1.0181	2.4205	29.878	0.0358	0.688
157	0.8128	1.0182	2.4246	29.998	0.0359	0.688
158	0.8109	1.0183	2.4287	30.118	0.0360	0.688
159	0.8090	1.0185	2.4328	30.237	0.0360	0.687
160	0.8070	1.0186	2.4370	30.357	0.0361	0.687
161	0.8051	1.0188	2.4411	30.476	0.0362	0.687
162	0.8031	1.0189	2.4452	30.596	0.0363	0.687
163	0.8012	1.0190	2.4493	30.716	0.0363	0.687
164	0.7992	1.0192	2.4534	30.835	0.0364	0.687
165	0.7973	1.0193	2.4576	30.955	0.0365	0.687
166	0.7954	1.0195	2.4617	31.074	0.0365	0.687
167	0.7934	1.0196	2.4658	31.194	0.0366	0.687
168	0.7915	1.0197	2.4699	31.314	0.0367	0.687
169	0.7895	1.0199	2.4740	31.433	0.0367	0.687
170	0.7876	1.0200	2.4782	31.553	0.0368	0.687
171	0.7857	1.0202	2.4823	31.672	0.0369	0.686
172	0.7837	1.0203	2.4864	31.792	0.0370	0.686
173	0.7818	1.0204	2.4905	31.912	0.0370	0.686
174	0.7798	1.0206	2.4946	32.031	0.0371	0.686
175	0.7779	1.0207	2.4988	32.151	0.0372	0.686
176	0.7759	1.0209	2.5029	32.270	0.0372	0.686
177	0.7740	1.0210	2.5070	32.390	0.0373	0.686
178	0.7724	1.0212	2.5109	32.518	0.0374	0.686
179	0.7709	1.0214	2.5148	32.646	0.0374	0.686
180	0.7693	1.0215	2.5186	32.774	0.0375	0.686
181	0.7678	1.0217	2.5225	32.902	0.0376	0.686
182	0.7662	1.0219	2.5264	33.030	0.0376	0.686
183	0.7647	1.0221	2.5303	33.158	0.0377	0.686
184	0.7631	1.0223	2.5342	33.286	0.0378	0.686
185	0.7616	1.0224	2.5380	33.414	0.0378	0.686
186	0.7600	1.0226	2.5419	33.542	0.0379	0.686
187	0.7585	1.0228	2.5458	33.670	0.0380	0.686
188	0.7569	1.0230	2.5497	33.798	0.0380	0.686
189	0.7554	1.0232	2.5536	33.926	0.0381	0.686
190	0.7538	1.0233	2.5574	34.054	0.0382	0.685
191	0.7523	1.0235	2.5613	34.182	0.0383	0.685
192	0.7507	1.0237	2.5652	34.310	0.0383	0.685
193	0.7492	1.0239	2.5691	34.438	0.0384	0.685
194	0.7476	1.0241	2.5730	34.566	0.0385	0.685
195	0.7461	1.0242	2.5768	34.694	0.0385	0.685
196	0.7445	1.0244	2.5807	34.822	0.0386	0.685

T °C	ρ kg/m^3	c_p kJ/kg·K	μ 10^5 kg /m·s	ν 10^6 m^2/s	k_l W/m·K	Pr_l -
197	0.7430	1.0246	2.5846	34.950	0.0387	0.685
198	0.7414	1.0248	2.5885	35.078	0.0387	0.685
199	0.7399	1.0250	2.5924	35.206	0.0388	0.685
200	0.7383	1.0251	2.5962	35.334	0.0389	0.685
201	0.7368	1.0253	2.6001	35.462	0.0389	0.685
202	0.7352	1.0255	2.6040	35.590	0.0390	0.685
203	0.7336	1.0257	2.6079	35.718	0.0391	0.685
204	0.7321	1.0259	2.6118	35.846	0.0391	0.685
205	0.7305	1.0260	2.6156	35.974	0.0392	0.685
206	0.7290	1.0262	2.6195	36.102	0.0393	0.685
207	0.7274	1.0264	2.6234	36.230	0.0393	0.685
208	0.7259	1.0266	2.6273	36.358	0.0394	0.685
209	0.7243	1.0268	2.6312	36.486	0.0395	0.685
210	0.7228	1.0269	2.6350	36.614	0.0395	0.685
211	0.7212	1.0271	2.6389	36.742	0.0396	0.685
212	0.7197	1.0273	2.6428	36.870	0.0397	0.685
213	0.7181	1.0275	2.6467	36.998	0.0397	0.685
214	0.7166	1.0277	2.6506	37.126	0.0398	0.685
215	0.7150	1.0278	2.6544	37.254	0.0399	0.684
216	0.7135	1.0280	2.6583	37.382	0.0400	0.684
217	0.7119	1.0282	2.6622	37.510	0.0400	0.684
218	0.7104	1.0284	2.6661	37.638	0.0401	0.684
219	0.7088	1.0286	2.6700	37.766	0.0402	0.684
220	0.7073	1.0287	2.6738	37.894	0.0402	0.684
221	0.7057	1.0289	2.6777	38.022	0.0403	0.684
222	0.7042	1.0291	2.6816	38.150	0.0404	0.684
223	0.7026	1.0293	2.6855	38.278	0.0404	0.684
224	0.7011	1.0295	2.6894	38.406	0.0405	0.684
225	0.6995	1.0296	2.6932	38.534	0.0406	0.684
226	0.6980	1.0298	2.6971	38.662	0.0406	0.684
227	0.6964	1.0300	2.7010	38.790	0.0407	0.684
228	0.6951	1.0302	2.7047	38.926	0.0408	0.684
229	0.6939	1.0304	2.7083	39.061	0.0408	0.684
230	0.6926	1.0306	2.7120	39.197	0.0409	0.684
231	0.6913	1.0308	2.7156	39.332	0.0410	0.684
232	0.6901	1.0310	2.7193	39.468	0.0410	0.684
233	0.6888	1.0312	2.7230	39.604	0.0411	0.684
234	0.6875	1.0314	2.7266	39.739	0.0411	0.684
235	0.6862	1.0316	2.7303	39.875	0.0412	0.684
236	0.6850	1.0318	2.7339	40.010	0.0413	0.684
237	0.6837	1.0320	2.7376	40.146	0.0413	0.684
238	0.6824	1.0322	2.7413	40.282	0.0414	0.684
239	0.6812	1.0324	2.7449	40.417	0.0415	0.684
240	0.6799	1.0326	2.7486	40.553	0.0415	0.684
241	0.6786	1.0328	2.7522	40.688	0.0416	0.684
242	0.6774	1.0330	2.7559	40.824	0.0417	0.684
243	0.6761	1.0332	2.7596	40.960	0.0417	0.684
244	0.6748	1.0334	2.7632	41.095	0.0418	0.684
245	0.6735	1.0336	2.7669	41.231	0.0419	0.684
246	0.6723	1.0338	2.7705	41.366	0.0419	0.684
247	0.6710	1.0340	2.7742	41.502	0.0420	0.684
248	0.6697	1.0342	2.7779	41.638	0.0420	0.684
249	0.6685	1.0344	2.7815	41.773	0.0421	0.684
250	0.6672	1.0346	2.7852	41.909	0.0422	0.684
251	0.6659	1.0348	2.7888	42.044	0.0422	0.684
252	0.6647	1.0350	2.7925	42.180	0.0423	0.684

T °C	ρ kg/m^3	c_p kJ/kg·K	μ 10^5 kg /m·s	ν 10^6 m^2/s	k_l W/m·K	Pr_l -
253	0.6634	1.0352	2.7962	42.316	0.0424	0.683
254	0.6621	1.0354	2.7998	42.451	0.0424	0.683
255	0.6608	1.0356	2.8035	42.587	0.0425	0.683
256	0.6596	1.0358	2.8071	42.722	0.0426	0.683
257	0.6583	1.0360	2.8108	42.858	0.0426	0.683
258	0.6570	1.0362	2.8145	42.994	0.0427	0.683
259	0.6558	1.0364	2.8181	43.129	0.0427	0.683
260	0.6545	1.0366	2.8218	43.265	0.0428	0.683
261	0.6532	1.0368	2.8254	43.400	0.0429	0.683
262	0.6520	1.0370	2.8291	43.536	0.0429	0.683
263	0.6507	1.0372	2.8328	43.672	0.0430	0.683
264	0.6494	1.0374	2.8364	43.807	0.0431	0.683
265	0.6481	1.0376	2.8401	43.943	0.0431	0.683
266	0.6469	1.0378	2.8437	44.078	0.0432	0.683
267	0.6456	1.0380	2.8474	44.214	0.0433	0.683
268	0.6443	1.0382	2.8511	44.350	0.0433	0.683
269	0.6431	1.0384	2.8547	44.485	0.0434	0.683
270	0.6418	1.0386	2.8584	44.621	0.0435	0.683
271	0.6405	1.0388	2.8620	44.756	0.0435	0.683
272	0.6393	1.0390	2.8657	44.892	0.0436	0.683
273	0.6380	1.0392	2.8694	45.028	0.0436	0.683
274	0.6367	1.0394	2.8730	45.163	0.0437	0.683
275	0.6354	1.0396	2.8767	45.299	0.0438	0.683
276	0.6342	1.0398	2.8803	45.434	0.0438	0.683
277	0.6329	1.0400	2.8840	45.570	0.0439	0.683
278	0.6304	1.0402	2.8875	45.712	0.0440	0.683
279	0.6279	1.0404	2.8910	45.855	0.0440	0.683
280	0.6254	1.0407	2.8944	45.997	0.0441	0.683
281	0.6229	1.0409	2.8979	46.140	0.0441	0.683
282	0.6205	1.0411	2.9014	46.282	0.0442	0.683
283	0.6180	1.0413	2.9049	46.424	0.0443	0.683
284	0.6155	1.0415	2.9084	46.567	0.0443	0.683
285	0.6130	1.0418	2.9118	46.709	0.0444	0.683
286	0.6105	1.0420	2.9153	46.852	0.0444	0.683
287	0.6080	1.0422	2.9188	46.994	0.0445	0.683
288	0.6055	1.0424	2.9223	47.136	0.0446	0.683
289	0.6030	1.0426	2.9258	47.279	0.0446	0.683
290	0.6005	1.0429	2.9292	47.421	0.0447	0.684
291	0.5980	1.0431	2.9327	47.564	0.0447	0.684
292	0.5956	1.0433	2.9362	47.706	0.0448	0.684
293	0.5931	1.0435	2.9397	47.848	0.0449	0.684
294	0.5906	1.0437	2.9432	47.991	0.0449	0.684
295	0.5881	1.0440	2.9466	48.133	0.0450	0.684
296	0.5856	1.0442	2.9501	48.276	0.0450	0.684
297	0.5831	1.0444	2.9536	48.418	0.0451	0.684
298	0.5806	1.0446	2.9571	48.560	0.0452	0.684
299	0.5781	1.0448	2.9606	48.703	0.0452	0.684
300	0.5756	1.0451	2.9640	48.845	0.0453	0.684
301	0.5731	1.0453	2.9675	48.988	0.0453	0.684
302	0.5707	1.0455	2.9710	49.130	0.0454	0.684
303	0.5682	1.0457	2.9745	49.272	0.0455	0.684
304	0.5657	1.0459	2.9780	49.415	0.0455	0.684
305	0.5632	1.0462	2.9814	49.557	0.0456	0.684
306	0.5607	1.0464	2.9849	49.700	0.0456	0.684
307	0.5582	1.0466	2.9884	49.842	0.0457	0.684
308	0.5557	1.0468	2.9919	49.984	0.0458	0.684

T °C	ρ kg/m^3	c_p kJ/kg·K	μ 10^5 kg /m·s	ν 10^6 m^2/s	k_l W/m·K	Pr_l -
309	0.5532	1.0470	2.9954	50.127	0.0458	0.684
310	0.5507	1.0473	2.9988	50.269	0.0459	0.684
311	0.5482	1.0475	3.0023	50.412	0.0459	0.684
312	0.5458	1.0477	3.0058	50.554	0.0460	0.684
313	0.5433	1.0479	3.0093	50.696	0.0461	0.684
314	0.5408	1.0481	3.0128	50.839	0.0461	0.684
315	0.5383	1.0484	3.0162	50.981	0.0462	0.685
316	0.5358	1.0486	3.0197	51.124	0.0462	0.685
317	0.5333	1.0488	3.0232	51.266	0.0463	0.685
318	0.5308	1.0490	3.0267	51.408	0.0464	0.685
319	0.5283	1.0492	3.0302	51.551	0.0464	0.685
320	0.5258	1.0495	3.0336	51.693	0.0465	0.685
321	0.5233	1.0497	3.0371	51.836	0.0465	0.685
322	0.5209	1.0499	3.0406	51.978	0.0466	0.685
323	0.5184	1.0501	3.0441	52.120	0.0467	0.685
324	0.5159	1.0503	3.0476	52.263	0.0467	0.685
325	0.5134	1.0506	3.0510	52.405	0.0468	0.685
326	0.5109	1.0508	3.0545	52.548	0.0468	0.685
327	0.5084	1.0510	3.0580	52.690	0.0469	0.685